

Dissection of drug resistance mechanisms in FGFR2 mutant endometrial cancer.

Fearon, Abbie Elizabeth

The copyright of this thesis rests with the author and no quotation from it or information derived from it may be published without the prior written consent of the author.

For additional information about this publication click this link.

<http://qmro.qmul.ac.uk/jspui/handle/123456789/9027>

Information about this research object was correct at the time of download; we occasionally make corrections to records, please therefore check the published record when citing. For more information contact scholarlycommunications@qmul.ac.uk

Dissection of drug resistance mechanisms in FGFR2 mutant endometrial cancer

Abbie Elizabeth Fearon

Submitted in partial fulfilment of the requirements for the Degree of Doctor of
Philosophy

January 2015

Queen Mary University of London

Barts Cancer Institute

Centre for Tumour Biology

John Vane Science Centre

Charterhouse Square

London

E1CM 6BQ

Declaration of authorship

I, Abbie Elizabeth Fearon, confirm that the research included within this thesis is my own work or that where it has been carried out in collaboration with, or supported by others, that this is duly acknowledged below and my contribution indicated. Previously published material is also acknowledged below.

I attest that I have exercised reasonable care to ensure that the work is original, and does not to the best of my knowledge break any UK law, infringe any third party's copyright or other Intellectual Property Right, or contain any confidential material.

I accept that the College has the right to use plagiarism detection software to check the electronic version of the thesis.

I confirm that this thesis has not been previously submitted for the award of a degree by this or any other university.

The copyright of this thesis rests with the author and no quotation from it or information derived from it may be published without the prior written consent of the author.

Signature: Abbie Elizabeth Fearon

Date: 30th January 2015

Acknowledgements

Firstly, I would like to express my sincere gratitude to Dr Richard Grose for his constant help, support and encouragement. I am extremely lucky to have had such a wonderful PhD supervisor, who understood and believed in me. I would also like to thank Dr Edward Carter, Yasmine Tanner, Ekaterina Kapitonova, Dr Myrto Chioni, Dr Luisa Robbez-Masson and Dr Stacey Coleman for being friends as well as colleagues. I will be forever grateful for the opportunity to work in such a fantastic group. I would also like to thank Cancer Research UK for the funding provided which allowed me to pursue my ambition of a career in academic research.

Thank you to everyone at Barts Cancer Institute for making the last three and a half years some of the best of my life. I am privileged to have worked alongside incredible scientists and am honoured to call so many of them my friends. I am extremely appreciative of the help I have received from Edmund Wilkes and Dr Pedro Cutillas. Thank you to everyone in the PhD office for the support and laughter they brought to my life every day. I would particularly like to thank Caroline Sproat and Rachel Nelan, in whom I have found lifelong friends.

There are so many friends to thank, each of whom have understood when I had to cancel, forgiven me when I didn't answer their calls and listened when I needed them. In particular, I would like to thank Faith, Katie Ebbrell and Katie Fox. After so many years, they are no longer my friends, they are my family.

I cannot let this moment pass without thanking my dear family. They are the constants in my ever changing world and for that I will be eternally grateful. Thank you to my parents, Jane and Peter, for their love and for helping to make me into the person I am today. Thank you to my sister Rachel and brother Lewis for being my friends as well as my siblings. The understanding and support they have given me means so much. I am very lucky to have each of them.

I would also like to thank my Nan and Da for their unwavering love and encouragement. I am very sad that my Nan didn't get to see me finish this chapter of my life but I'm so happy she saw it begin. Thank you also to Ann, for her kindness and warmth. We are all privileged to have her in our lives. I would also like to take this opportunity to thank Patricia and Michael for their encouragement and many wise words. And thank you to Caleb and Kaden who, without even knowing it, helped me to keep things in perspective.

And finally to my darling Richard, whose beautiful words brighten my days. I am very fortunate to have found someone who understands me, whose love and support is unwavering and who believes in me even when I have lost belief in myself. Thank you will never be enough.

Abstract

Mutations in FGFR2 are common in a subset of endometrial carcinomas. Given the emergence of small molecule inhibitors specific to this receptor tyrosine kinase, FGFR2 is an attractive therapeutic target. However, compensatory and adaptation mechanisms limit the clinical utility of compounds that target nodes in the receptor tyrosine kinase network. Here, we analysed the impact of FGFR inhibition in endometrial cancer cells and observed the emergence of a resistant population in an FGFR2-mutant cell line. To understand the mechanisms underlying this adaptation response, we used a phosphoproteomics approach to measure the kinase network in an unbiased manner. These experiments led to the identification of an AKT-related compensatory mechanism underpinning this resistance. Further dissection of this resistance mechanism utilising gene expression analysis showed *PHLDA1*, a negative regulator of AKT, was significantly down-regulated in resistant cells. This was further confirmed at the protein level. siRNA knockdown of *PHLDA1* conferred immediate drug resistance in the FGFR2-mutant endometrial cancer cell line. Therefore, we identified *PHLDA1* down-regulation as a mediator of drug resistance in FGFR2 mutant cancer cells, the first demonstration of the role of *PHLDA1* in the acquisition and maintenance of drug resistance. Using a 3D physiometric model, we demonstrated that AKT inhibition alone also led to generation of a drug-resistant population. Most importantly, dual-drug therapy inhibited proliferation and induced cell death. Our data highlight how mass spectrometry and microarray gene expression analysis can complement each other in the identification of novel resistance mechanisms in cancer cells. These data suggest that combination treatment of FGFR2-mutant endometrial cancers, targeting both FGFR2 and AKT, represents a promising therapeutic approach.

Table of contents

Chapter 1:	Introduction.....	24
1.1.	Endometrial cancer.....	25
1.2.	Fibroblast growth factor (FGF) and FGFR signalling.....	29
1.2.1.	FGFs and FGFRs.....	29
1.2.2.	FGFR activation.....	33
1.2.3.	FGFR signalling pathways.....	36
1.2.4.	Regulation of FGFR signalling.....	41
1.2.5.	FGFR2 and disease.....	46
1.3.	Targeted drug therapy.....	54
1.4.	Drug resistance in cancer.....	59
1.5.	Screening of signalling networks.....	62
1.5.1.	Microarray gene expression analysis.....	62
1.5.2.	Mass spectrometry.....	63
1.6.	Cell culture models.....	69
1.7.	Aims and objectives.....	72
Chapter 2:	Materials and methods.....	73
2.1.	Cell culture.....	74
2.2.	Cell line sequencing.....	75
2.3.	PCR.....	78
2.4.	Serum starvation assay.....	81
2.5.	Stimulation assay.....	81
2.6.	Western blotting.....	81

2.7.	2D cell survival assay and generation of FGFR-inhibitor resistant cell lines.....	82
2.8.	3D physiomimetic model.....	83
2.9.	Immunofluorescence.....	84
2.10.	Microscope image acquisition.....	85
2.11.	Data analysis.....	85
2.12.	Isolation, purification, growth and maintenance of primary cells, and cell immortalisation.....	86
2.13.	Mass spectrometry.....	88
2.13.1.	Cell culture.....	88
2.13.2.	Cell lysis, digestion and solid-phase extraction.....	88
2.13.3.	TiO ₂ Metal Oxide Affinity Chromatography (MOAC).....	89
2.13.4.	Nanoflow-liquid chromatography tandem mass spectrometry (LC-MS/MS).....	89
2.13.5.	Identification and quantification of phosphopeptides.....	90
2.14.	Cell tracker.....	91
2.15.	Receptor tyrosine kinase (RTK) and signalling node phosphoprotein immunofluorescence assay.....	92
2.16.	Microarray.....	92
2.17.	Fractionation.....	93
2.18.	siRNA knockdown.....	93
2.19.	PHLDA1 over expression and cell cycle analysis.....	94
Chapter 3:	Results: Endometrial cancer cell line characterisation.....	95
3.1.	Introduction.....	96

3.2.	Endometrial cancer cell line characterisation.....	97
3.3.	Differential signalling in the presence and absence of FGFR inhibition in endometrial cancer cell lines.....	104
3.4.	Primary cell line immortalisation.....	109
3.5.	Development of a 3D organotypic model to investigate endometrial cancer cell behaviour.....	113
3.6.	Summary of results.....	125
3.7.	Discussion.....	126
Chapter 4:	Results: Investigation of FGFR inhibitor resistance in MFE-296 cells.....	131
4.1.	Introduction.....	132
4.2.	Phosphoproteomic investigation of resistance acquisition in MFE-296 cells.....	133
4.3.	Effect of AKT inhibition alone and in combination with FGFR inhibition in MFE-296 cells.....	143
4.4.	Summary of results.....	150
4.5.	Discussion.....	151
Chapter 5:	Results: Investigation of FGFR inhibitor resistance mechanisms in MFE-296 cells.....	156
5.1.	Introduction.....	157
5.2.	Generation and characterisation of an FGFR inhibitor resistant cell line.....	158
5.3.	Investigation of the MFE-296 ^{PDR} FGFR inhibitor resistance pathway.....	169
5.4.	Investigation of the role of PHLDA1 in FGFR inhibitor resistance.....	178
5.5.	Summary of results.....	185

5.6.	Discussion.....	186
Chapter 6:	General discussion.....	193
6.1.	Overview.....	194
6.2.	Generation of a 3D model of endometrial cancer and its use in investigation of small molecule inhibition of FGFR signalling.....	196
6.3.	Identification of changes in the phosphoproteome upon drug resistance acquisition using MS.....	198
6.4.	Dissection of drug resistance mechanisms using transcriptomic analysis.....	202
6.5.	Concluding remarks.....	205
Chapter 7:	References.....	206
Appendix 1:	Supplementary figures.....	246
Appendix 2:	Genomic editing of <i>FGFR2</i> mutation status using ZFN technology...	261
2.1.	Introduction.....	262
2.2.	Materials and Methods.....	267
2.2.1.	Custom-made <i>FGFR2</i> ZFN.....	267
2.2.2.	Bacterial transformation.....	267
2.2.3.	ZFN mRNA synthesis.....	267
2.2.4.	Alternative repair construct.....	267
2.2.5.	Site directed mutagenesis.....	268
2.2.6.	ZFN transfection – lipofection.....	272
2.2.7.	ZFN transfection – nucleofection.....	273
2.2.8.	Surveyor assay.....	273
2.2.9.	Single cell cloning.....	278

2.2.10.	FGFR2 N550K mutation sequencing.....	280
2.2.11.	Neomycin PCR.....	281
2.3.	ZFN cleavage in endometrial cancer cells.....	284
2.4.	Generation of FGFR2 mutant alternative repair templates.....	288
2.5.	Transfection and screening of MFE-296 cells following ZFN and FGFR2IIIb-GFP-neo construct transfection.....	291
2.6.	Summary of results.....	297
2.7.	Discussion.....	298
Appendix 3:	International Journal of Biochemistry and Cell Biology review: FGFR signalling in women's cancers.....	301
Appendix 4:	Nature Structural and Molecular Biology review: Grb-ing receptor activation by the tail.....	313
Appendix 5:	Trends in Cell Biology review: Careless talks costs lives: fibroblast growth factor receptor signalling and the consequences of pathway malfunction.....	316

List of Figures

Figure 1.1.	Structure of the uterus and localisation of endometrial tumours at surgical stages I-IV of the disease.....	26
Figure 1.2.	Somatic <i>FGFR2</i> mutations in endometrial cancer are the same as germline mutations found in a range of developmental disorders.....	28
Figure 1.3.	FGFR signalling.....	32
Figure 1.4.	Canonical FGFR activation.....	35
Figure 1.5.	Negative regulation of FGFR signalling.....	45
Figure 1.6.	Frequency of <i>FGFR2</i> point mutations, copy number and gene expression variations in cancer.....	52
Figure 1.7.	Mechanisms of aberrant FGFR signalling in disease.....	53
Figure 1.8.	Mechanisms of FGFR inhibition.....	58
Figure 1.9.	Schematic representation of the 3D organotypic cell culture model.....	71
Figure 3.1.	Effect of serum starvation on basal signalling in FGFR2 mutant endometrial cancer cell lines.....	100
Figure 3.2.	Baseline expression of FGFR1, FGFR2 and downstream signalling molecules in endometrial cancer cell lines.....	103
Figure 3.3.	Effect of FGFR inhibition on endometrial cancer cell number in 2D culture.....	105
Figure 3.4.	Effect of FGF2 stimulation and FGFR2 inhibition on cell signalling.....	107
Figure 3.5.	Immortalisation of non-malignant primary endometrial tissue.....	111
Figure 3.6.	Effect of PD173074 on fibroblasts in 2D culture.....	114

Figure 3.7.	Effect of FGFR2 inhibition on endometrial cancer cells in a 3D physiomimetic model.....	116
Figure 3.8.	AN3CA cells adhere to the stromal equivalent layer in a 3D organotypic model in the presence of PD173074.....	118
Figure 3.9.	The emergence of a drug resistant population in FGFR inhibitor treated MFE-296 cells.....	120
Figure 3.10.	Effect of FGFR inhibitor treatment on free circulating cells in a 3D model.....	123
Figure 4.1.	Workflow of MS employed to detect changes in the phosphoproteome of MFE-296 cells upon inhibition of FGFR signalling.....	134
Figure 4.2.	Phosphoproteomic analysis of FGFR-inhibitor resistance acquisition in MFE-296 cells.....	139
Figure 4.3.	Phosphopeptides showing significant up-regulation after 14 days PD173074 treatment.....	141
Figure 4.4.	Effect of FGFR inhibition on MFE-296 cells after one day PD173074 treatment.....	142
Figure 4.5.	Effect of AKT inhibition, alone and in combination with FGFR inhibition, in MFE-296 cells in a 3D physiomimetic model.....	144
Figure 4.6.	Effect of AKT inhibition, alone and in combination with FGFR inhibition, in Ishikawa cells in a 3D physiomimetic model.....	146
Figure 4.7.	AKT inhibition in combination with the FGFR inhibitor AZD4547, for seven days, overcomes FGFR inhibitor resistance in MFE-296 cells.....	149
Figure 5.1.	Effect of PD173074 treatment on MFE-296 ^{PDR} cells in 2D culture.....	159
Figure 5.2.	Changes in signalling upon PD173074 treatment in MFE-296 parental and MFE-296 ^{PDR} cells.....	161

Figure 5.3.	Effect of drug removal on MFE-296 ^{PDR} cell number and proliferation in a 3D physiomimetic model.....	162
Figure 5.4.	Effect of AKT inhibition, in the presence or absence of PD173074, in MFE-296 ^{PDR} cells in a 3D organotypic model.....	164
Figure 5.5.	Effect of FGFR and AKT inhibition, alone and in combination, on a mixed population of MFE-296 and MFE-296 ^{PDR} cells.....	166
Figure 5.6.	Effect of PI3K inhibition on MFE-296 and MFE-296 ^{PDR} cells in 2D culture.....	168
Figure 5.7.	Schematic representation of the PathScan array.....	170
Figure 5.8.	Changes in signalling node phosphorylation in MFE-296 ^{PDR} vs MFE-296 parental cells.....	171
Figure 5.9.	Transcriptomic changes induced upon FGFR inhibitor resistance acquisition in MFE-296 cells.....	174
Figure 5.10.	Schematic representation of the opposing cellular effects of the PIP ₃ binding proteins AKT and PHLDA1.....	177
Figure 5.11.	PHLDA1 expression in the basal state and after PD173074 treatment of MFE-296 and MFE-296 ^{PDR} cells.....	179
Figure 5.12.	Cellular localisation of PHLDA1, P-AKT and total AKT in MFE-296 and MFE-296 ^{PDR} cells.....	181
Figure 5.13.	Induction of FGFR inhibitor resistance in MFE-296 cells upon PHLDA1 knockdown.....	183
Figure 5.14.	Proposed mechanism of FGFR inhibitor drug resistance in MFE-296 endometrial cancer cells.....	191

List of Tables

Table 2.1.	Primers used to sequence endometrial cancer cell point mutations.....	76
Table 2.2.	HotStarTaq Plus DNA Polymerase PCR programme.....	77
Table 2.3.	FGFR PCR primers.....	79
Table 2.4.	PCR cycle for amplification of FGF and FGFR sequences.....	80
Table 3.1.	<i>FGFR2</i> , <i>PTEN</i> , <i>PIK3CA</i> and <i>PIK3R1</i> mutation status of endometrial cancer.....	98
Table 3.2.	FGFR isoform expression profile.....	102

List of Appendix 1 Figures

Appendix Figure 1.1.	<i>FGFR2</i> mutation sequencing of endometrial cancer cell lines.....	247
Appendix Figure 1.2.	<i>PTEN</i> and <i>PIK3CA</i> mutation sequencing of MFE-296 cells.....	249
Appendix Figure 1.3.	<i>PTEN</i> and <i>PIK3CA</i> mutation sequencing of AN3CA cells.....	250
Appendix Figure 1.4.	<i>PTEN</i> and <i>PIK3CA</i> mutation sequencing of Ishikawa cells.....	251
Appendix Figure 1.5.	FGFR isoform expression in MFE-296 and AN3CA.....	252
Appendix Figure 1.6.	FGFR2 antibody validation.....	253
Appendix Figure 1.7.	Effect of varying HFF2:MFE-296 ratio in a 3D organotypic model of endometrial cancer.....	254
Appendix Figure 1.8.	False discovery rate (FDR) and quantile normalisation of phosphopeptide ions.....	255
Appendix Figure 1.9.	<i>FGFR2</i> mutation sequencing of MFE-296 ^{PDR} cells.....	257
Appendix Figure 1.10.	Effect of PD173074 on PHLDA1 levels in MFE-296 cells.....	258
Appendix Figure 1.11.	PHLDA1 knockdown does not affect MFE-296 ^{PDR} cell number.....	259
Appendix Figure 1.12.	PHLDA1 over expression in MFE-296 and MFE-296 ^{PDR} cells.....	260

List of Appendix 2 Figures

Appendix Figure 2.1.	ZFN-mediated genome editing.....	265
Appendix Figure 2.2.	Schematic representation of single cell cloning by serial dilution.....	279
Appendix Figure 2.3.	Utilisation of the surveyor nuclease assay to assess the efficiency of ZFN genomic DNA editing.....	286
Appendix Figure 2.4.	Sequence alignment of FGFR2 wild type and mutant constructs generated via SDM.....	290
Appendix Figure 2.5.	GFP expression in a polyclonal population of MFE-296 cells transfected with pGFP or ZFN in combination with the FGFR2IIIb-GFP-neo construct.....	292
Appendix Figure 2.6.	Neomycin gene amplification in MC1 cells after ZFN and FGFR2IIIb-GFP-neo transfection.....	294
Appendix Figure 2.7.	MC1 cells are N550K FGFR2 mutant.....	296

List of Appendix 2 Tables

Appendix Table 2.1.	Primers used to produce mutant FGFR2IIIb-GFP constructs via SDM.....	269
Appendix Table 2.2.	Primers used to sequence endometrial cancer cells for point mutations.....	270
Appendix Table 2.3.	HotStarTaq Plus DNA polymerase PCR programme...	261
Appendix Table 2.4.	Sequencing and ZFN-induced mutation detection PCR primers.....	275
Appendix Table 2.5.	ZFN-induced mutation detection PCR primers.....	276
Appendix Table 2.6.	Cycler conditions for re-annealing of PCR products in ZFN-induced mutation detection PCR.....	277
Appendix Table 2.7.	Neomycin resistance gene primers.....	282
Appendix Table 2.8.	PCR conditions for amplification of neomycin resistance gene product.....	283

List of abbreviations

ACN	Acetonitrile
AKT	Protein kinase B
BCL2	B-cell lymphoma 2
BICC1	Bicaudal C homolog 1
BMI-1	Polycomb group RING finger protein 4
bp	Base pair
BRAF	Serine-threonine protein kinase b-raf
CBL	Casitas B-lineage lymphoma
cDNA	Complementary DNA
CID	Collision induced dissociation
CML	Chronic myeloid leukaemia
c-MYC	Cellular homologue of v-MYC
COSMIC	Catalogue of somatic mutations in cancer
CRISPR	Clustered regulatory interspaced short palindromic repeat
DAG	Diacylglycerol
DAPI	4', 6-diamidino-2-phenylindole
DDA	Data-dependent acquisition
DMSO	Dimethyl sulphoxide
DSB	Double strand break
DTT	Dithiothreitol
ECD	Electron capture dissociation
ECL	Enhanced chemiluminescence

ECM	Extracellular matrix
EDTA	Ethylenediaminetetraacetic acid
EIF4EBP	Eukaryotic translation initiation factor 4E binding protein
EMT	Epithelial to mesenchymal transition
ER	Endoplasmic reticulum
ERK	Extracellular signal regulated kinase
ETD	Electron transfer dissociation
FA	Formic acid
FBS	Foetal bovine serum
FGF	Fibroblast growth factor
FGFR	Fibroblast growth factor receptor
FGFRL1	Fibroblast growth factor receptor like 1
FRS2	Fibroblast growth factor receptor substrate 2
GAS	Gamma-activated site
gDNA	Genomic DNA
Grb2	Growth factor receptor-bound protein 2
GWAS	Genome wide association studies
H&E	Hematoxylin-eosin
HCD	Higher energy C-trap dissociation
HER2	Human epidermal growth factor 2
HFF2	Human foreskin fibroblast 2
HPLC	High performance-liquid chromatography
HPV	Human papilloma virus

HR	Homologous repair
HS	Heparan sulphate
HSC70	Heat shock chaperone 70
HSPG	Heparan sulphate proteoglycans
hTERT	Human telomerase reverse transcriptase
IAM	Iodoacetamide
Ig	Immunoglobulin
IP ₃	Inositol 1, 4, 5 trisphosphate
iTRAQ	Isobaric tag for relative and absolute quantification
JAK	Janus kinase
K-RAS	Kirsten-rat sarcoma viral oncogene homologue
KSEA	Kinase substrate enrichment analysis
LB	Luria Broth
LC-MS	Liquid chromatography-MS
MAPK	Mitogen activated protein kinase
MC1	Monoclonal cell line 1
MDM2	Minute 2 homologue
MEK	MAPK kinase
MEM	Modified Eagle's medium
MOAC	Metal oxide affinity chromatography
MS	Mass spectrometry
MSA	Multistage activation
mTOR	Mammalian target of rapamycin

mTORC	mTOR complex
NBR1	Neighbor of BRCA1
NHEJ	Non-homologous end joining
p16	Cyclin-dependent kinase inhibitor 2A
P-AKT	Phospho-AKT
PANDA	Peptide ANalysis and Database Assembly
PBS	Phosphate buffered saline
PCBP1	Poly(rC)-binding protein 1
PCR	Polymerase chain reaction
PD	PD173074
PDGFR β	Platelet derived growth factor receptor β
PDK1	Phosphoinositide-dependent kinase 1
PEI	Polyethylenimine
pELM	PhosphoELM
P-ERK	Phospho-ERK
PESCAL	PEak Statistical CALculator
P-FRS2	Phospho- FRS2
PHLDA	Pleckstrin homology like domain A
PI3K	Phosphoinositide 3-kinase
PI3K α	Phosphoinositide 3-kinase alpha
PI3K β	Phosphoinositide 3-kinase beta
PI3K δ	Phosphoinositide 3-kinase delta
PI3K γ	Phosphoinositide 3-kinase gamma

PIK3CA	Phosphoinositide 3-kinase catalytic subunit alpha
PIK3CB	Phosphoinositide 3-kinase catalytic subunit beta
PIK3CD	Phosphoinositide 3-kinase catalytic subunit delta
PIK3CG	Phosphoinositide 3-kinase catalytic subunit gamma
PIK3R1	Phosphoinositide 3-kinase regulatory subunit 1
PIK3R2	Phosphoinositide 3-kinase regulatory subunit 1
PIK3R3	Phosphoinositide 3-kinase regulatory subunit 1
PIP ₂	Phosphatidylinositol (4, 5) bisphosphate
PIP ₃	Phosphatidylinositol (3, 4, 5) triphosphate
PLC γ	Phospholipase C γ
PMSF	Phenylmethylsulphonyl fluoride
pPoint	PhosphoPoint
pSite	PhosphoSite
PTB	Phosphotyrosine-binding
PTEN	Phosphatase and tensin homologue
RAF	Rapidly accelerated fibrosarcoma
RAS	Rat sarcoma
RIPA	Radioimmunoprecipitation assay
RNAi	RNA interference
RTK	Receptor tyrosine kinase
S6K	Ribosomal S6 kinase
SDM	Site directed mutagenesis
SEF	Similar expression to FGF

SEM	Standard error of the mean
SH2	Src homology-2
SH3	Src homology-3
SH3BP4	SH3 binding protein 4
SILAC	Stable isotope labelling with amino acids in cell culture
siRNA	Short interfering RNA
SLC45A3	Solute Carrier Family 45, Member 3
SNP	Small nucleotide polymorphism
SOS	Son of sevenless
SPRED1/2	Sprouty-related enabled/vasodilator-stimulated homology 1/2 domain phosphoprotein
SPRY	Sprouty
STAT	Signal transducer and activator of transcription
TALEN	Transcription activator-like effector nuclease
TBST	Tween20-TBS
TFA	Trifluoroacetic acid
TSPAN11	Tetraspanin 11
VEGFR2	Vascular endothelial growth factor receptor 2
Vps15	Vacuolar protein sorting 15
Vps34	Vacuolar protein sorting 34
YAP1	Yes-associated protein 1
ZFN	Zinc finger nuclease

Chapter 1

Introduction

1.1 Endometrial cancer

Endometrial cancer is the most common gynaecological malignancy in the developed world and the fourth most common cancer in women (Byron et al., 2008, Jemal et al., 2011, Pollock et al., 2007). In 2011, approximately 8500 women were diagnosed with endometrial cancer in the UK alone (CRUK, 2014). Patients commonly present at an early stage where the tumour is confined to the endometrium, the lining of the uterus, with little or no migration into the surrounding tissue (Amant et al., 2005) (Figure 1.1 A). In this early stage disease, surgical treatment with full hysterectomy is most common and usually curative, with greater than 85% of patients surviving for over five years (Amant et al., 2005). However, such surgery is associated with the effects of long term oestrogen deprivation, for example increased risk of cardiovascular disease (Atsma et al., 2006), as well as the additional impact of a loss of fertility in the 14-30% of patients who are premenopausal upon diagnosis (Lau et al., 2014, Wright et al., 2009). In light of this, alternative treatments are desirable.

Endometrial cancer is split predominantly into two types, endometrioid and non-endometrioid, with further subdivision of the latter into serous and clear-cell carcinomas. Although only around 20% of all endometrial cancers are non-endometrioid, these tumours are higher grade by definition (Amant et al., 2005). Endometrioid endometrial cancer accounts for the remaining 80% of tumours of the uterus. These lesions are generally oestrogen-related and usually associated with endometrial hyperplasia, resulting in excessive proliferation of the endometrium (Amant et al., 2005). Endometrioid and non-endometrioid cancers present with distinct genetic alterations, however, a minority of cases present with mixed features (Yeramian et al., 2013).

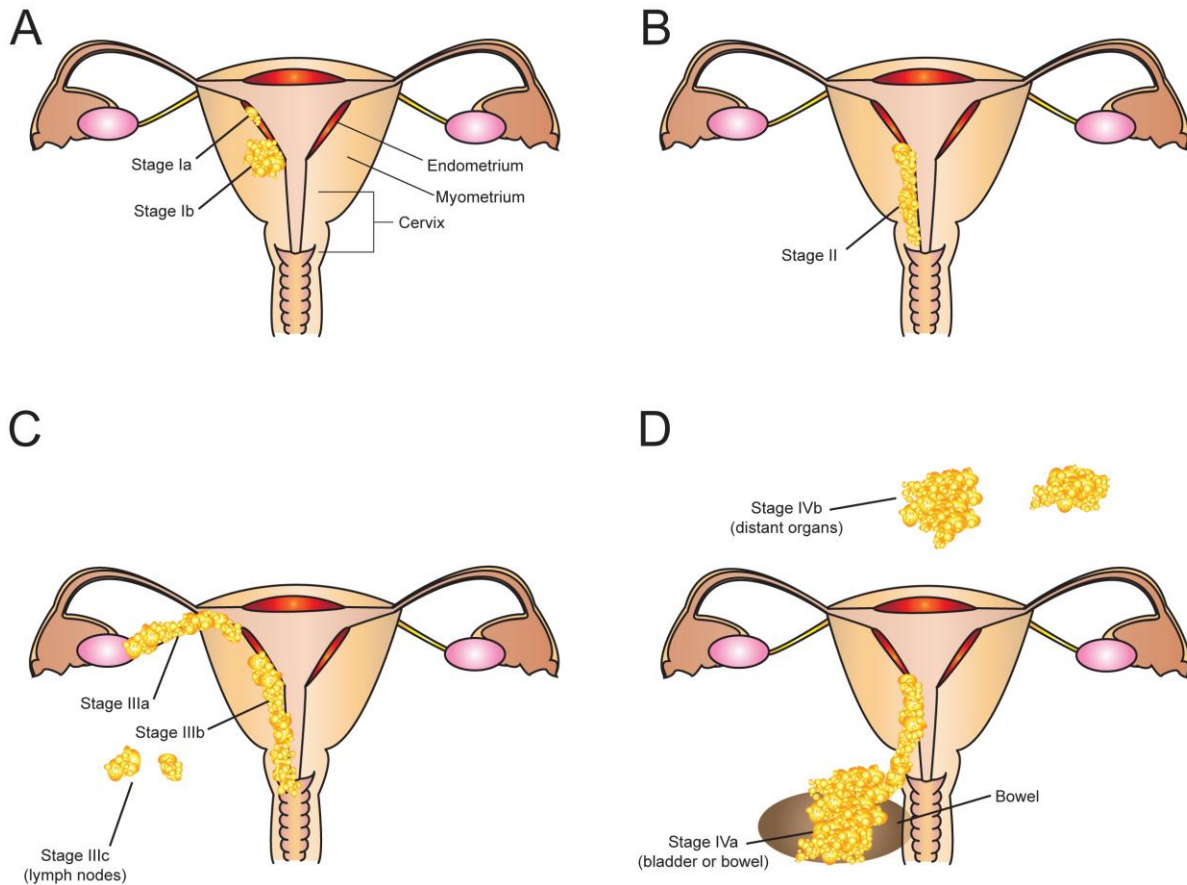


Figure 1.1. Structure of the uterus and localisation of endometrial tumours at surgical stages I-IV of the disease.

(A) Stage Ia endometrial tumours are confined to the endometrium while stage Ib tumours commonly penetrate halfway into the muscle wall. (B) Higher grade stage II tumours grow into the cervix. (C) Stage III cancer is characterised by spread of the tumour to other parts of the pelvis and can be subdivided into tumours spreading to the ovaries (IIIa), into the vagina (IIIb) and those which have spread to the lymph nodes (IIIc). (D) The highest grade tumours are those which have metastasised to the bladder or bowel (IVa) or to distant organs (IVb). The surgical stage of tumours reflects the five year survival rate of approximately 85% for stage I, 75% for stage II, 45% for stage III and 25% for stage IV (Amant et al., 2005).

Patients presenting with advanced stage and higher grade endometrial cancer commonly relapse despite surgery, adjuvant radiotherapy and chemotherapy (Chaudhry and Asselin, 2009). Overall patient survival has not improved significantly and so endometrial cancer remains among the top ten leading causes of female cancer related deaths (Chaudhry and Asselin, 2009). In order to address this, a greater understanding of the molecular mechanisms underlying the disease is required.

A range of genetic abnormalities are found in endometrial cancer. Microsatellite instability is seen in 25-30% of cases (Catasus et al., 1998, Duggan et al., 1994), while phosphatase and tensin homologue (PTEN) alterations have been detected in 37-61% of endometrial cancers, leading to the deregulation of the phosphoinositide 3-kinase (PI3K) pathway (Yeramian et al., 2013). Other common mutations include those in genes encoding phosphoinositide 3-kinase catalytic subunit alpha (*PIK3CA*) and Kirsten-rat sarcoma viral oncogene homologue (*K-RAS*) (Byron et al., 2008, Yeramian et al., 2013).

Mutations in the receptor tyrosine kinase fibroblast growth factor receptor 2 (FGFR2) occur in up to 16% of endometrial cancers (Byron et al., 2008, Byron et al., 2012, Fearon et al., 2013). Interestingly, many of these somatic oncogenic mutations are the same as germline mutations found in developmental disorders, for example craniosynostosis dysplasias (Pollock et al., 2007) (Figure 1.2). Such FGFR2 mutations also give mutant clones of spermatogonia a selective advantage in the testes (Wilkie, 2005), suggesting that they are capable of conferring a growth advantage at the cellular level and are thus likely driver mutations in endometrial cancer (Dutt et al., 2008, Jemal et al., 2011). Thus, this pathway is an attractive therapeutic target and so a greater understanding of the role of FGFR2 signalling in endometrial cancer is of paramount importance.

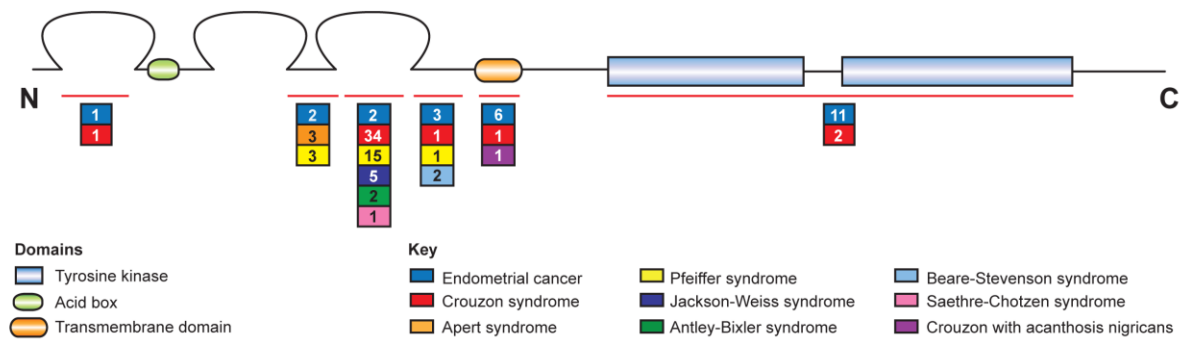


Figure 1.2. Somatic *FGFR2* mutations in endometrial cancer are the same as germline mutations found in a range of developmental disorders.

Schematic representation of *FGFR2*. In the lower panel, mutations in various regions of the receptor (red lines) in both developmental disorders and endometrial cancer are shown (boxes). The diseases represented by each colour are detailed in the key. The number of *FGFR2* mutations found in each region in the various disorders is noted in the corresponding box. Mutations were collated from the literature (Freitas et al., 2006, Lajeunie et al., 2006, Passos-Bueno et al., 1998) and the catalogue of somatic mutations in cancer (COSMIC). Data correct as of September 2014. N, N terminus; C, C terminus.

1.2 Fibroblast growth factor (FGF) and FGFR signalling

1.2.1 FGFs and FGFRs

FGFs are responsible for a plethora of cellular functions, from embryogenesis to metabolism (Bottcher and Niehrs, 2005, Dubrulle and Pourquie, 2004, Feldman et al., 1995, Ghabrial et al., 2003, Huang and Stern, 2005, Polanska et al., 2009, Sun et al., 1999). FGFs exert their cellular effects by interacting with FGFRs in a complex with heparan sulphate (HS) (Yayon et al., 1991). Upon ligand binding, FGFRs dimerise and undergo transphosphorylation of their split kinase domain (Coughlin et al., 1988) (Figure 1.3 A), leading to the recruitment of adaptor proteins and initiation of downstream signalling (Figure 1.3 B). This results in a range of cellular outcomes, including proliferation, migration, differentiation and survival (Belov and Mohammadi, 2013, Carter et al., 2014).

The extended FGF family is composed of 22 members, varying in size from 17-34 kDa. All members share a conserved 120 amino acid sequence and show 16-65% sequence homology (Ornitz and Itoh, 2001). However, only 18 FGFs signal via FGFR interactions (FGF1-10 and FGF16-23), while FGF11-14, which lack a signal peptide, act in an intracellular manner and do not bind FGFRs (Smallwood et al., 1996). Thus, many consider the FGF family to comprise only 18 members. Furthermore, although they are numbered from 1-23, Fgf15 is the mouse orthologue of human FGF19. The 18 true FGFs cluster into six subfamilies; one endocrine subfamily, that acts globally in metabolic processes such as glucose metabolism, and five paracrine subfamilies acting locally to initiate processes such as organogenesis (Belov and Mohammadi, 2013). Each ligand binds to FGFRs with varying specificity; some are promiscuous, for example FGF1, and bind to multiple receptors, while others, such as FGF7, bind to only one receptor isoform (Ornitz et al., 1996).

There are seven signalling receptors, encoded by four *FGFR* genes, *FGFR1-4* (Johnson and Williams, 1993). Each of the receptors consists of an intracellular split tyrosine kinase domain, a transmembrane region and an extracellular domain

containing three Immunoglobulin (Ig) loops (Igl-III) (Figure 1.3 A). FGFR1-3 have highly conserved intron/exon boundaries (Ornitz et al., 1996). Alternative splicing of exons 8 and 9, encoding IgIII of FGFR1-3, results in translation of two distinct isoforms capable of signal transduction (Johnson et al., 1991). These isoforms are termed IIIb and IIIc, depending on which exons are spliced out. This third Ig loop encodes the ligand binding domain; alternative splicing of this region is responsible for ligand binding specificity. A third isoform exists for FGFR1 and 2, termed IIIa. This variant results in a truncated, secreted protein, which is unable to transduce a signal and may have an auto-inhibitory role in FGF signalling, possibly by sequestering ligands (Wheldon et al., 2011). FGFR4 is distinct in that it has only one isoform, homologous to the IIIc variant of FGFR1-3 (Vainikka et al., 1992). Receptor expression is generally cell type specific, for example IIIb and IIIc isoforms of FGFR1 and 2 are expressed in epithelial and mesenchymal cells, respectively (Orr-Urtreger et al., 1993, Yan et al., 1993). However, this cell type specificity is subject to change when FGFRs are associated with diseases such as cancer (Shirakihara et al., 2011, Yan et al., 1993).

A fifth member of the FGFR family, fibroblast growth factor receptor like 1 (FGFRL1), has also been identified. This protein, which exists as a homodimer consisting of the three characteristic extracellular Ig domains, acid box between Igl and IgII and a transmembrane helix, differs from the classic receptors in that it has no intracellular tyrosine kinase domain (Sleeman et al., 2001, Trueb et al., 2003, Wiedemann and Trueb, 2000). Instead, the intracellular portion of FGFRL1 consists of only 100 residues including a histidine-rich sequence and a tandem tyrosine-based motif (Rieckmann et al., 2009, Sleeman et al., 2001, Zhuang et al., 2009). These two sequences function as signals for FGFRL1 trafficking from the plasma membrane to endosomes and lysosomes. Deletion of these sequences result in inefficient FGFRL1 internalisation and prolonged localisation at the plasma membrane (Rieckmann et al., 2009).

As FGFRL1 does not contain a tyrosine kinase domain, it is not able to signal in the classical FGFR fashion. Its function is yet to be fully determined but a number of

theories have been postulated. Firstly, the receptor could have an inhibitory effect on FGF signalling, by sequestering ligands and therefore preventing them from binding to FGFR1-4 (Sleeman et al., 2001, Steinberg et al., 2010, Trueb et al., 2003). However, recent work has suggested FGFR1 does indeed have some form of signalling potential (Silva et al., 2013). Although not itself a receptor tyrosine kinase, it is clear that FGFR1 can play an important role in FGF/FGFR signalling.

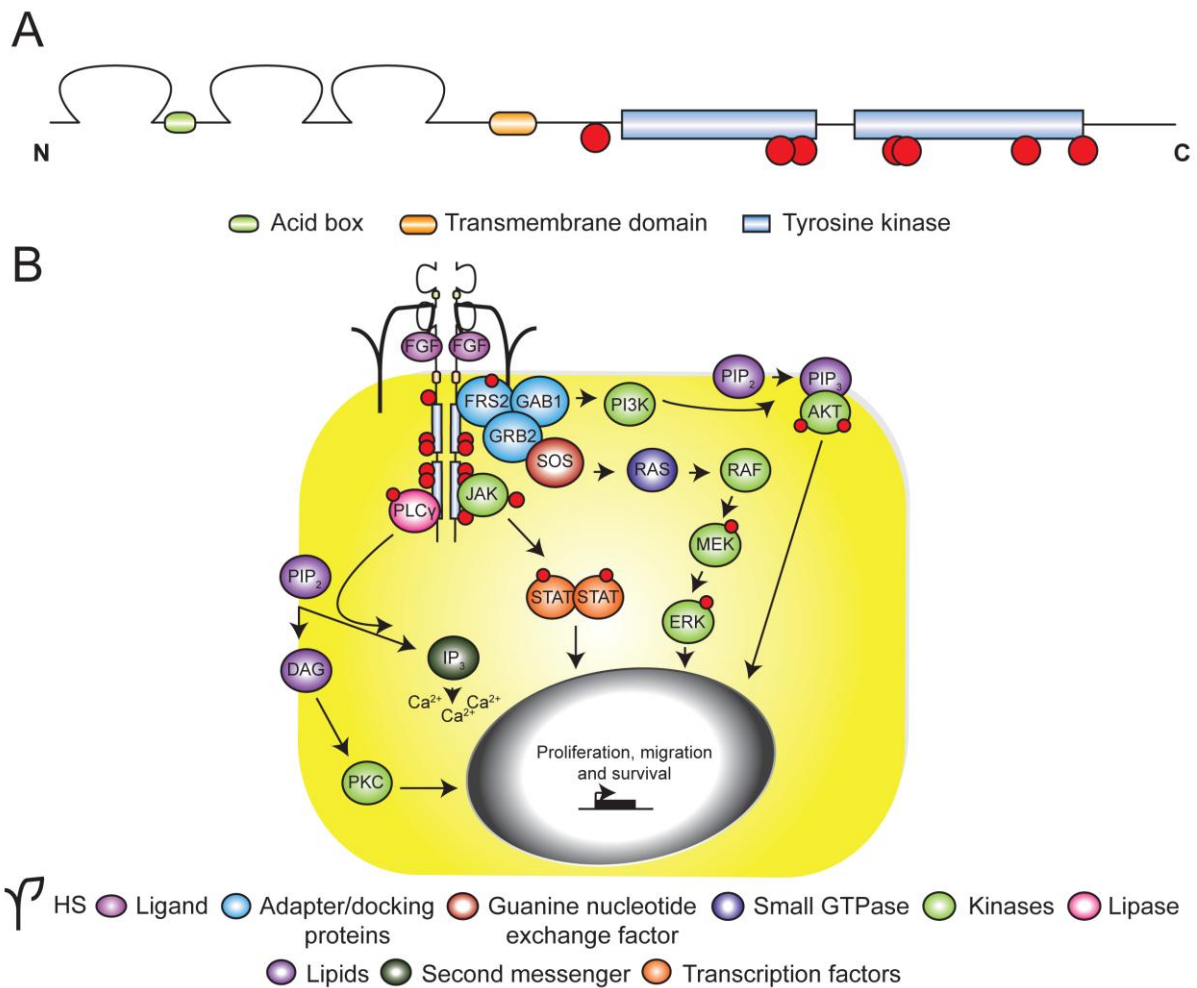


Figure 1.3. FGFR signalling.

(A) Schematic representation of FGFR2 depicting the three extracellular Ig loops, the third of which is responsible for ligand binding. Alternative splicing of this loop leads to varying affinity for different FGF ligands (Ornitz et al., 1996). The acid box (green) between the first and second Ig loops is involved in HS binding (Kalinina et al., 2012). The transmembrane domain is shown in orange. The intracellular portion of the receptor consists of a split kinase domain (blue). Upon ligand binding, dimerisation and subsequent transphosphorylation of the receptor occurs on seven tyrosine residues (red spheres) (Furdui et al., 2006, Mohammadi et al., 1996). (B) Receptor transphosphorylation induces four key downstream pathways: ERK, PI3K/AKT, PLCγ and JAK/STAT. These pathways comprise a series of phosphorylation events, culminating in regulation of target genes, which dictate cellular processes, for example proliferation and migration (Carter et al., 2014). Figure adapted from Carter et al., 2014.

1.2.2 FGFR activation

Heparin, used *in vitro* as the model HS, is a member of the HS family of proteoglycans (HSPGs) and has been used to establish the necessity of HS binding in FGFR activation (Lindahl and Hook, 1978). This acidic molecule resembles the highly sulfated saccharide chains of HS (Gambarini et al., 1993). The heparin-binding residues found in the IgII loop and acid box of FGFRs are highly conserved, while heparin-binding residues of FGFs are diverse (Kalinina et al., 2012, Schlessinger et al., 2000). Because of this, different FGFs require various HS sulfation patterns and/or length of chains for their optimum activity. Variability of HS sulfation patterns and length across cell types has an effect on FGF-FGFR interactions and may be a mediator of the biological activity of FGFRs (Gambarini et al., 1993, Guimond and Turnbull, 1999, Ornitz et al., 1992, Ornitz et al., 1995).

The widely accepted model of FGFR activation is of FGF:FGFR:HS complex formation in a 2:2:2 ratio (Schlessinger et al., 2000) (Figure 1.4). Two independent FGF:FGFR:HS ternary complexes are formed in a 1:1:1 ratio, via HS binding to both receptor and ligand. These two complexes bind via receptor interactions, as well as interactions between the ligand in one complex and the receptor in another, thus forming a stable, symmetrical dimer. Direct ligand-ligand interactions are not observed.

However, it has recently been shown that FGFR2 can exist in a dimerised state prior to ligand binding, primed to activate downstream signalling upon receiving its extracellular ligand (Lin et al., 2012, Ahmed et al., 2013). Growth factor receptor-bound protein 2 (Grb2), an adapter protein consisting of a Src homology-2 (SH2) and two Src homology-3 (SH3) domains, is well known to facilitate activation of extracellular signal regulated kinase (ERK – also known as mitogen activated protein kinase, MAPK) and PI3K signalling, downstream of receptor-ligand binding (Gotoh, 2008, Eswarakumar et al., 2005). This protein was found to have a novel function in stabilisation of an inactive FGFR2 dimer (Lin et al., 2012). Dimeric Grb2 binds, via an SH3 domain, to the C-terminal tail of unstimulated FGFR2 molecules to form a

tetrameric 2:2 complex, in which Grb2 functions to prevent the recruitment of downstream signalling proteins. Ligand binding results in Grb2 phosphorylation and its subsequent dissociation from the FGFR2 cytoplasmic tail, enabling the activation of canonical signalling (Lin et al., 2012). While the 2:2:2 FGF:FGFR:HS model is acknowledged as the canonical method of FGFR activation, this work provides evidence of alternative mechanisms of FGFR2 stabilisation, and control of activation, in basal cellular conditions.

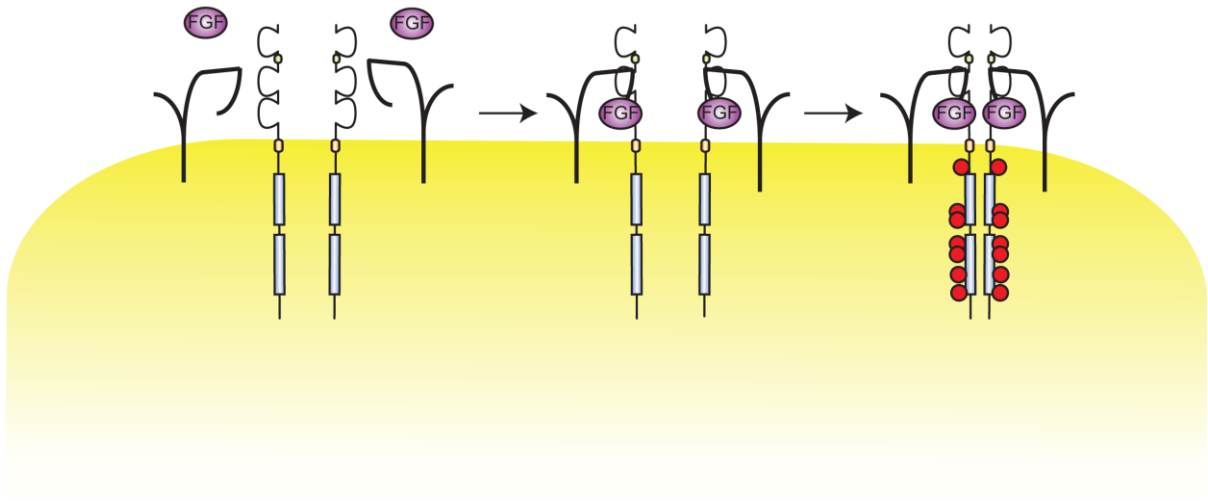


Figure 1.4. Canonical FGFR activation.

The classical model of FGFR activation proposes a symmetrical dimer utilising two HS chains, which bind both ligands and receptor monomers, bringing them into close proximity and facilitating receptor dimerization (Schlessinger et al., 2000). The binding of the HS chains to both ligands and receptors forms a complete, active molecule capable of autophosphorylation and subsequent phosphorylation of downstream signalling molecules.

1.2.3 FGFR signalling pathways

Upon FGFR dimerisation and reciprocal phosphorylation of the tyrosine kinase domains, the phosphorylated receptors act as docking sites for intracellular proteins, leading to activation of signalling cascades (Furdui et al., 2006, Mohammadi et al., 1992, Mohammadi et al., 1996) (Figure 1.3 B). This autophosphorylation occurs in a specific order; 'first-phase' phosphorylation increases the catalytic activity of the kinase after ligand binding, while 'second-phase' phosphorylation creates phosphotyrosine-binding sites for docking molecules containing SH2 and phosphotyrosine-binding (PTB) domains (Furdui et al., 2006). From this, four signalling pathways can be activated: PI3K, ERK, phospholipase C γ (PLC γ) and janus kinase/signal transducer and activator of transcription (JAK/STAT) (Furdui et al., 2006). The key difference between FGFRs in signalling is the strength of their tyrosine kinase activity; their target proteins are the same (Raffioni et al., 1999). However, as will be discussed later, recent work on FGFR2 has highlighted how differential ligand binding can result in activation of specific downstream pathways and subsequently lead to initiation of distinct cellular processes (Francavilla et al., 2013).

Lipid-anchored fibroblast growth factor receptor substrate 2 (FRS2) plays an integral role in the PI3K and ERK pathways, while PLC γ and JAK/STAT pathways are mediated through mechanisms independent of this adapter protein. FRS2 binds to the receptor via its PTB domain and undergoes phosphorylation (Dhalluin et al., 2000, Kouhara et al., 1997, Ong et al., 2000). Grb2 is then recruited to FRS2, from which the PI3K and ERK pathways can be activated.

PI3K

Phosphoinositide lipids are a key component of the plasma membrane (Balla, 2013); their phosphorylation status is important in cellular signalling and is therefore tightly regulated by kinases and phosphatases. PI3K is one such important regulator of lipid phosphorylation status, particularly in response to FGFR activation.

PI3K can be divided into three families, class I, II and III, based on their structure and substrate specificities. The best understood of these is class I, known to be activated downstream of receptor phosphorylation (Vanhaesebroeck et al., 2010).

Class I

The class I PI3Ks can be further subdivided into class IA and IB. Class IA PI3Ks exist as a heterodimer formed of a regulatory subunit coupled to a catalytic subunit. The three potential catalytic subunits, p110 α (*PI3KCA*), p110 β (*PIK3CB*) and p110 δ (*PIK3CD*) can be associated with any of the following five regulatory subunit isoforms: p85 α and its splice variants p55 α and p50 α (*PIK3R1*), p85 β (*PIK3R2*) and p55 γ (*PIK3R3*). The class IB PI3Ks are unique in that the p110 γ (*PIK3CG*) subunit can bind one of two regulatory subunits, p101 and p87 (Thorpe et al., 2014). Thus, four distinct PI3K class I isoforms exist: PI3K α , PI3K β , PI3K δ and PI3K γ . Upon FGFR activation, the PI3K α , β or δ isoforms are activated, as is common in response to receptor tyrosine kinase signalling (Ong et al., 2001).

Upon receptor activation, Grb2/FRS2 binds to GAB1 via the SH3 domain of Grb2 (Gotoh, 2008), whereupon GAB1 is phosphorylated by FGFR2. This FRS2/Grb2/GAB1 complex recruits PI3K to the receptor via its regulatory subunit, causing a conformational change in the catalytic subunit, rendering it catalytically active. PI3K is then able to convert its lipid substrate, phosphatidylinositol (4, 5) bisphosphate (PIP₂), to phosphatidylinositol (3, 4, 5) trisphosphate (PIP₃).

PIP₃ generation leads to recruitment of downstream signalling molecules containing a PH domain, for example the serine-threonine kinases protein kinase B (AKT) and phosphoinositide-dependent kinase 1 (PDK1). Once engaged at the membrane, AKT is phosphorylated, and therefore activated, by PDK1 on the threonine 308 (thr308) residue (Alessi et al., 1997, Franke et al., 1995). This in turn affects a number of signalling proteins, including tuberous sclerosis complex (TSC), whereupon

mammalian target of rapamycin (mTOR) is activated (Inoki et al., 2002, Potter et al., 2002).

mTOR, a protein complex that functions as a serine/threonine kinase, exists in two forms; mTOR complex 1 (mTORC1) and mTORC2. AKT can be further phosphorylated at the serine 473 (ser473) residue by mTORC2, resulting in its complete activation (Facchinetti et al., 2008, Sarbassov et al., 2005). Indeed, this full activation exhibits a fivefold increase in activity over the thr308 phosphorylated protein alone (Sarbassov et al., 2005). AKT is then able to promote cell survival through regulation of its anti-apoptotic targets, such as B-cell lymphoma 2 (BCL2). Cell survival is further promoted by mTORC1 via activation of ribosomal S6 kinase (S6K). This protein releases eukaryotic translation initiation factor 4E binding protein 1 (EIF4EBP1) transcriptional repression and allows for translation of prosurvival factors (Wang et al., 2006).

The differential role of PI3K signalling outcomes following FGFR2 activation, in response to distinct ligands, has recently been elucidated (Francavilla et al., 2013). Interaction between PI3K and phosphorylated residue tyrosine 734 (tyr734) of FGFR2IIIb following FGF10 stimulation results in increased cell migration. Here, the PI3K p85 subunit binds phospho-tyr734 and recruits the adaptor protein SH3 binding protein 4 (SH3BP4), leading to receptor recycling via endosomes. In contrast, FGF7 stimulation does not result in PI3K/SH3BP4 complex formation, and instead induces a more transient stimulation and rapid degradation, resulting in increased proliferation rather than migration. This study serves as evidence of the complex role of PI3K signalling downstream of FGFR2 and the importance of ligand-receptor interactions in dictating cell fate.

Class II and III

The functional importance of class II and III PI3K subfamilies remains unclear. Two of the three class II isoforms, PI3KC2 α and β , are widely distributed throughout

mammalian tissue; less is known about the third γ isoform. Interestingly, this subfamily harbors a catalytic subunit only. The solitary class III PI3K, vacuolar protein sorting 34 (Vps34), also known as *PIK3C3* in mammals, forms complexes with a variety of proteins. Vps34, with intrinsic catalytic activity, binds vacuolar protein sorting 15 (Vps15) to form an intracellular membrane bound heterodimer. Its function then depends on the multi-protein complex formed, where interaction with specific proteins leads to a defined cellular outcome, including autophagy or endosomal trafficking (Vanhaesebroeck et al., 2010).

ERK

In mammals, 14 MAPKs have been described and can be subdivided into conventional and unconventional MAPKs (Cargnello and Roux, 2011). Typical MAPKs, for example ERK1/2 and p38, are activated via a three-tiered kinase cascade culminating in the phosphorylation of the MAPK protein on a threonine and tyrosine residue. Whilst unconventional MAPKs are activated via other means, all activated MAPKs are proline-directed kinases (Coulombe and Meloche, 2007).

The most extensively studied group of MAPKs are ERK1/2, which are principally activated by receptor tyrosine kinases (Cargnello and Roux, 2011) and promote cell proliferation and survival (Eswarakumar et al., 2005). ERK1/2 share 83% amino acid homology and are expressed in a wide range of tissues (Bogoyevitch et al., 1994, English and Sweatt, 1997). FRS2 is constitutively bound to the juxtamembrane region of the FGFR and, upon receptor activation, Grb2 is recruited to the FGFR/FRS2 complex (Dhalluin et al., 2000, Kouhara et al., 1997, Ong et al., 2000). Son of sevenless (SOS) is subsequently recruited from the cytosol to the plasma membrane via interaction with Grb2 (Olivier et al., 1993), whereupon rat sarcoma (RAS), a membrane-tethered GTPase, is activated by SOS catalysed dissociation of GDP from RAS, which allows GTP binding in its place, rendering RAS active. GTP-bound RAS is then able to directly interact with its target proteins, including the MAPK kinase kinase rapidly accelerated fibrosarcoma (RAF). RAF is recruited to the plasma membrane via RAS-GTP, whereupon RAF is phosphorylated and thereby

activated. Activated RAF subsequently phosphorylates and activates MAPK or ERK kinase (MEK), a dual-specificity kinase. MEK then phosphorylates and activates ERK1/2, the final kinase in the core three-tiered cascade. This phosphorylation occurs within a conserved threonine-glutamic acid-tyrosine (TEY) motif located in the activation loop of ERK1/2 (Marshall, 1995). Phosphorylated ERK is then able to activate transcription factors in the nucleus, for example cellular homologue of v-MYC (c-MYC), and regulate G1-to-S phase cell cycle progression (Chen et al., 1992, Lenormand et al., 1993).

PLC γ

Autophosphorylation of the tyrosine 769 (tyr769) residue in FGFR2 creates a specific binding site for the SH2 domain of PLC γ , leading to its tyrosine phosphorylation and subsequent catalytic activation (Mohammadi et al., 1991). PLC γ is recruited to the membrane by PIP $_3$ and PIP $_2$, where catalytically active PLC γ is able to hydrolyse PIP $_2$ into inositol 1, 4, 5 trisphosphate (IP $_3$) and diacylglycerol (DAG) (Carpenter and Ji, 1999, Klint and Claesson-Welsh, 1999). IP $_3$ can then release calcium stored in the endoplasmic reticulum (ER), which, along with DAG, activate protein kinase C (PKC) (Rameh et al., 1998). PKC is then able to relieve inhibition of RAF and activate the ERK pathway (Corbit et al., 2003).

As discussed in section 1.2.2, FGFR2 can exist in a dimerised form, primed for receptor activation, in the absence of ligand (Lin et al., 2012). In this scenario, Grb2 binding to the C-terminus of FGFR2 allows low level phosphorylation of the receptor but inhibits downstream signalling until ligand is bound and full tyrosine kinase phosphorylation of the intracellular portion of the receptor occurs (Lin et al., 2012). However, recent investigations have indicated a novel signalling mechanism downstream of this pre-dimerised FGFR2 complex, in the absence of ligand binding (Timsah et al., 2014). Although recruitment of PLC γ to the membrane is usually associated with ligand-dependent receptor activation, Timsah et al., have shown that PLC γ 1 can also bind to the C terminus of FGFR2 in an SH3-dependent manner, to initiate signalling in the absence of FGF ligand. This occurs when the cellular

concentrations of PLC γ 1 exceeds that of Grb2, thus potentially explaining why tumour cells expressing low levels of Grb2 often exhibit enhanced PLC γ 1 activity and metastatic behaviour (Fearon and Grose, 2014). While ligand-receptor binding is acknowledged as the canonical signalling mechanism, this work illustrates the presence of alternative mechanisms of FGFR signalling in basal cellular conditions.

JAK/STAT

The STAT family of cytoplasmic transcription factors can be activated by non-receptor tyrosine kinases, JAKs, leading to cell proliferation and differentiation (Ebong et al., 2004). Upon FGFR dimerisation and autophosphorylation, JAKs are phosphorylated by the receptor, forming a FGFR/JAK complex. This acts as a docking site for STATs, which are in turn tyrosine phosphorylated in their SH2 domain (Darnell, 1997). STAT dimers form and translocate to the nucleus, where they bind to gamma-activated site (GAS) enhancers to activate or repress gene transcription (Darnell, 1997).

1.2.4 Regulation of FGFR signalling

Regulation of FGF signalling is critical to ensure a balanced response to receptor stimulation. This occurs largely through negative feedback mechanisms (Figure 1.5), including receptor internalisation, where recruitment of the casitas B-lineage lymphoma (CBL) protein to FRS2 leads to ubiquitination of both FGFR and FRS2 and therefore attenuation of FGFR-mediated signalling (Wang et al., 2002), and induction of negative regulators, for example sprouty (SPRY) (Hacohen et al., 1998). SPRYs are thought to act through two possible mechanisms. Firstly, via interaction with Grb2, interrupting the FRS2/Grb2 complex and therefore decreasing signal transduction (Thisse and Thisse, 2005). Secondly, SPRY-RAF interactions can occur, preventing RAF phosphorylation and therefore inhibiting ERK signalling (Sasaki et al., 2003).

ERK signalling can also be inhibited by sprouty-related enabled/vasodilator-stimulated phosphoprotein homology 1 domain-containing proteins (SPRED1 and 2) (Wakioka et al., 2001). SPRED proteins prevent RAF activation of MEK by forming a complex between RAS and RAF. Co-localisation of SPRED2 with the protein neighbor of BRCA1 (NBR1) results in sequestration of FGFR and its lysosomal degradation (Mardakheh et al., 2009).

Similar expression to FGF (SEF) proteins also negatively regulate FGF signalling via a number of mechanisms. These include targeted inhibition at, or downstream of, MEK (Yang et al., 2003) and inhibition of RAS activation, which also inhibits the PI3K pathway (Kovalenko et al., 2003). Direct interaction between SEF and the FGFR leads to inhibition of FGFR and FRS2 phosphorylation (Kovalenko et al., 2003, Tsang et al., 2002, Xiong et al., 2003), while SEF can also act as a spatial regulator of phospho-ERK migration to the nucleus and therefore attenuate ERK signalling (Torii et al., 2004).

Another mechanism of negative regulation is via direct phosphorylation of ERK pathway proteins, for example, the RAS guanine nucleotide exchange factor SOS and RAF. Phosphorylation of SOS by ERK disrupts interactions between SOS and Grb2, in turn decreasing recruitment of SOS to the membrane and resulting in diminished RAS activation (Buday et al., 1995). ERK can also phosphorylate RAF, reducing RAF kinase activity and therefore decreasing MEK and ERK phosphorylation (Ueki et al., 1994). ERK can also negatively regulate the PI3K pathway via direct phosphorylation of GAB1, subsequently decreasing PI3K recruitment to GAB1 and in turn reducing AKT pathway activation (Gual et al., 2001). The PI3K pathway is also commonly modulated by PTEN, a phosphatase that converts PIP_3 back to PIP_2 (Makker et al., 2014).

There is emerging evidence of the importance of the pleckstrin homology like domain A (PHLDA) family of proteins in negative regulation of the PI3K pathway (Kawase et al., 2009, Ohki et al., 2014). This family, of which there are three known members,

contain a PH domain, via which they may be able to bind to phosphoinositide lipids. While PHLDA2 seems to be important in embryonic development, PHLDA1 and 3 are expressed in adult tissue (Frank et al., 1999).

PHLDA3 is the most well characterised of the family, with clear evidence of its role as a negative regulator of AKT (Kawase et al., 2009). PHLDA3 competes with AKT for PIP₃ binding and therefore induces apoptosis by inhibiting AKT phosphorylation; in this way, PHLDA3 acts as a tumour suppressor (Kawase et al., 2009, Ohki et al., 2014).

PHLDA1 is also known to interact with PIP₃ and attenuate AKT signalling (Murata et al., 2014). Though the potential role of PHLDA1 in anti-apoptotic signalling has been described, the mechanism of this action remains unclear (Toyoshima et al., 2004, Neef et al., 2002, Hossain et al., 2003, Murata et al., 2014).

PHLDA3 has also been shown to be a direct target of p53 (Kawase et al., 2009). Indeed, a p53-mediated negative feedback loop between AKT and PHLDA3 has been illustrated (Liao and Hung, 2010). Here, AKT is recruited to the membrane as a result of PI3K activation, as previously described. Following phosphorylation of one of its downstream targets, the ubiquitin ligase mouse double minute 2 homologue (MDM2), p53 is ubiquitinated and subsequently degraded. This in turn leads to decreased expression of PHLDA3 and PTEN and allows for unopposed AKT signalling. However, under cell stress, p53 expression is increased, leading to upregulation of PHLDA3 and subsequent initiation of apoptotic signalling (Liao and Hung, 2010).

Alternative internal control mechanisms of FGF signalling exist, including autoinhibition of the receptor (Plotnikov et al., 1999, Schlessinger et al., 2000, Stauber et al., 2000). The FGFRs exist in 'closed' and 'open' conformation equilibrium (Kalinina et al., 2012). The Igl loop and the Igl/IgII linker region containing the acid box, a glutamate, aspartate and serine-rich sequence (Johnson

and Williams, 1993), are responsible for formation of the 'closed', autoinhibited state. Spectroscopic investigations have shown the acid box engages in electrostatic interactions with the HS-binding site of the IgII loop, inhibiting receptor-HS interactions and, therefore, receptor activation. This then encourages intramolecular interactions between IgI and the ligand-binding sites of the IgII and IgIII loops, further aiding the acquisition of a closed conformation (Olsen et al., 2004). Alternative splicing of exons encoding the IgI and/or acid box region leads to enhanced affinity of the receptor for its ligand and HS, increasing downstream signalling (Olsen et al., 2004). Loss of this region has been implicated in cancer (Kobrin et al., 1993, Mansson et al., 1989). This mechanism of autoinhibition supports FGF binding specificity of receptors, as only specific ligands with high affinity for the receptors will overcome this inhibition and bind to the receptor.

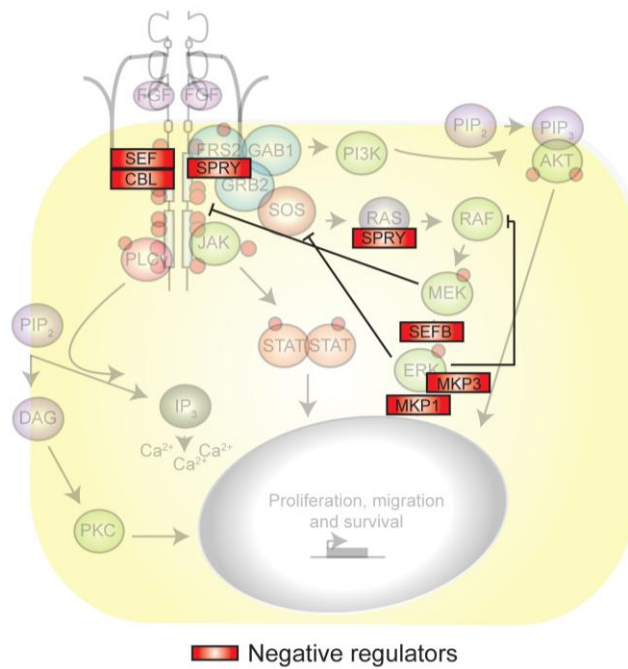


Figure 1.5. Negative regulation of FGFR signalling.

A number of mechanisms exist to negatively regulate FGFR signalling. These include recruitment of additional proteins (red boxes) (Hacohen et al., 1998, Wakioka et al., 2001, Wang et al., 2002, Yang et al., 2003) as well as downstream elements of, for example, the ERK pathway acting upstream to modulate activity (black lines) (Buday et al., 1995, Gual et al., 2001, Ueki et al., 1994). Figure adapted from Carter et al., 2014.

1.2.5 FGFR2 and disease

Developmental disorders

The importance of the FGF signalling axis in development is well documented, with integral functions in, for example, organ morphogenesis and limb function (Pownall and Isaacs, 2010). As such, germline mutations in FGFRs are known drivers in a range of developmental disorders.

Point mutations in FGFR2 can manifest in skeletal malformations and dwarfism (Hatch, 2010). FGFR2 mutations common in the craniosynostosis dysplasias Crouzon, Jackson-Weiss, Pfeiffer and Apert syndromes cluster in the linker region between the IgII and IgIII loops, which alter the ligand binding specificity of the receptor (Eswarakumar et al., 2004, Chen et al., 2003, Ibrahimi et al., 2001, Yu et al., 2000). Mutations in two conserved cysteine residues within IgIII of FGFR2 are also common. In normal receptor signalling, these cysteine residues form intramolecular bonds, preventing receptor dimerisation until ligand binding. In mutant FGFR2, substitution of one of these cysteine residues creates an unpaired cysteine able to form an intermolecular disulphide bridge, leading to receptor dimerisation and activation (Eswarakumar et al., 2005).

Mouse models of the most common of these gain-of-function mutations, S252W (Oldridge et al., 1997, Webster and Donoghue, 1997), show phenotypic traits of Apert syndrome, including impaired bone growth (Wang et al., 2005). Additional studies have suggested this mutation enhances FGFR2IIIb expression, as well as one of its ligands, FGF10, which may be responsible for the premature fusion of the cranial plates characteristic of this disorder (Yokota et al., 2014). It is also postulated that the S252W mutation leads to the modified receptor remaining on the cell surface for an extended period of time, rather than undergoing rapid recycling like its wild type counterpart. Downstream signalling pathways are affected, leading to increased ERK phosphorylation and therefore increased cell proliferation and migration capabilities, as well as premature differentiation (Ahmed et al., 2008).

Cancer

In 2000, Hanahan and Weinberg first proposed six hallmarks of cancer: sustainment of proliferative signalling, evasion of growth suppressors, activation of invasion and metastasis, establishment of replicative immortality, induction of angiogenesis and evasion of cell death (Hanahan and Weinberg, 2000). This notion has recently been revised and two additional hallmarks added; deregulation of energetics, i.e. the reprogramming of metabolic processes to enhance cellular proliferation, and evasion of immune destruction (Hanahan and Weinberg, 2011). The tumour microenvironment is also known to be of particular importance in maintaining tumour growth and progression (Gligorijevic et al., 2014, Langley and Fidler, 2011, Onuigbo, 1975, Suh et al., 2014, Witz and Levy-Nissenbaum, 2006). For example, pancreatic cancer is known to have a dense stromal cell component, which communicates with tumour cells and subsequently aids tumour growth (Froeling et al., 2009). Another characteristic of cancer progression elucidated over recent years is that of infiltration of tumours by the immune system, causing an inflammatory response (Hanahan and Weinberg, 2011). Rather than eradicating tumour growth, it appears such inflammation is capable of promoting tumour progression by supplying growth factors and enzymes that facilitate angiogenesis and metastasis (DeNardo et al., 2010, Grivennikov et al., 2010, Qian and Pollard, 2010).

Whilst it is generally accepted that the evolution of normal cells to a malignant state involves acquisition of these hallmarks in a multistep process, genomic instability is also known to be an important feature in enabling neoplastic progression (Hanahan and Weinberg, 2011). Such instability can confer a selective advantage in a subpopulation of cells in a polyclonal environment, eventually leading to dominance in the population. Indeed, such selective advantage can lead to clonal expansions over the evolution of the tumour, resulting in a malignant phenotype (Vogelstein et al., 2013).

An important facet of this idea of clonal expansion of cells within a tumour is that of driver and passenger mutations (McFarland et al., 2014). Tumour progression is now

known to be driven by a relatively small selection of mutations and chromosomal abnormalities (Lawrence et al., 2014, Zack et al., 2013). Acquisition of a mutation in an oncogene or tumour suppressor can provide a cell with a distinct advantage over others in the population, allowing for outgrowth and, potentially, dominance in the tumour (Hanahan and Weinberg, 2011). Due to the rapid rate of cell division in tumours, additional mutations also arise that do not confer a selective advantage to the tumour but are inherited alongside advantageous mutations, and are thus known as passenger mutations (Lawrence et al., 2014).

Whilst tumours often contain multiple subpopulations of clonal expansions, resulting from a small number of driver mutations, tumour cells can become dependent on a particular driver mutation (McFarland et al., 2014). One hypothesis for such addiction is genetic streamlining, whereby cancer cells dismiss signalling pathways that do not provide a fitness advantage. This can provide a therapeutic window, where inhibition of this dominant signalling pathway can lead to tumour eradication (Torti and Trusolino, 2011).

Given the ability of the FGF signalling pathway to facilitate cell survival and proliferation, amongst other cellular responses, it is not surprising this pathway is hijacked in cancer cells. According to the catalogue of somatic mutations in cancer (COSMIC), *FGFR2* aberrations have been identified in 23 tissue types (COSMIC, 2014) (Figure 1.6). The majority of these mutations are activating, resulting in increased proliferation, migration and angiogenesis and are generally indicative of a more malignant phenotype (Turner and Grose, 2010). This deregulation in *FGFR2* signalling is known to occur via a range of mechanisms (Figure 1.7):

Receptor amplification

Amplification of *FGFR2* correlates with poor survival in a range of different cancers (Figure 1.6). However, patients who present with *FGFR2* amplified tumours respond favourably to FGFR targeted therapies, compared to those harbouring non-amplified

tumours (Andre et al., 2013, Cheng and Alper, 2014, Soria et al., 2014). Interestingly, recent work investigating the use of the EGFR-targeted monoclonal antibody cetuximab found that while patients responded initially, they quickly acquired resistance to the treatment (Zhang et al., 2014). Through use of xenograft models, this was shown to be the result of concomitant *FGFR2* amplification. Drug therapy directed against FGFR2 led to re-sensitisation to cetuximab, highlighting the complex role of receptor tyrosine kinases in cell signalling. FGFR1, 3 and 4 amplifications are also found in a range of cancers, including lung and breast, and show enhanced sensitivity to FGFR-directed therapies (Carter et al., 2014).

Isoform switching/autocrine stimulation

Epithelial cells commonly express FGFR2IIIb, while mesenchymal cells express the IIIc isoform. However, a change in isoform expression is frequently seen in cancer and is indicative of a more malignant phenotype (Ishiwata et al., 2012, Kawase et al., 2010, Peng et al., 2014, Turner and Grose, 2010) . In breast cancer, epithelial cell lines expressing the FGFR2IIIc isoform displayed a more invasive phenotype (Shirakihara et al., 2011), while pancreatic cells over-expressing FGFR2IIIc in *in vivo* models display enhanced tumour growth (Ishiwata et al., 2012).

Induction of autocrine signalling is common in cancer and such a method of enhanced signalling via FGFR2 has been noted in epithelial ovarian cancer (Steele et al., 2001). Here, over-expression of FGFR2IIIb, as well as its cognate ligand, FGF7, was observed in cancer cells of epithelial origin. As such, it was suggested that induction of this autocrine signalling axis may play a role in development of ovarian carcinoma.

Fusion proteins

A number of novel FGFR2 fusion proteins have recently been described (Wu et al., 2013). One such fusion protein, FGFR2-bicaudal C homolog 1 (BICC1) found in cholangiocarcinoma, was shown to consist of full length FGFR2 fused to BICC1, an

RNA binding protein known to regulate gene expression. Such fusion proteins are proposed to lead to enhanced receptor activity by mediating oligomerisation (Wu et al., 2013). Importantly, inclusion of the kinase domain makes such fusion proteins potential therapeutic targets (Arai et al., 2014).

One fusion protein of particular interest was identified in prostate cancer (Wu et al., 2013). This protein, solute carrier family 45, member 3 (SLC45A3)-FGFR2, consists of the entire *FGFR2* gene fused to, and under the control of, an androgen-regulated promoter, *SLC45A3*, resulting in over-expression of FGFR2. One would postulate that patients harbouring this fusion should respond to both anti-androgens and FGFR inhibition.

Another fusion protein of interest involving an FGFR family member is FGFR3-transforming acidic coiled coil 3 (TACC3), described in bladder and lung carcinomas (Wang et al., 2014b, Williams et al., 2013). FGFR3-TACC3 promotes constitutive kinase activity, enhancing cellular proliferation (Singh et al., 2012, Williams et al., 2013).

Activating mutations

A number of cancers have been found to contain somatic mutations identical to germ line mutations in FGFRs associated with developmental disorders. FGFR2 mutations commonly seen in Apert and Pfeiffer Syndromes are frequently identified in endometrial cancer (Pollock et al., 2007), for example S252W and N550K, both of which result in receptor activation (Greulich and Pollock, 2011a). Other FGFR2 mutations in endometrial cancer include S373C and Y376C, which result in gain of a cysteine residue, allowing formation of intermolecular disulphide bonds, leading to constitutive receptor dimerisation and therefore downstream signalling (Wilkie, 2005).

Other FGFR2 mutations of note include those in breast cancer, which have been shown to enhance kinase activity (Reintjes et al., 2013). The functionality of these mutations in tumour development, and their potential to be targeted therapeutically, has been demonstrated in mouse models (Tchaicha et al., 2014).

Receptor mutation is particularly important in non-muscle invasive bladder cancer, where approximately 70% of tumours harbour FGFR3 mutations, which correlate with enhanced PI3K signalling (Juanpere et al., 2012, Liu et al., 2014). *In vivo* studies have shown the functional role of FGFR3 mutations in bladder cancer, whereby FGFR3-mutant mice exhibit enhanced urothelial cell proliferation and hypertrophy (Foth et al., 2014).

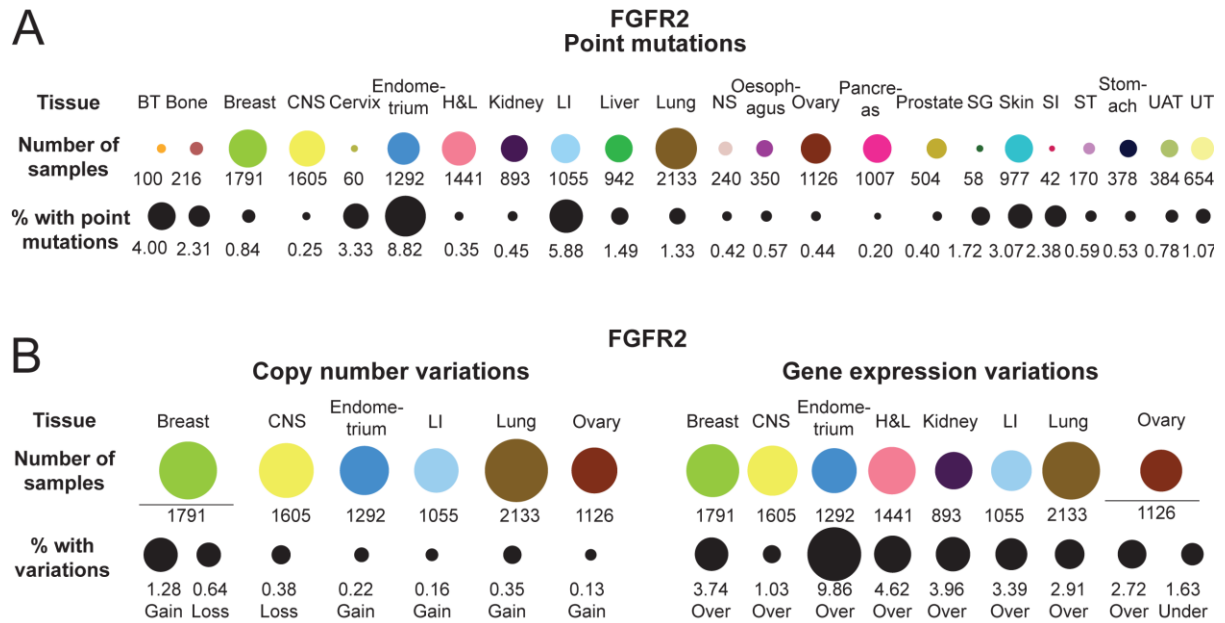


Figure 1.6. Frequency of *FGFR2* point mutations, copy number and gene expression variations in cancer.

FGFR2 mutations are found in a range of tumour types and their proportions differ depending on the tissue of origin. Here, we show all tissue types and number of tumours screened (A and B, top panels), as well as the proportion of these tumours harbouring an *FGFR2* point mutation (A, bottom panel) and copy number or gene expression variations (B, bottom panels), as listed in COSMIC. All dots in the plot are in proportion within the same panel. BT, biliary tract; CNS, central nervous system; H&L, haematopoietic and lymphoid; LI, large intestine; NS, not specified; SG, salivary gland; SI, small intestine; ST, soft tissue; UAT, upper aerodigestive tract; UT, urinary tract. Gain and loss indicate increased and decreased copy number respectively; over and under indicate increased and decreased gene expression respectively. Data correct as of September 2014. Figure adapted from Carter et al., 2014.

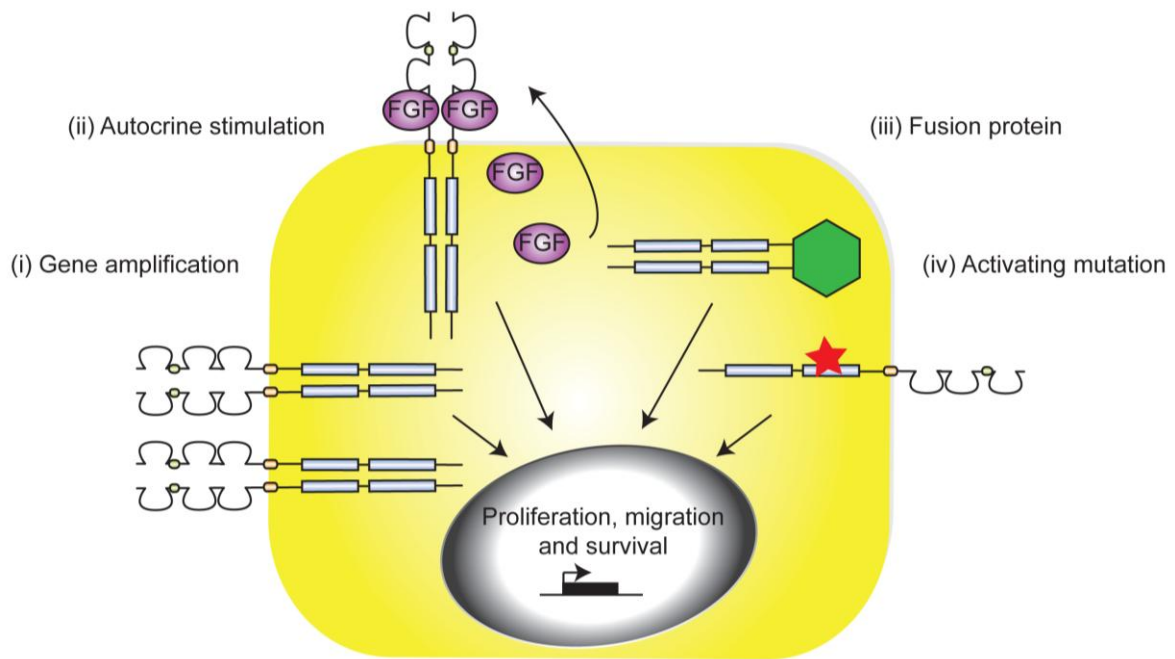


Figure 1.7. Mechanisms of aberrant FGFR signalling in disease.

Increased signalling downstream of FGFRs, in both developmental disorders and cancer, occurs via four main mechanisms: (i) gene amplification, where overexpression of the receptor leads to augmented intracellular signalling (Turner and Grose, 2010); (ii) autocrine stimulation by release of ligands with high affinity for the receptor expressed on the cell (Ishiwata et al., 2012, Kawase et al., 2010, Peng et al., 2014, Shirakihara et al., 2011, Steele et al., 2001); (iii) fusion proteins, whereby the kinase domain is fused to, for example, BICC1 (Wu et al., 2013); (iv) activating mutations, for example in the kinase domain, which lead to constitutive activation of the receptor (Greulich and Pollock, 2011b, Pollock et al., 2007, Wilkie, 2005). Figure adapted from Carter et al., 2014.

1.3 Targeted drug therapy

Historically, tumour burden has been relieved by surgical and radiotherapeutic measures. Whilst classic systemic treatment of malignant lesions using chemotherapy is still a common treatment option, continuing research into the molecular mechanisms underpinning cancer has led to the advent of a range of drugs targeting a variety of pathways, for example small molecule inhibitors towards receptor tyrosine kinases (Hojjat-Farsangi, 2014). An emerging therapeutic option is that of immunotherapy, which aims to utilise and augment the ability of the immune system to eradicate cancer cells (Perica et al., 2015). One key aspect of this emerging treatment strategy relies on tumour-associated T-cells. As T-cell responses are specific and can potentially distinguish between healthy and cancerous tissue, their utility in cancer treatment is particularly promising (Perica et al., 2015).

One immunotherapy option is the use of cancer vaccines, whereby delivery of tumour-associated antigens expands and activates the tumour-specific T-cell population (Finn, 2014). However, the current treatment choice that seems to offer a paradigm shift in harnessing the power of the immune system is the use of immune checkpoint antagonists. Immune checkpoints negatively regulate T-cells, therefore decreasing T-cell function (Emens and Middleton, 2015). Using antagonists of these checkpoints, the negative signals that diminish T-cell activity at the tumour site can be abrogated, resulting in increased tumour-associated T-cell activity (Pardoll, 2012). For example, the immune checkpoint molecule cytotoxic T-lymphocyte-associated antigen 4 (CTLA-4) down-regulates T-cell activation (Melero et al., 2007). The monoclonal antibody Ipilimumab blocks CTLA-4, thereby promoting anti-tumour immunity (Fong and Small, 2008, O'Day et al., 2007, Robert and Ghiringhelli, 2009, Weber, 2009). Indeed, Ipilimumab monotherapy in metastatic melanoma has proven successful in phase 2 clinical trials (O'Day et al., 2010, Weber et al., 2009, Wolchok et al., 2010). The ultimate aim of this emerging treatment option is to establish a population of tumour-specific T-cells with the ability to lyse tumour cells and to combine such measures with existing systemic therapies to achieve the greatest clinical benefit to patients (Emens and Middleton, 2015).

The high rate of FGFR mutations in a range of diseases makes this family of proteins an attractive therapeutic target. Numerous studies have shown the benefits of FGFR knockdown and inhibition in cancer cell lines where the result is, for example, a decrease in cell proliferation (Byron et al., 2008, Chioni and Grose, 2012, Coleman et al., 2014). However, translating this into a therapy for patients has proven difficult, due to even specific FGFR inhibitors having off-target effects (Mohammadi et al., 1998). However, given the importance of these receptors in a range of pathologies, numerous drugs have been, and currently are, under development. A number of different approaches to develop therapeutics to target this pathway have been employed (Figure 1.8).

Kinase inhibitors

The most clinically advanced FGFR inhibitors to date are multi-kinase inhibitors, targeting the kinase domain of receptors to prevent downstream signalling (Figure 1.8 (iv)) and include Dovitinib (Trudel et al., 2006) and SU6668 (Fabbro and Manley, 2001). While these compounds are known to be promiscuous, hitting receptor tyrosine kinases outside of the FGFR family, recent analysis has shown that Dovitinib and Lucitanib have better responses in clinical trials in patients with cancers harbouring *FGFR* amplifications than those that do not (Andre et al., 2013, Soria et al., 2014). However, broad-reaching tyrosine kinase inhibitors have shown dismal toxicity profiles, evidenced in Ponatinib's recent temporary withdrawal from the treatment of chronic myeloid leukaemia (CML) due to a high proportion of patients exhibiting arterial and venous thromboses (Report, 2014). As such, work in recent years has focused on development of more potent, FGFR-selective inhibitors.

One inhibitor, PD173074, a pyrazoloamide derivative targeting the intracellular ATP binding pocket of FGFRs, preferentially binds to FGFRs, with weak activity against other receptor tyrosine kinases (Mohammadi et al., 1998). However, due to toxicity issues, this drug can only be used as a laboratory tool in the investigation of the effects of FGFR inhibition (Knights and Cook, 2010). More success has been achieved with an alternative FGFR kinase inhibitor, AZD4547, which is currently in

phase II clinical trials for solid tumours (Clinicaltrials.gov, 2014, Gavine et al., 2012). This ATP-competitive small molecule inhibitor targets FGFR1, 2 and 3 and results in both inhibition of growth and induction of apoptosis, specifically in cancer cell lines with known FGFR mutations or amplifications. While selectivity for FGFRs is high with this compound, at high concentrations this inhibitor too has off-target effects, for example activity against vascular endothelial growth factor receptor 2 (VEGFR2). However, the potency of this off-target inhibition is much lower than that versus FGFRs.

Orthosteric receptor binding

While small molecule kinase inhibitors remain the most clinically advanced method of FGFR-targeted therapeutics, alternative methods, in the form of antibody-based approaches, allow for more direct action against FGFRs by targeting specific receptor isoforms (Figure 1.8 (i)). For example, an anti-FGFR2IIIb antibody, GP369, has demonstrated promising results in animal models where FGFR2-mutant xenograft tumours have shown reduced growth in GP369-treated mice (Bai et al., 2010). Moreover, an FGFR3 antibody, MGFR1877S, is currently in phase I clinical trials for multiple myeloma and solid tumours (Clinicaltrials.gov, 2014).

In an alternative approach, FGF-ligand trap antibodies have been developed, for example FP-1039, to prevent ligand-receptor binding (Harding et al., 2013) (Figure 1.8 (iii)). FP-1039 is currently in phase I clinical trials for solid tumours. However, while this form of inhibition may temper FGF-stimulated activation of FGFRs, such therapeutics provide little benefit against tumours with kinase mutations which lead to constitutive activation of the receptor.

Allosteric receptor binding

Recently, the potential use of allosteric inhibitors has been described (Figure 1.8 (ii)). Interestingly, initial *in vivo* investigations of one such drug, SSR128129E, have

shown no evidence of vascular side effects, suggesting this may be a preferable alternative to use of receptor tyrosine kinase inhibitors (Herbert et al., 2013).

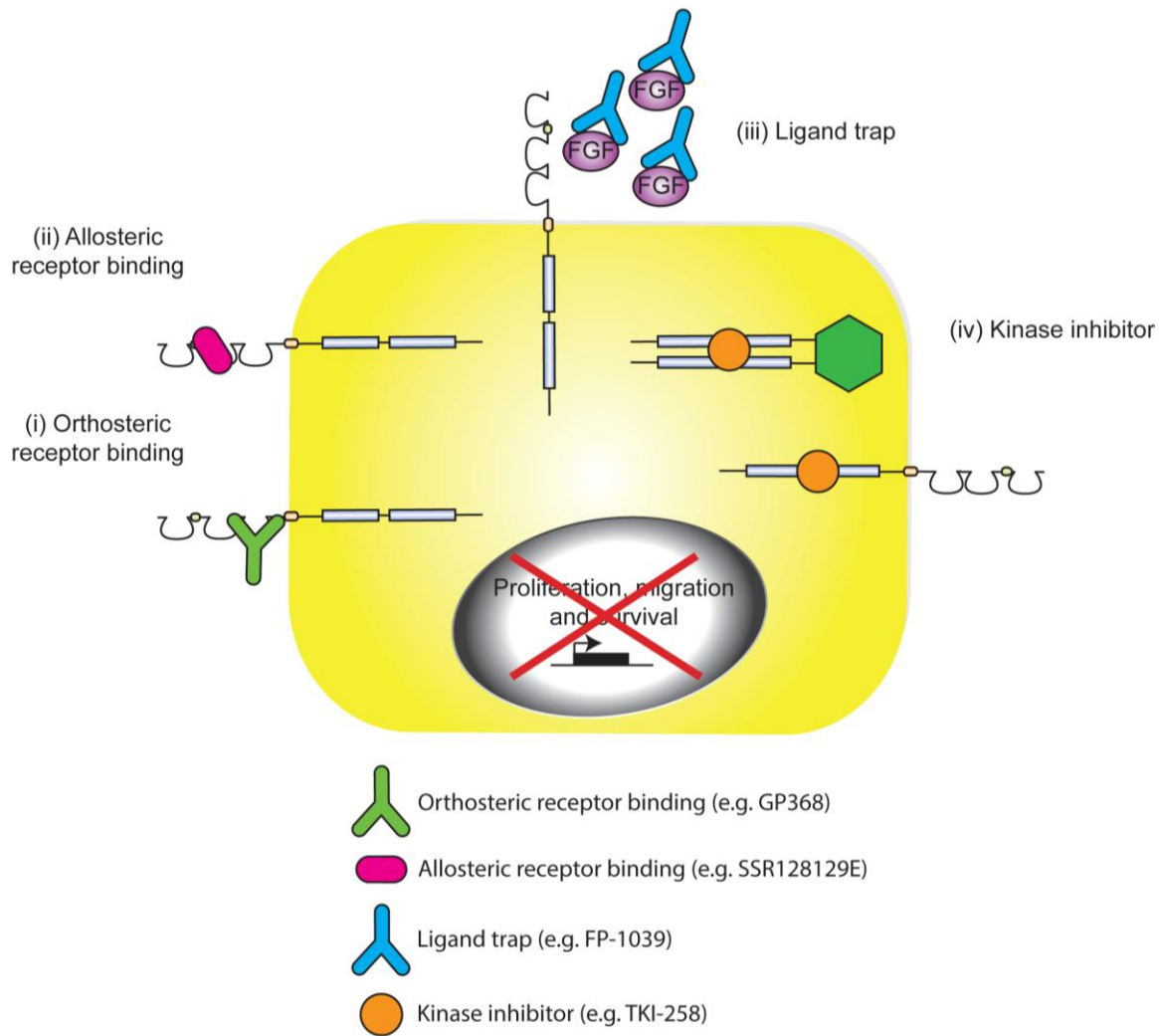


Figure 1.8. Mechanisms of FGFR inhibition.

Given the importance of FGFR signalling in a range of pathologies, numerous drugs have been, and currently are, under development to target this pathway. These therapeutics fall in to one of four categories: (i) orthosteric inhibitors, where inhibitors target the ligand binding domain of the receptor, therefore preventing FGF attachment and induction of downstream signals (Bai et al., 2010, Clinicaltrials.gov, 2014); (ii) allosteric inhibitors, which bind to the extracellular portion of the receptor, preventing it being internalised and transducing a signal, even when ligand is bound (Herbert et al., 2013); (iii) ligand trap, consisting of the ligand binding domain of, for example, FGFR1 bound to the Fc portion of IgG1, resulting in sequestration of ligand and therefore prevention of receptor stimulation (Harding et al., 2013); (iv) small molecule kinase inhibitors, the most common therapeutic option, targeting the ATP-binding pocket of the intracellular kinase domain of the receptor (Fabbro and Manley, 2001, Gavine et al., 2012, Mohammadi et al., 1998, Trudel et al., 2006). Figure adapted from Carter et al., 2014.

1.4 Drug resistance in cancer

Continuing research into the molecular mechanisms underpinning cancer has led to the advent of a range of drugs targeting a variety of pathways. Whilst this has led to the beginnings of personalised medicine, where therapeutics are prescribed on the basis of the molecular aberrations present in the tumour, resistance to these new drugs, as well as to classic chemotherapeutics, continues to be one of the major barriers in successfully treating cancer patients (Holohan et al., 2013). This is of particular importance in endometrial cancer, where patients with advanced disease often relapse due to drug resistance (Chaudhry and Asselin, 2009). To overcome this, a thorough understanding of the mechanisms implemented by cancer cells to circumvent drug treatment is necessary.

One common mechanism of multidrug resistance is up-regulation of efflux proteins, resulting in removal of drugs from cells and therefore preventing them reaching their targets (Ambudkar et al., 1999, Gottesman et al., 2002). Alterations in signalling, leading to activation of pro-survival or inactivation of pro-apoptotic pathways, are also common. For example, deregulation of the PI3K/AKT pathway is seen in a variety of cancer types (Faratian et al., 2009, Goltsov et al., 2011, Goltsov et al., 2012). Indeed, this pathway has been postulated as a potential therapeutic target in chemoresistant endometrial cancer, where administration of doxorubicin in combination with PTEN over-expression in resistant cells led to cell death (Wan et al., 2007).

A particularly striking example of resistance to targeted therapies is that of vemurafenib-treated melanoma (Flaherty et al., 2010, Wagle et al., 2011). Approximately 50% of melanomas carry a mutation in the serine-threonine protein kinase b-raf (BRAF); of these 90% harbour the V600E mutation, leading to constitutive activation of the protein and therefore its downstream ERK signalling pathway (Davies et al., 2002, Flaherty et al., 2010). The prevalence of this mutation makes it an attractive therapeutic target, and led to the development of Vemurafenib, a small molecule inhibitor that preferentially binds to the V600E mutant form of BRAF

(Tsai et al., 2008). Initial clinical trials showed excellent results, with complete or partial regression in approximately 80% of patients (Flaherty et al., 2010). However, resistance to the drug occurred and the duration of response lasted only two to 18 months (Flaherty et al., 2010).

Dissection of this resistance by mutation profiling revealed several mechanisms of importance. Activating mutations in MEK1 were seen in vemurafenib resistant populations (Wagle et al., 2011), as well as increased expression of MAP3K8 (Johannessen et al., 2010). Activation of CRAF has been noted in resistant cells (Montagut et al., 2008), as has up-regulation of platelet derived growth factor receptor β (PDGFR β) (Nazarian et al., 2010). All of these aberrations ultimately lead to activation of the ERK pathway, therefore circumventing BRAF inhibition. Together, these data show the multitude of mechanisms cancer cells can employ to elude death in response to drug treatment.

Modelling of resistance to vemurafenib in mice has indicated that cyclical administration of the drug could delay acquisition of resistance and therefore potentially prolong patient life (Das Thakur et al., 2013). *In vivo* studies have shown that mice implanted with BRAF mutant tumour cells and sequentially treated with the drug for four weeks followed by removal for two weeks did not develop tumours, while control mice continuously dosed did. Tumour heterogeneity can give rise to drug resistance through positive selection of a resistant subpopulation; these data indicate that some drug resistant cells confer a fitness deficit in the tumour environment, in the absence of drug. Understanding the balance between molecular subtypes within tumours and utilising this knowledge, not only in drug choice but also in how drugs are administered, may prove crucial in overcoming drug resistance.

Although current clinical trials of FGFR-targeted therapies have reported favourable results, based on knowledge of other small molecule inhibitors, it is possible that treatment of FGFR-mutant tumours with such drugs will result in resistance in a subpopulation of patients. Recent work in FGFR2-mutant gastric cancer aimed to

pre-empt possible resistance mechanisms and alluded to potential combination therapies that may overcome such issues (Grygielewicz et al., 2014). The authors noted a compensatory signalling mechanism in FGFR-inhibitor resistant cells that could be overcome by blockade of human epidermal growth factor 2 (HER2) and attributed this change in signalling to induction of epithelial to mesenchymal transition (EMT). Acquired resistance to FGFR-inhibition in FGFR3-dependent bladder cancer cells has also been ascribed to EMT and a change in signalling from FGFR3 to HER2/3 (Wang et al., 2014a). In another study, investigation of small molecule inhibition of FGFR3 mutant cell lines revealed a secondary gatekeeper mutation critical for acquired resistance to a selection of FGFR inhibitors, including the AZD4547 compound currently in clinical trials (Chell et al., 2013). Such work is important in the anticipation of drug resistance mechanisms that may affect the utility of drugs in the clinic.

High throughput technologies, such as mass spectrometry (MS), gene microarray profiling and next generation sequencing, afford greater insight into the processes employed by drug resistant cells and therefore offer opportunities to overcome resistance using rational drug combinations (Holohan et al., 2013). Ultimately, to overcome the hurdle of drug resistance in the treatment of cancer, we require a greater understanding of how resistance is acquired and to view cell signalling as an interconnected network, capable of rewiring upon inhibition of the dominant signalling pathways.

1.5 Screening of signalling networks

As discussed in section 1.4, a common mechanism of drug resistance is via reprogramming of signalling networks upon inhibition of a mutant receptor (Holohan et al., 2013). This 'kinome reprogramming' is the product of pathway redundancy in cancer cells, where blockade of one receptor tyrosine kinase is compensated for by re-wiring of the signalling network either downstream of the receptor or via up-regulation of a different receptor tyrosine kinase. To dissect an intracellular signalling network, it is essential to use an unbiased, quantitative and well-validated assay. Microarray and MS provide two effective ways to assess gene and protein levels, respectively, and can be used to complement each other in the dissection of signalling networks.

1.5.1 Microarray gene expression analysis

Advances in genome sequencing have facilitated high resolution gene expression studies. Microarray technology has increased hugely the efficiency of gene expression analysis, as well as measuring gene expression in a global, unbiased fashion. Using this technology, the levels of thousands of gene transcripts can be measured simultaneously from one RNA sample. While the specifics vary between providers, the format is generally one of a chip composed of DNA probes specific to a gene. For example the Illumina platform provides probes for over 47000 gene transcripts. RNA is extracted from tissue or cells, reverse transcribed and labelled with a fluorescent dye. Upon hybridisation, fluorescent imaging provides a measure of relative gene expression across and, in the case of chips whereby multiple samples can be analysed in tandem, between samples (Tarca et al., 2006). Whilst this approach has been used to great effect to garner a wealth of transcriptomic data, it is being superseded by direct RNA sequencing, which offers greater resolution and also encompasses analysis of mRNA splice variants (Qian et al., 2014).

Although transcriptome investigation omits information about the posttranslational modifications proteins undergo to perform their various functions, expression arrays

have been crucial in identifying important players in a range of cellular processes, as well as aiding identification of therapeutic targets in disease states (Aguan et al., 2000, Banwait and Bastola, 2014, Critchley et al., 2006, Ohgino et al., 2014, Olivera-Martinez et al., 2014).

1.5.2 Mass spectrometry

Microarray transcriptomics represents an important breakthrough in the global identification and quantification of gene expression in distinct cell populations. While this has often been used as a proxy for protein expression, it is important to assess cellular activity at the protein level in a similar global, unbiased fashion. MS provides the ideal tool for such analysis.

The initial step of all proteomic experiments is sample preparation, which is typically performed in one of two ways: labelled or label-free. While these terms denote sample preparation methods, ultimately they determine how proteins in the samples are identified and quantified. The labelled system can be further subdivided into two distinct processes: chemical labelling using isobaric tag for relative and absolute quantification (iTRAQ) and metabolic stable isotope labelling with amino acids in cell culture (SILAC) (Ong et al., 2002, Ross et al., 2004).

The iTRAQ system utilises isotope-containing tags, which react with primary amine groups of peptides and act as reporter molecules. These tags are fragmented in the mass spectrometer and the difference in the intensity of the various reporters is employed to derive the relative abundance of the proteins in the starting cell population (Ross et al., 2004). The SILAC method involves incorporation of 'heavy' isotope-containing amino acids (Ong et al., 2002). Arginine and lysine labelled with ^{13}C and/or ^{15}N are fed to cells as a medium supplement, leading to the incorporation of these heavy labels into newly synthesised proteins in the cell. At the end of experimental treatment, differentially labelled cell populations can be mixed and, because the heavy and light proteins can be distinguished from each other, run

through the mass spectrometer together. The ability to run all sample conditions through the spectrometer at once is advantageous, as the influence of differences in MS runs between samples on peptide quantification is minimised. However, experimental conditions are limited to the number of labels available, both in iTRAQ and SILAC systems, and sample preparation is both costly and time consuming.

The label-free approach of sample preparation is advantageous in that it allows for analysis of an unlimited number of samples and removes cumbersome culturing techniques. In this system, cells are grown in their normal culture medium and run through the mass spectrometer separately. Historically, this has been associated with difficulty in normalising between samples. However, advances in computational methods have allowed for internal normalisation controls, minimising this problem (Cutillas and Vanhaesebroeck, 2007).

MS identifies proteins based on their weight, or mass-to-charge (m/z) ratio. In the 'bottom-up' MS approach, sample proteins are identified based on their constituent peptides. Peptide fragments are obtained by digestion of whole proteins, commonly using trypsin. This method is generally considered more sensitive than the 'top-down' alternative, where whole proteins are detected; therefore the fragmentation approach allows identification of a more complete protein network (Moradian et al., 2014).

In liquid chromatography (LC)-MS, solid phase extraction of peptides typically follows tryptic digest, after which peptides are run through high performance-LC (HPLC), separating peptides based on their hydrophobicity. Peptides are then transferred from liquid to gas phase by passing through an electrospray ionisation unit, producing multiply charged ions. The ions then pass into the vacuum of the mass spectrometer, where an electromagnetic field is applied and peptides are separated based on their m/z ratio, which is recorded by the detector. From these data, the isotopic distribution and charge of the peptides in the sample can be deduced, as well as its retention time, i.e. the time taken for the analyte to pass from the HPLC

inlet to the detector (Ens and Standing, 2005). To garner information about the peptide sequence from the MS spectra, the peptide must be fragmented along its backbone, giving an MS/MS, or 'tandem MS', spectrum. This is performed on a number of top multiply charged ions, the number of which is defined by the user, typically in the range of 5-7 ions. The resulting MS/MS spectra is essentially a list of m/z ratios of the various fragments (Walther and Mann, 2010).

From comparison of tandem mass spectra, peptide molecular weights or mass data and amino acid sequence data with an annotated database, for example Mascot, peptide identification can be achieved (Perkins et al., 1999). Reference values of peptides listed in the database are calculated by applying appropriate cleavage rules to known proteins. Experimental data can be compared to those listed in the database and given a score based on the likelihood of each peptide belonging to a particular protein. The peptide match with the highest score, with this score representing the probability that the pairing is not a chance event, is reported as the best match and the peptide assigned accordingly.

Following identification of the proteins present in the experimental sample, quantification of these peptides can be performed. Label-free MS can be quantified by using an internal control such as inclusion of yeast extracts spiked with standard proteins in the experimental sample (Old et al., 2005). One method developed for accurate quantification of peptides from label-free MS is the *peak statistical calculator* (Pescal) programme (Cutillas and Vanhaesebroeck, 2007). Here, the retention time and m/z ratio of a given peptide is used to generate an extracted ion chromatogram. These ion intensities are then normalised by subtracting the intensities of the particular ion in a blank sample from the experimental peptide intensity and subsequently dividing this by the peptide intensities of the internal standard (Cutillas and Vanhaesebroeck, 2007). The relative quantity of peptide is calculated relative to the mean of normalised ion intensities of the peptide of interest across the samples being compared. Further calculations are employed to garner intensity values of peptides matching each protein and are ultimately reported as fold expression relative to the mean expression (Cutillas and Vanhaesebroeck, 2007). Other

methods of quantitation of label-free proteomics have been described (Ishihama et al., 2005, Mallick et al., 2007). However, as these methods only allow for approximation of protein abundance from spectral count, they lack the precision of Pascal (Cutillas and Vanhaesebroeck, 2007).

As well as identifying total protein levels in cells, MS can be used to identify post-translationally modified proteins, for example those which have been phosphorylated. Protein kinase signalling plays an essential role in mediating cell behaviour, and changes in signalling via phosphorylation status of proteins provide valuable information in both normal and disease states. The phosphoprotein signature of cells is a reflection of kinase pathways active in the population, and allows us to acquire greater understanding of the complexity of cellular signalling (Choudhary and Mann, 2010).

The phosphoproteome can be deduced using MS by including an enrichment step. Following proteolytic digest of the sample proteins, phosphopeptides are selected using, for example, TiO₂ chromatography or incubation with phospho-selective antibodies (Boersema et al., 2009). The resulting fraction can then be run through the mass spectrometer as described, as can the total protein fraction, therefore providing a wealth of information regarding both the phospho- and total proteome. This fully quantitative method is capable of identifying at least 2000 phosphopeptides (Casado et al., 2013a).

Although the changes in phosphoprotein levels have routinely been assessed using antibody-based methods, such as western blotting, such methods only shed light on pre-selected signalling pathways and are limited to the number of proteins that can be investigated at one time. As such, only hints of the myriad signalling changes which occur between cell populations are identified. The ability of MS to identify changes in thousands of phosphoproteins in one run gives a much broader, quantifiable and unbiased insight into multiple signalling pathways. From such data, a detailed model can be built and an assessment of the networks involved in discreet

populations can be made. Indeed, MS-based phosphoproteomics has been reported as a tool capable of identifying signalling pathways that contribute to intrinsic drug resistance to targeted therapies (Alcolea et al., 2012, Casado and Cutillas, 2011, Casado et al., 2013a, Casado et al., 2013b).

As noted previously, MS/MS spectra are produced by fragmentation of peptides along their amino acid backbone. The most popular method of gas phase fragmentation is collision induced dissociation (CID) (Boersema et al., 2009). In CID, ionised peptides are accelerated by an electric potential in a vacuum and allowed to collide with an inert gas, such as helium or nitrogen. These collisions convert the kinetic energy of the peptide ion to internal energy distributed throughout the molecule. This causes disruption of the peptide bonds and leads to their fragmentation, typically at the amide bond, producing b- and y-ions, from which the amino acid sequence can be deduced (Biemann, 1988, Boersema et al., 2009, Roepstorff and Fohlman, 1984). However, when fragmenting phosphorylated peptides, CID can cause the phosphate group to break away from the peptide, an energetically more favourable process than backbone fragmentation. This is termed 'neutral loss' and results in a dominant peak in the MS/MS spectrum that can hinder identification of the rest of the fragments and therefore prevent accurate peptide sequence information being obtained (DeGnove and Qin, 1998, Tholey et al., 1999).

To overcome this, an additional step can be added to the MS process. The standard LC-MS/MS process involves the initial MS scan to determine peptide masses and charge state, after which ions are selected and fragmented for MS/MS (MS^2) scans. A third step is then introduced, isolating the neutral loss fragment ion and fragmenting the precursor ion again so as to achieve more efficient backbone fragmentation (MS^3) (Schroeder et al., 2004). However, this additional step increases analysis time and so MS^2 and MS^3 steps can be combined in a process known as 'multistage activation' (MSA) (Schroeder et al., 2004). Therefore, CID-MSA gives more accurate identification of phosphopeptides than its CID predecessor (Boersema et al., 2009).

Additional advances in peptide fragmentation have been achieved in recent years, for example electron capture dissociation (ECD) and electron transfer dissociation (ETD) methods, which are ideal for post-translationally modified peptides, as neutral loss is not observed (Syka et al., 2004, Zubarev, 2004). Higher energy C-trap dissociation (HCD) can also be used to identify peptide modification with very high confidence (Olsen et al., 2007).

MS presents a valuable tool in assessing protein activity within cells. As well as looking at global proteomes, signatures of post-translationally modified proteins can be assessed and modification of the technique can allow for investigation of discreet protein complexes, for example RNA polymerases (Melnik et al., 2011). Indeed, this technique represents an opportunity to assess both cell line and human tissue proteomes and use these data to identify therapeutic targets and subsequently guide both pre-clinical and clinical research.

1.6 Cell culture models

Whilst *in vitro* 2D culture of cells allows dissection of molecular events, it is important to assess cellular behaviour in a more physiological environment, where interactions between different cell types can be taken into consideration. This is particularly important in the investigation of cancer, where the tumour microenvironment is known to play a critical part in cancer cell signalling and therefore tumour progression (Gligorijevic et al., 2014, Langley and Fidler, 2011, Onuigbo, 1975, Suh et al., 2014, Witz and Levy-Nissenbaum, 2006). One useful pre-clinical investigative model is the genetically modified mouse, where the impact of tumour microenvironment, vasculature and immune response can be taken into account. However, such models are expensive and time consuming and are not readily available for all cancer and molecular aberrations, as is the case for FGFR2 mutant endometrial cancer. As such, an intermediary model is required where cell-cell interactions in a 3D environment, as well as the effects of targeted drugs, can be assessed in a cost- and time-effective manner.

3D cell culture models are particularly important in assessing and visualising cancer cell invasion. Transwell assays, where cells invade through a membrane towards a chemoattractant, have been used to this effect and allow for quantification of cell invasion (Nystrom et al., 2005). However, this system fails to incorporate a stromal population of mesenchymal cells and therefore omits the effect of paracrine signalling between the two cell types (De Wever and Mareel, 2003, Liotta and Kohn, 2001, Mueller and Fusenig, 2002). Incorporation of such a layer allows for recapitulation of physiologically-relevant cancer cell-stroma interactions and assessment of their effect on growth and migration.

To address this issue, the organotypic culture model was created (Fusenig et al., 1983). This system has since been modified and used to assess the 3D culture properties of a range of cancer types (Chioni and Grose, 2012, Coleman et al., 2014, Froeling et al., 2009, Mauchamp et al., 1998, Nystrom et al., 2005, Sakamoto et al., 2001, Sanderson et al., 1996, Vukicevic et al., 1990). In general, this system

consists of fibroblasts mixed with collagen and Matrigel, acting as the extracellular matrix, to form a stromal equivalent, and cancer cells are seeded on top of this layer. These cultures are then raised to an air-liquid interface and fed from underneath. After a given time course, cultures are formalin-fixed and stained for various markers (Figure 1.9 A). While this method lacks insight into the role of the full range of physiological factors, it is arguably as clinically relevant as mouse xenograft models using nude mice, which also lack infiltrating immune responses and clinically accurate *in situ* tumour phenotypes (Kahn et al., 2012).

The optimal 3D cell culture would consist of either primary or immortalised stromal cells from the tissue of origin of the cancer under investigation (Coleman et al., 2014). However, the successful use of these cells in such cultures is influenced by the amenability of the primary cells to tissue culture, as well as access to adequate amounts of primary tissue. To overcome such obstacles, immortalised primary mesenchymal cells from another tissue may be used as a substitute (Nystrom et al., 2005). In scenarios where primary cells are available, a 'mini' organotypic model has been established to accommodate small quantities of cells (Coleman et al., 2014) (Figure 1.9 B).

An attractive feature of this model is its amenability for investigation of a range of cancer types and as a tool in aiding the answer of an array of molecular questions. For example, in addition to quantification of invasion, this system can be used to assess the effects of drug compounds on cell growth of both cancer and stromal cells, and immunofluorescence can be performed on sections to quantify proliferative cells and localisation of proteins (Chioni and Grose, 2012, Coleman et al., 2014). In short, this 3D physiometric system serves as a relatively high throughput, preclinical model in the analysis of cell-cell interactions and the evaluation of the effects of pharmacological agents.

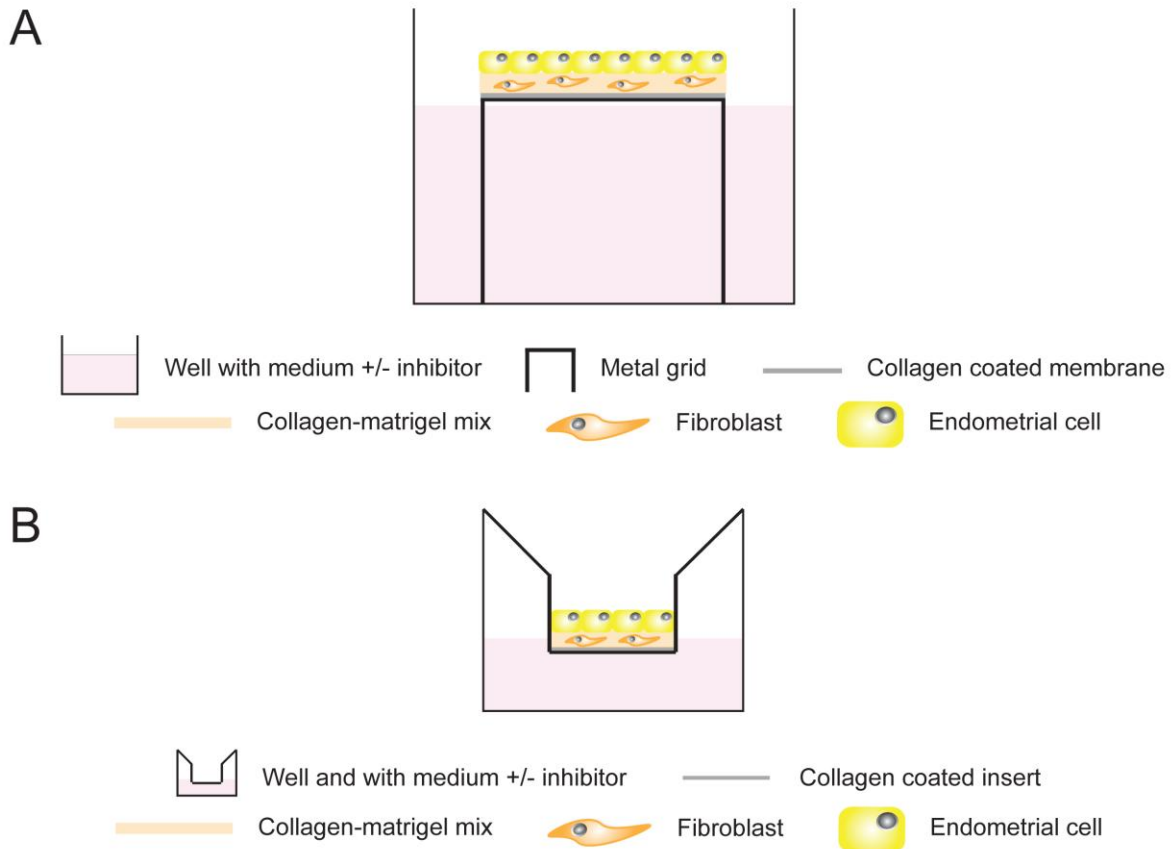


Figure 1.9. Schematic representation of the 3D organotypic cell culture model.

(A) The standard organotypic model consists of a collagen/Matrigel stromal equivalent containing embedded fibroblasts, upon which cancer cells are seeded. This culture is raised onto a collagen-coated membrane placed on a metal grid in a 6-well plate. Cultures are fed from underneath. This model can be used to assess the effects of pharmacological agents by inclusion of such drugs in the medium (Chioni and Grose, 2012, Coleman et al., 2014, Froeling et al., 2009). (B) An alternative method of organotypic culture has been developed, where fibroblasts and cancer cells are seeded in the same ratios as shown in A but in a smaller total volume (Coleman et al., 2014). In this method, the organotypic is created as before, this time using a Transwell insert placed inside the well of a 24-well plate. In both systems, cells are fed every 2-3 days for the duration of the experiment, after which they are formalin fixed, sectioned and stained for a range of cellular markers.

1.7 Aims and objectives

FGFR2 is mutated in approximately 16% of endometrial cancers and, while these aberrations are known to be the driver mutations in a range of developmental disorders, little is known about their relevance in endometrial cancer (Byron et al., 2008, Byron et al., 2012, Pollock et al., 2007). Small molecule inhibition of FGFR signalling in FGFR2 mutant endometrial cancer has been postulated as a viable therapeutic target (Byron et al., 2008, Dutt et al., 2008, Konecny et al., 2013). However, as resistance to both chemotherapy and hormone therapy is common in recurrent endometrial cancer, and acquired and intrinsic resistance to small molecule inhibitors have been documented in other carcinomas (Goltsov et al., 2011, Goltsov et al., 2012, Lito et al., 2013, Wagle et al., 2011, Zhang et al., 2009), the efficacy of prolonged FGFR-targeted therapy is an important area of study.

To ascertain the role of mutant FGFR2 in endometrial cancer, and to decipher the susceptibility of various cell populations to acquisition of FGFR inhibitor resistance, the first aim of this project was to establish a 3D cell culture model to interrogate these populations using pharmacological agents.

The second objective was to use phosphoproteomics to analyse differential signalling behaviour in cells prior to and post FGFR-targeted drug resistance acquisition and use these data to identify viable therapeutic targets to abrogate resistance pathways.

The third objective was to determine the mechanism of drug resistance in FGFR2 mutant cell lines using a combination of microarray gene expression analysis and biochemical techniques.

Chapter 2

Materials and methods

2.1 Cell culture

MFE-296 cells (Health Protection Agency, HPA) were grown in Modified Eagle's Medium (MEM) (Sigma-Aldrich) supplemented with 10% foetal bovine serum (FBS) (GE Healthcare). AN3CA (American Type Culture Collection, ATCC) and HFF2 cells (ATCC) were grown in Dulbecco's Modified Eagle's Medium (DMEM, Sigma-Aldrich) supplemented with 10% FBS and 1% L-glutamine (GE Healthcare). Ishikawa cells (Sigma-Aldrich) were grown in MEM supplemented with 5% FBS, 1% L-glutamine and 1% Non-Essential Amino Acids (Sigma-Aldrich). All cells were incubated at 37°C, 8% CO₂ and 100% relative humidity.

When cells reached approximately 80-90% confluence, medium was removed and trypsin/ethylenediaminetetraacetic acid (EDTA) (GE Healthcare) was added for 5-7 min at 37°C, 8% CO₂ in order to detach cells from the flask surface. Once cells were detached, trypsin was inactivated with the relevant medium. Cell suspensions were centrifuged at 240 x g for 3 min at room temperature. Following centrifugation, supernatant was removed and the cell pellet re-suspended in standard medium. If counting of cells was required, 10 µL of cell suspension was added to a haemocytometer and cells counted manually under a light microscope. Cells were sub-cultured at a 1:3 ratio.

For storage of cells, cell pellets were re-suspended in 2 mL of a 90% FBS and 10% dimethyl sulphoxide (DMSO) (Sigma-Aldrich) solution. Aliquots were frozen slowly at -80°C and then transferred to liquid nitrogen for long-term storage.

When recovering cells from liquid nitrogen stocks, cell suspensions were thawed at 37°C and transferred to a 15 mL Falcon tube containing standard medium. To remove DMSO, the cell suspension was centrifuged at 240 x g for 3 min. The supernatant was removed and cells were re-suspended in standard medium and plated into a tissue culture flask.

2.2 Cell line sequencing

To ensure each cell line contained the *FGFR2*, *PIK3CA*, *PIK3R1* and *PTEN* mutations detailed in the literature, PCR-based cell line sequencing was performed. Primers were designed using Primer3Plus (Primer3Plus, 2015) to amplify an approximately 200 base pairs (bp) region around the mutation site (Table 2.1). PCR using HotStarTaq Plus DNA Polymerase (QIAGEN) was then performed according to the manufacturer's instructions and using the PCR conditions detailed in Table 2.2.

The PCR product was subsequently run on a 1.5% agarose gel, containing Gel Red (Biotium), and visualised under UV light to ensure a single, strong band was produced from the PCR. The PCR product was then sent to Barts Genome Centre for cycle sequencing and the resulting data analysed using BioEdit and CLC Sequence Viewer (v6) software.

Table 2.1. Primers used to sequence endometrial cancer cell point mutations

Primer name	Sequence	Source
<i>FGFR2</i> N550K F	GCT GCC CAT GAG TTA GAG GA	Eurogentec
<i>FGFR2</i> N550K R	GGA AGC CCA GCC ATT TCT A	Eurogentec
<i>FGFR2</i> K310R F	TCT TCC CTC TCT CCA CCA GA	Eurogentec
<i>FGFR2</i> K310R R	CAT GAA GGA GAC CCC AGT TG	Eurogentec
<i>PTEN</i> R130Q/R130fs*1 F	AGA CCA TAA CCC ACC ACA GC	Eurogentec
<i>PTEN</i> R130Q/R130fs*1 R	ATC TAG GGC CTC TTG TGC CT	Eurogentec
<i>PIK3CA</i> P539R F	CCA CGC AGG ACT GAG TAA CA	Eurogentec
<i>PIK3CA</i> P539R R	ACA GAC AGA AGC AAT TTG GGT	Eurogentec

Table 2.2. HotStarTaq Plus DNA Polymerase PCR programme

Step	Temperature (°C)	Time (min)	Cycles
Initial denaturation	94	3	1
Denaturation	94	0.5	35
Annealing	58	0.5	
Extension	72	0.5	
Final extension	72	7	1
Hold	4	Indefinitely	

2.3 PCR

To establish the FGFR expression status of each cell line, primers for each FGFR (Table 2.3) were used and the PCR cycle in Table 2.4 followed. PCR products were then run on an agarose gel containing Gel Red and visualised under UV light. All experiments were performed in duplicate.

Table 2.3. FGFR PCR primers

Primer name	Sequence	Source
FGFR1IIIa F	AAA GCA CAT CGA GGT GAA CG	Eurogentec
FGFR1IIIa R	TTC ATG GAT GCA CTG GAG TC	Eurogentec
FGFR1IIIb F	TTA ATA GCT CGG ATG CGG AG	Eurogentec
FGFR1IIIb R	ACG CAG ACT GGT TAG CTT CA	Eurogentec
FGFR1IIIc F	TGC TGG AGT TAA TAC CAC CG	Eurogentec
FGFR1IIIc R	CCA GAA CGG TCA ACC ATG CA	Eurogentec
FGFR2IIIa F	AAG GTT TAC AGC GAT GCC CA	Eurogentec
FGFR2IIIa R	CTG CTG AAG TCT GGC TTC TT	Eurogentec
FGFR2IIIb R	AGA GCC AGC ACT TCT GCA TT	Eurogentec
FGFR2IIIc F	GTG TTA ACA CCA CGG ACA AA	Eurogentec
FGFR2IIIc R	TGG CAG AAC TGT CAA CAA TG	Eurogentec
FGFR3IIIb R	AAA TTG GTG GCT CGA CAG AG	Eurogentec
FGFR3IIIc F	AGA ACC TCT AGC TCC TTG TC	Eurogentec
FGFR4 F	TAT CTG GAG TCC CGG AAG TG	Eurogentec
FGFR4 R	GTG TGT GTA CAC CCG GTC AA	Eurogentec

Table 2.4. PCR cycle for amplification of FGF and FGFR sequences

Step	Temperature (°C)	Time (min)	Cycles
Initial denaturation	94	5	1
Denaturation	94	0.5	35
Annealing	58	0.5	
Extension	72	0.5	
Final extension	72	7	1
Hold	16	Indefinitely	

2.4 Serum starvation assay

Cells were seeded in six well plates in standard medium and incubated at 37°C, 8% CO₂. After 16 h, medium was removed and cells were serum starved in FBS-free medium for 1, 2, 4, 8 or 16 h. Control cells were treated with full serum for 16 h, after which all cells were lysed and protein isolated as outlined in section 2.6. All experiments were performed in duplicate.

2.5 Stimulation assay

Cells were seeded in six well plates in standard medium and incubated at 37°C, 8% CO₂. After 16 h, medium was removed and cells were serum starved in FBS-free medium for 4-6 h. Medium was removed and cells were treated with FBS-free medium supplemented with PD173074 (Sigma-Aldrich) at a final concentration of 2 µM, 1 µM AZD4547 (AstraZeneca, UK) or the equivalent volume of DMSO for control wells, for 1 h. 300 ng/mL heparin (Sigma-Aldrich) was added to each well and cells were stimulated with 100 ng/mL FGF2 (PeproTech) for 15 and 60 min. After 1 h, cells were lysed and protein isolated as outlined in section 2.6. All experiments were performed in triplicate.

2.6 Western blotting

Cell lysates were prepared using radioimmunoprecipitation assay (RIPA) buffer (Millipore) supplemented with protease inhibitor (Millipore) and phosphatase inhibitor (Millipore) at a dilution of 1:100. Protein concentration was then determined with a BioRad DC protein assay (BIORAD, Reagent A; Reagent B; Reagent S) according to the manufacturer's instructions. Equal concentrations of denatured protein at 20-40 µg were loaded onto 4-12% NuPage Bis-Tris pre-cast gels (Invitrogen). After protein separation by electrophoresis, proteins were transferred to a nitrocellulose membrane (GE Healthcare) for 4 h at 4°C, run at 44 V. Membranes were blocked in 5% milk in phosphate buffered saline (PBS) (Fisher Scientific) at room temperature for 30 min and then incubated with primary antibody in 3% BSA/PBS overnight at 4°C. All antibodies were rabbit polyclonal at a dilution of 1:1000 unless otherwise

stated: anti-Actin (goat polyclonal; Santa Cruz, sc-1615), anti-AKT (Cell Signalling Technology, 9272S), anti-Calnexin (Cell Signalling Technology, 2433S), anti-Cyclophilin A (Abcam, ab58144), anti-ERK (Millipore, 06-182), anti-FGFR1 (rabbit monoclonal; Cell Signalling Technology, 9740S), anti-FGFR2 (Santa Cruz, sc-122), anti-FRS2 (Santa Cruz, sc-8318), anti-HSC70 (mouse monoclonal; Santa Cruz, sc-7298), anti-P-AKT (Ser473) (Cell Signalling Technology, 9271S), anti-P-ERK (Thr202/Tyr204) (Cell Signalling Technology, 9101S), anti-P-RFS2 (Cell Signalling Technology, 3861), anti-PHLDA1 (Sigma-Aldrich, HPA019000-100UL).

Membranes were incubated with HRP-conjugated secondary antibodies for 1 h at room temperature. All secondary antibodies were obtained from Dako. Specific protein bands were visualised using Amersham Enhanced chemiluminescence (ECL) Western Blotting Detection Kit (GE Healthcare) and photographic film (Super RX).

All washes after primary and secondary antibody incubations were performed in 0.1% Tween20-TBS (TBST) (Applichem) for 3 x 5 min. Densitometric analysis was performed using ImageJ 1.429 software (National Institutes of Health), Microsoft Excel (2007) and Prism (v5.03). Where phospho-antibodies were used, signal density was normalised to the total protein level, unless otherwise stated. Signal density was normalised to the anti-actin, anti-HSC70, anti-calnexin or anti-cyclophilin A level as a loading control/reference in all other western blots.

2.7 2D cell survival assay and generation of FGFR-inhibitor resistant cell lines

Cells were seeded in their respective culture medium, as detailed previously, in 12 well plates at the following densities: MFE-296 9×10^3 , AN3CA 1×10^4 and Ishikawa 9×10^3 . After 24 h, the relevant concentration of inhibitor or DMSO control was added. Medium was changed every 2-3 d. After 7 or 14 d, cells were detached from the well using trypsin/EDTA and cells counted manually under a light microscope using a haemocytometer. All experiments were performed in triplicate. The MFE-

296^{PDR} cell line was generated by treating MFE-296 cells with 5 μ M PD173074 continuously. MFE-296^{AZR} cells were generated by treating MFE-296 cells with 2.5 μ M AZD4547.

2.8 3D physiomimetic model

This was modified from previously published protocols (Chioni and Grose, 2012, Coleman et al., 2014). Organotypic cultures were prepared as shown in Figure 1.9 A. The stromal extracellular matrix (ECM) equivalent was composed of 70% 3.48 mg/mL collagen type I (BD Bioscience) and 30% Matrigel (BD Bioscience), (80% of the final volume of the ECM). 10x Hanks buffer (Sigma-Aldrich) was added to the mix (10% of the final volume) and the pH adjusted to 7.4 using 2 M NaOH. HFF2 cells were re-suspended in FBS (10% of the final volume), at 5×10^5 cells/mL and added to the mix. The final mixture was added to a 24-well plate (1 mL/well) and incubated at 30°C, 8% CO₂ for 4 h to polymerise. The gels were equilibrated by immersion in DMEM for 16 h, whereupon the medium was replaced by 1 mL culture medium containing 1×10^6 endometrial cancer cells/mL. Cells were left to adhere to the gel at 37°C, 8% CO₂ for 16 h.

250 μ L collagen mix (7 vol collagen type I, 1 vol each of 10x Hanks buffer, FBS and culture medium neutralized with 2 M NaOH) was added drop-wise onto 400 mm² Nylon membranes (100 μ m pore; Tetko, Inc.). Membranes were incubated at 37°C for 15 min, fixed in 1% glutaraldehyde (Sigma-Aldrich) in PBS and incubated at 4°C for 1 h. After fixation, the membranes were washed 3 x for 5 min with PBS and incubated for 16 h in culture medium at 4°C. The coated membranes were placed on 25 mm² sterile stainless steel grids in 6 well plates. Gels were lifted from the 24 well plate and laid on top of the coated membranes. An appropriate amount of culture medium supplemented with either 2 μ M PD173074, 1 μ M AKTVIII (Sigma-Aldrich), 1 μ M MK2206 (Selleckchem), 2 μ M PD173074 in combination with 1 μ M AKTVIII or MK2206 or the equivalent volume of DMSO, for control wells, was added to each well until it reached the lower part of the gel, so that cultures were maintained at the air-liquid interface. 5 μ M PD173074 was used for MFE-296^{PDR} cell cultures. Fresh

inhibitor or DMSO was added to the medium at each medium change. In all cases, medium was changed every 2-3 d. At the relevant time point, gels were fixed in 10% neutral buffered formalin (CellPath) for 16 h at 4°C. After fixation, gels were washed thoroughly in PBS, bisected and dehydrated in 70% ethanol before paraffin embedding. Each treatment was performed in biological duplicates or triplicates with one to three technical replicates of each.

The mini organotypic model was prepared as shown in Figure 1.9 B. All reagents and cells were used in the same ratio but in a total volume of 120 µL. 200 µL of the Matrigel/collagen mix containing 6.25×10^4 HFF2 cells was added to the insert of a Transwell in a 24 well plate. Gels were equilibrated by immersion in DMEM for 2 h, after which the medium was replaced with 200 µL medium containing 1.25×10^5 endometrial cancer cells. Cells were left to adhere to the gel at 37°C, 8% CO₂ for 16 h, upon which medium was removed and the inserts placed into a new 24 well plate. 350 µL medium containing the relevant drug or vehicle control was added to the base of the well. Medium was changed every 2-3 d and gels removed, formalin fixed, paraffin embedded and sectioned as previously described.

The mini organotypic procedure was modified where stated by fully submerging the Transwell insert throughout drug treatment. All other parameters were kept constant.

2.9 Immunofluorescence

Four µm paraffin sections of organotypic cultures were dewaxed in xylene, rehydrated through a graded ethanol series and transferred to PBS. Antigens were retrieved by microwaving in 10 mM citrate buffer (pH 6) for 20 min. Sections were washed 3 x with PBS, blocked for 1 h at room temperature with 6% BSA/PBS and incubated with anti-Ki67 primary antibody (rabbit, 1:200; AbCam, ab15580) diluted in 6% BSA/PBS for 1 h at room temperature.

After incubation with primary antibody, cells were washed 3 x for 5 min in PBS and incubated with a secondary antibody conjugated with FITC (goat anti-rabbit IgG (H+L)-FITC; 1:200; Invitrogen, A11008) diluted in 6% BSA/PBS for 1 h at room temperature. Cells were washed 3 x in PBS for 5 min and a final wash of H₂O was performed. Finally, slides were mounted using aqueous mounting medium supplemented with 4', 6-diamidino-2-phenylindole (DAPI) (Life Technologies). Hematoxylin-eosin (H&E) staining was performed by the BCI Pathology service, according to standard procedures.

2.10 Microscope image acquisition

Confocal images were acquired at room temperature using a confocal microscope (LSM510 Axio; Carl Zeiss). Images were taken using a Plan Apochromat 40x objective, 1.3 oil differential interference contrast M27. Immersol 518 F (Carl Zeiss) was used as an imaging medium. The acquisition software used was ZEN 2011 (Carl Zeiss). Thresholds were set per slide and kept constant for all images analysed.

Bright-field images were acquired at room temperature using a light microscope (Axiophot; Carl Zeiss) connected to a camera (AxioCam HRz; Carl Zeiss). The objective used was Plan Neofluar with 10x magnification and 0.3 aperture. The acquisition software used was AxioVision Release 4.8 (Carl Zeiss).

2.11 Data analysis

In all experiments, excluding those using MS, all quantitative data are presented as means \pm standard errors. Statistical significance was determined with Student's *t* test.

Cell number and percentage Ki67 staining in the confocal images of organotypic cultures were analysed using ImageJ 1.429 software. Six random fields of each

organotypic culture, and three fields of each mini organotypic culture, were analysed. Percentage Ki67 staining was calculated as Ki67 positive cells as a percentage of the total number of cells (DAPI stained nuclei) per field of view. An average was taken from the multiple fields per slide.

2.12 Isolation, purification, growth and maintenance of primary cells, and cell immortalisation

Endometrial tissue was collected from a healthy uterus after hysterectomy (collaboration with Dr Michelle Lockley, Barts Cancer Institute, Barts Gynae Tissue Bank ethics number 10/H0304/14). Tissue was transported on ice, washed in 70% ethanol for 20 s and subsequently washed three times in RPMI-1640 medium (RPMI; Sigma-Aldrich) supplemented with 5% FBS. Tissue was dissected into 1mm³ pieces and added to 15 mL RPMI supplemented with 1% FBS. Tissue was digested in a final volume of 0.05% trypsin and 0.01% EDTA in PBS, incubated at 37°C for 1 hour with rotation at 200 rpm. Digestion was stopped by dilution with RPMI + 1% FBS. The cell suspension was then centrifuged at 380 x g for 5 min. The supernatant was removed and the remaining tissue/cell pellet was re-suspended in RPMI + 1% FBS and passed through a 40 µm cell strainer (BD Biosciences) to remove undigested tissue. The supernatant was collected and centrifuged at 380 x g for 5-10 min at room temperature. The pellet was re-suspended in RPMI + 1% FBS and cells were counted as described in section 2.1.

Epithelial cell isolation was achieved using Epcam-coated magnetic beads (Invitrogen). Beads were washed in 10 mL RPMI + 1% FBS and placed on a magnet for 2 min. The supernatant was removed and the process repeated using 5 mL and 2 mL of medium, respectively. Finally, supernatant was removed and beads re-suspended in 100 µL of RPMI + 1% FBS.

Based on personal recommendation (collaboration with Dr Jenny Gomm, Barts Cancer Institute), it was assumed 50% of these cells were epithelial. Bead solution was added in a 1:1 ratio of beads:target cells where 2.5 µL of bead solution is equivalent to 1x10⁶ beads. Beads:target cell suspension was incubated at 4°C for 20 min. The suspension was then placed on a magnet for 2 min. The supernatant, containing non-epithelial cells, was removed

and stored in freezing medium containing RPMI supplemented with 40% FBS and 6% DMSO at -80°C for one day, then transferred to liquid nitrogen for long term storage. The bead:target cell mixture was then re-suspended in RPMI + 1% FBS in a final volume of 1 mL. The suspension was centrifuged at 380 x g for 5 min and the pellet re-suspended in freezing medium and stored as per the epithelial fraction.

Isolated cells were then cultured as an adherent monolayer in sterile tissue culture flasks at 37°C and 8% CO₂. Cells were grown in DMEM:F12 (50:50) (Sigma-Aldrich) supplemented with 10% FBS, 10% Pen Strep (Invitrogen), 0.25 µg/mL fungizone (Invitrogen), 0.5 ng/mL hydrocortisone (Sigma-Aldrich), 2.5 ng/mL insulin (Sigma-Aldrich), 0.1 ng/mL epidermal growth factor (EGF) (Sigma-Aldrich) and 10 ng/mL Apo-transferrin (Sigma-Aldrich).

HEK293T cells were seeded in a T175 flask and allowed to reach 90% confluence. 50 µg vector construct, 17.5 µg pMD.G2 envelope plasmid (Addgene 12259) and 32.5 µg pCMVΔ8.74 packaging plasmid (Addgene 22036) were added to 6 mL OptiMEM and mixed with a further 6 mL OptiMEM plus 1 µL 10 mM Polyethylenimine (PEI). The solution was incubated for 20 min at room temperature. Medium was removed from cells and 12 mL of the PEI/DNA complex was added. Cells were incubated at 37°C, 5% CO₂ for 3 h, after which medium was removed and replaced with 15 mL DMEM and 10% FBS. Medium change was repeated after 24 h. Cell supernatant was harvested at 48 and 72 h and centrifuged at 3400 x g for 10 min at room temperature. The supernatant was removed and passed through a 0.22 µm filter (Millex). Virus was concentrated by centrifugation at 23000 x g for 2 h at 4°C. Supernatant was removed and tubes inverted for 2 min, after which 50 µL OptiMEM was added. The suspension was incubated on ice for 1 h under intermittent agitation. Concentrated virus was stored at -80°C.

Primary cells, isolated from endometrial tissue, were seeded in a six well plate in 1 mL media and 20 µL of concentrated virus. Cells were incubated at 37°C, 5% CO₂

for 3 d. Cells were transferred to a T25 flask and medium was changed every 5-7 d. Cells were split as per section 2.1.

2.13 Mass spectrometry

2.13.1 Cell culture

MFE-296 cells were plated at 7×10^5 per 10cm plate in their appropriate culture medium, as previously outlined earlier in this chapter. After 16 h, an appropriate amount of fresh culture medium was added to untreated (UT) control plates, supplemented with DMSO as a vehicle control, or 2 μ M PD173074 (PD). Medium was changed every 2-3 d. Cells were lysed at 1, 7 or 14 d. Experiments were performed in duplicate.

2.13.2 Cell lysis, digestion and solid-phase extraction

Cells were washed with PBS supplemented with 1 mM Na_3VO_4 (Sigma-Aldrich) and 0.5 mM NaF (Sigma-Aldrich) on ice. Cells were lysed in 8 M urea in 20 mM HEPES (Sigma-Aldrich) (pH 8.0) supplemented with 100 mM Na_3VO_4 , 0.5 M NaF, 1 M β -Glycerol Phosphate (Sigma-Aldrich) and 0.25 M $\text{Na}_2\text{H}_2\text{P}_2\text{O}_7$ (Sigma-Aldrich). Lysates were sonicated on ice at 50% intensity 3 x for 15 s followed by centrifugation for 10 min at 4°C. Protein concentration in the supernatant was determined using Bradford assay reagent (Sigma-Aldrich) according to the manufacturer's instructions. Cysteines were reduced using 1 M dithiothreitol (DTT) (Sigma-Aldrich) with 30 min incubation at room temperature in darkness. Samples were subsequently alkylated by addition of 415 mM iodoacetamide (IAM) (Sigma-Aldrich) and incubated at room temperature for 30 min in darkness. Samples were diluted 1:4 with 20 mM HEPES to a final volume of 4 mL. Proteins were digested using immobilized trypsin beads (GL Sciences) re-suspended in 20 mM HEPES. Samples were incubated at 37°C for 16 h with constant agitation. Trypsin was removed by centrifugation and the resultant peptide solutions desalted by reversed solid-phase extraction with OASIS HLB cartridges (Waters Corp.) using a vacuum manifold ($P = 5.0$ inHg, ± 0.5). Digested sample peptides were kept on ice during desalting but were allowed to equilibrate to

room temperature prior to loading into the OASIS cartridge. Cartridges were conditioned with 1 mL 100% acetonitrile (ACN) (Sigma-Aldrich) and columns equilibrated by purging of 1 mL 1% ACN + 0.1% TFA followed by 0.5 mL of 1% ACN + 0.1% trifluoroacetic acid (TFA) (Sigma-Aldrich). Samples were loaded into the corresponding cartridge and purged at a low flow rate. Columns were subsequently washed with 1 mL 1% ACN + 0.1% TFA and desalted peptides then eluted 0.5 mL 1 M glycolic acid (50% ACN, 5% TFA).

2.13.3 TiO₂ Metal Oxide Affinity Chromatography (MOAC)

Phosphopeptides were enriched using MOAC by TiO₂. Desalted peptides were normalised to 1 mL with 1 M glycolic acid and incubated with 50 µL TiO₂ beads, re-suspended in 1% TFA, at room temperature with constant agitation for 5 min. TiO₂ beads were re-suspended in 4 x 200 µL supernatant and loaded into Glygen TopTips (Glygen) previously washed with 100% ACN. The samples in spin tips were centrifuged. Unbound peptides were discarded and beads were sequentially washed with 1M glycolic acid, 100 mM ACN and 2 x 10% ACN, centrifuging between each wash. Bound peptides were eluted from the beads, washing with 4 x 5% NH₄OH (10% ACN) followed by centrifugation. Samples were snap-frozen on dry ice, vacuum dried overnight and stored at -80°C.

2.13.4 Nanoflow-liquid chromatography tandem mass spectrometry (LC-MS/MS)

Immediately prior to LC-MS analysis, samples were reconstituted with 20 µL 50 nM enolase peptide digest and dissolved in 5% ACN + 0.1% TFA, followed by bath sonication for 15 min at room temperature and centrifugation for 5 min at 5°C. The supernatant was recovered for LC-MS analysis.

Phosphopeptide LC separations were carried out on a Dionex Ultimate 3000 nRSLC system with an Acclaim PepMap RLSC C18 Analytical Column (75 µm x 25 cm, 2µm, 100Å) (Thermo Scientific) and an Acclaim PepMap 100 C18 Trap Column (100

$\mu\text{m} \times 2 \text{ cm}$, $5 \mu\text{m}$, 100\AA) (Thermo Scientific). Solvent A consisted of 2% ACN + 0.1% formic acid (FA). Solvent B was made up of 80% ACN + 0.1% FA. Sample injections of $3 \mu\text{L}$ were loaded onto the trap column at a flow rate of $8 \mu\text{L}\cdot\text{min}^{-1}$ for 5 min. Once loaded, samples were eluted over an 85 min gradient from 6.3% to 43.8% solvent A. Following elution, the column was cleaned with 90% solvent B for 10 min, and subsequently equilibrated with 6.3% solvent A for 10 min.

All analyses were completed on a Thermo Scientific LTQ Orbitrap-Velos hybrid instrument, operated in data-dependent acquisition (DDA) mode. In the DDA method used, a full MS^1 survey scan (m/z 350-1500) was performed at a resolution of 30000 FWHM (at m/z 400) and the ions analysed in the Orbitrap. The top seven most intense multiply charged precursor ions present in the MS^1 scan were automatically mass-selected and fragmented by collision-induced dissociation (CID – normalised collision energy = 35%) with multi-stage activation enabled, and analysed in the LTQ-Velos linear ion trap (m/z 190-2000). Neutral losses of 98, 49, 32.7 and 24.5 were accounted for (representing differentially charged phosphate losses) and dynamic exclusion was enabled (avoiding repeat analysis of identical precursor ions within a 60 min window). Samples were run in duplicate.

2.13.5 Identification and quantification of phosphopeptides

Mascot Daemon and Distiller (v2.3.0.0 and v2.4.2.0 respectively, Matrix Science) were used in conjunction to automate the conversion of Thermo Scientific .raw files to MS^2 smoothed and centroided peak lists (.mgf files) and to search the peak lists against the Uniprot/Swissprot human database. LTQ Orbitrap-Velos data were searched using the following criteria: ± 10 ppm precursor and ± 600 mmu fragment ion m/z tolerances; enzyme = trypsin (2 missed cleavages tolerated); fixed modification: carbamidomethyl (C); variable modifications: gln \rightarrow pyro-glu (N-term Q), oxidation (M), phospho (ST), and phospho (Y).

Phosphopeptide identification data produced by Mascot search engine results were collated using a combination of a Perl script (Barts Cancer Institute, London) and Peptide ANalysis and Database Assembly (PANDA) software (v1.1), (Barts Cancer Institute, London). The data were algorithmically curated to include only unique phosphopeptide ions with a q-value ≤ 0.05 (calculated via comparison to searches against a randomised database). All phosphopeptides with a Mascot delta score < 10 were reported as 'Protein (residues), charge, modification(s)'. All those with a score ≥ 10 were reported as the specific phosphorylation site.

Phosphopeptides were quantified using PEAk Statistical CALculator (PESCAL) (Barts Cancer Institute, London) (Cutillas and Vanhaesebroeck, 2007). This automatically generates extracted ion chromatograms (XIC) for the first three isotopes of each phosphopeptide ion within the created database (± 7 ppm m/z tolerance, ± 1.5 min retention time tolerance, isotope correlation > 0.8), subsequently calculating the peak heights of each constructed XIC. Peak heights for each phosphopeptide ion were \log_2 -transformed and quantile normalised. Each of the phosphopeptide ions was then fitted to a linear model, and the difference in magnitude and statistical significance between conditions calculated using an empirical Bayes shrinkage of standard deviations (Smyth, 2004). The resulting p-values were then multiple-testing corrected using the Benjamini-Hochberg procedure. All of the described analysis was performed using the limma package (v3.16.2) within the R statistical computing environment (v3.0.0). Data were processed further and analysed within Microsoft Excel (2007/2010) and R (v3.1.2). Kinase Substrate Enrichment Analysis (KSEA) was performed as previously described (Casado et al., 2013b).

2.14 Cell tracker

Cells were seeded in T175 tissue culture flasks at 40% confluence and incubated for 16 h at 37°C, 8% CO₂. Medium was removed and cells were washed with sterile PBS. Medium was replaced with standard culture medium supplemented with 1 μ L/mL of the relevant CellTracker fluorescent dye (Invitrogen). Cells were incubated at 37°C for 30 min, after which cells were detached from the surface of the flask and

counted using a haemocytometer, as outlined in section 2.1. MFE-296 and MFE-296^{PDR} cells were re-seeded at a 1:1 ratio (4.5×10^4 cells each) on 35 x10 mm glass bottomed plates (SPL Life Sciences) and were incubated at 37°C, 8% CO₂ for 16 h. Following incubation, cells were treated with 5 µM PD173074, 1 µM MK2206, PD173074 in combination with MK2206, or DMSO as a vehicle control. Cells were monitored on a Confocal microscope every day for four days. Confocal images were acquired at room temperature using a confocal microscope (LSM510 Axio; Carl Zeiss). Images were taken using a Plan Apochromat 40x objective, 1.3 oil differential interference contrast M27. Immersol 518 F (Carl Zeiss) was used as an imaging medium. The acquisition software used was ZEN 2011 (Carl Zeiss). Thresholds were set per slide and kept constant for all images analysed. Images of six random fields were taken. Cell number of each population was quantified using ImageJ, Microsoft Excel and Prism. Experiments were performed in duplicate or triplicate.

2.15 Receptor tyrosine kinase (RTK) and signalling node phosphoprotein immunofluorescence assay

Cells were seeded on 10cm plates to be 70% confluent the following day. Cells were lysed and a slide-based Immunofluorescence assay performed using the PathScan RTK Signalling Antibody Array Kit (Cell Signalling Technology) according to the manufacturer's instructions. Slides were read using an ODYSSEY SA Infrared Imaging System (Li-COR) with excitation at 680 nm and detection at 700 nm. Spot intensities were quantified using ImageJ software and data analysed in Microsoft Excel and Prism.

2.16 Microarray

MFE-296, MFE-296^{PDR} and MFE-296^{AZR} cells were seeded on T75 tissue culture flasks at 40% confluence. After 16 h incubation at 37°C, 8% CO₂, total RNA was extracted using the RNeasy Plus RNA extraction kit (QIAGEN) according to the manufacturers instructions. From this, cDNA was synthesised using the first-strand cDNA synthesis using SuperScript II reverse transcriptase kit (Invitrogen) according to the manufacturer's instructions. cDNA of two biological replicates of each cell line

was then sent for microarray gene expression analysis using the Illumina platform at Barts Genome Centre. Each sample was run on the array in duplicate. The resulting data were analysed using Genome Studio, Microsoft Excel and Prism software.

2.17 Fractionation

Cells were seeded in 10 cm dishes and incubated at 37°C, 8% CO₂ for 16 hr. Cells were then washed in PBS and lysed in hypotonic buffer consisting of 20 mM Tris-HCl (pH 7.5) (Sigma-Aldrich), 10 mM MgCl₂ (Sigma-Aldrich), 5 mM (EDTA) (Sigma-Aldrich), 250 µM sucrose (Sigma-Aldrich) and 200 µM phenylmethylsulphonyl fluoride (PMSF) (Sigma-Aldrich). Cells were incubated on ice for 15 min. Lysates were then centrifuged at 100000 x g for 1 h at 4°C. Supernatants (cytosolic fraction) were transferred to a fresh tube and pellets (membrane fraction) were re-suspended in hypertonic buffer. Western blot analysis with the relevant antibodies was then performed as described in section 2.6.

2.18 Short interfering RNA (siRNA) knockdown

Cells were seeded in six well plates in standard medium. The following day, at approximately 40% confluence, the medium was removed and replaced with 1 mL of standard medium. Cells were transfected with either a pool of four siRNA oligonucleotides targeting FGFR2 or PHLDA1 (GE Healthcare) at a final concentration of 10 nM. Control cells were transfected with a pool of non-targeting siRNA at the same concentration. Transfection was achieved using INTERFERin (Polyplus). INTERFERin and siRNA complexes were prepared in OptiMEM (Gibco By Life Technologies), vortexed and incubated at room temperature for 20 min before the total mixture was added to cells in culture medium. Cells were incubated for 48 or 120 h before cell lysis and confirmation of knockdown by western blot (section 2.6).

2.19 PHLDA1 over expression

Cells were seeded in a T75 flask at 40% confluence in standard medium. The following day, medium was removed and cells were washed with PBS. OptiMEM was warmed to 37°C and 5 mL added to each flask. For transfection control wells, 1 µg/µL pmaxGFP (pGFP) (Lonza) was added to 1.25 mL OptiMEM in a Falcon tube. A second Eppendorf tube containing 25 µL Lipofectamine 2000 (Invitrogen) with 1.25 mL OptiMEM was prepared and both solutions incubated at room temperature for 5 min. The contents of both tubes were then mixed and incubated at room temperature for 20 min. The total volume was then added to control flasks and incubated at 37°C for 4 hours. Medium was then removed and replaced with standard culture medium and cells incubated at 37°C for 16 h.

The PHLDA1 plasmid with GFP fluorescent tag was a gift from Richard C. Austin (Addgene 32699). For pPHLDA1 transfection, 1 µg/µL of plasmid was added to 1.25 mL OptiMEM and mixed with the Lipofectamine 2000 preparation as above and added to the cells. After 16 h, flasks were inspected under UV light for GFP expression. Cells were lysed and PHLDA1 levels analysed via western blot, as outline in section 2.6.

Chapter 3

Results: Endometrial cancer cell line characterisation and model development

3.1 Introduction

Whilst approximately 16% of endometrial cancers harbour FGFR2 mutations, little is known about their importance in driving progression of this tumour type (Byron et al., 2008, Byron et al., 2012, COSMIC, 2014). As these same FGFR2 mutations are known to be integral to the aetiology of a range of developmental syndromes, for example craniosynostoses, their characterisation in endometrial cancer is of utmost importance (Dutt et al., 2008, Jemal et al., 2011, Pollock et al., 2007). The effect of targeting FGFR2 mutant tumours with small molecule inhibitors is of particular interest, given the abundance of such drugs currently in clinical trials for other cancer types (Clinicaltrials.gov, 2014). A thorough investigation of the phenotypic and mechanistic effects of these mutations, and the effects of targeted drug treatment, should be considered in the context of other cell types and compared to FGFR2 wild type endometrial cells. Of particular importance is the characterisation of the effects of these drugs over a prolonged period, given the prevalence of acquired resistance to these inhibitors seen in carcinomas of other tissues (Flaherty et al., 2010, Holohan et al., 2013, Wagle et al., 2011).

3.2 Endometrial cancer cell line characterisation

To establish the role of mutant FGFR2 in endometrial cancer, three endometrial cancer cell lines were selected (Table 3.1). Two cell lines, MFE-296 and AN3CA, harbour the N550K FGFR2 mutation (COSMIC, 2014), which results in constitutive activation of kinase activity (Byron et al., 2008). Both of these cell lines also display the FGFR2 IgIII loop mutation K310R (COSMIC, 2014), suggested in previous studies to be a passenger mutation with no obvious phenotype (Dutt et al., 2008). Both cell lines are heterozygous for the N550K and K310R mutations (Pollock et al., 2007)

The MFE-296 cell line also possesses one copy of the activating *PIK3CA* mutation P539R (COSMIC, 2014, Gymnopoulos et al., 2007, Konstantinova et al., 2010, Weigelt et al., 2013), and is heterozygous for the I20M *PIK3CA* mutation of unknown consequence (COSMIC, 2014, Weigelt et al., 2013). The inactivating R130Q and N323 frameshift (fs) PTEN mutations are also expressed in MFE-296 cells (COSMIC, 2014, Han et al., 2000, Weigelt et al., 2013).

Whilst the AN3CA cell line is R130fs*1 PTEN mutant, the *PIK3CA* locus is wild type (Byron et al., 2008, COSMIC, 2014). The AN3CA cell line is, however, heterozygous for the PI3K regulatory subunit R557_D560del mutation, which can interfere with PTEN binding (Cheung et al., 2011, COSMIC, 2014, Van Allen et al., 2014).

The Ishikawa cell line, which expresses wild type FGFR2 (Byron et al., 2013, COSMIC, 2014), multiple inactivating PTEN mutations (COSMIC, 2014, Weigelt et al., 2013) and a PI3K regulatory subunit mutation (COSMIC, 2014, Weigelt et al., 2013) was used as a control. The mutation status of FGFR2, PTEN and PIK3CA in each cell line was confirmed by Sanger sequencing (Table 3.1, Appendix Figures 1.1-1.4).

Table 3.1. *FGFR2*, *PTEN*, *PIK3CA* and *PIK3R1* mutation status of endometrial cancer cell lines

Cell line	<i>FGFR2</i>	<i>PTEN</i>	<i>PIK3CA</i>	<i>PIK3R1</i>
MFE-296	N550K, K310R	R130Q, N323fs*?	P539R, I20M	wt
AN3CA	N550K, K310R	R130fs*1	wt	R557_D560del
Ishikawa	wt	V290fs*1, V317fs*?, T319fs*1	wt	L570P

Mutations listed in COSMIC as of January 2015.

To establish the levels and activation of various proteins under basal conditions, it is common to serum starve cells overnight. However, serum starvation can induce cellular stress responses, consequently leading to changes in protein abundance (Pirkmajer and Chibalin, 2011). Because of this, the effect of serum starvation on MFE-296 and AN3CA cells was assessed via western blot (Figure 3.1). ERK phosphorylation (P-ERK) returned to levels seen in full serum culture conditions after 16 hours serum starvation in both MFE-296 and AN3CA cells. P-ERK levels reached basal levels between four and six hours starvation. On this basis, all further experiments requiring serum starvation were performed after culturing for four to six hours in serum-free medium.

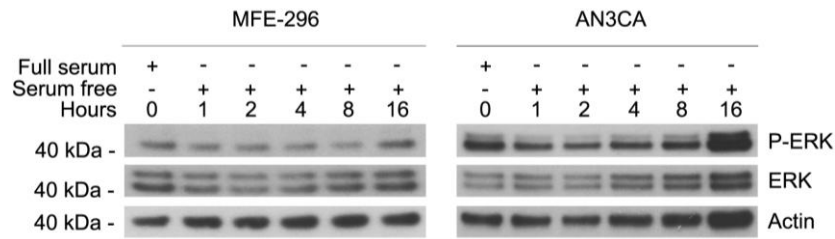


Figure 3.1. Effect of serum starvation on basal signalling in FGFR2 mutant endometrial cancer cell lines.

Cells were cultured in serum free medium for one to 16 hours, or full serum for 16 hours as a control. A decrease in ERK phosphorylation was observed up to eight hours in MFE-296 cells. Minimum P-ERK levels of AN3CA cells were reached at between two and four hours. P-ERK levels increased to full serum levels after 16 hours in both cell lines. As a result, all subsequent experiments requiring serum starvation were performed after four to six hours of serum starvation. 20 µg protein was used for each lane. Protein bands are representative of two independent experiments.

Expression levels of all isoforms of FGFR1-4 in MFE-296 and AN3CA cell lines were established via PCR (Table 3.2, Appendix Figure 1.5). Expression of FGFR1 isoforms IIIa, IIIb and IIIc was apparent in both cell lines, while only isoforms IIIa and IIIc of FGFR2 were expressed. Neither MFE-296 nor AN3CA cells expressed either isoform of FGFR3. FGFR4 was expressed in both cell lines.

FGFR1 and FGFR2 expression in all endometrial cancer cell lines was also established at the protein level (Figure 3.2). The efficacy of the FGFR2 antibody was validated via siRNA knockdown of FGFR2 (Appendix Figure 1.6). There was no significant difference in FGFR1 levels between the three cell lines (Figure 3.2 A and B, left panel). AN3CA cells expressed the highest levels of FGFR2, followed by the MFE-296 and Ishikawa cell lines, respectively (Figure 3.2 A and B, left panel). There was no significant difference in FGFR2 levels between MFE-296 and Ishikawa cells (Figure 3.2 A and B, right panel).

Basal levels of various important signalling nodes downstream of FGFR2 activation were also evaluated. FRS2 phosphorylation (P-FRS2) was lower in Ishikawa cells than in FGFR2 mutant cell lines, as was the total FRS2 protein level (Figure 3.2 A and C, left panel). Basal ERK phosphorylation was significantly higher in AN3CA cells than the MFE-296 and Ishikawa cell lines (Figure 3.2 A and C, middle panel). Baseline AKT phosphorylation (P-AKT) was equivalent across all three cell lines (Figure 3.2 A and C, right panel).

Table 3.2. FGFR isoform expression profile

Cell line	FGFR1			FGFR2			FGFR3		FGFR4
	IIIa	IIIb	IIIc	IIIa	IIIb	IIIc	IIIb	IIIc	
MFE-296	✓	✓	✓	✓	✗	✓	✗	✗	✓
AN3CA	✓	✓	✓	✓	✗	✓	✗	✗	✓

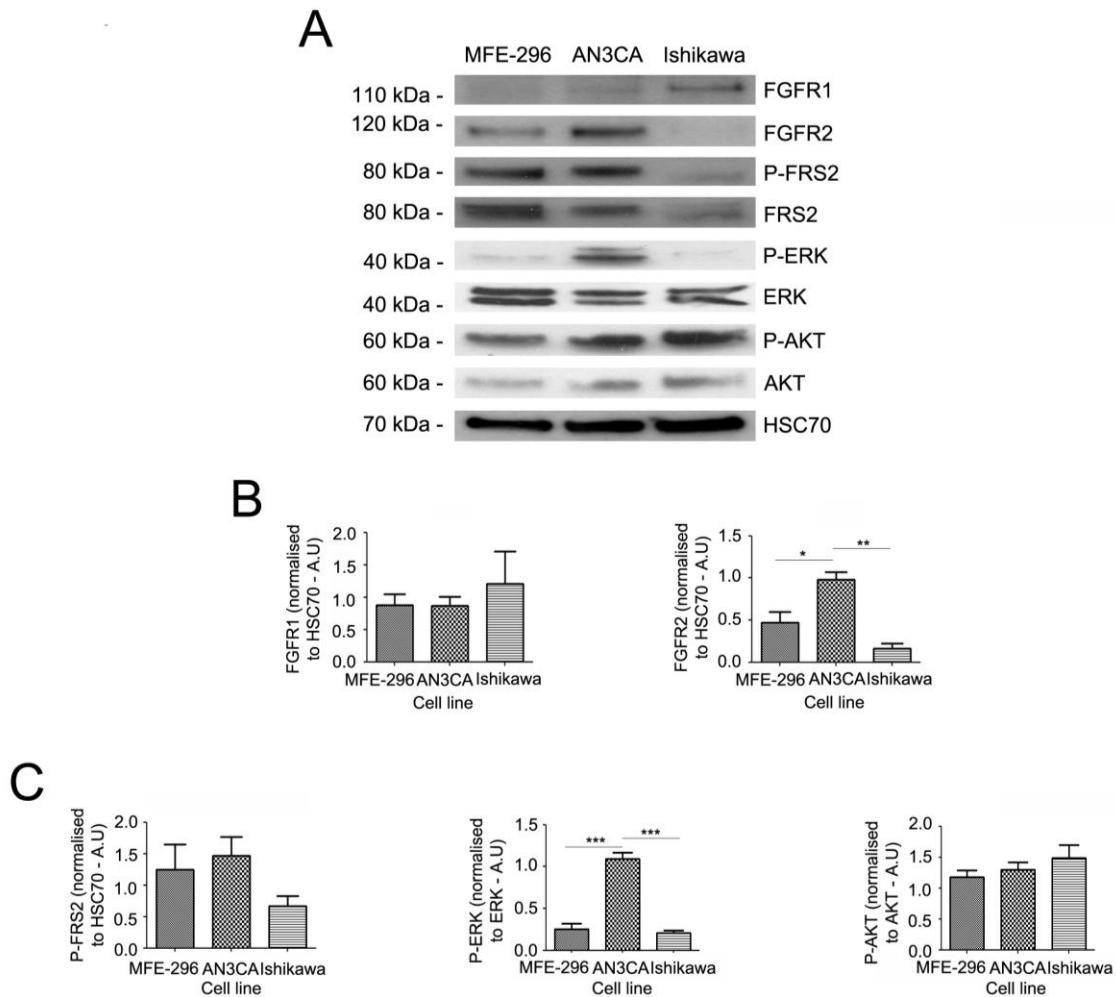


Figure 3.2. Baseline expression of FGFR1, FGFR2 and downstream signalling molecules in endometrial cancer cell lines.

Cells were starved in serum free medium for six hours. There was no significant difference in FGFR1 levels between the three cell lines (A and B, left panel). AN3CA cells expressed significantly higher levels of FGFR2 than both MFE-296 and Ishikawa cells; there was no significant difference in FGFR2 expression between MFE-296 and Ishikawa cell lines (A and B, right panel). FRS2 phosphorylation was lower in Ishikawa cells than in MFE-296 and AN3CA cell lines, as was total FRS2 protein level (A and C, left panel). ERK phosphorylation was significantly higher in the AN3CA cell line than in MFE-296 and Ishikawa cells (A and C, middle panel). There was no significant difference in AKT phosphorylation between any of the endometrial cancer cell lines (A and C, right panel). *, $P \leq 0.05$; **, $P \leq 0.01$; ***, $P \leq 0.001$ (Student's *t* test). 20 μ g protein was used for each lane. Error bars show means \pm SEM of three replicates.

3.3 Differential signalling in the presence and absence of FGFR inhibition in endometrial cancer cell lines

Given that FGFR inhibitors are currently in clinical trials for a range of cancer types (Clinicaltrials.gov, 2014), we sought to establish the differential effects of FGFR inhibition in endometrial cancer cells. Two FGFR inhibitors were used: PD173074, an FGFR-targeted small molecule inhibitor tool compound (Knights and Cook, 2010) and AZD4547, another ATP-competitive inhibitor currently in clinical trials for FGFR2-mutant solid tumours (Clinicaltrials.gov, 2014, Gavine et al., 2012).

The effect of increasing concentration of PD173074 (10-10000 nM) on cell number in 2D culture over seven days was assessed in all three cell lines (Figure 3.3 A). Cell number decreased with increasing inhibitor concentration in both FGFR2 mutant cell lines (Figure 3.3 A, left and middle panels). The AN3CA cell line was more sensitive to PD173074 treatment than the MFE-296 cell line, with cell number reduced to 50% of the DMSO control at approximately 100 nM PD173074 in AN3CA cells compared to approximately 5000 nM in MFE-296 cells. 50 nM to 500 nM PD173074 increased Ishikawa cell number, after which cell number remained broadly constant, regardless of increasing PD173074 concentration (Figure 3.3 A, right panel).

MFE-296 cells were further interrogated with 5 nM to 5000 nM of the more potent AZD4547 (Figure 3.3 B). The effect of this drug on cell number was comparable to that observed with PD173074 (Figure 3.3 A, left panel and B).

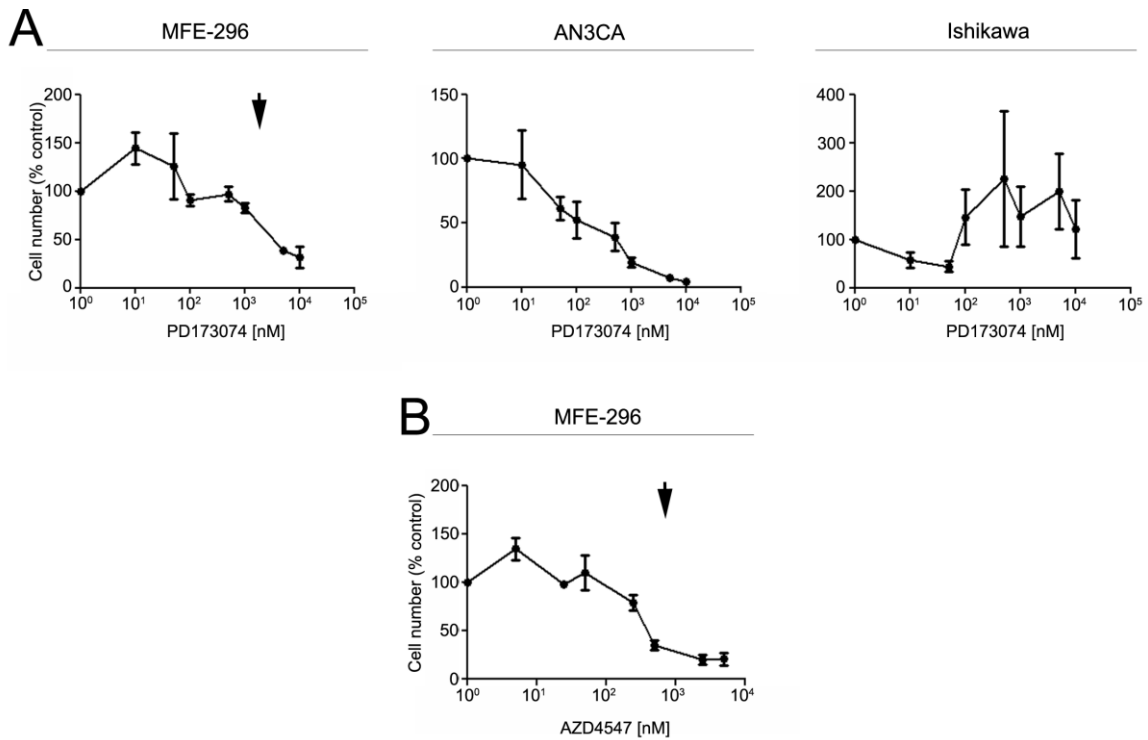


Figure 3.3. Effect of FGFR inhibition on endometrial cancer cell number in 2D culture.

MFE-296, AN3CA and Ishikawa cells were treated with increasing concentrations of PD173074 (10-10000 nM) for seven days, after which cells were counted using a haemocytometer and cell number as a percentage of the DMSO control calculated. (A and B) Cell number was decreased with increasing PD173074 concentration in both FGFR2 mutant cell lines. The AN3CA cell line was more sensitive to FGFR inhibition with a 50% reduction in DMSO control-normalised cell number at 100 nM compared to 5000 nM in MFE-296 cell. Cell number was increased at 500 nM PD173074 compared to 50 nM in Ishikawa cells, after which cell number remained broadly constant, irrespective of treatment with PD173074 concentration. (B) Treatment of MFE-296 cells with increasing concentration of AZD4547 (5-5000 nM) recapitulates PD173074 treatment. Arrows indicate the concentration of inhibitor used in subsequent 2D and 3D experiments (2 μ M PD173074, 1 μ M AZD4547). Error bars show means \pm SEM of three replicates.

To assess the effect of FGFR2 stimulation and inhibition on cell signalling, cells were treated with 100 ng/ml FGF2 for 15 or 60 minutes, either in the presence of PD173074 or AZD4547, or DMSO as a vehicle control (Figure 3.4 A and B respectively). FGF2 was chosen since it efficiently activates the IIIc variants of FGFR1 and FGFR2, which are expressed by the tumour cells (Table 3.2).

FGF2 stimulation activated the ERK pathway in all cell lines, indicated by increased ERK phosphorylation on threonine and tyrosine residues; this was inhibited upon FGFR inhibition (Figure 3.4 A and B, top panels). The extent of inhibition varied between cell lines, with near complete abolition of ERK phosphorylation in AN3CA cells (Figure 3.4 A and B, top and middle panels).

FGF2 treatment also increased AKT signalling in MFE-296 cells; whilst this was decreased following FGFR inhibition, the effect was not significant (Figure 3.4 A and B, top and bottom panels). However, in AN3CA and Ishikawa cells, the AKT pathway was unaffected by FGF2 stimulation. AKT phosphorylation (P-AKT) on serine 473 (ser473) was decreased in AN3CA cells upon PD173074 treatment, while AKT signalling in Ishikawa cells was unaffected by FGFR inhibition. Overall, comparable data were observed between PD173074 and AZD4547 treated cells across all cell lines.

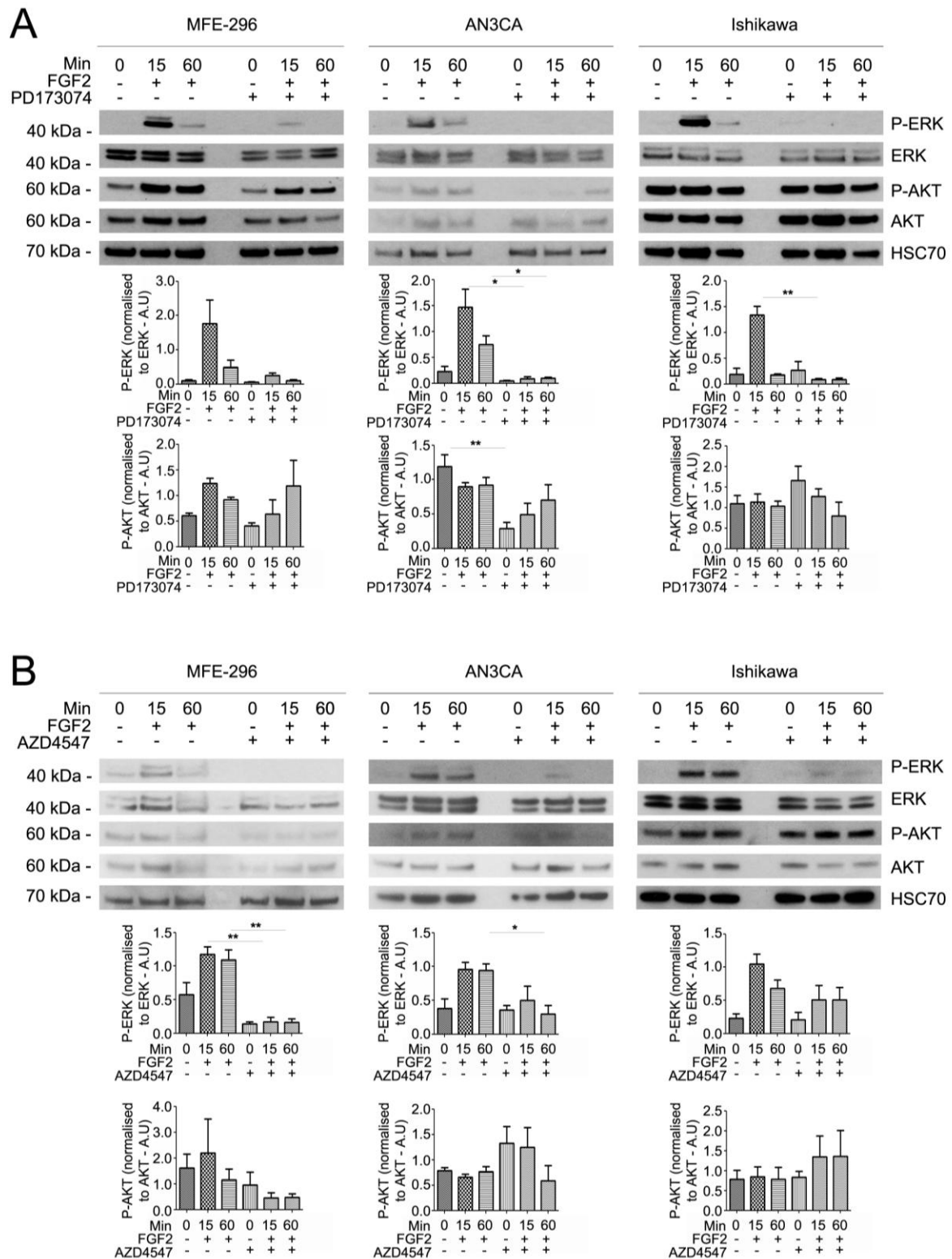


Figure 3.4. Effect of FGF2 stimulation and FGFR2 inhibition on cell signalling.

Cells were serum-starved for six hours and stimulated with 100 ng/mL FGF2 in the presence of 300 ng/mL heparin in serum-free medium for 15 and 60 min. Where indicated, cells were pre-treated with 2 μ M PD173074 or 1 μ M AZD4547 (one hour). Stimulation of all cell lines

activated the ERK pathway; this was inhibited by PD173074 and AZD4547. FGF2 stimulation also increased AKT phosphorylation in MFE-296 cells; AKT signalling was unaffected by stimulation in the AN3CA and Ishikawa cell lines. FGFR inhibition decreased AKT phosphorylation in the MFE-296 and AN3CA cell lines; AKT phosphorylation was unaffected by PD173074 or AZD4547 treatment in Ishikawa cells. 20 µg protein was used for each lane. Error bars show means \pm SEM of three replicates. *, $P \leq 0.05$; **, $P \leq 0.01$ (Student's *t* test).

3.4 Primary cell line immortalisation

Whilst all analysis of the effect of FGFR inhibition in endometrial cancer cell lines has been performed on FGFR2 mutant cells and wild type cells as a control, another important consideration is the effect of such drug treatment on normal epithelial cells. However, such endometrial cells are not commercially available, so benign primary tissue was obtained and primary cell culture attempted.

Endometrial tissue was taken from a 46 year old pre-menopausal patient after abdominal hysterectomy and bilateral salpingo-oophorectomy due to the presence of fibroids and menorrhagia. Pathological investigation showed the tissue to be benign (Figure 3.5 A).

Cell culture of non-malignant primary cells is often hindered by the limited proliferative capabilities of diploid cells (Hayflick and Moorhead, 1961). As such, their culture often leads to immediate cell death or senescence after only a few of rounds of the cell cycle (Condon et al., 2002). Because of this, an attempt to immortalise the primary endometrial cells was undertaken using lentiviral infection with polycomb group RING finger protein 4 (BMI-1), a polycomb protein that suppresses cyclin-dependent kinase inhibitor 2A (p16), thereby preventing cellular senescence (Ganey et al., 2006, Silva et al., 2006).

Epithelial and stromal cells were extracted from the endometrial tissue using an affinity bead-based method (Gomm et al., 1995). Both primary cell fractions were then cultured separately on plastic. The BMI-1 lentivirus was prepared by transfection of the lentivirus plasmid (pFCRu), with BMI-1 and a puromycin resistance cassette under control of a ubiquitous promoter (Feng et al., 2010), into HEK293T cells alongside pMD.G2 envelope and pCMV Δ 8.74 packaging plasmids. The supernatant was harvested after 48 and 72 hours, from which the fully packaged BMI-1 lentivirus was isolated. Primary cells were then transduced using this

concentrated virus. A sub fraction of epithelial and stromal cells were not infected with the lentivirus and were cultured on plastic as a control.

After approximately one week, these slow growing non-transduced primary cells began lifting off the culture plate. BMI-1 lentivirus infected cells remained adhered to the plate; however, the morphology of the epithelial cell fraction became more mesenchymal-like (Figure 3.5 B). To assess whether these cells had undergone epithelial to mesenchymal transition (EMT), epithelial cells were stained for the mesenchymal marker vimentin, as were stromal primary cells as a control (Figure 3.5 C). Cells from both fractions stained positive for vimentin, indicating a transition to a mesenchymal phenotype in the epithelial cell fraction. As EMT subsequently changes the signalling characteristics of cells (Lamouille et al., 2014), these cells could not be used in the comparison of non-malignant epithelial cells and FGFR2 mutant endometrial cancer cells.

Cells from the stromal fraction were cultured for potential use in the analysis of endometrial cancer cells in a 3D environment (Section 3.5). However, these slow growing cells stopped proliferating after approximately two weeks of culture and were therefore unavailable for use.

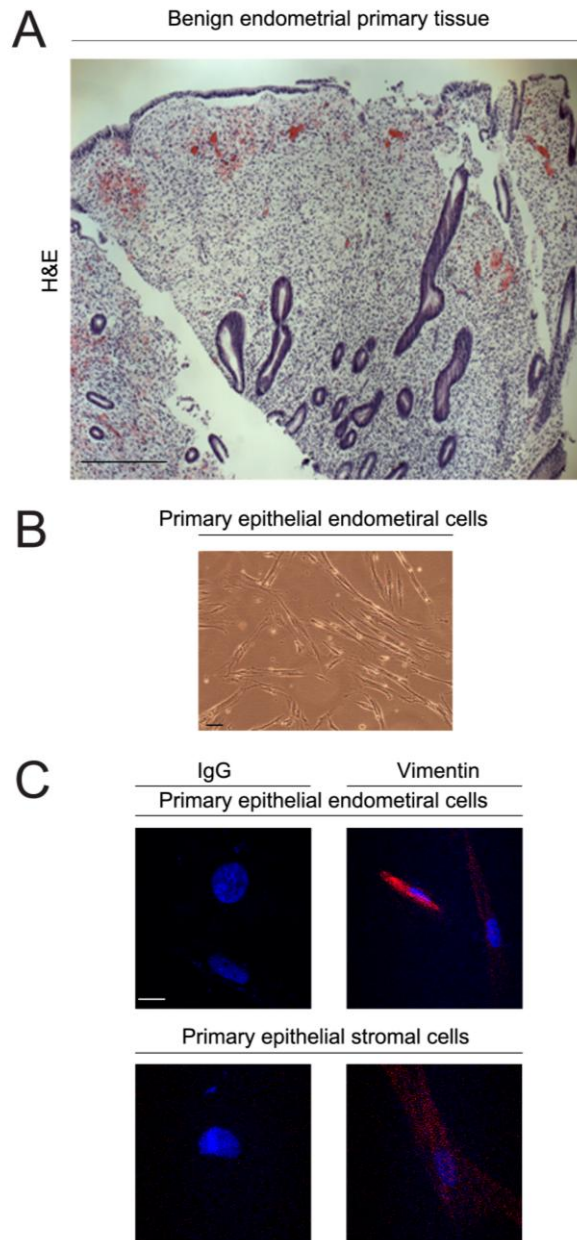


Figure 3.5. Immortalisation of non-malignant primary endometrial tissue.

Tissue was taken from a pre-menopausal patient following abdominal hysterectomy and bilateral salpingo-oophorectomy due to fibroids and menorrhagia. (A) Pathological investigation showed the tissue to be benign. (B) Tissue was homogenised and epithelial and stromal cells were separated. The resulting cell fractions were cultured separately. To immortalise these non-malignant cells, cells were infected with fully packaged BMI-1 lentivirus. Primary epithelial cells showed mesenchymal morphology approximately one week post infection with BMI-1 lentivirus. (C) Cells from both the epithelial and stromal fractions were stained for the mesenchymal marker, vimentin. Epithelial cells stained positive for vimentin expression, indicating EMT had taken place. Original magnification of H&E

image, 10X objective; bar, 100 μm . Original magnification of bright field image, 10X objective; bar 100 μm . Original magnification of confocal images, 40X objective; bar, 25 μm . Confocal images representative of three images acquired from imaging of one biological replicate.

3.5 Development of a 3D organotypic model to investigate endometrial cancer cell behaviour

To investigate the effect of FGFR inhibition in a more physiologically relevant form, a 3D organotypic model was developed. This consisted of a collagen/Matrigel mix with human foreskin fibroblasts (HFF2) embedded, acting as a stromal equivalent in the absence of immortalised non-malignant endometrial stromal cells. Gels were overlaid with MFE-296, AN3CA or Ishikawa cells and raised to an air-liquid interface. Cultures were treated for seven or 14 days in the presence of PD173074 or DMSO vehicle control (Figure 1.9 A).

Preliminary investigations showed the optimum ratio of HFF2:endometrial cancer cells to be 1:2 and so this ratio was used throughout (Appendix Figure 1.7). Analysis of the effect of FGFR inhibition on HFF2 cell number in 2D culture showed there was no significant change with increasing PD173074 concentration (Figure 3.6). Previous work has also successfully used this cell line in stromal matrices of breast cancer cell models (Chioni and Grose, 2012).

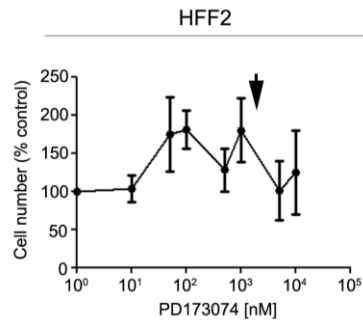


Figure 3.6. Effect of PD173074 on fibroblasts in 2D culture.

HFF2 cells were treated with increasing concentrations of PD173074 for seven days, after which cells were counted using a haemocytometer and cell number as a percentage of the DMSO control calculated. FGFR inhibition did not induce cell death in FGFR2 wild type HFF2 cells. Arrow indicates the concentration of inhibitor used in subsequent 2D and 3D experiments. Error bars show means \pm SEM of three replicates.

Hematoxylin and eosin (H&E) staining showed that endometrial cancer cells did not invade into the stroma in either control or PD173074 treated cultures (Figure 3.7 A-C, top panels). Ki67 staining (green) was used to assess proliferation in all cultures (Figure 3.7 A-C, middle panels). MFE-296 cell number and proliferation decreased significantly in PD173074 treated cells compared to the DMSO control after seven days (Figure 3.7 A, left panels). However, while cell number in PD173074 treated cultures remained lower relative to the control, there was no significant difference in the percentage of cells capable of proliferation after 14 days, as indicated by Ki67 staining (Figure 3.7 A, right panels). Thus, after 14 days, a potentially inhibitor resistant population of cells was established. In contrast, treatment of AN3CA cells with PD173074 led to cell death after seven days (Figure 3.7 B). To ensure this effect was due to induction of cell death upon FGFR signalling inhibition, and not the result of the inability of this cell line to adhere to the stromal equivalent layer in the presence of the drug, cultures were assessed after three days (Figure 3.8). These data showed adhesion of AN3CA cells to the stromal layer, as well as decreased cell number upon drug treatment.

There was no significant difference between PD173074 and control treated Ishikawa cell number or proliferation rate after either seven or 14 days (Figure 3.7 C), suggesting that FGFR inhibition specifically affects FGFR2 mutant cell lines.

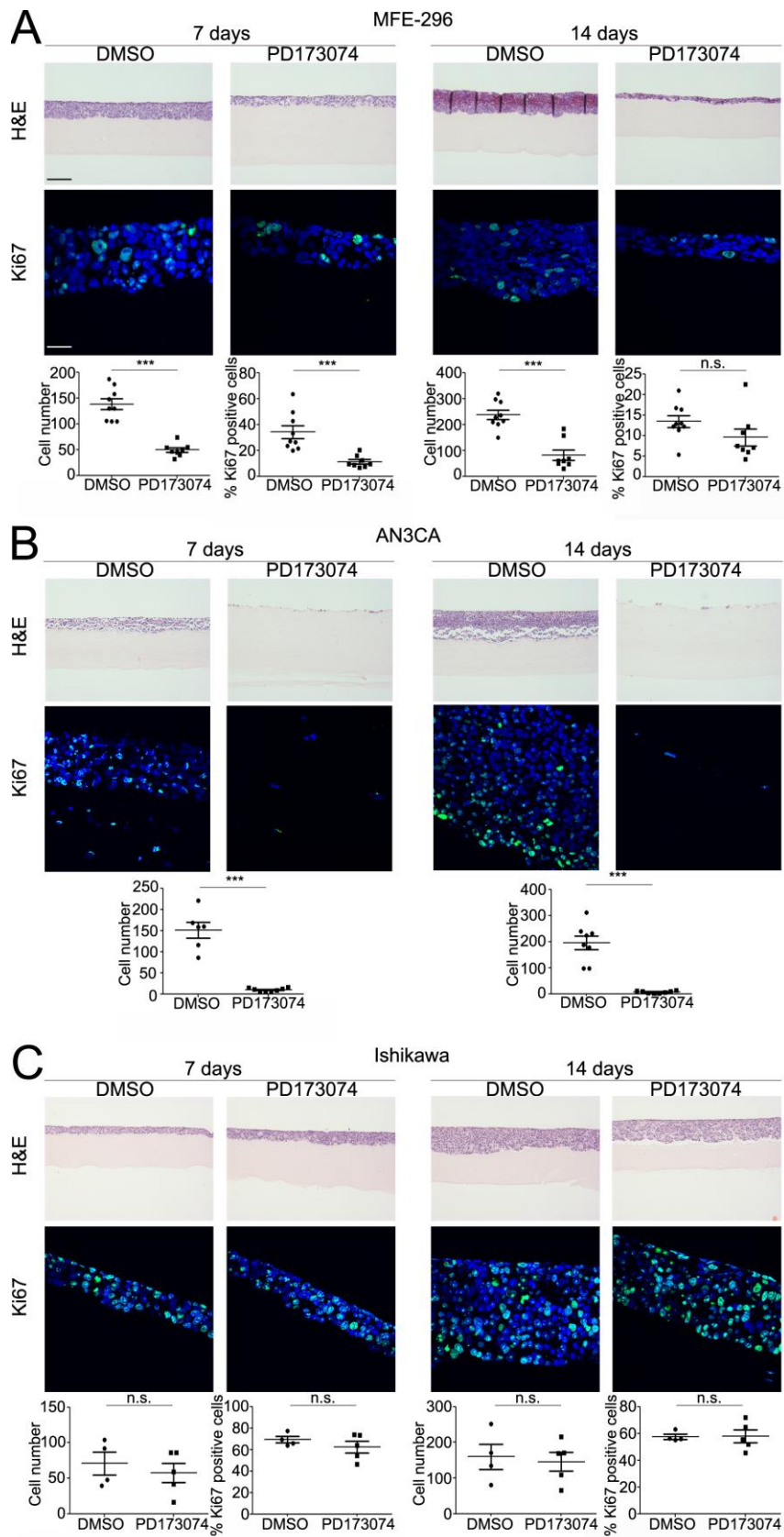


Figure 3.7. Effect of FGFR2 inhibition on endometrial cancer cells in a 3D physiometric model.

An endometrial cancer cell model was designed using a collagen/Matrigel mix, containing HFF2 cells as a stromal equivalent, overlaid with either MFE-296, AN3CA or Ishikawa cells. Organotypic cultures were raised to an air-liquid interface and cultured for seven or 14 days in the presence of 2 μ M PD173074 or DMSO control. (A) After seven days PD173074 treatment of MFE-296 cells, cell number was decreased (left panels). H&E staining showed endometrial cancer cells did not invade into the stroma (top panel). Sections were stained with Ki67 (green) to identify cell proliferation. Proliferation decreased following seven days treatment with PD173074. Cell number in PD173074 treated cells also decreased compared to the DMSO vehicle control at 14 days, however, there was no significant difference in proliferation. An inhibitor-resistant population of MFE-296 cells was apparent. (B) Treatment of AN3CA cells with PD173074 led to cell death after seven days. (C) FGFR2 inhibitor treatment did not affect cell number or proliferation of Ishikawa cells after either seven or 14 days. n.s., not significant ($P > 0.05$); ***, $P \leq 0.001$ (Student's *t* test). Nuclei were stained with DAPI (blue). Original magnification of H&E images, 10X objective; bar, 100 μ m. Original magnification of confocal images, 40X objective; bar, 25 μ m. Error bars show means \pm SEM. Data points represent the average cell number/percentage of Ki67 positive cells of six fields of view of one to three technical replicates of three biological replicates. Cell number and percent Ki67 positive cells represents average values per field of view.

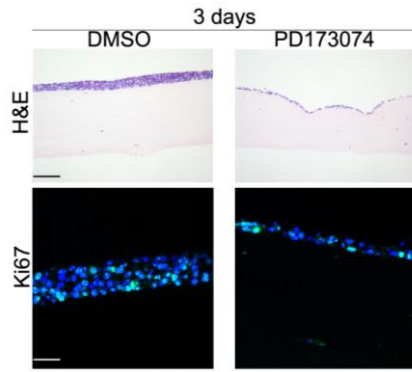


Figure 3.8. AN3CA cells adhere to the stromal equivalent layer in a 3D organotypic model in the presence of PD173074.

Cultures were prepared as in Figure 3.7. AN3CA cells adhered to the stromal equivalent in the 3D endometrial cancer model in the presence of PD173074. Cell number was decreased in the presence of the FGFR inhibitor. Nuclei were stained with DAPI (blue). Proliferating cells were visualised using the Ki67 marker (green). Original magnification of H&E images, 10X objective; bar, 100 μ m. Original magnification of confocal images, 40X objective; bar, 25 μ m. Images representative of three technical repeats of one biological replicate. Six fields of view per replicate were analysed.

These data, showing the emergence of an FGFR inhibitor resistant population of MFE-296 cells, were further interrogated using a mini organotypic model (Figure 1.9 B). Firstly, the validity of this alternative mini model was assessed by repetition of the experiment outlined in Figure 3.7 using MFE-296 cells (Figure 3.9). In this model, cell number was decreased compared to the DMSO control after both seven and 14 days (Figure 3.9 A). There was no significant difference in the percentage of cells positive for Ki67 staining after 14 days, recapitulating the data obtained in the original model, where an inhibitor resistant population of MFE-296 cells was apparent.

The effect of the AZD4547 inhibitor in this mini 3D model was then assessed (Figure 3.9 B). Treatment of MFE-296 cells with AZD4547 gave strikingly similar results to those seen in the PD173074-treated cultures (Figures 3.7 A and 3.9 A), thereby demonstrating the emergence of an FGFR inhibitor resistant population using two independent FGFR-targeted small molecule inhibitors.

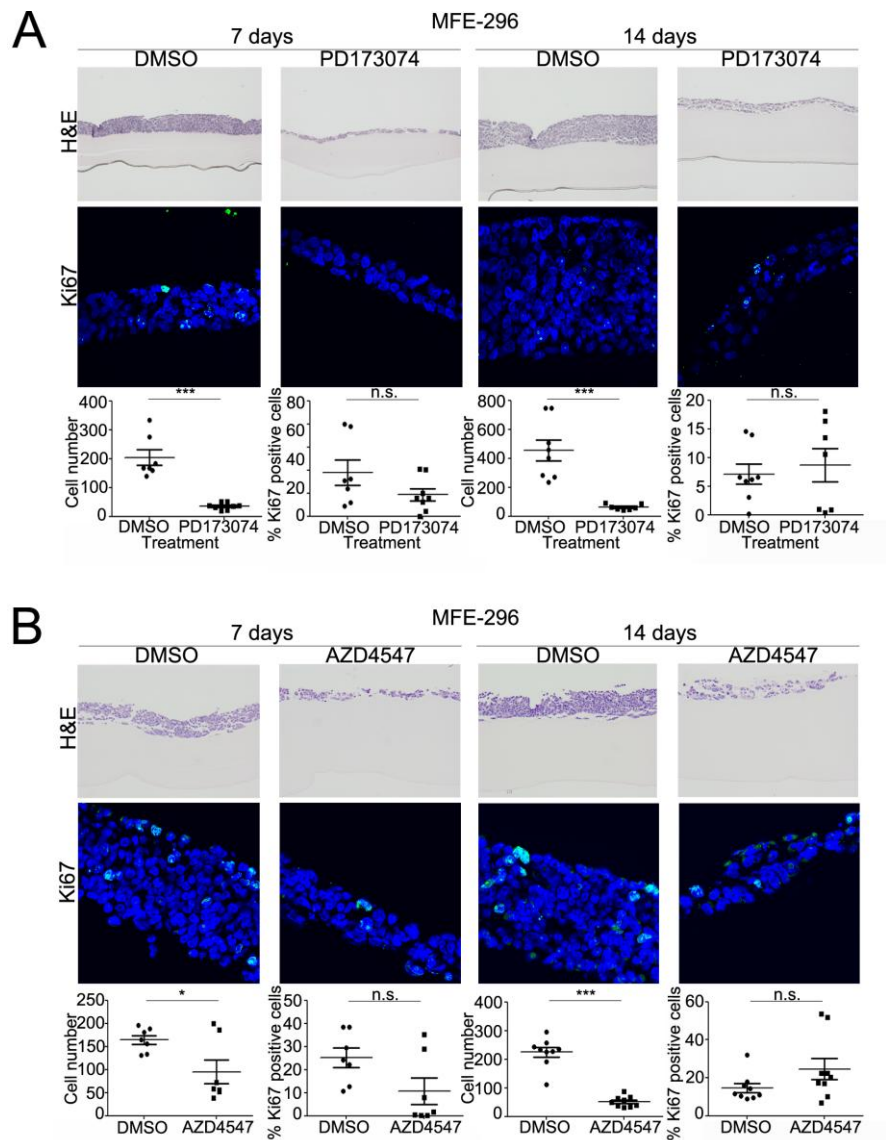


Figure 3.9. The emergence of a drug resistant population in FGFR inhibitor treated MFE-296 cells.

An endometrial cancer cell model was designed using a collagen/Matrigel mix containing HFF2 cells as a stromal equivalent, overlaid with MFE-296 cells in a Transwell insert, respecting the cell ratios previously outlined. Cells were cultured at an air-liquid interface for seven or 14 days in the presence of an FGFR inhibitor or DMSO control. (A) Cell number was significantly decreased in cultures treated with 2 μ M PD173074 for seven and 14 days. There was no significant difference in the percentage of cells positive for Ki67 staining (green) in PD173074 treated cells compared to the DMSO control at either seven or 14 days. (B) Whilst cell number was decreased in cultures treated with 1 μ M AZD4547, there was no significant difference in the percentage of cells positive for the Ki67 proliferation marker. In both PD173074 and AZD4547 treated cultures, an inhibitor resistant population was identified. n.s., not significant ($P > 0.05$); *, $P \leq 0.05$; ***, $P \leq 0.001$ (Student's *t* test).

Nuclei were stained with DAPI (blue). Original magnification of H&E images, 10X objective; bar, 100 μ m. Original magnification of confocal images, 40X objective; bar, 25 μ m. Error bars show means \pm SEM. Data points represent the average cell number/percentage of Ki67 positive cells of three fields of view of one to three technical replicates of three biological replicates. Cell number and percent Ki67 positive cells represents average values per field of view.

Further investigation of the validity of this model and the resulting data were assessed via modification of the culture conditions. It is well established that endometrial cancer metastasis to the ovaries can occur through endometrial cancer cell implantation as a result of retrograde menstruation (Kurman and Shih le, 2011). In our organotypic model, cancer cell invasion is not observed. However, as this cancer type can spread via the budding off of malignant cells from the endometrium into the menstrual fluid, from where cell implantation on the ovaries can occur, the propensity of these cancer cells to behave in this way, and the effect of FGFR inhibition on this, was assessed.

Using the mini organotypic model, MFE-296 cell cultures were set up as outlined previously (Figure 1.9 B). However, medium was also added to the Transwell insert so the organotypic culture was fully immersed. Cells were treated with PD173074 or DMSO as a control and cell number and proliferating cells assessed using H&E and Ki67 staining (Figure 3.10 A). In this model, the viability of cells collected from the medium and found adhered to the bottom of the plate was also assessed, using trypan blue staining (Figure 3.10 B).

These cultures showed the same trend as previous data with regards to cell number and percentage of Ki67 positive cells after 14 days, where an inhibitor resistant population of cells was established upon PD173074 treatment (Figure 3.10 A). Trypan blue staining showed that, while there was no significant difference in the number of cells either free in the medium or adhered to the well of the plate after seven days, the viability of these cells was significantly decreased upon FGFR inhibitor treatment (Figure 3.10 B, left panels). However, while the number of free cells in the media and adhered to the plate was decreased after 14 days inhibitor treatment, there was no significant difference in the percentage of viable cells between those which were control and PD173074 treated, indicating the emergence of an inhibitor resistant population of free cells in the media and adhered to plastic outside of the organotypic culture (Figure 3.10 B, right panels).

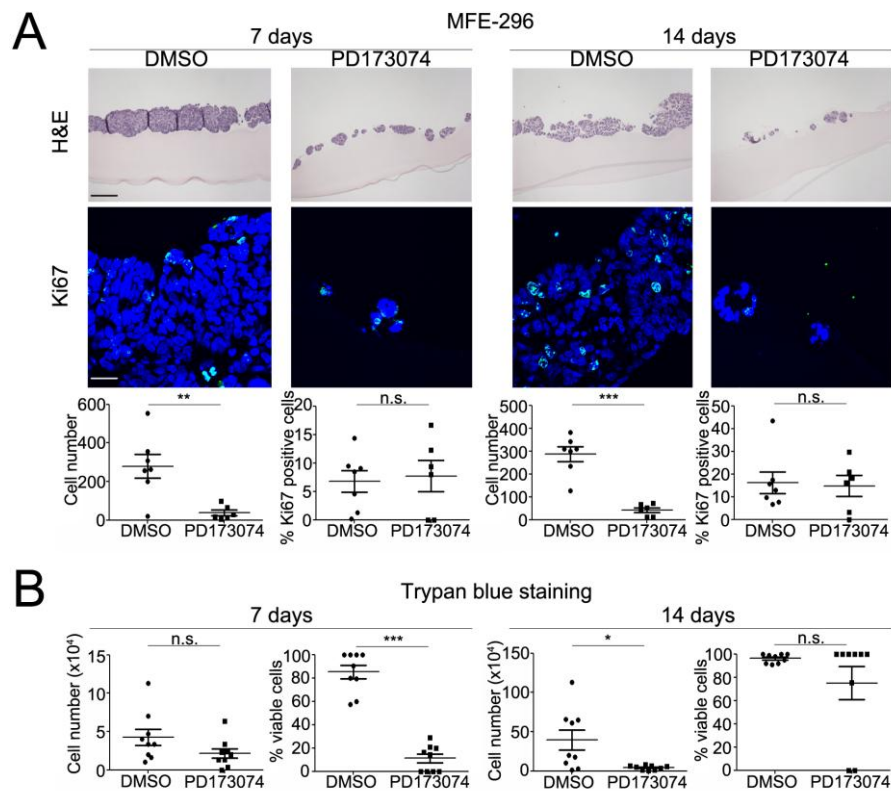


Figure 3.10. Effect of FGFR inhibitor treatment on free circulating cells in a 3D model.

Cultures were prepared as outlined in Figure 3.9 using MFE-296 cells. However, the experimental conditions were modified so that the cultures were fully submerged in medium containing either 2 μ M PD173074 or DMSO as a control. After either seven or 14 days, cultures were assessed for cell number and Ki67 staining as previously detailed. Culture medium was also collected, as were cells adhered to the plate, via trypsinisation. These two populations were then pooled and the number of cells counted using a haemocytometer. Trypan blue staining was used to assess viability of these cells. (A) Cell number was significantly decreased upon PD173074 treatment compared to the DMSO control at both seven and 14 days. However, a resistant population of MFE-296 cells emerged that retained their proliferative capability, as shown by Ki67 staining (green). (B) There was no significant difference in the number of free cells in the culture medium or adhered to the plate between drug or control treated cultures after seven days. However, free cells from PD173074 treated cultures were less viable than DMSO treated cells (left panels). After 14 days, this trend was reversed, whereby free cell number was decreased in FGFR inhibitor treated cultures compared to the control; the viability of these free cells was the same regardless of drug treatment. An inhibitor population of free cells was identified. n.s., not significant ($P > 0.05$); *, $P \leq 0.05$; **, $P \leq 0.01$; ***, $P \leq 0.001$ (Student's *t* test). Nuclei were stained with DAPI (blue). Original magnification of H&E images, 10X objective; bar, 100 μ m. Original magnification of

confocal images, 40X objective; bar, 25 μm . Error bars show means \pm SEM. Data points represent the average cell number/percentage of Ki67 positive cells of three fields of view of one to three technical replicates of three biological replicates. Cell number and percent Ki67 positive cells represents average values per field of view.

3.6 Summary of results

- The MFE-296 cell line harbours *FGFR2*, *PTEN* and *PIK3CA* mutations; the AN3CA cell line harbours *FGFR2*, *PTEN* and *PIK3R1* mutations; the Ishikawa cell line harbours *PTEN* and *PIK3R1* mutations
- Minimal signalling levels in MFE-296 and AN3CA cells are achieved by four to six hours of serum starvation
- Both MFE-296 and AN3CA cell lines express the FGFR2IIIc isoform
- AN3CA cells have higher baseline expression levels of FGFR2 and P-ERK than MFE-296 and Ishikawa cells; MFE-296 and AN3CA cells have higher P-FRS2 levels than Ishikawa cells
- AN3CA cells are more sensitive to FGFR inhibition than MFE-296 cells in 2D culture; FGFR inhibition does not decrease cell number in Ishikawa cell cultures
- The AZD4547 small molecule inhibitor has a similar effect on cell number of MFE-296 cells as PD173074
- ERK and AKT pathways are stimulated in response to FGF2 in FGFR2 mutant cell lines; the inhibitory effect of FGFR targeted drug treatment on these pathways is greater in AN3CA cells
- Primary epithelial cell immortalisation using BMI-1 lentivirus infection leads to EMT
- Development of a 3D organotypic model of endometrial cancer allowed analysis of the effects of prolonged drug treatment on cell number and proliferation
- 3D modelling confirmed the sensitivity of AN3CA cells to FGFR inhibition
- Ishikawa cell proliferation was unaffected by FGFR inhibition
- Treatment of MFE-296 cells with an FGFR inhibitor led to the selection of an inhibitor resistant population

3.7 Discussion

In these initial investigations, we provide new insight into the significance of *FGFR2* mutations in endometrial cancer. We have established differences in oncogene addiction between *FGFR2* mutant cell lines using two small molecule inhibitors, providing evidence that in some cases, as seen in AN3CA cells, *FGFR2* inhibition alone was sufficient to induce cell death throughout the cancer cell population. However, a drug resistant population was established in another *FGFR2* mutant cell line, MFE-296, after prolonged *FGFR* inhibitor treatment. Importantly, the effects of small molecule inhibition outlined in these data were *FGFR2* mutation status dependent, as shown by the absence of growth inhibition of the *FGFR2* wild-type Ishikawa cell line.

Differential signalling of endometrial cancer cells

Previous studies have used PD173074 treatment to investigate the effect of *FGFR* inhibition on endometrial cancer cell lines (Dutt et al., 2008, Byron et al., 2008, Byron et al., 2013). Where 2D cell proliferation was measured, the findings were consistent with our data, showing that AN3CA cells are more sensitive to *FGFR* inhibition than MFE-296 cells (Dutt et al., 2008, Byron et al., 2008). Similarly, a recent study has shown that the IC_{50} of PD173074 was higher in MFE-296 cells than the AN3CA cell line (Byron et al., 2013), further validating their differential response to *FGFR* inhibition.

As both MFE-296 and AN3CA cell lines harbour the same *FGFR2* mutation, N550K, it is interesting that differences in signalling response are invoked upon *FGFR* inhibition (Byron et al., 2008, Byron et al., 2013). Recent work has debated the status of N550K as a gatekeeper mutation (Byron et al., 2013). However, as cell lines harbouring this mutation have varying responses to *FGFR* inhibition, it is possible that, rather than N550K conferring innate resistance to receptor inhibition, the effect of drug treatment in mutant cell lines varies depending on relative addiction to oncogenic *FGFR2* signalling (Sharma and Settleman, 2007). For example, our initial signalling data show that baseline *FGFR2* and P-ERK levels are higher in the

AN3CA cell line compared to those observed in MFE-296 cells, suggesting that the AN3CA cell line has evolved to preferentially depend on the effects of this particular mutation.

Cell line immortalisation

Ideally, the effects of tumourigenic mutations would be compared to non-malignant cells arising from the same tissue of origin. However, primary cell culture of such tissue is difficult and so induced immortalisation is particularly useful. One method commonly used is transfection of human telomerase reverse transcriptase (hTERT) expression vectors, whereby hTERT transfection of primary cells maintains telomere length and thereby extends their cell culture lifespan (Bodnar et al., 1998, Condon et al., 2002, Dickson et al., 2000, Fanning, 1992, Farwell et al., 2000, Morales et al., 1999, Vaziri et al., 1999). However, this method has limitations, for example over-expression of hTERT can compromise regulation of cell differentiation (Georgopoulos et al., 2011). While such epithelial cells of endometrial origin are not commercially available, one laboratory has reported successful generation of such cells via transfection of hTERT alongside human papilloma virus (HPV) E7 to overcome telomere-independent senescence (Kyo et al., 2003). Collaboration was attempted with the only laboratory still in possession of these cells. However, upon their receipt, they were found to have undergone EMT. For this reason, we began attempts to generate our own immortalised non-malignant endometrial cell lines.

A potential alternative to hTERT transfection is induction of BMI-1 expression in primary cells (Douillard-Guilloux et al., 2009, Fulcher et al., 2009). BMI-1 is a polycomb protein that suppresses p16 and therefore enhances cell survival (Guney et al., 2006, Silva et al., 2006). This protein has been shown to be required for self-renewal of stem cells in a range of tissues, such as lung epithelial stem cells (Zacharek et al., 2011). As such, it is an attractive candidate for use in immortalisation of non-malignant primary cells. Early work using lentiviral induced expression of a combination of both hTERT and BMI-1 showed a normal diploid karyotype over 15 passages (Fulcher et al., 2009). Indeed, BMI-1 expression via

lentivirus infection has been observed by other members of Barts Cancer Institute to result in immortalised cells with superior karyotypic stability over 20 passages compared to those transfected with hTERT (personal communication – Dr Tyson Sharp). Lentiviral technology is particularly useful in this context as it is a robust method of achieving long-term expression of a transgene *in vitro* (Kumar and Woon-Khiong, 2011).

Non-malignant endometrial tissue was obtained following hysterectomy and both epithelial and stromal cells were isolated and prepared for lentiviral transfection of BMI-1. After approximately one week of cell culture post-infection, the epithelial cells began displaying a mesenchymal morphology and EMT was confirmed by vimentin staining. The propensity of BMI-1 to induce EMT has recently been documented (Li et al., 2014) and so it is possible that this process was induced as a result of the immortalisation method employed. Whilst immortalised stromal cells behaved as expected, they did not adhere to the plastic culture dish for longer than two weeks. Due to limitations on the availability of non-malignant endometrial tissue, repetition of primary cell immortalisation was not possible. However, future attempts of stromal cell immortalisation should assess the effect of coating culture plates with collagen prior to cell culture to increase efficiency of cell attachment and proliferation.

Identification of an FGFR-inhibitor resistant population of MFE-296 cells using a 3D organotypic model

The use of 3D cell culture models has been used to great effect in delineating cell-cell interactions as well as the phenotypic consequences of drug treatment in a range of cancer types (Chioni and Grose, 2012, Coleman et al., 2014, Froeling et al., 2009, Mauchamp et al., 1998, Nystrom et al., 2005, Sakamoto et al., 2001, Sanderson et al., 1996, Vukicevic et al., 1990). An *in vitro* model of endometrial cancer has been lacking and so we set out to establish such organotypic cultures.

One advantage of the organotypic model is the ability to assess the effect of drug treatment over prolonged time periods. Our 3D culture model identified the differential effects of FGFR inhibitor treatment on two FGFR2 mutant cell lines, which were consistent with our previous 2D culture data. The importance of mutant FGFR2 in the AN3CA cell line was demonstrated by induction of cell death upon FGFR inhibition after seven days.

The reduced sensitivity of MFE-296 cells to FGFR inhibition, demonstrated in 2D culture, was recapitulated in the organotypic model. Most interestingly, while cell number was decreased upon PD173074 and AZD4547 treatment, compared to the DMSO control, the beginnings of an inhibitor resistant population remained after 14 days and retained its ability to proliferate. The specificity of these data to FGFR2 mutant cell lines was demonstrated using the FGFR2 wild type Ishikawa cell line. The absence of cell growth and proliferation inhibition in Ishikawa cells suggests the effects observed in the FGFR2 mutant cell lines are due to blockade of aberrant FGFR2 signalling rather than off target effects of the inhibitor. However, further validation using additional cell lines should be performed in the future to confirm the specificity of the effect to FGFR2 mutant cells.

Similar organotypic models have been used to evaluate the invasive capacity of a range of cancer cell types (Chioni and Grose, 2012, Coleman et al., 2014). Our model did not show invasion of endometrial cancer cells into the stromal equivalent layer. However, endometrial cancer cell metastasis can occur through retrograde menstruation and subsequent implantation of endometrial cells in, for example, the ovaries (Kurman and Shih le, 2011). Therefore, the model was modified to encompass this possibility and to assess the effect of FGFR inhibition on this mode of migration.

Full submersion of the organotypic cultures in medium showed the ability of MFE-296 cells to bud from the organotypic culture and either remain free in the medium or re-adhere to the culture plate. After 14 days of FGFR inhibition, free and re-adhered

cell number was decreased; however, the viability of these cells, relative to the DMSO treated control cultures, was demonstrated using trypan blue staining. These data, as with those from the supporting organotypic models of MFE-296 cells, show the establishment of an FGFR inhibitor resistant population.

Whilst the 3D culture was useful in assessing the effects of drug treatment on endometrial cancer cells and could be modified to answer a range of questions, the model was time consuming. As such, it may be of more value to proceed with 2D culture experiments in the future, especially as we have shown the results thus far can be recapitulated in both systems. This would allow for analysis of more cell lines and use of more small molecule inhibitors in a similar timeframe.

Emergence of drug resistant clones of cancer cells in a population can be acquired through a number of mechanisms, from up-regulation of efflux proteins to rewiring of signalling cascades to compensate for inhibition of an important pathway (Ambudkar et al., 1999, Faratian et al., 2009, Flaherty et al., 2010, Goltsov et al., 2011, Goltsov et al., 2012, Gottesman et al., 2002, Wagle et al., 2011). To fully understand the potential of FGFR inhibitors in treatment of FGFR2 mutant endometrial cancer, as well as assess viable strategies to overcome this observed resistance, the mechanism underlying the development of this population was subsequently explored (Chapters 4 and 5).

Chapter 4

Results: Investigation of FGFR inhibitor resistance in MFE-296 cells

4.1 Introduction

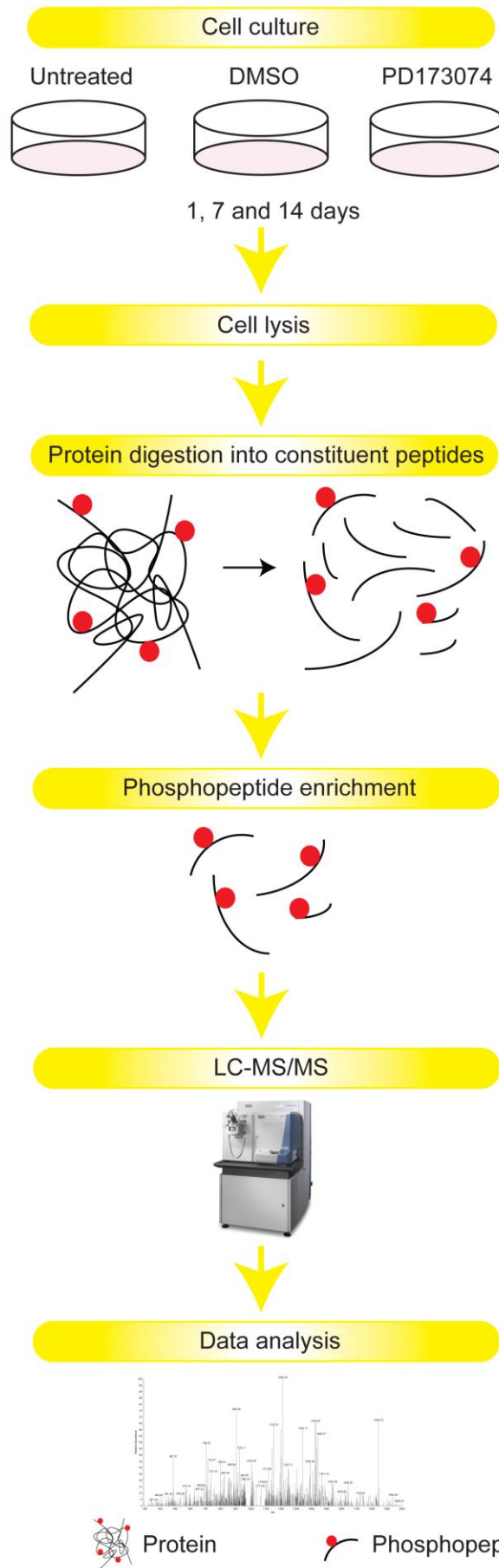
Small molecule inhibition of FGFR signalling in FGFR2 mutant endometrial cancer has been postulated as a viable therapeutic target (Byron et al., 2008, Dutt et al., 2008, Konecny et al., 2013). However, as resistance to both chemotherapy and hormone therapy is common in recurrent endometrial cancer, and acquired and intrinsic resistance to small molecule inhibitors have been documented in other carcinomas (Chell et al., 2013, Goltsov et al., 2012, Goltsov et al., 2011, Lito et al., 2013, Wagle et al., 2011, Zhang et al., 2009), the efficacy of prolonged FGFR-targeted therapy is an important area of study.

Drug resistance remains one of the biggest challenges in cancer therapeutics (Holohan et al., 2013). To overcome this, we require a greater understanding of how resistance is acquired and need to view cell signalling as an interconnected network, capable of rewiring upon inhibition of the dominant signalling pathways. To dissect the changes in an intracellular signalling network, it is essential to have an unbiased, quantitative and well-validated assay. MS-based phosphoproteomics has previously been reported as a tool capable of identifying signalling pathways that contribute to intrinsic resistance to targeted therapies (Alcolea et al., 2012, Casado et al., 2013a, Casado and Cutillas, 2011, Casado et al., 2013b). This technique could also, in principle, be used to define potential compensatory pathways that could be targeted alongside FGFR inhibition.

Initial data assessing the effect of FGFR inhibition in FGFR2 mutant endometrial cancer showed one cell line acquired resistance to drug treatment over 14 days exposure to an FGFR-targeted small molecule inhibitor. To investigate the mechanism of this resistance, MS was employed. Measuring signalling networks using global phosphoproteomics should allow us to: (i) further understand the plasticity of signalling networks upon perturbation of one of their components and (ii) define compensatory pathways in drug resistant cell lines.

4.2 Phosphoproteomic investigation of resistance acquisition in MFE-296 cells

An unbiased phosphoproteomic approach was adopted to investigate the mode of resistance to FGFR inhibition in MFE-296 cells. Cells were treated with PD173074 (PD), DMSO vehicle control (DMSO) or left untreated (UT) for one, seven or 14 days in 2D culture, after which MS was used to assess changes in the global phosphoproteome (Figure 4.1).



 10cm² dish

 Protein

 Phosphopeptide

 Peptide

Figure 4.1. Workflow of MS employed to detect changes in the phosphoproteome of MFE-296 cells upon inhibition of FGFR signalling.

Cells were cultured for one, seven and 14 days in the presence of PD173074, DMSO as a vehicle control, or were left untreated. Cells were then lysed and digested into their constituent peptides by trypsinisation. The resulting peptide mixture was enriched for phosphopeptides via MOAC using TiO₂ affinity beads. The phosphopeptide fraction was then run through the MS. A full MS¹ survey scan was performed; the top seven most intense multiply charged precursor ions were automatically mass selected and fragmented by CID-MSA and analysed in the LTQ-Velos linear ion trap. Two biological replicates of each condition were run through the MS in duplicate. Phosphopeptides were identified using the Mascot search engine and quantified using PESCAL.

We identified a total of 6706 unique phosphopeptide ions (i.e. phosphorylation sites) across four replicates (two biological and two technical). The false discovery rate (FDR) was <1% for 95% of identifications and <5% for the remainder (Appendix Figure 1.8 A). A previously described, well established, label-free methodology was used to identify (Mascot) and quantify (PESCAL) the phosphorylation sites (Alcolea et al., 2012, Casado et al., 2013a). After quantile normalisation (Appendix Figure 1.8 B and C), statistical analysis was performed.

Hierarchical clustering of the average intensities of the resulting phosphorylation motifs was used to assess the similarity of the phosphoproteome across the time points and treatments (Figure 4.2 A). The resulting dendrogram showed all treatments at one day (blue) and 14 days (orange) clustered together, indicating a high degree of similarity between the intensities of phosphopeptides identified in these samples. However, the seven day PD173074 treatment (green) clustered away from the DMSO and UT controls at the same time point, as well as from all samples at one and 14 days. This indicated that the seven day treatment of MFE-296 cells with PD173074 induced a change in the global phosphoproteome of this cell line that was distinct from the DMSO or UT samples.

Of the 6706 phosphopeptides identified, 525 were significantly up- or down-regulated in the PD samples compared to the DMSO control for at least one time point (adjusted $P < 0.05$). These phosphopeptides were grouped according to their temporal profile (Figure 4.2 B, left panel), with 412 down-regulated at seven days, but returning to baseline levels after 14 days of exposure to PD173074 (Figure 4.2 B, clusters 1 and 2). An increase in the \log_2 fold-ratio of 104 phosphopeptides was induced after seven days, which returned to baseline levels after 14 days PD173074 treatment (Figure 4.2 B, cluster 3). Clustering analysis also identified nine phosphopeptides whose abundance was stable at one and seven days, but increased after 14 days PD173074 treatment compared to the DMSO control (Figure 4.2 B, cluster 4, Figure 4.3).

Interestingly, FGFR inhibition did not induce a significant change in the phosphoproteome compared to the DMSO control after one day of exposure to inhibitor (Figure 4.2 B). This lack of phenotypic change upon one day of FGFR inhibition in MFE-296 cells was confirmed in our 3D organotypic model (Figure 4.4). Cultures were prepared as detailed in Figure 1.9 A and treated with 2 μ M PD173074 or a DMSO control for one day, upon which cultures were formalin fixed and sectioned for histochemical and immunohistochemical analysis. There was no significant difference in cell number or proliferation (Ki67 staining, green) in MFE-296 cells after seven days of drug treatment.

To determine kinase activity from these data, the 525 significantly changed phosphopeptides were analysed using Kinase Substrate Enrichment Analysis (KSEA) (Casado et al., 2013b) (Figure 4.2 B, middle panel). This analysis allows phosphopeptides to be grouped according to their upstream kinase, based on annotated kinase-substrate relationships from three, independent databases (PhosphoPoint, Phospho.ELM and PhosphoSite). KSEA thus allows inference of the activities of kinases active in the system. Analysis of the KSEA output demonstrated that phosphopeptides known to be downstream of AKT and AKT-related pathways were significantly enriched (according to a hypergeometric t-test) in clusters 1 and 2 (Figure 4.2 B and C). For example, as well as direct AKT targets, mTOR, serine/threonine protein kinase Pim-2 (PIM2) and PIM3 substrates were significantly down-regulated at seven days and returned to basal levels at 14 days. All of these molecules are associated with AKT signalling (Facchinetti et al., 2008, Inoki et al., 2002, Meja et al., 2014, Narlik-Grassow et al., 2013, Potter et al., 2002, Sarbassov et al., 2005, Wang et al., 2006). The down-regulation and subsequent re-establishment of AKT signalling in FGFR inhibitor treated MFE-296 cells indicates this pathway may be critical to acquisition of drug resistance in this cell line.

The potential importance of AKT related signalling in establishment of an FGFR inhibitor resistant cell line is highlighted further by the nine phosphopeptides that are up-regulated at 14 days drug exposure, compared to the DMSO control (Figure 4.2 B, Figure 4.3). The phosphorylation sites of these peptides could not be identified

with absolute certainty, owing to their inadequate fragmentation, i.e. multiple potential phosphorylation sites exist closely together within the peptide. Because of this, these peptides could not be clustered using KSEA. However, whilst their exact phosphorylation site could not be determined, peptide identification could be achieved from the MS¹ spectra. Of these nine peptides, four of them, poly(rC)-binding protein 1 (PCBP1), eukaryotic translation initiation factor 4E binding protein 2 (EIF4EBP2) (two phosphopeptides identified) and Yes-associated protein 1 (YAP1), are implicated in AKT signalling (Chaudhury et al., 2010, Hussey et al., 2011, Ma et al., 2014, Morita et al., 2013, Roux and Topisirovic, 2012, Song et al., 2014, Zhang and Dou, 2014). This further reinforced the potential importance of the AKT pathway in FGFR inhibitor resistance acquisition. This was subsequently investigated using the 3D organotypic model.

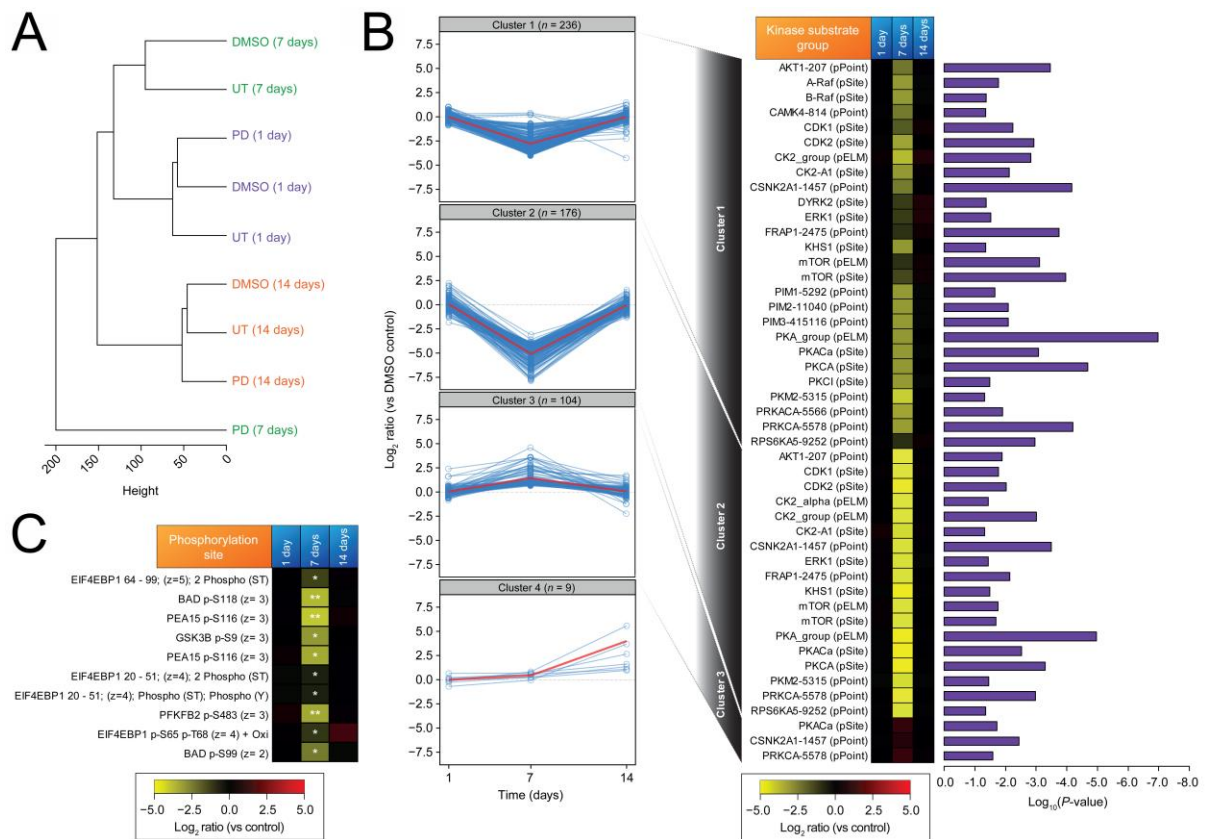


Figure 4.2. Phosphoproteomic analysis of FGFR-inhibitor resistance acquisition in MFE-296 cells.

MFE-296 cells were treated with DMSO vehicle control (DMSO), 2 μ M PD173074 (PD) or untreated (UT) for one, seven or 14 days, after which lysates were collected, tryptic digest performed and the resulting peptides enriched for phosphopeptides. MS was employed to analyse differences in phosphorylation patterns of peptides upon FGFR inhibition. (A) To determine the similarity of phosphorylation patterns across the various treatments and time points, hierarchical clustering (Pearson Correlation distance metric) of the average intensities of the resulting phosphorylation motifs represented in the phosphopeptides identified was employed. The dendrogram shows all treatments at one (blue) and 14 days (orange) clustered together, indicating a high degree of similarity between the intensities of the phosphopeptides identified in these samples. At seven days (green) the PD sample clustered away from the DMSO and UT controls, as well as from all samples at one and 14 days. Treatment of MFE-296 cells with PD173074 for seven days induced a change in the global phosphoproteome of this cell line. (B) MS identified 6706 unique phosphopeptides in total across all samples. Of these, 525 were significantly up- or down-regulated in the PD samples compared to the DMSO control for at least one time point, and were grouped according to their phosphorylation pattern using unsupervised clustering (clusters 1-4; left panel). The resulting phosphopeptides were analysed using Kinase Substrate Enrichment

Analysis (KSEA) and grouped in a heatmap according to their upstream kinases (middle panel). P values of each group are shown as bars (right panel). pPoint, pSite and pELM in the heatmap represent the database employed by KSEA to cluster substrates into their kinase groups (phosphoPoint, phosphoSite and phospho.ELM respectively). Blue lines in the clusters represent individual phosphopeptides; the red lines represent the line of best fit. (C) Heatmap of phosphopeptides downstream of AKT which were significantly down-regulated at seven days PD173074 treatment, compared to the DMSO control. z indicates number of potential phosphorylation sites identified on each peptide; 2 phospho indicates two phosphorylation sites were identified on the preceding residues (S, serine; T, threonine; Y, tyrosine); pS118 etc indicates phosphorylation on S or T at the residue indicated by the number; Oxi indicates the phosphopeptide was oxidised; numbers preceding protein name indicate phosphopeptide length. Data represent average of two technical replicates of two biological replicates, i.e. each replicate was run through the MS twice. *, $P \leq 0.05$, **, $P \leq 0.01$.

Phosphorylation site	Phosphorylation site		
	1 day	7 days	14 days
PCBP1 244 - 268; (z=3); Gln->pyro-Glu (N-term Q); Oxidation (M); Phospho (ST)			*
EIF4EBP2 21 - 57; (z=4); Phospho (ST); Phospho (Y)			*
YAP1 350 - 375; (z=3); Oxidation (M); Phospho (ST)			**
PTPN23 1113 - 1152; (z=4); Phospho (ST)			*
EIF4EBP2 21 - 51; (z=3); Phospho (ST)			*
ARHGEF17 498 - 535; (z=4); 2 Phospho (ST)			***
SYAP1 259 - 292; (z=3); Phospho (ST)			*

Figure 4.3. Phosphopeptides showing significant up-regulation after 14 days PD173074 treatment.

Significantly up- or down-regulated phosphopeptides, identified via MS, were clustered according to their upstream kinases (Figure. 4.2 B); KSEA analysis was unable to identify the upstream kinases of phosphopeptides identified in cluster 4. These phosphopeptides, and their up-regulation compared to the DMSO control, are shown in the heatmap. Four of these are implicated in AKT signalling (PCBP1, EIF4EBP2 - two phosphopeptides identified, YAP). z indicates number of potential phosphorylation sites identified on each peptide; 2 phospho indicates two phosphorylation sites were identified on the preceding residues (S, serine; T, threonine; Y, tyrosine); M, methionine; N-term Q indicates the N terminus of the peptide was a glutamine residue; numbers preceding protein name indicate phosphopeptide length. *, P < 0.05, **, P < 0.01, ***, P < 0.001.

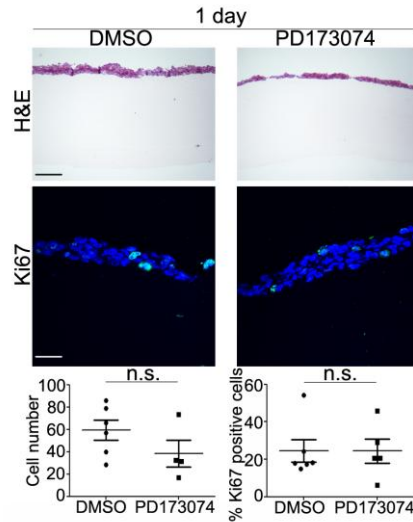


Figure 4.4. Effect of FGFR inhibition on MFE-296 cells after one day PD173074 treatment.

The 3D organotypic model was prepared as detailed in Figure 1.9 A. MFE-296 cells were treated with of 2 μ M PD173074 or DMSO control for one day. There was no difference in cell number or proliferation, indicated by Ki67 staining (green), between FGFR inhibitor treated and control treated cultures. Original magnification of H&E images, 10X objective; bar, 100 μ m. Original magnification of confocal images, 40X objective; bar, 25 μ m. Error bars show means \pm SEM. Data points represent the average cell number/percentage of Ki67 positive cells of six fields of view of two to three technical replicates of two biological replicates. Cell number and percent Ki67 positive cells represents average values per field of view.

4.3 Effect of AKT inhibition alone and in combination with FGFR inhibition in MFE-296 cells

To explore the significance of AKT signalling in FGFR inhibitor resistance, MFE-296 cells were treated with one of two AKT inhibitors, alone or in combination with PD173074, in the 3D organotypic model (Figure 4.5). The AKT inhibitors used were AKTVIII, an allosteric AKT1 and 2 inhibitor (Lindsley et al., 2005), and MK2206, which allosterically targets AKT1, 2 and 3 (Hirai et al., 2010). Ishikawa cells were treated in an identical fashion as a control (Figure 4.6).

Treatment with AKTVIII alone for seven days did not significantly change either cell number or the percentage of proliferating cells (Figure 4.5 A). MK2206, alone and in combination with PD173074, did significantly reduce cell number over seven days. However, only AKTVIII/PD173074 and MK2206/PD173074 treatments led to a reduction in the percentage of proliferating cells.

Over 14 days, cell number was decreased upon all drug treatments compared to the control (Figure 4.5. B). However, only MK2206, MK2206/PD173074 and AKTVIII/PD173074 combination treatments led to a significant reduction in the number of cells capable of proliferation compared to the DMSO control. In MK2206 treated cultures, a distinct cell population remained. In MK2206/PD173074 treated cells, few cells remained and thus FGFR and AKT1, 2 and 3 inhibition was sufficient to overcome FGFR inhibitor resistance in MFE-296 cells.

Ishikawa cells were largely unaffected by drug treatments, indicating the effects seen in MFE-296 cells were potentially FGFR mutation status dependent (Figure 4.6).

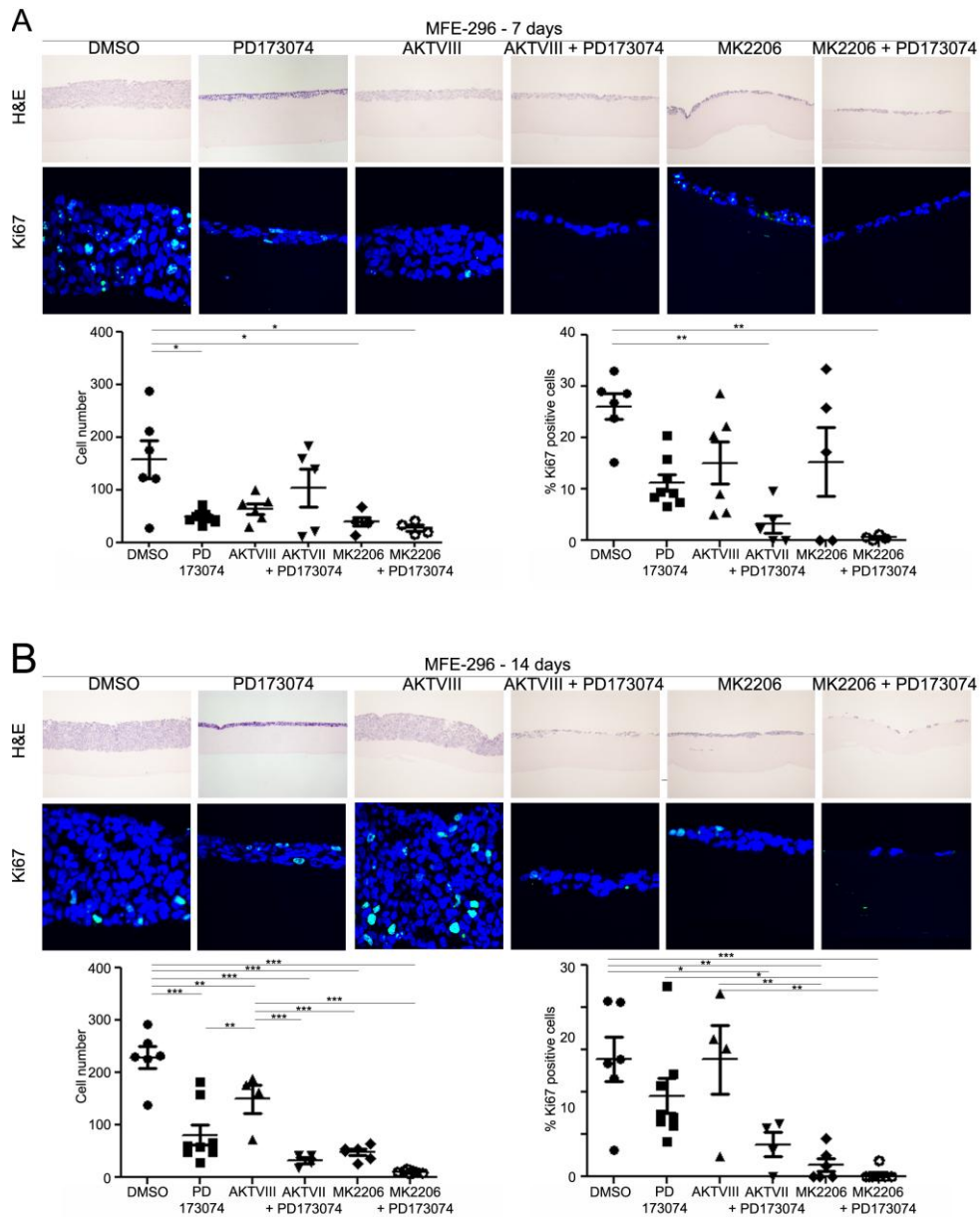


Figure 4.5. Effect of AKT inhibition, alone and in combination with FGFR inhibition, in MFE-296 cells in a 3D physiometric model.

Cultures were prepared as outlined in Figure 1.9 A. (A) MFE-296 cells were treated with 2 μ M PD173074, 1 μ M AKTVIII, 1 μ M MK2206, 2 μ M PD173074 in combination with 1 μ M of either AKTVIII or MK2206 or DMSO as a control for seven days. Cell number was significantly decreased in PD173074, MK2206 and MK2206/PD173074 treated cells compared to the DMSO control. Proliferation (Ki67 staining, green) was significantly reduced in cultures treated with AKTVIII/PD173074 and MK2206/PD173074 compared to the DMSO control. (B) MFE-296 cells were treated as in A for 14 days. Cell number was significantly decreased in all cultures compared to the DMSO control. However, cell number was significantly higher in cultures treated with AKTVIII compared to all other small molecule

inhibitor treated cultures. Cell proliferation was only decreased in MK2206, MK2206/PD173074 and AKTVIII/PD173074 treated cultures compared to the DMSO control. *, $P \leq 0.05$; **, $P \leq 0.01$; ***, $P \leq 0.001$ (one-way ANOVA). Nuclei were stained with DAPI (blue). Original magnification of H&E images, 10X objective; bar, 100 μm . Original magnification of confocal images, 40X objective; bar, 25 μm . Error bars show means \pm SEM. Data points represent the average cell number/percentage of Ki67 positive cells of six fields of view of one to three technical replicates of three biological replicates. Cell number and percent Ki67 positive cells represents average values per field of view.

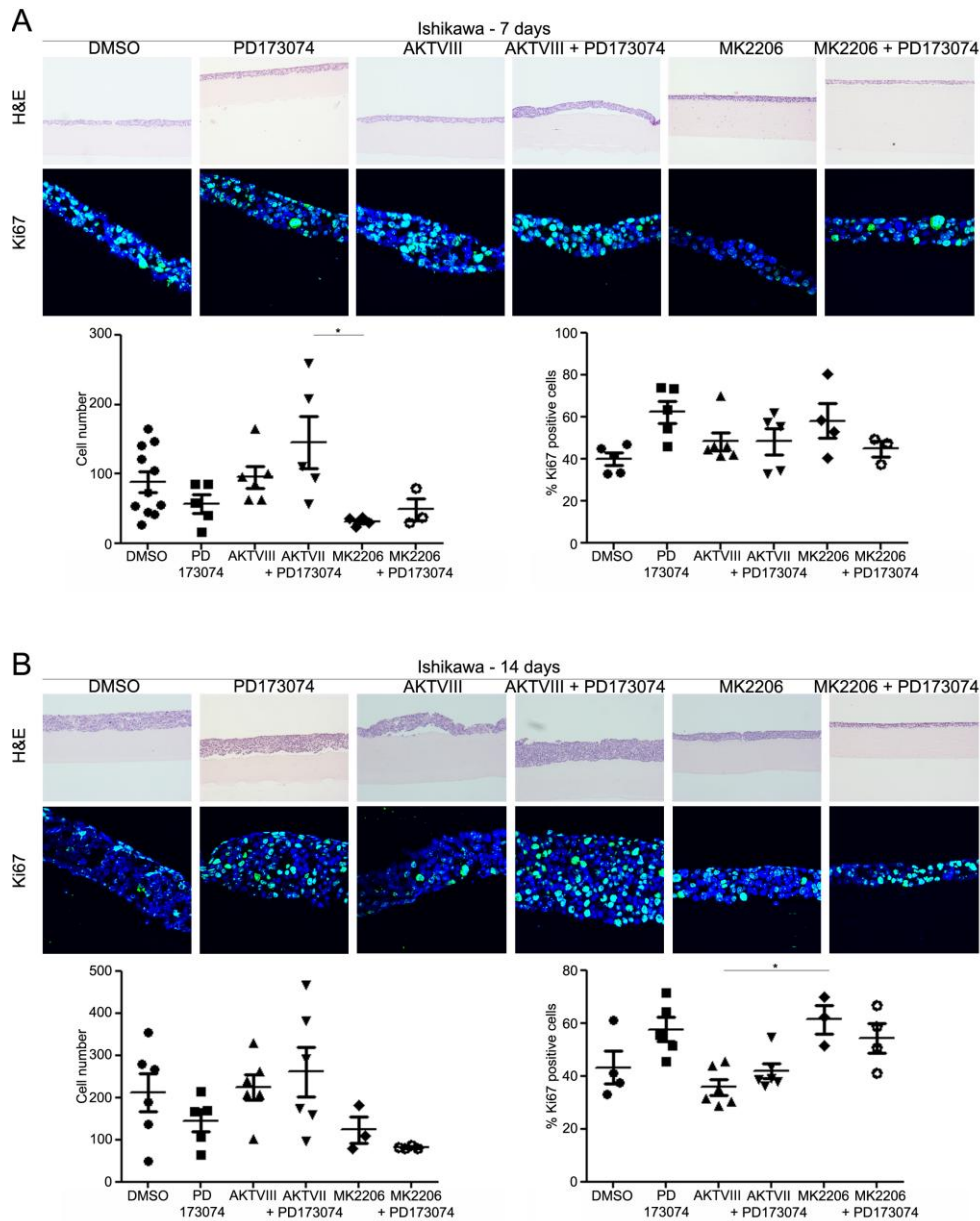


Figure 4.6. Effect of AKT inhibition, alone and in combination with FGFR inhibition, in Ishikawa cells in a 3D physiomimetic model.

Cultures were prepared as described in Figure 1.9 A. (A) Ishikawa cells were treated with 2 μ M PD173074, 1 μ M AKTVIII, 1 μ M MK2206, 2 μ M PD173074 in combination with 1 μ M of either AKTVIII or MK2206 or DMSO as a control for seven days. Cell number was significantly decreased in MK2206 cultures compared to AKTVIII/PD173074 treated cells only. There was no significant effect on the percentage of cells positive for Ki67 in any treatment. (B) Ishikawa cells were treated as in A for 14 days. Cell number was unaffected by any of the small molecule inhibitor treatments. There was, however, a significant increase in the percentage of cells positive for Ki67 between AKTVIII and MK2206 treated cultures. *, $P \leq 0.05$; **, $P \leq 0.01$; ***, $P \leq 0.001$ (one-way ANOVA). Nuclei were stained with DAPI (blue).

Original magnification of H&E images, 10X objective; bar, 100 μm . Original magnification of confocal images, 40X objective; bar, 25 μm . Error bars show means \pm SEM. Data points represent the average cell number/percentage of Ki67 positive cells of six fields of view of one to three technical replicates of three biological replicates. Cell number and percent Ki67 positive cells represents average values per field of view.

The reproducibility of these data was examined by seven day treatment of organotypic cultures with AKTVIII and MK2206 in combination with 1 μ M of the FGFR inhibitor AZD4547 (Figure 4.7). In both treatments, cell number and proliferation was significantly decreased compared to the control, recapitulating the effect of seven day combination treatment with PD173074 (Figure 4.5 A).

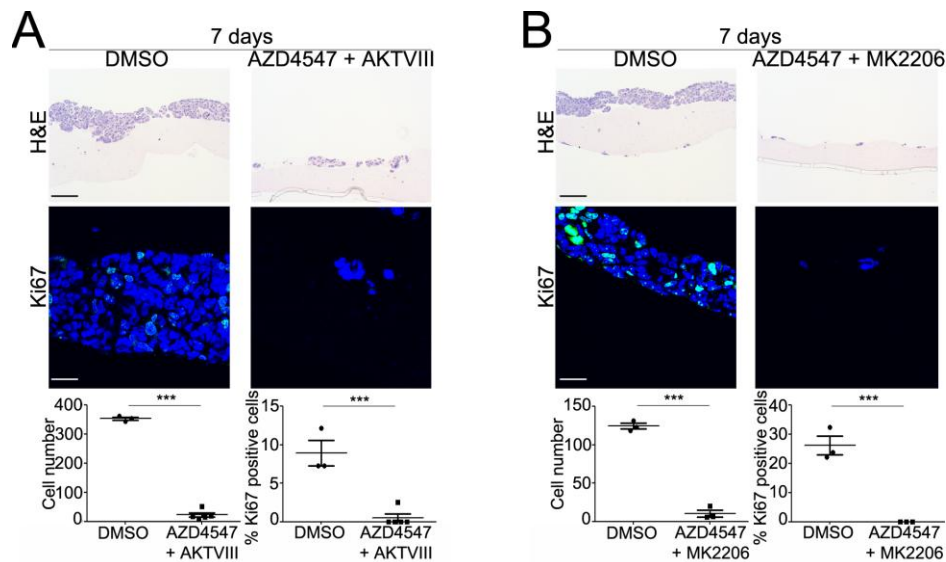


Figure 4.7. AKT inhibition in combination with the FGFR inhibitor AZD4547, for seven days, overcomes FGFR inhibitor resistance in MFE-296 cells.

Cultures were prepared as outlined in Figure 1.9 B and treated with 1 μ M AZD4547 in combination with 1 μ M AKTVIII (A) or 1 μ M MK2206 (B). (A) AKT1 and 2 inhibition, in combination with FGFR inhibitor treatment, significantly decreased both cell number and proliferation (Ki67 staining, green) after seven days. (B) Inhibition of AKT1, 2 and 3 in combination with FGFR signalling significantly reduced both cell number and proliferation. These data recapitulate those seen with another FGFR inhibitor, PD173074 (Figure 4.5 B and 4.6 B). ***, $P \leq 0.001$ (Student's t test). Nuclei were stained with DAPI (blue). Original magnification of H&E images, 10X objective; bar, 100 μ m. Original magnification of confocal images, 40X objective; bar, 25 μ m. Error bars show means \pm SEM. Data points represent the average cell number/percentage of Ki67 positive cells of three fields of view of one to three technical replicates of three biological replicates. Cell number and percent Ki67 positive cells represents average values per field of view.

4.4 Summary of results

- MS can be used to delineate changes in signalling upon drug treatment in endometrial cancer cells
- Approximately 7000 phosphopeptides were identified using MS; of these over 500 were significantly up- or down-regulated in PD173074-treated samples compared to the control
- A change in the phosphoproteome was induced after seven days FGFR inhibition; approximately 400 phosphopeptides were significantly down-regulated compared to the control. These returned to basal levels at 14 days; direct substrates of AKT or pathways associated with AKT were enriched in this subset of phosphopeptides
- Nine phosphopeptides were significantly up-regulated after 14 days FGFR inhibition. Four of these were implicated in AKT signalling
- AKT was identified as having a potential role in FGFR inhibitor resistance acquisition
- The 3D organotypic model of endometrial cancer was used to assess the effect of AKT inhibition alone and in combination with FGFR inhibition
- Inhibition of AKT1 and 2 or AKT1, 2 and 3 resulted in generation of an inhibitor resistant population
- Drug combination treatment targeting FGFR and AKT1, 2 and 3 led to cell death in FGFR2 mutant endometrial cancer cells

4.5 Discussion

Using an MS phosphoproteomic approach, we have demonstrated the changes in signalling networks upon acquisition of FGFR inhibitor resistance in MFE-296 cells, a FGFR2 mutant cell line. By investigating this, using an unbiased and quantitative approach, we have provided evidence of the importance of AKT signalling in acquisition of FGFR inhibitor resistance. Importantly, the effects of small molecule inhibition outlined in these data are FGFR2 mutation status dependent, as shown by the absence of growth inhibition in the FGFR2 wild-type Ishikawa cell line, in the presence of FGFR inhibitor. Thus, we provide evidence of the utility of phosphoproteomics in elucidating inhibitor resistance mechanisms and identifying viable therapeutic targets. In addition, we have also demonstrated the successful use of 2D and 3D cell culture to complement each other in the delineation of cell signalling changes upon perturbation of a given pathway.

FGFR inhibition induces a distinct change in the global phosphoproteome of MFE-296 cells

Having established that MFE-296 cells acquire resistance to PD173074 treatment, we aimed to identify the underlying changes in cell signalling induced by receptor inhibition. To do this, we used MS, comparing the global phosphoproteome of PD173074 treated MFE-296 cells to control cells. Utilising this technique, we were able to assess differences in the levels of phosphopeptides induced by drug treatment in an unbiased manner and investigate the mechanisms that underlie resistance to targeted compounds (Casado et al., 2013a, Casado et al., 2013b, Cutillas and Vanhaesebroeck, 2007, Alcolea et al., 2012). This highlights the use of MS as a tool to elucidate signalling pathways that play a role in adaptation to small-molecule inhibitor treatment and underscores how this information can be used to identify druggable targets to overcome resistance.

Of the 6706 phosphopeptides identified across all samples, changes in the abundance of 525 were statistically significant in PD173074 treated samples, compared to the DMSO control. Analysis of this subset of phosphopeptides showed

the predominant pattern of phosphorylation across the time points in PD173074 treated cells to be the same as DMSO samples at one day treatment, significant down-regulation at seven days drug exposure, and a return to baseline levels at 14 days. The absence of a significant change in phosphorylation of PD173074-treated cells at one day was surprising, given our initial western blot analysis showing abrogation of P-ERK and decreased P-AKT after two hours PD173074 treatment of MFE-296 cells. However, it was apparent from the MS data that signalling was recovered after 24 hours, while constant exposure to PD173074 for seven days resulted in changes in the phosphoproteome. This was supported by our 3D organotypic analysis, which showed no change in cell number or proliferation of MFE-296 cells treated with PD173074 for one day and a significant decrease in both of these parameters at seven days of inhibitor treatment.

To better understand the signalling pathways identified by the differentially phosphorylated sites, their upstream kinases were inferred using KSEA. Interestingly, a number of phosphorylation sites known to be downstream of AKT followed the baseline – down-regulation – baseline pattern over the three time points in PD173074 treated cells. Phosphorylation sites known to be substrates of kinases downstream of AKT, including mTOR, were also found to follow this pattern, further supporting the findings that the change in AKT signalling identified in the MS data was transmitted downstream. The potential role of AKT signalling in overcoming FGFR inhibitor resistance in MFE-296 cells was further highlighted by up-regulation of four phosphopeptides, each implicated in AKT signalling, after 14 days of drug exposure (Chaudhury et al., 2010, Hussey et al., 2011, Ma et al., 2014, Morita et al., 2013, Roux and Topisirovic, 2012, Song et al., 2014, Zhang and Dou, 2014).

The exact phosphorylation sites of a small number of phosphopeptides could not be determined definitively, due to inadequate fragmentation of the peptide. Furthermore, these peptides possessed multiple potential phosphorylation sites and so the specific phosphorylated residues remained elusive. Whilst the fragmentation method employed in our work (CID-MSA) is routinely used in phosphopeptide analysis (Boersema et al., 2009), more sensitive methods do exist, for example ECD and

HCD, which could be used in future to determine the exact phosphorylated residues in these peptides (Olsen et al., 2007, Syka et al., 2004, Zubarev, 2004). Notably, total protein levels were not assessed in this study. Our work has focused primarily on changes in signalling peptides upon drug exposure, of which phosphopeptides are the most important (Cohen, 2000, Manning et al., 2002). We do, however, acknowledge that analysis of total protein levels adds an additional layer of information to changes within the cell upon drug treatment, and so repetition of this experiment to elucidate such changes may be of interest in the future.

Another potential shortcoming of this study is the number of repeats of the experiment. Due to time constraints, only two biological replicates of each condition were performed. Although these were analysed on the MS twice, producing an n of four for each sample, a more robust experiment would include more biological and technical replicates. Repetition of this experiment using the Ishikawa cell line should also be considered in future work. This would assess the specificity of signalling changes seen in MFE-296 cells upon FGFR inhibition with regards to the FGFR2 mutation status of the cell line.

MS generates a large quantity of data, and validation of all potential pathways highlighted in this analysis is outside of the scope of this study. Whilst the AKT pathway was associated with the most de-regulated phosphopeptides identified in our study, we are nevertheless mindful that pathways other than AKT could have been selected to target alongside FGFR2. Rather than this diminishing the validity of this work, we believe it: (i) reinforces the known complexity of cell signalling; (ii) validates the use of MS as a tool in drug target discovery and (iii) provides evidence of how prior knowledge of the importance of certain proteins in signalling networks can be used to aid selection of potentially important phosphopeptides from MS data.

Inhibition of FGFR in combination with AKT1, 2 and 3 overcomes FGFR inhibitor resistance in MFE-296 cells

To investigate the significance of AKT1, 2 and 3 in this FGFR inhibitor resistance mechanism, two small molecule inhibitors were used; AKTVIII, targeting AKT1 and 2 (Lindsley et al., 2005), and MK2206, which blocks AKT1, 2 and 3 (Hirai et al., 2010). As MK2206 has a more marked effect on cell number and proliferation on MFE-296 cells than AKTVIII, both alone and in combination with PD173074, our data suggest a specific role for AKT3 in the compensatory mechanism. While *in vivo* studies investigating the role of AKT in development and disease have shown different phenotypes for individual knockout of AKT1, 2 and 3, little is known about the specific functions of these isoforms and how they are regulated (Madhunapantula and Robertson, 2011). However, increased AKT3 activity has been shown to play an important role in the development of melanoma (Stahl et al., 2004). AKT1 and 3 have also been shown to be involved in regulation of splicing of FGFR2 in lung cancer (Sanidas et al., 2014). As such, the role of the individual isoforms of AKT in the resistance mechanism outlined in this chapter warrants further investigation.

Dual drug therapy in FGFR2 mutant cancer

The prospect of treating endometrial cancer with a combination of chemotherapeutic drugs or small molecule inhibitors and chemotherapeutics has been outlined previously (Gozgit et al., 2013, Byron et al., 2012). Although these studies investigated the synergistic effects of dual drug therapy, we present the first study to investigate potential resistance mechanisms upon FGFR inhibition and use these data as the rationale for choosing an additional therapeutic target.

FGFR2 mutations are known to be putative oncogenic drivers in other cancers (Su et al., 2014, Hong et al., 2013). It remains to be investigated whether *FGFR2* mutant cell lines derived from such cancers undergo similar reorganisation of their signalling pathways upon FGFR inhibition as that seen in MFE-296 cells. However, we have identified the importance of AKT signalling in overcoming FGFR inhibition, a relationship that may also be important in other *FGFR2* mutant cancers. The

relevance of AKT in relation to FGFR signalling has already been demonstrated in lung and gastric cancers (Sanidas et al., 2014, Hu et al., 2013), yet the implications of AKT signalling in relation to, but not necessarily downstream of, FGFR signalling remain to be fully understood. As such, it is possible that the dual drug treatment identified in this study is applicable to a range of FGFR2 mutant cancers.

Since we have shown that AKT inhibition can overcome FGFR inhibitor resistance in MFE-296 cells, further *in vivo* investigations should be undertaken to establish the potential viability of this FGFR/AKT drug combination in the treatment of endometrial cancer. Although combination trials are not currently underway, initial investigations into neuroblastoma and glioma, amongst others, suggest use of MK2206 alongside other small molecule inhibitors and chemotherapeutics provides an advantage in inducing cancer cell death (Cheng et al., 2012, Li et al., 2012, Agarwal et al., 2013). It is also promising that use of MK2206 alone is currently in clinical trials (Molife et al., 2014), as is the AZD4547 FGFR inhibitor (Xie et al., 2013, Zamora et al., 2014). The combinatorial use of both drugs represents an exciting line of clinical investigation, with the potential to overcome chemoresistance in FGFR2-driven cancers.

While we have established the importance of AKT in acquiring inhibitor resistance in MFE-296 cells, it is important to delineate the mechanism of this compensatory response. As such, further investigation was undertaken to establish the inducer/s of this AKT-mediated recovery in FGFR inhibitor resistance in MFE-296 cells (Chapter 5).

Chapter 5

Results: Investigation of FGFR inhibitor resistance mechanisms in MFE-296 cells

5.1 Introduction

Initial data assessing the effect of FGFR inhibition in FGFR2 mutant endometrial cancer showed the MFE-296 cell line acquired resistance to drug treatment, over 14 days exposure to an FGFR-targeted small molecule inhibitor. To investigate the effect of resistance acquisition on intracellular signalling pathways, MS was employed. From these data, the importance of AKT signalling recovery in drug resistant cells was established and validated using a 3D organotypic model of endometrial cancer. Dual drug therapy targeting FGFR and AKT signalling overcame drug resistance and, importantly, this effect was FGFR2 mutation status dependent.

To fully understand the cellular changes responsible for AKT pathway recovery in FGFR inhibitor resistant cells, microarray gene expression analysis was employed. These data, coupled with the knowledge garnered from MS analysis, were used to delineate the FGFR inhibitor resistance mechanism of FGFR2 mutant endometrial cancer cells.

5.2 Generation and characterisation of an FGFR inhibitor resistant cell line

To investigate the phenotypic and mechanistic consequences of sustained FGFR inhibitor resistance, an FGFR inhibitor resistant population of cells was generated by continuous treatment of MFE-296 cells with 5 μ M PD173074. This inhibitor concentration was decided upon based on initial data showing over 50% reduction in MFE-296 cell number relative to DMSO control treated cells after seven days of 5 μ M PD173074 (Figure 3.3). It was therefore assumed that the resulting population was resistant to PD173074 treatment. This population was named MFE-296^{PDR}. The standard medium for these cells was supplemented with 5 μ M PD173074 from this point onwards.

The FGFR2 mutation status of MFE-296^{PDR} cells was assessed at approximately passage 15. The resistant cell line harboured the same N550K and K310R mutations as its MFE-296 parental cell line (Appendix Figure 1.9).

At approximately the same passage, the effect of increasing PD173074 concentration on MFE-296^{PDR} cells after seven days in 2D culture was assessed. The same PD173074 concentrations as those used to treat parental cells in our initial investigations were used (Figure 3.3). PD173074 treatment of MFE-296^{PDR} cells from 10–10000 nM did not decrease cell number (Figure 5.1).

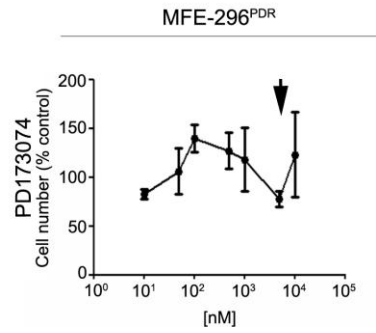


Figure 5.1. Effect of PD173074 treatment on MFE-296^{PDR} cells in 2D culture.

MFE-296^{PDR} cells were treated with the same concentrations of PD173074 as the parental MFE-296 cell line had been treated previously (Figure 3.3). After seven days, cells were counted using a haemocytometer and the values displayed as a percentage of DMSO control treated cell number. FGFR inhibition did not induce cell death in MFE-296^{PDR} cells. Arrow indicates concentration of PD173074 supplemented in MFE-296^{PDR} cell medium in all subsequent experiments (5 μ M PD173074). Error bars show means \pm SEM of three replicates.

Changes in the signalling capacity of MFE-296 parental cells, upon 5 μ M PD173074 treatment, and MFE-296^{PDR} cells, upon removal of the drug, were investigated. ERK phosphorylation was decreased upon PD173074 treatment in MFE-296 cells after both seven and 14 days (Figure 5.2 A, left panel). Interestingly, removal of PD173074 from the medium of MFE-296^{PDR} cells significantly increased P-ERK levels (Figure 5.2 A and B, right panel). Indeed, ERK phosphorylation in MFE-296^{PDR} cells in the absence of PD173074 was increased compared to the MFE-296 parental cell line. AKT phosphorylation remained unchanged in both MFE-296 and MFE-296^{PDR} cells regardless of PD173074 treatment (Figure 5.2 A and B).

The consequences of drug removal from the established MFE-296^{PDR} cell line were investigated further in 3D culture. There was no significant difference in cell number, or the percentage of cells able to proliferate, between cultures grown in 5 μ M PD173074 or DMSO vehicle control (Figure 5.3).

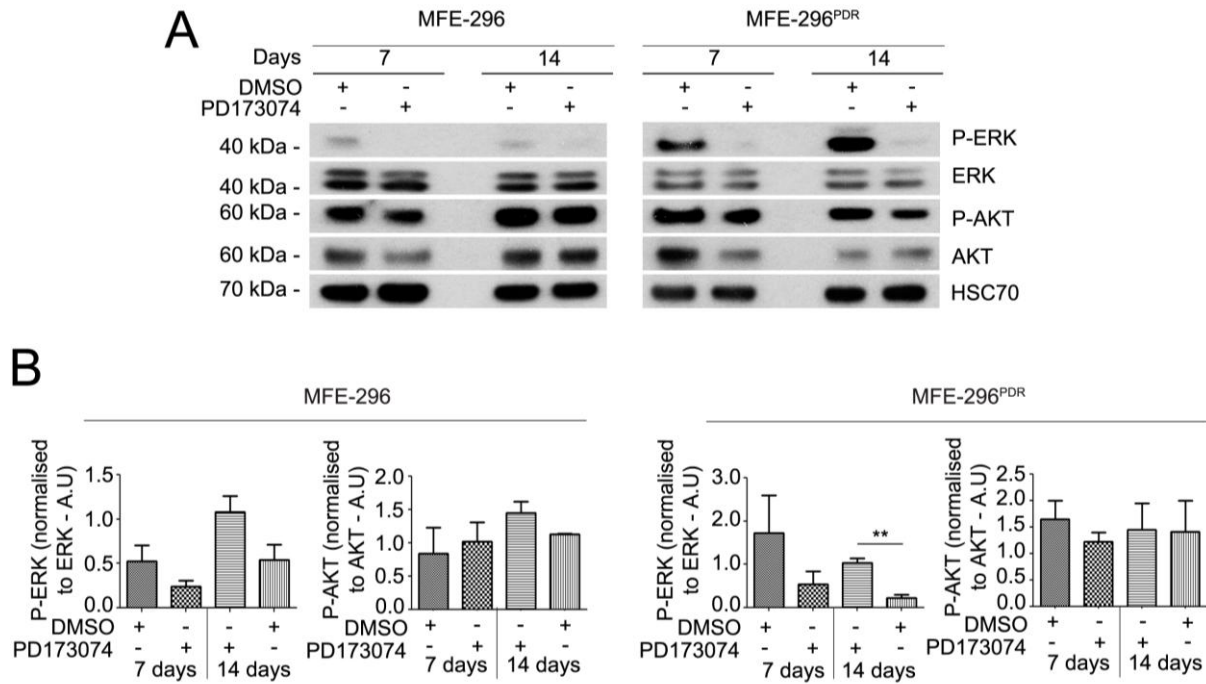


Figure 5.2. Changes in signalling upon PD173074 treatment in MFE-296 parental and MFE-296^{PDR} cells.

MFE-296 and MFE-296^{PDR} cells were cultured in the presence or absence of 5 μ M PD173074 for seven and 14 days, after which western blot analysis was performed to investigate changes in key signalling pathways. (A) ERK phosphorylation was inhibited upon PD173074 treatment in MFE-296 cells. Removal of PD173074 from MFE-296^{PDR} cell medium resulted in a significant increase in ERK phosphorylation. AKT phosphorylation was unchanged regardless of the presence or absence of PD173074 after seven or 14 days. (B) Densitometric analysis of P-ERK and P-AKT levels compared to their total protein counterparts. **, $P \leq 0.01$ (Student's *t* test). 20 μ g protein was used for each lane. Error bars show means \pm SEM of three replicates.

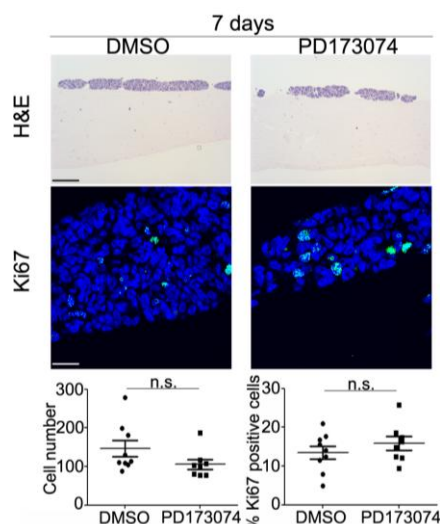


Figure 5.3. Effect of drug removal on MFE-296^{PDR} cell number and proliferation in a 3D physiomimetic model.

Organotypic cultures of MFE-296^{PDR} cells were prepared as detailed in Figure 1.9 B. MFE-296^{PDR} cells were grown in the presence or absence of 5 μ M PD173074 for seven days. There was no significant difference in cell number, or the percentage of proliferative cells (Ki67, green), between cultures in the presence or absence of PD173074. n.s., not significant, $P > 0.05$ (Student's t test). Nuclei were stained with DAPI (blue). Original magnification of H&E images, 10X objective; bar, 100 μ m. Original magnification of confocal images, 40X objective; bar, 25 μ m. Error bars show means \pm SEM. Data points represent the average cell number/percentage Ki67 positive cells of three fields of view of two to three technical replicates of three biological replicates. Cell number and percent Ki67 positive cells represent average values per field of view.

Analysis of changes in the phosphoproteome of MFE-296 cells upon inhibition of FGFR signalling, via exposure to PD173074, indicated a potential role for AKT signalling in acquiring this resistance (Figures 4.2 and 4.3). Subsequent 3D organotypic modelling showed that dual drug treatment, targeting the AKT1, 2, 3 and FGFR pathways, could overcome this resistance in MFE-296 cells (Figure 4.6). The effect of these drug combinations on cells with established PD173074 resistance was investigated.

MFE-296^{PDR} cells were cultured for seven days in the presence of two AKT inhibitors alone or in the presence of PD173074. Control culture medium was supplemented with 5 μ M PD173074.

MFE-296^{PDR} cells were resistant to inhibition of AKT1 and 2 using 1 μ M AKTVIII (Figure 5.4. A). However, dual drug treatment using AKTVIII in combination with PD173074 significantly decreased both cell growth and the percentage of cells capable of proliferation (Figure 5.4 B). Inhibition of AKT1, 2 and 3 for seven days with 1 μ M MK2206 significantly decreased both cell number and proliferation of MFE-296^{PDR} cells (Figure 5.4 C), as did MK2206 and PD173074 dual drug treatment (Figure 5.4 D).

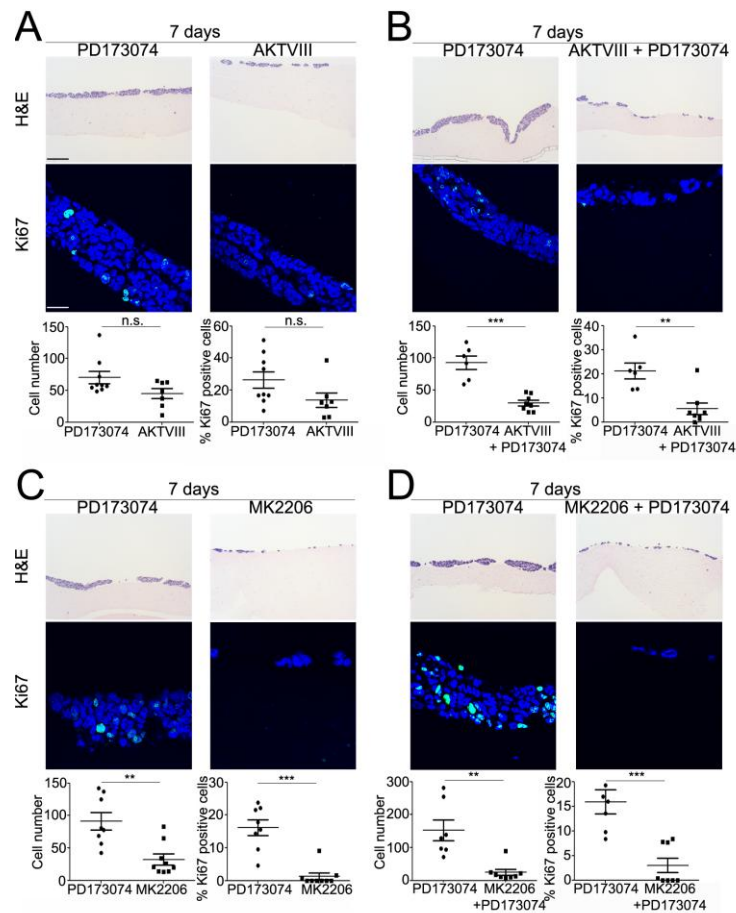


Figure 5.4. Effect of AKT inhibition, in the presence or absence of PD173074, in MFE-296^{PDR} cells in a 3D organotypic model.

3D cultures of MFE-296^{PDR} cells were prepared as detailed in Figure 1.9 B. Cultures were treated with 5 μ M PD173074 as a control. (A) There was no significant difference in cell number or percentage of proliferative cells (Ki67, green), between cells treated with PD173074 and those treated with 1 μ M AKTVIII for seven days. (B) Both cell number and percentage of Ki67 positive cells decreased in cultures treated with both PD173074 and AKTVIII for seven days. (C) Cell number and the percentage of cells that stained positive for Ki67 significantly decreased upon 1 μ M MK2206 treatment. (D) Both cell number and percentage of Ki67 positive cells decreased in cultures treated with both PD173074 and MK2206 for seven days. n.s., not significant, $P > 0.05$; **, $P \leq 0.01$; ***, $P \leq 0.001$ (Student's t test). Nuclei were stained with DAPI (blue). Original magnification of H&E images, 10X objective; bar, 100 μ m. Original magnification of confocal images, 40X objective; bar, 25 μ m. Error bars show means \pm SEM. Data points represent the average cell number/percentage of Ki67 positive cells of three fields of view of two to three technical replicates of three biological replicates. Cell number and percent Ki67 positive cells represents average values per field of view.

MK2206 treatment, both alone and in combination with PD173074, had a significant effect on both cell number and the proliferative capacity of MFE-296^{PDR} cells. The effect of MK2206 alone, as well as PD173074 removal, PD173074 alone and MK2206/PD173074 combination treatment, on a mixed population of parental MFE-296 and MFE-296^{PDR} cells was investigated.

Both cell lines were labelled with distinct fluorescent dyes. An equal number of MFE-296 (red) and MFE-296^{PDR} (green) cells were seeded and images taken using a confocal microscope every day for four days (Figure 5.5). The dyes used were cell permeable. However, their intracellular reaction products were retained within the cell and passed to their progeny, enabling efficient tracing of cells over several generations. Importantly, these dyes could not be passed to adjacent cells, enabling reliable analysis of a mixed cell population.

Culture of the mixed population in a DMSO control showed growth of both cell lines, with MFE-296^{PDR} cell number significantly higher than the parental cell line at both one and three days (Figure 5.5 A). MFE-296 cell number was decreased compared to the control upon treatment with 5 μ M PD173074; MFE-296^{PDR} cell number was significantly higher than that of MFE-296 in the presence of PD173074 (Figure 5.5 B). The number of cells in both populations was decreased upon MK2206 treatment (Figure 5.5 C). However, the effect of MK2206 in combination with PD173074 blocked any increase in cell number of both MFE-296 parental and MFE-296^{PDR} cells over the course of the four days experiment (Figure 5.5 D).

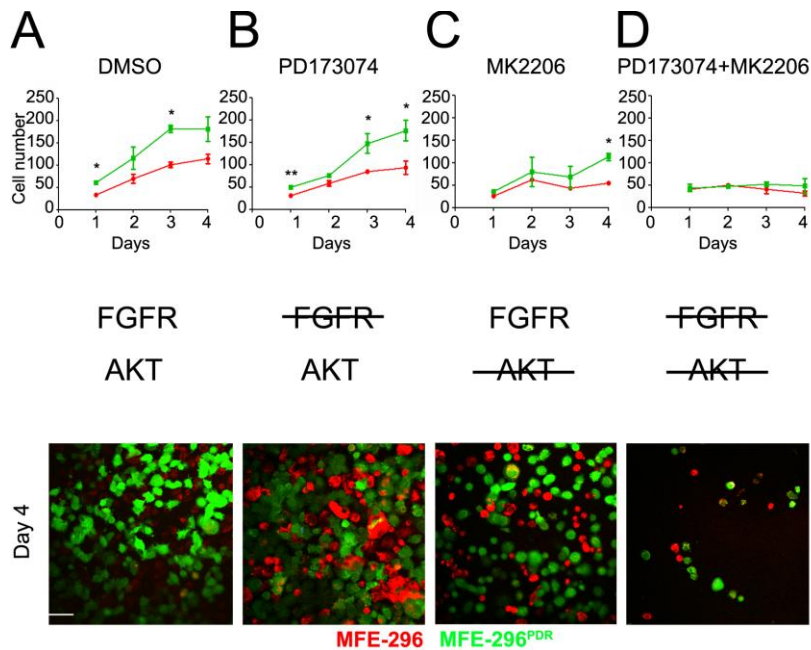


Figure 5.5. Effect of FGFR and AKT inhibition, alone and in combination, on a mixed population of MFE-296 and MFE-296^{PDR} cells.

MFE-296 and MFE-296^{PDR} cells were labelled with a cell permeable fluorescent dye (red and green, respectively). The intracellular reaction products of these dyes were cell impermeable, therefore preventing passage of the dye to adjacent cells. The tag was, however, passed on to daughter cells. (A) Cell number increased over four days in both MFE-296 and MFE-296^{PDR} cells in the presence of a DMSO vehicle control. (B) MFE-296 cell number was significantly lower than MFE-296^{PDR} cells at one, three and four days upon 5 μ M PD173074 treatment. (C) Cell number of both cell populations was decreased compared to the DMSO and PD173074 treated cells upon 1 μ M MK2206 treatment. MFE-296^{PDR} cell number was significantly higher than that of parental cells at four days treatment. (D) Both MFE-296 and MFE-296^{PDR} cells failed to increase in number upon PD173074 and MK2206 dual drug treatment. Lines through 'FGFR' and 'AKT' signify which pathways were targeted using small molecule inhibitors under each condition. *, $P \leq 0.05$; **, $P \leq 0.01$, (Student's *t* test). Original magnification of confocal images, 40X objective; bar, 25 μ m. Error bars show means \pm SEM. Data points represent the average cell number of six fields of view of three technical replicates of three biological replicates. Cell number and percent Ki67 positive cells represents average values per field of view.

MFE-296 cell line sequencing showed that this cell line was heterozygous for an activating *PIK3CA* mutation (Table 3.1). As this mutation leads to activation of PI3Ka (Gymnopoulos et al., 2007, Konstantinova et al., 2010, Weigelt et al., 2013), the effect of inhibition of PI3K signalling in MFE-296 and MFE-296^{PDR} cells was assessed using the ZSTK474 class I PI3K inhibitor.

Cells were treated with increasing concentrations of ZSTK474 for seven days, after which cell number was counted using a haemocytometer. MFE-296^{PDR} cell medium was also supplemented with 5 μ M PD173074 throughout the investigation. A similar decrease in cell number with increasing drug concentration was seen in both MFE-296 and MFE-296^{PDR} cells (Figure 5.6 A and B, respectively), indicating that sensitivity to PI3K inhibition was independent of FGFR inhibitor resistance. Interestingly, both MFE-296 and MFE-296^{PDR} cells showed PI3K inhibitor sensitivity comparable to that seen in MFE-296 cells upon FGFR inhibitor treatment (Figure 3.3). These data suggested that MFE-296 cells relied on both FGFR2 and PI3K mutant pathways for optimal cell survival in contrast to AN3CA cells, which were FGFR2 oncogene addicted (Figure 3.7 B).

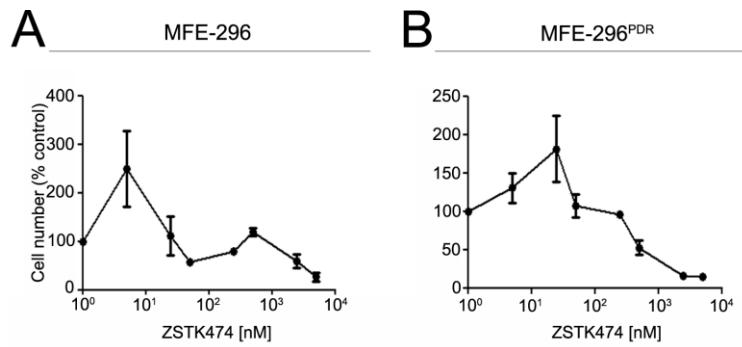


Figure 5.6. Effect of PI3K inhibition on MFE-296 and MFE-296^{PDR} cells in 2D culture.

Increasing concentration of ZSTK474 pan PI3K inhibitor reduced cell number of both parental and PD173074 inhibitor resistant cells in 2D culture after 7 days (A and B respectively). (A) Data displayed as average of three replicates and values normalised to DMSO control treated cells. (B) Data displayed as average of two replicates and values normalised to control cells treated with 5 μ M PD173074. MFE-296^{PDR} cells were treated with 5 μ M PD173074 in addition to various ZSTK474 concentrations throughout the experiments. Error bars show means \pm SEM.

5.3 Investigation of the MFE-296^{PDR} FGFR inhibitor resistance pathway

After establishing the importance of AKT signalling in FGFR inhibitor resistance, further analysis was employed to dissect this mechanism. The phosphoproteomics method outlined in Chapter 4 primarily detected peptides phosphorylated on serine and threonine residues. Whilst this gives great insight into the activity of intracellular signalling cascades, changes in phosphotyrosine residues can go unnoticed, since they are much less abundant than serine and threonine phosphorylations (Delom and Chevet, 2006). As up-regulation of alternative receptor tyrosine kinase (RTK) pathways is a common mechanism of resistance in RTK mutant cancers (Niederst and Engelman, 2013), a fluorescence-based assay allowing for detection of a range of phosphorylated RTKs, as well as other important signalling nodes, was performed. In the PathScan array used, antibodies specific to each protein of interest were spotted on to a chip, to which cell lysates were added (Figure 5.7, left and middle panels). A pan-phosphoprotein detection antibody was applied, followed by Streptavidin-conjugated DyLight 680, to visualise the bound detection antibody (Figure 5.7, right panel). The fluorescent image produced was then used to quantify each spot, and therefore phosphoprotein, intensities.

MFE-296 and MFE-296^{PDR} cells were analysed using the PathScan assay. A down-regulation of ERK phosphorylation of almost two-fold was seen in MFE-296^{PDR} cells compared to the parental cell line (Figure 5.8 A and B). The array also showed an approximately one-fold decrease in AKT phosphorylation on both serine 473 (ser473) and threonine 308 (thr308). None of the RTKs investigated in this assay showed increased phosphorylation levels in MFE-296^{PDR} cells, relative to the parental cell line. Four phosphoproteins were more abundant in the MFE-296^{PDR} cell line relative to MFE-296 parental cells, however, this was a small increase of approximately one-fold.

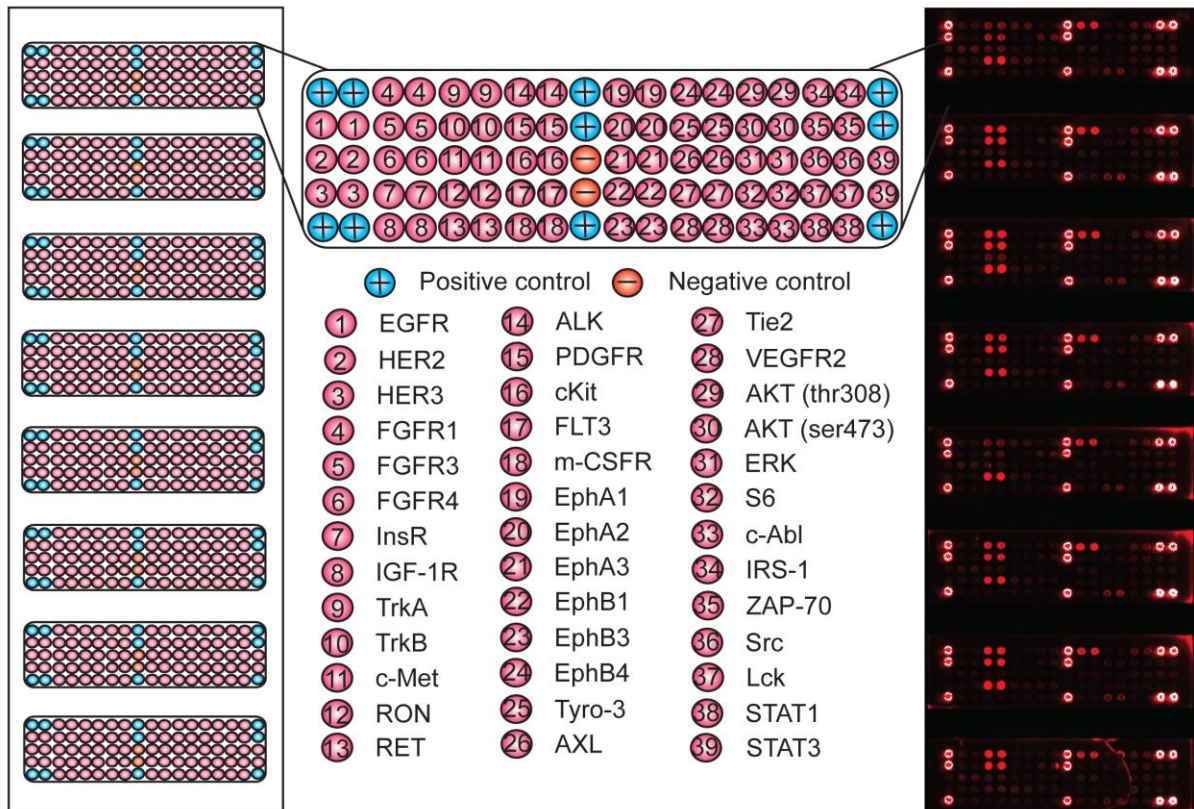
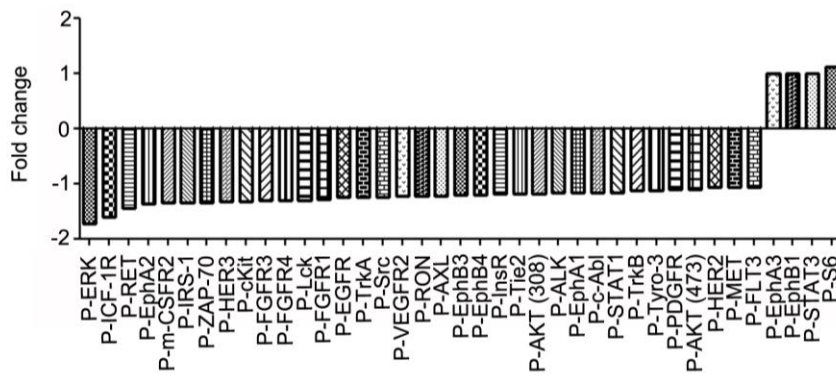


Figure 5.7. Schematic representation of the PathScan array.

The PathScan array used to analyse phosphoprotein levels in MFE-296 and MFE-296^{PDR} cells was based on sandwich immunoassay technology. Each nitrocellulose-coated glass slide contained eight pads, spotted with antibodies for a range of signalling proteins, as well as a biotinylated positive control and a nonspecific IgG negative control (left and middle panels). Samples were incubated on each pad, followed by a biotinylated detection antibody specific to phosphoproteins. A Streptavidin-conjugated DyLight 680 was then used to visualise the bound detection antibody (right panel). The resulting fluorescent image was used to quantify spot, and therefore phosphoprotein, intensities.

A



B

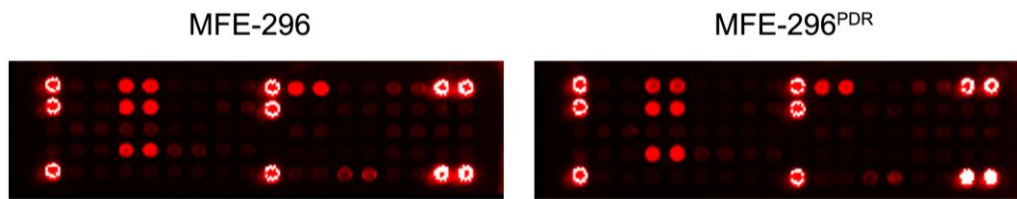


Figure 5.8. Changes in signalling node phosphorylation in MFE-296^{PDR} vs MFE-296 parental cells.

The PathScan assay was employed to determine changes in a range of RTKs and downstream effectors in MFE-296^{PDR} vs MFE-296 parental cells. (A and B) Phosphorylation of all RTKs investigated decreased upon FGFR inhibitor resistance. A 1-fold increase in phosphorylation of four downstream signalling nodes was exhibited upon acquisition of resistance. Values represent fold change in signal intensity of each phosphoprotein in MFE-296^{PDR} cells vs MFE-296 cells. The average of two technical replicates from one PathScan slide pad was used to calculate the fold change.

To further dissect changes induced upon FGFR inhibitor resistance acquisition in MFE-296 cells, transcriptomic analysis was employed. RNA from MFE-296 and MFE-296^{PDR} cells was isolated and sent to Barts Genome Centre. Following reverse transcription and labelling, it was run on an Illumina microarray gene expression chip, containing approximately 45000 probes specific to various gene transcripts. Relative expression levels for each of these transcripts was then analysed using Genome Studio, Microsoft Excel and Prism software.

An additional inhibitor resistant cell line, termed MFE-296^{AZR}, was generated by continuous exposure to 2.5 μ M AZD4547. cDNA from this cell line was run on the Illumina microarray chip in tandem with the MFE-296 and MFE-296^{PDR} cell lines. Two biological replicates of each cell line were run on the chip in duplicate, giving a total of four data points per gene transcript for each cell line.

MFE-296 and MFE-296^{PDR} cell replicates one to four were clustered according to their transcriptomic profile (Figure 5.9 A). MFE-296 and MFE-296^{PDR} cells formed two distinct clusters, indicating distinct transcriptomes. The four replicates of each experiment also clustered together, indicative of the reproducibility of these data.

We identified 1129 transcripts that were significantly up- or down-regulated in MFE-296^{PDR} cells compared to the parental cell line, of which 586 were up-regulated and 543 were down-regulated (Figure 5.9 B and C, respectively). The top 10 up-regulated genes included *IGFBP5*, the expression of which is known to be elevated in the absence of FGFR2 in keratinocytes *in vivo* (Grose et al., 2007, Schlake, 2005) (Figure 5.9 B, bottom panel). Moreover, *DUSP6* and *SPRY4* were down-regulated in both resistant populations compared to the parental controls, both of which are transcriptional targets of FGFR and play an important role in negative feedback of FGFR signalling (Furthauer et al., 2001, Li et al., 2007).

The most significantly down-regulated gene was *PHLDA1* (Figure 5.9 C, bottom panel), a negative regulator of AKT signalling (Murata et al., 2014). Interestingly, levels of many of the top 10 up- and down-regulated transcripts identified in MFE-296^{PDR} cells were similarly regulated in MFE-296^{AZR} cells (Figure 5.9 D and E, respectively). Indeed, *PHLDA1* was down-regulated by equivalent levels in this inhibitor resistant cell line as in MFE-296^{PDR} cells.

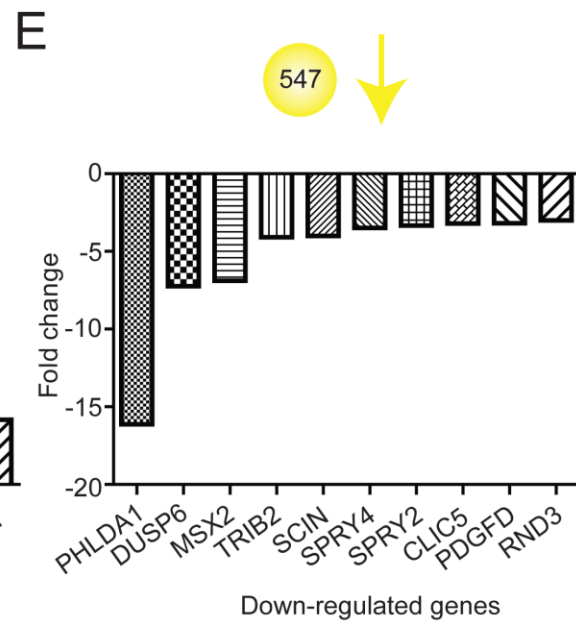
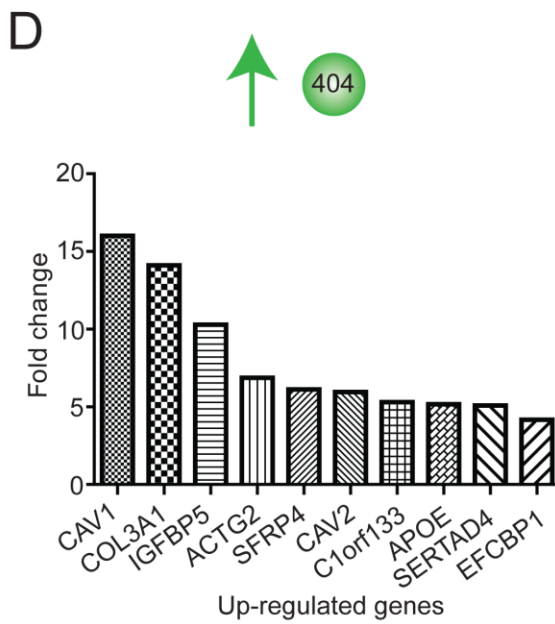
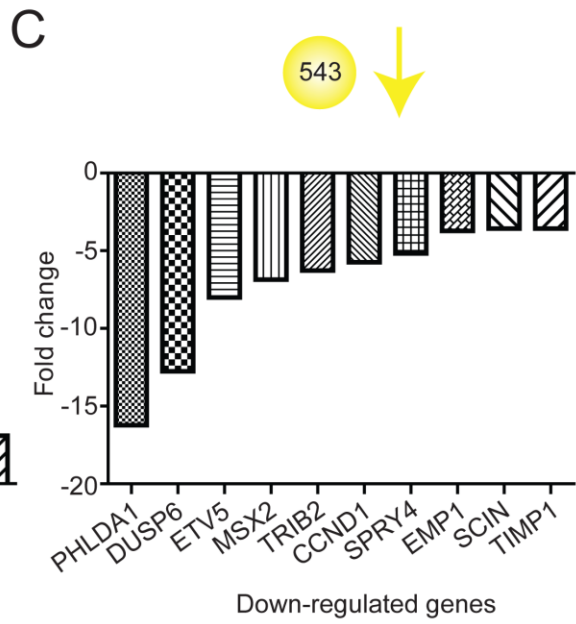
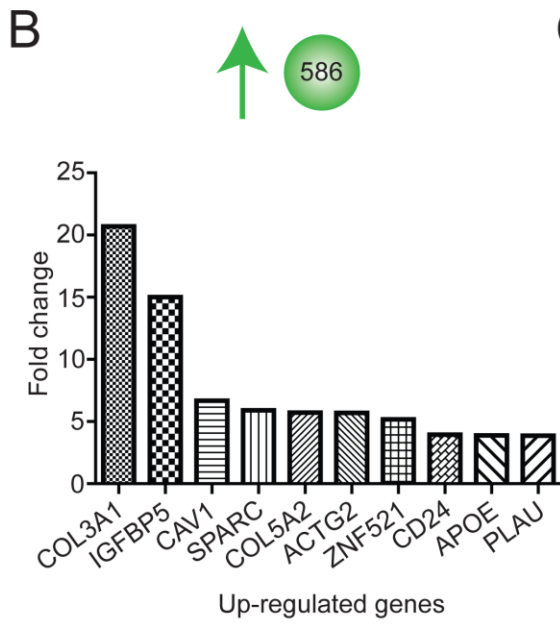
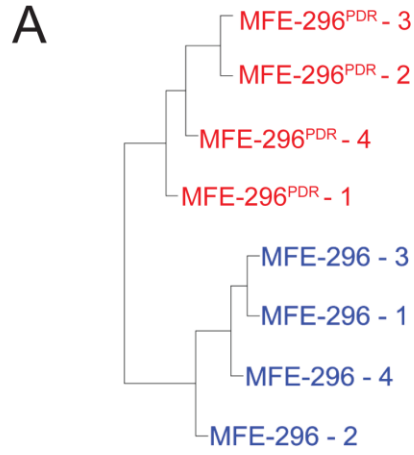


Figure 5.9. Transcriptomic changes induced upon FGFR inhibitor resistance acquisition in MFE-296 cells.

RNA was extracted from MFE-296, MFE-296^{PDR} and MFE-296^{AZR} cells and gene expression analysis performed using the Illumina microarray platform. (A) Hierarchical clustering of the four MFE-296 and MFE-296^{PDR} cells resulted in generation of two distinct clusters, indicative of discrete transcriptome signatures in the two cell populations. (B) 586 gene transcripts were up-regulated in MFE-296^{PDR} cells compared to the MFE-296 parental cell line (top panel). The 10 transcripts with the highest fold change relative to the parental cells included IGFBP5, previously shown to increase in response to FGFR2 inhibition *in vivo* (Schlake, 2005) (bottom panel). (C) Of the 543 transcripts that were significantly down-regulated in MFE-296^{PDR} cells compared to the parental cell line (top panel), PHLDA1, a negative regulator of AKT signalling, showed the largest fold decrease. (D) Comparison of an additional FGFR inhibitor resistant cell line generated via exposure to the AZD4547 compound, MFE-296^{AZR}, showed a similar number of up-regulated transcripts, as well as overlap of five genes in the top 10 highest fold up-regulation with that seen in figure B (top and bottom panels respectively). (E) Of the 547 significantly down-regulated transcripts identified in MFE-296^{AZR} cells relative to the parental cell line, six of the top 10 with the highest fold decrease in the resistant cell line were also seen in figure C (top and bottom panels respectively). Of note, PHLDA1 was down-regulated by equivalent amounts compared to the parental cells in both FGFR inhibitor resistant populations. Two technical replicates of two biological replicates of each cell line were run on the Illumina microarray assay. The average signal intensity of each transcript probe in each sample was quantile normalised, to adjust sample signals in order to minimise the effects of variation arising from non-biological factors. The average signal of the four replicates was taken for each gene transcript in each cell line examined. Values in MFE-296^{PDR} and MFE-296^{AZR} cells were then compared to those obtained in the parental cell line. Gene transcripts with values significantly higher or lower than the parental cells were identified (diff score >65). The fold change between the resistant populations compared to the parental cells, in these significantly up- or down-regulated transcripts, was then calculated. Circle sizes in figures B-E are proportional to each other.

Upon PI3K activation, PIP₂ is converted to PIP₃, to which PH domain containing proteins can bind. In the case of AKT, recruitment to the membrane via PIP₃ binding leads to phosphorylation of the thr308 residue by PDK1 and subsequent activation of AKT (Alessi et al., 1997, Franke et al., 1995). This in turn leads to mTORC2 activation, which can further phosphorylate AKT, resulting in its complete activation and subsequent pro-survival signalling (Facchinetti et al., 2008, Sarbassov et al., 2005) (Figure 5.10 A).

PHLDA1, another PH domain containing protein, is also a known binding partner of PIP₃ (Murata et al., 2014). In this way, it competes with AKT, as well as many other PH domain-containing proteins (Varnai et al., 2005), for PIP₃ binding. Upon PIP₃-PHLDA1 interaction, AKT phosphorylation and subsequent activation is prevented, leading to inhibition of AKT signalling (Figure 5.10 B). Therefore, a balance between AKT and PHLDA1 exists, whereby an increase in AKT displaces PHLDA1-PIP₃ binding and leads to anti-apoptotic signalling, while up-regulation of PHLDA1 protein levels inhibits pro-survival activity (Figure 5.10 C).

The dramatic decrease in PHLDA1 in drug resistant cell lines, identified via microarray gene expression analysis, was particularly interesting given our previous data implicating the importance of AKT signalling in FGFR inhibitor resistance (Figures 4.2, 4.3 and 4.6). Previous studies have shown down-regulation of PHLDA1 correlated with poor prognosis in breast cancer tissue samples and has also been reported in melanoma (Nagai et al., 2007, Neef et al., 2002). However, this was the first potential demonstration of the down-regulation of PHLDA1 in an apparent compensatory capacity in response to inhibition of a mutant RTK pathway. Therefore, the validity of these transcriptomics data and their importance in the FGFR inhibitor resistance mechanism were investigated further.

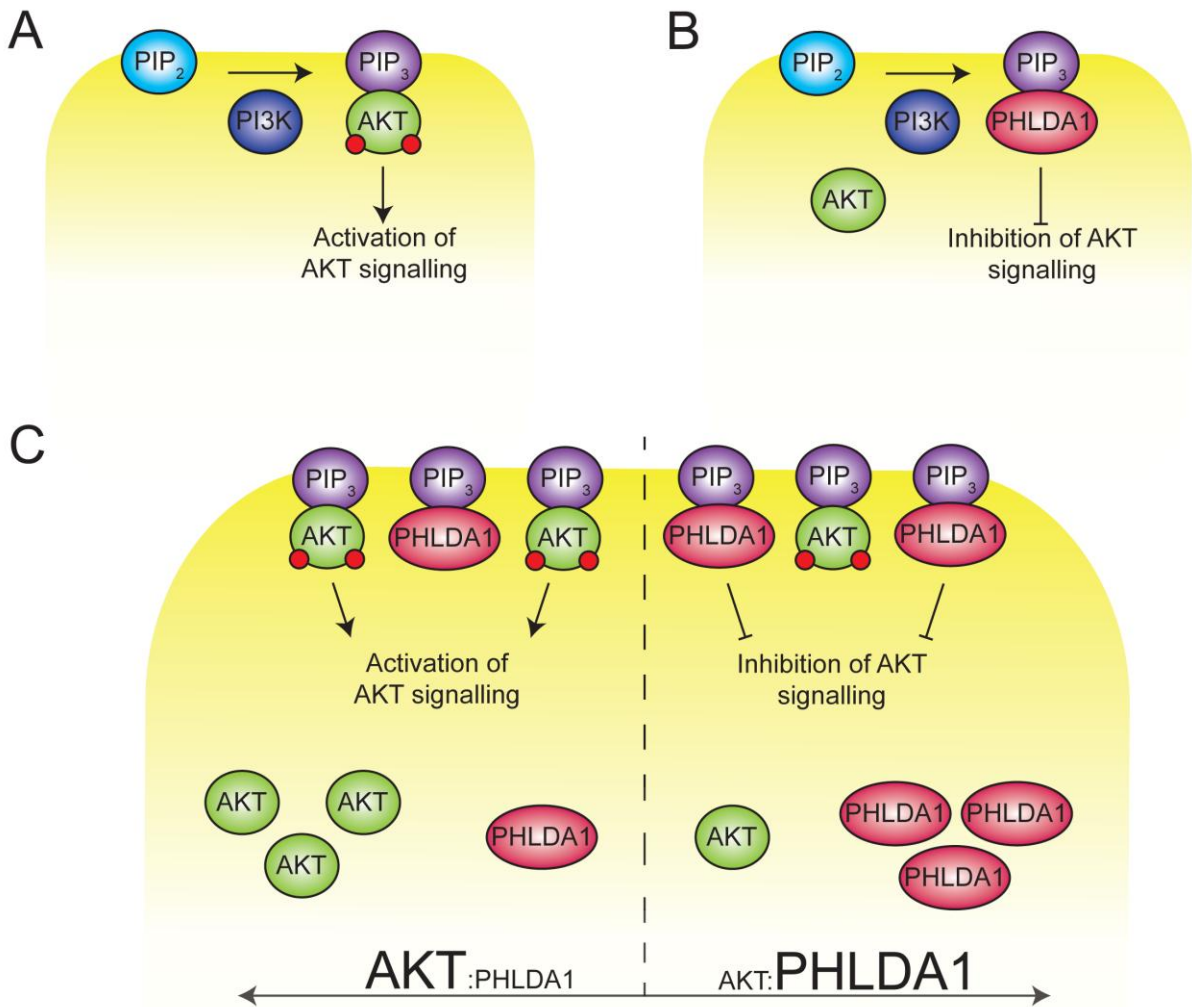


Figure 5.10. Schematic representation of the opposing cellular effects of the PIP_3 binding proteins AKT and PHLDA1.

(A) PI3K activation leads to conversion of membrane-bound PIP_2 to PIP_3 . AKT binds to PIP_3 via its PH domain, upon which it is phosphorylated by PDK1 (Alessi et al., 1997, Franke et al., 1995). This, in turn, leads to activation of mTORC2, which further phosphorylates AKT, leading to full activation of the protein and subsequent activation of pro-survival signals (Facchinetti et al., 2008, Sarbassov et al., 2005). (B) PHLDA1 is also able to bind to PIP_3 , therefore preventing AKT recruitment to the membrane and subsequently inhibiting AKT-induced anti-apoptotic signalling (Murata et al., 2014). (C) AKT and PHLDA1 levels exist in a state of balance, whereby a higher ratio of AKT:PHLDA1 favours pro-survival signalling and vice versa.

5.4 Investigation of the role of PHLDA1 in FGFR inhibitor resistance

To establish the validity of microarray gene expression data at the protein level, PHLDA1 levels in MFE-296 and MFE-296^{PDR} cells were assessed via western blot (Figure 5.11). MFE-296 cells expressed PHLDA1 in the basal state. PHLDA1 levels in MFE-296 cells were significantly decreased upon treatment with 5 μ M PD173074 for seven days (Figure 5.11, left). Preliminary data showed that, whilst PHLDA1 levels decreased after one and three days PD173074 treatment, the down-regulation of this protein was significant after seven days (Appendix Figure 1.10). PHLDA1 was not expressed in MFE-296^{PDR} cells. Expression of PHLDA1 was not recovered when resistant cells were cultured in PD173074-free medium (Figure 5.11, right).

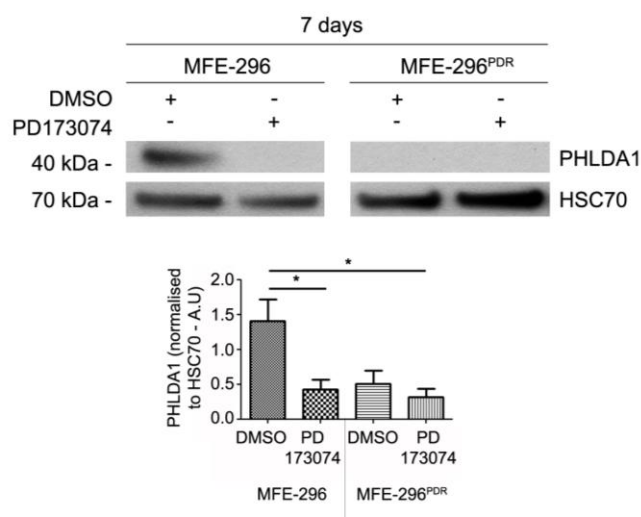


Figure 5.11. PHLDA1 expression in the basal state and after PD173074 treatment of MFE-296 and MFE-296^{PDR} cells.

MFE-296 and MFE-296^{PDR} cells were cultured in medium supplemented with 5 μ M PD173074 or a DMSO vehicle control for seven days. MFE-296 cells expressed PHLDA1 in the basal state; this expression was significantly decreased upon PD173074 treatment (left panel). MFE-296^{PDR} cells did not express PHLDA1 in either the presence or the absence of PD173074. *, $P \leq 0.05$ (Student's *t* test). 40 μ g protein was used for each lane. Error bars show means \pm SEM of three replicates.

As detailed in Figure 5.10, PHLDA1 negatively regulates AKT signalling via direct competition with AKT for PIP₃ binding at the membrane. As such, an indicator of the importance of the balance between PHLDA1 and AKT in MFE-296 cells is the cellular localisation of both proteins. We assessed cellular localisation of PHLDA1, P-AKT and total AKT in MFE-296 and MFE-296^{PDR} cells via fractionation of cells, into their membrane and cytoplasmic components (Figure 5.12). PHLDA1 was predominately localised to the membrane in MFE-296 cells, while MFE-296^{PDR} cells did not express PHLDA1 at either the membrane or in the cytoplasm (Figure 5.12 A and B, left panel). There was no significant difference in AKT levels at the membrane or in the cytoplasm in MFE-296 cells. However, there was significantly more AKT localised to the membrane in MFE-296^{PDR} cells (Figure 5.12 A and B, middle panel). AKT phosphorylation was significantly higher in the cytoplasm than at the membrane in both MFE-296 and MFE-296^{PDR} cells (Figure 5.12 A and B, right panel).

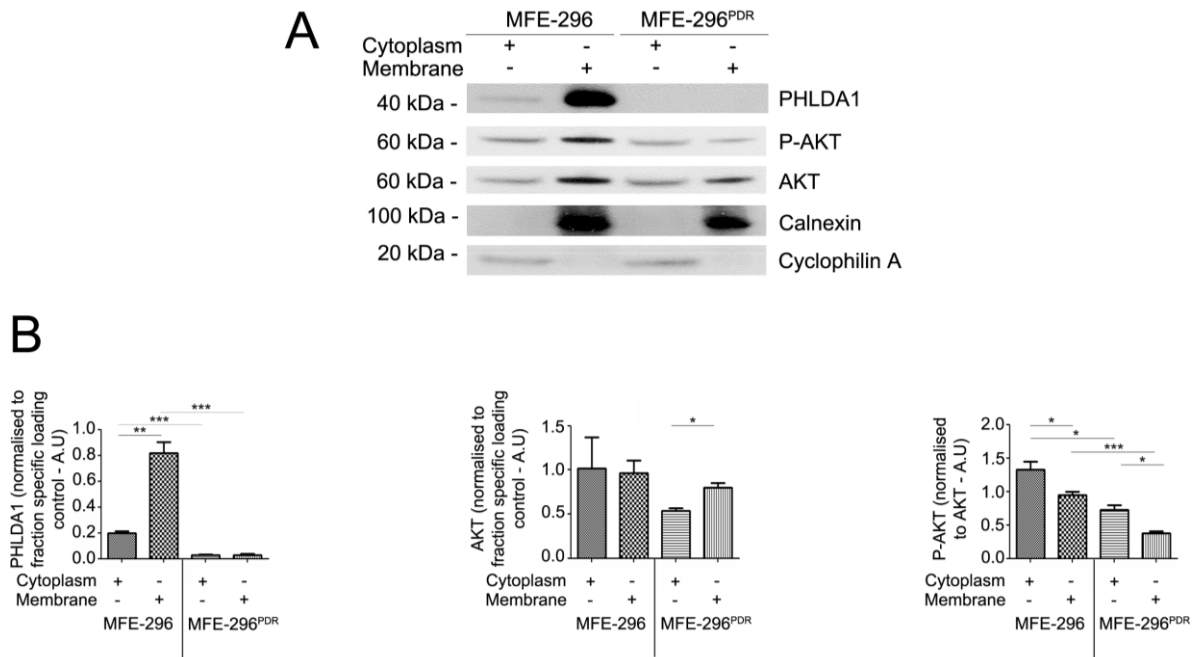


Figure 5.12. Cellular localisation of PHLDA1, P-AKT and total AKT in MFE-296 and MFE-296^{PDR} cells.

PHLDA1, P-AKT and total AKT localisation in MFE-296 and MFE-296^{PDR} cells was assessed, via fractionation of both cell lines into their cytoplasmic and membrane portions. (A and B) PHLDA1 was predominantly expressed at the membrane in MFE-296 cells. MFE-296^{PDR} cells did not express PHLDA1. Total AKT levels were equivalent in the membrane and cytoplasmic portions in MFE-296 cells, whilst AKT was significantly higher at the membrane in MFE-296^{PDR} cells. P-AKT was higher in the cytoplasm than at the membrane in both cell lines. Calnexin and Cyclophilin A were used as loading controls for membrane and cytoplasmic fractions, respectively. *, $P \leq 0.05$; **, $P \leq 0.01$; ***, $P \leq 0.001$ (Student's *t* test). 40 μ g protein was used for each lane. Error bars show means \pm SEM of three replicates.

Having confirmed down-regulation of PHLDA1 in resistant cells, and established that PHLDA1 was down regulated in MFE-296 parental cells upon seven days PD173074 treatment, we aimed to assess the effect PHLDA1 on sensitivity to FGFR inhibitor treatment in MFE-296 cells. To investigate this, siRNA knockdown of PHLDA1 was utilised. Initial investigations showed significantly decreased protein levels of PHLDA1 in MFE-296 cells upon two days exposure to siRNA (Figure 5.13, A, left). This returned to levels equivalent to cells treated with a non-targeting siRNA control after five days (Figure 5.13 A, right). MFE-296^{PDR} cells did not express PHLDA1. The effect of PHLDA1 knockdown on cell number was assessed, after two days siRNA treatment. This showed no significant difference in cell number between non-targeting scrambled control and PHLDA1 siRNA treated MFE-296 cells (Figure 5.13 B).

As MFE-296 cell number was significantly decreased compared to a DMSO control after three days 5 μ M PD173074 treatment (Figure 5.13 C), the effect of loss of PHLDA1 on MFE-296 cell line sensitivity to PD173074 was investigated. Cells were treated with PHLDA1-targeting siRNA for two days, followed by incubation with 5 μ M PD173074 for three days, after which cell number was determined. There was no difference in cell number between siRNA/drug treated cells compared to those treated with non-targeting siRNA/DMSO vehicle control (Figure 5.13 D). The same treatment did not affect MFE-296^{PDR} cells (Appendix Figure 1.11). Therefore, loss of PHLDA1 expression in MFE-296 cells induced FGFR-inhibitor resistance.

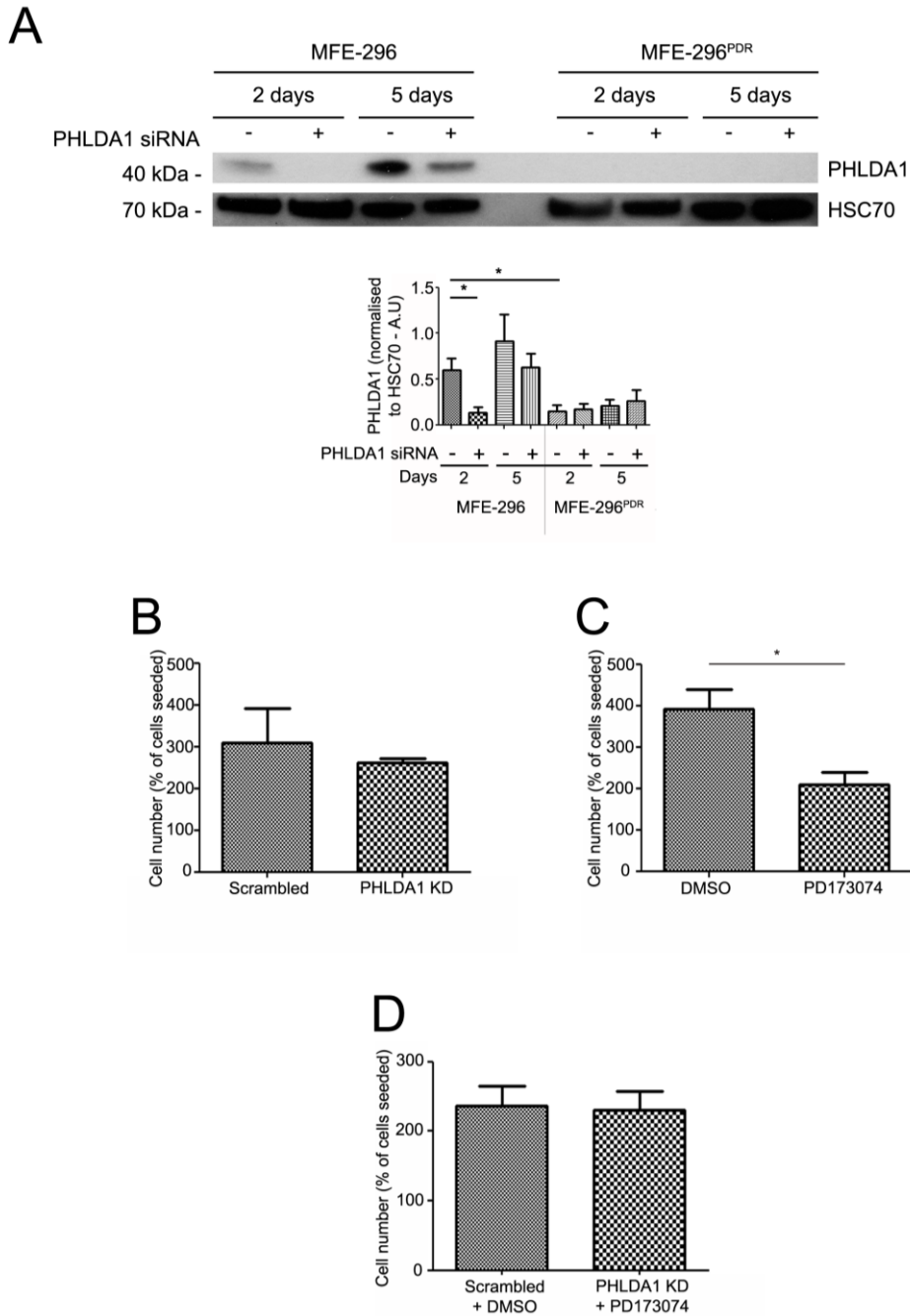


Figure 5.13. Induction of FGFR inhibitor resistance in MFE-296 cells upon PHLDA1 knockdown.

(A) MFE-296 and MFE-296^{PDR} cells were treated with PHLDA1 targeted siRNA or a non-targeting control for two or five days. PHLDA1 expression was significantly decreased in MFE-296 cells upon two day siRNA treatment. However, this returned to near control levels after five days exposure to PHLDA1 targeted siRNA. PHLDA1 was not expressed in MFE-296^{PDR} cells. (B) MFE-296 cells were treated with PHLDA1 targeted siRNA or a non-targeting control for two days, after which cell number was counted using a haemocytometer. There was no significant difference in cell number upon PHLDA1

knockdown. (C) MFE-296 cells were treated with 5 μ M PD173074 or a DMSO control for three days, after which cell number was assessed as previously described. Cell number was significantly decreased after three days exposure to PD173074. (D) MFE-296 cells were treated with PHLDA1 targeting siRNA for two days and treated subsequently with PD173074 for three days, after which cell number was assessed. Control cells were treated with non-targeting siRNA, followed by DMSO for three days. There was no significant difference in cell number between control and PHLDA1 knockdown/PD173074 treated cells. Therefore, knockdown of PHLDA1 induced inhibition to FGFR inhibition in MFE-296 cells. *, $P \leq 0.05$ (Student's *t* test). 40 μ g protein was used for each lane. Error bars show means \pm SEM of three replicates. Cell number data displayed as average of three replicates and values expressed as percentage of number of cells seeded. Error bars show means \pm SEM.

5.5 Summary of results

- Two FGFR inhibitor resistant populations of MFE-296 cells were generated by continuous treatment with PD173074 or AZD4547
- ERK phosphorylation was inhibited in MFE-296^{PDR} cells whilst P-AKT levels in resistant and parental cells were equivalent
- Seven day treatment of MFE-296 and MFE-296^{PDR} cells with MK2206 or MK2206 in combination with PD173074 significantly reduced cell number and proliferation
- Compensatory signalling via an alternative RTK was not induced in MFE-296^{PDR} cells
- Comparison of MFE-296^{PDR} transcriptomic data with that of MFE-296 cells showed PHLDA1, a negative regulator of AKT signalling, was down-regulated by approximately 15-fold; this was recapitulated in MFE-296^{AZR} cells
- A lack of PHLDA1 expression in MFE-296^{PDR} cells was confirmed at the protein level
- MFE-296 cells expressed PHLDA1; this was significantly decreased upon seven day PD173074 treatment
- PHLDA1 was located predominantly at the membrane in MFE-296 cells
- AKT was located predominantly at the membrane in MFE-296^{PDR} cells, however, P-AKT was higher in the cytoplasm
- PHLDA1 siRNA knockdown in MFE-296 cells induced PD173074 inhibitor resistance
- First evidence of PHLDA1 down-regulation in response to small molecule inhibitor treatment leading to drug resistance

5.6 Discussion

Initial work showed generation of a drug resistant population of MFE-296 cells upon FGFR inhibition, in which the importance of AKT signalling recovery and maintenance was implicated via phosphoproteomic analysis. To dissect this drug resistance mechanism further, an inhibitor resistant population of MFE-296 cells was produced, by continuous exposure to PD173074, and named MFE-296^{PDR}. Comparison of this cell line to its parental counterpart facilitated discovery of a PHLDA1 down-regulation mediated compensatory mechanism of signalling in FGFR inhibitor resistant endometrial cancer cells.

Differential signalling in MFE-296 and MFE-296^{PDR} cells

Changes in the signalling capacity of MFE-296^{PDR} cells were shown via western blot analysis. ERK phosphorylation was inhibited in MFE-296^{PDR} cells, but P-ERK returned to levels equivalent to that of parental cells upon removal of the drug. This reversible inhibition of ERK phosphorylation in resistant cells implies that FGFR2 signalling was indeed blocked by PD173074 in MFE-296^{PDR} cells and that drug resistance was acquired by an alternative signalling method, rather than resulting from mutation of the receptor so as to overcome small molecule inhibition.

The validity of the drug combinations detailed in Chapter 4 were further shown in MFE-296^{PDR} cells, whereby AKTVIII treatment alone resulted in an inhibitor resistant population, while dual drug treatment with MK2206 and PD173074 induced cell death. Interestingly, FGFR inhibitor resistance in MFE-296^{PDR} cells was also overcome by MK2206 inhibition alone, suggesting a key role for AKT signalling in this resistant population, as inferred from the phosphoproteomic data.

To probe this AKT related mechanism further, we addressed the question of possible up-regulation of an alternative RTK pathway to compensate for loss of FGFR signalling, as has been noted elsewhere in the literature (Niederst and Engelman, 2013). As tyrosine phosphorylation events occur at a reduced rate compared to that

of serine and threonine (Delom and Chevet, 2006), it was possible that our MS investigations failed to highlight increased phosphorylation of an alternative RTK. However, PathScan analysis revealed low level down-regulation of alternative RTKs in MFE-296^{PDR} cells, implying the resistance mechanism was acquired via alternative means.

The MFE-296 cell line also harboured a mutant copy of *PIK3CA*, leading to activation of PI3Ka. Although treatment of MFE-296 cells with AKT inhibitors alone generated a resistant population, we investigated the effects of PI3K inhibition in MFE-296 and MFE-296^{PDR} cells. The growth curve resulting from increasing concentration of ZSTK474, a PI3Ka inhibitor (Dan et al., 2002, Kong et al., 2009), was similar to that seen when MFE-296 cells were exposed to PD173074 and AZD4547. This suggested both of these mutations are important in maintaining full signalling capacity in MFE-296 cells, whereas the AN3CA cell line was oncogene addicted to mutant FGFR2. Interestingly, MFE-296^{PDR} cells showed a similar dose response to ZSTK474 treatment to their MFE-296 parental cell line, indicating the significance of this pathway to their survival. With the potential importance of AKT signalling in mind, we used transcriptomic analysis of parental and drug resistant cells to further delineate the mechanism of FGFR inhibitor resistance.

Changes in the global transcriptome of MFE-296 drug resistant cells

Use of microarray gene expression analysis of transcriptomic changes in drug resistant cells allowed insight into events in a global, unbiased fashion. Transcriptomic analysis of MFE-296^{PDR} cells and MFE-296^{AZR} cells, an additional inhibitor resistant cell line, showed a distinct gene expression signature common to drug resistant cells compared to their parental counterparts.

1129 transcripts were significantly up- or down-regulated in MFE-296^{PDR} cells, compared to the parental cell line. The top 10 up-regulated genes included *IGFBP5*, the expression of which is known to be elevated in the absence of FGFR2 in

keratinocytes *in vivo* (Grose et al., 2007, Schlake, 2005), therefore potentially validating our data. The most significantly down-regulated gene was *PHLDA1*, a negative regulator of AKT signalling. MFE-296^{AZR} cells produced similar results in terms of significantly up- and down-regulated genes. Of note, *PHLDA1* was also down-regulated by approximately 15 fold in the MFE-296^{AZR} cell line, recapitulating the data obtained from MFE-296^{PDR} cells.

In light of our data identifying a role for AKT in maintaining FGFR inhibitor resistance in MFE-296 cells, it was of particular interest that a negative regulator of AKT signalling was the most significantly down-regulated of all genes analysed on the microarray. Published work has noted the down-regulation of this gene in patient samples of melanoma and has postulated its use as a biomarker of disease progression (Nagai et al., 2007, Neef et al., 2002). However, this was the first demonstration of a potential role for *PHLDA1* in the acquisition and maintenance of drug resistance in cancer cells.

We sought to validate the importance of this protein in our parental and resistant cells at the protein level and found expression was down regulated in MFE-296 cells, upon seven days exposure to PD173074. *PHLDA1* was not expressed in MFE-296^{PDR} cells. The importance of down-regulation of this protein was shown upon siRNA knockdown of *PHLDA1* in the parental MFE-296 cell line, which induced PD173074 inhibitor resistance after just three days of drug exposure.

Interestingly, *PHLDA1* expression was not recovered upon removal of PD173074 from the medium of resistant cells, suggesting this down regulation may be of a permanent nature, potentially induced by epigenetic modulation of the gene. Whilst this mechanism of *PHLDA1* down-regulation is speculative, future work will aim to validate the means by which *PHLDA1* is modulated. Another intriguing line of enquiry is the potential feedback loop between AKT and p53 resulting in down-regulation of *PHLDA1*, as has been noted in signalling of its protein family member, *PHLDA3* (Kawase et al., 2009, Liao and Hung, 2010).

In an alternative approach, the effect of PHLDA1 over-expression on MFE-296 and MFE-296^{PDR} cells will be assessed. Initial experiments validated the efficiency of transfection with a GFP-tagged PHLDA1 plasmid or GFP alone as a control (Appendix Figure 1.12). GFP expression and PHLDA1 protein levels were assessed one day post transfection, which showed PHLDA1 expression in both MFE-296 and MFE-296^{PDR} cell lines (Appendix Figure 1.12 A and B). PHLDA1 over-expressing cells, alongside GFP transfected controls, will undergo DAPI stained cell cycle analysis, as well as annexin V staining, as a marker of apoptosis, using flow cytometry.

As with MS, transcriptomic analysis generates a large amount of data, the interrogation of all aspects of which was beyond the scope of this work. However, while we are mindful that other genes, just as other phosphoproteins, could have been selected for investigation from these data sets, we believe the current thesis (i) validates the known complexity of signalling networks and their changes upon perturbation of a single pathway and (ii) demonstrates the compatibility of MS and gene microarray to complement each other in large scale studies.

PHLDA1 down-regulation led to FGFR inhibitor resistance in MFE-296 cells

Based on these data, we propose the following model (Figure 5.14): Inhibition of mutant FGFR signalling in MFE-296 cells decreased cell growth and proliferation over seven days. Although FGFR2 signalling was blocked, the cells were able to continue signalling at a reduced level. This most likely occurred via the mutant copy of PI3Ka harboured in this cell line. As FGFR2 also induces PI3K signalling, decreased downstream effects of PI3K were observed via MS analysis following seven days exposure to PD173074. This decreased PI3K signalling subsequently led to a decrease in PIP₃ at the membrane. To compensate for the decrease in PI3K signalling upon FGFR2 inhibition, PHLDA1 expression was decreased. Therefore, whilst there was reduced PI3K signalling, the AKT available in the cells was able to bind to PIP₃ free of competition with PHLDA1. In this way, AKT signalling could be sustained, even in the absence of mutant FGFR2 signalling.

Important to this mechanism is the cellular localisation of PHLDA1 and AKT in parental and resistant cells. Via cellular fractionation, we were able to determine that PHLDA1 was expressed predominantly at the membrane of MFE-296 cells, whilst it was not expressed in the resistant cell line. Therefore AKT could bind to the membrane unhindered in the MFE-296^{PDR} cells. Another important aspect of this mechanism is the differential level of PIP₂ and PIP₃ in MFE-296 and MFE-296^{PDR} cells. Whilst we postulate PIP₃ levels are lower in the resistant cell line, requiring PHLDA1 down-regulation in order to maintain AKT signalling, we aim to validate this using a PIP₃ competition assay in future work.

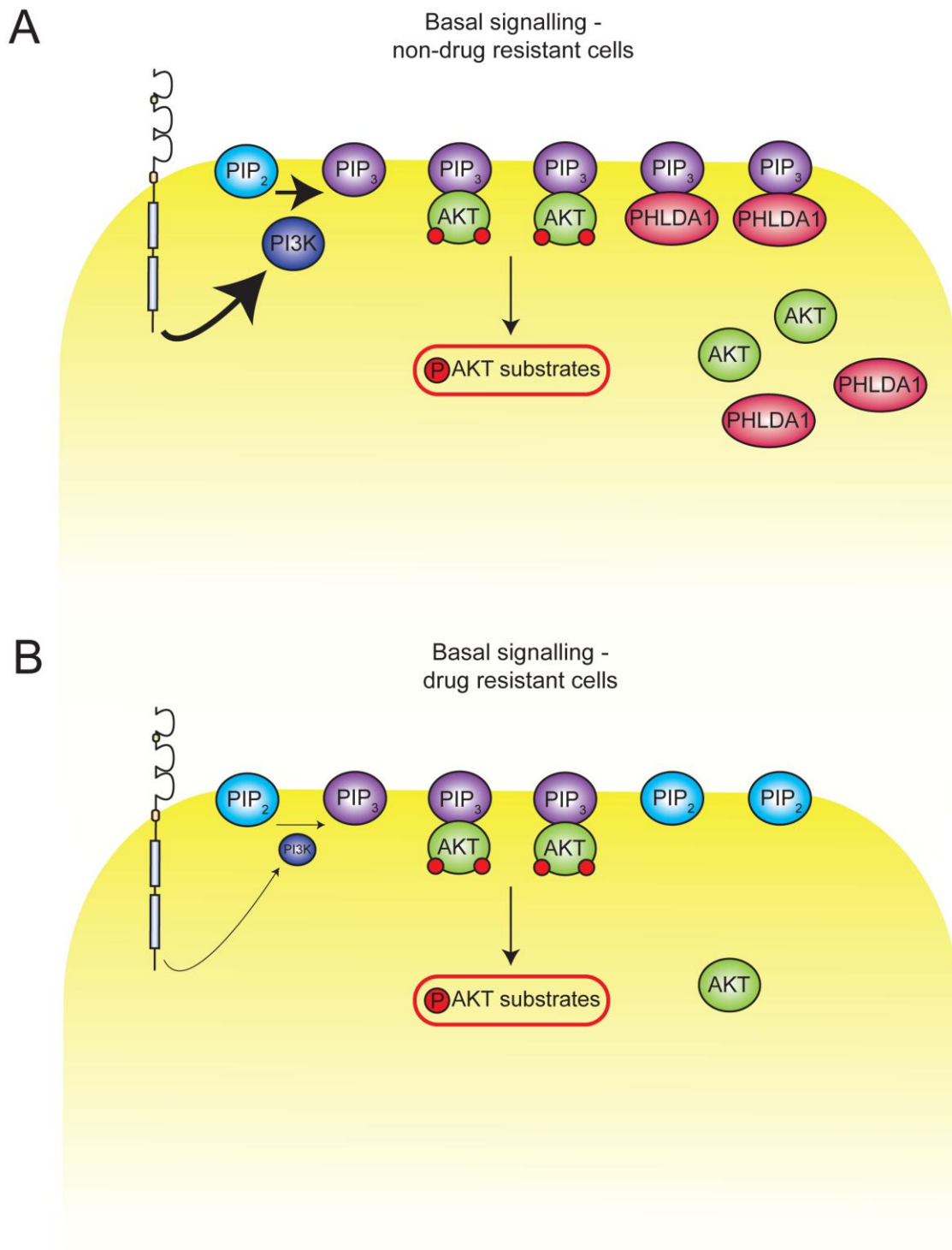


Figure 5.14. Proposed mechanism of FGFR inhibitor drug resistance in MFE-296 endometrial cancer cells.

(A) In the basal state, FGFR2 mutant MFE-296 cells signal via mutant FGFR2. This induces activation of downstream signalling pathways, including PI3K. Signalling via the PI3K pathway is further enriched due to the presence of mutant PI3Ka in MFE-296 cells. This leads to an abundance of PIP₃ at the cell membrane, to which AKT can bind and induce its

pro-survival downstream signalling cascades. MFE-296 cells also express PHLDA1, which competes with AKT for PIP₃ binding. However, due to the dual activation of PI3K signalling via mutant FGFR2 and mutant PI3Ka, PIP₃ is abundant and freely available for both AKT and PHLDA1 to bind. (B) Upon continuous treatment of MFE-296 cells with an FGFR inhibitor, PI3K signalling is reduced; therefore the cells now rely on only the mutant version of PI3Ka. Overall, membrane bound PIP₃ levels are decreased due to less PIP₂ to PIP₃ conversion as a result of diminished total PI3K signalling. In response, PHLDA1 is down-regulated in these FGFR inhibitor exposed cells. Therefore, AKT can bind to PIP₃ unhindered and continue to signal at the same rate as in non-inhibitor treated cells. In this way, an FGFR inhibitor resistant population is generated.

Chapter 6

General discussion

6.1 Overview

FGFs and their receptors mediate a variety of processes, from embryonic development to cellular growth and proliferation (Bottcher and Niehrs, 2005, Dubrulle and Pourquie, 2004, Feldman et al., 1995, Ghabrial et al., 2003, Huang and Stern, 2005, Polanska et al., 2009, Sun et al., 1999). It is therefore unsurprising that these receptors are often co-opted by cancer cells to drive cell growth and tumour progression. With the advent of small molecule inhibitor treatment of cancers harbouring mutations in a range of RTKs, the therapeutic viability of targeting mutant FGFR with such inhibitors has been much discussed in the literature (Byron et al., 2008, Carter et al., 2014, Pollock et al., 2007). Indeed, a wide range of RTK inhibitors are showing success in the clinical setting (Clinicaltrials.gov, 2014, Gavine et al., 2012). However, drug resistance is a major issue (Holohan et al., 2013). As such, alternative regimens must be investigated based upon the cellular alterations acquired in response to small molecule inhibition.

The most common gynaecological malignancy in the western world is that of the endometrium, with approximately 8500 women diagnosed with endometrial cancer in 2011 in the UK alone (CRUK, 2014). At present, the most common treatment is a full hysterectomy. However, whilst curative in the majority of cases, an alternative approach to surgery would be of great benefit to patients. Up to 16% of endometrial cancers harbour FGFR2 mutations analogous to those found in a range of developmental disorders (Pollock et al., 2007). As such, tumours harbouring these mutations have been postulated to be reliant on aberrant FGFR2 signalling and so inhibition of this RTK is of therapeutic interest.

Whilst initial studies of the role of these mutations in endometrial cancer has shown targeting FGFR2 reduced cell number *in vitro*, effects of prolonged exposure to FGFR inhibitors, particularly AZD4547 which is currently in clinical trials in the treatment of FGFR2 mutant solid tumours, have not been investigated. Signalling deregulation upon small molecule inhibitor treatment of a dominant pathway often leads to induction of compensatory signalling (Holohan et al., 2013). Therefore,

investigation of the effect of such treatment in endometrial cancer is of paramount importance, prior to commencement of clinical trials.

6.2. Generation of a 3D model of endometrial cancer and its use in investigation of small molecule inhibition of FGFR signalling

In order to fully assess the effect of a compound *in vitro*, a viable cell model is required. Organotypic cultures, such as those used in the study of breast and pancreatic cancers (Chioni and Grose, 2012, Coleman et al., 2014), provide a tool capable of assessing the effects of small molecule inhibition in the context of a 3D environment, comprising an ECM-like stromal cell-containing component. Since such tools are not currently available for the study of endometrial cancer, we developed and validated a novel 3D organotypic model.

This model facilitated the identification of differential effects of FGFR inhibition in two FGFR2 mutant endometrial cell lines, consistent with our previous 2D culture data. The importance of mutant FGFR2 in the AN3CA cell line was demonstrated by induction of cell death upon FGFR inhibition after seven days.

Both 2D and 3D models showed reduced sensitivity of the MFE-296 cell line to FGFR2 inhibition, compared to AN3CA cells. Most interestingly, while cell number was decreased upon treatment with two FGFR inhibitors, PD173074 and AZD4547, compared to the DMSO control, an inhibitor resistant population remained after 14 days and retained its ability to proliferate. The absence of cell growth and proliferation inhibition in FGFR2 wild type Ishikawa cells suggested the effects observed in both FGFR2 mutant cell lines were due to blockade of aberrant FGFR2 signalling rather than off target effects of the inhibitor.

Our model was further modified to simulate endometrial cancer cell metastasis, via retrograde menstruation, and the effect of FGFR2 inhibition on the viability of migrating cells. Full submersion of the organotypic cultures in medium showed the ability of MFE-296 cells to bud from the organotypic culture and either remain free in the medium or re-adhere to the culture plate. After 14 days of FGFR inhibition, the

viability of these cells was demonstrated and showed the establishment of an FGFR inhibitor resistant population.

Future directions

Ideally, the effects of tumourigenic mutations would be compared to non-malignant cells arising from the same tissue of origin. While such epithelial cells of endometrial origin are not commercially available, we attempted to generate our own immortalised non-malignant endometrial cell lines. However, epithelial cells underwent EMT and so could not be used, and stromal cells did not survive the culture conditions. Future attempts at stromal cell immortalisation should assess the effect of coating culture plates with collagen prior to cell culture, to increase efficiency of cell attachment and proliferation. Successful generation of these immortalised stromal cells would be of great benefit for use in the ECM component of the organotypic model, in place of the HFF2 cells used in our investigations, so as to provide a more physiomimetic model. Culture of endometrial cancer cells in the presence of cancer-related stromal endometrial cells would also be of benefit in delineating the possible effects of paracrine signalling between the two populations.

6.3 Identification of changes in the phosphoproteome upon drug resistance acquisition using MS

Having established that MFE-296 cells acquire resistance to FGFR inhibition, we used MS-based phosphoproteomics to identify underlying changes in cell signalling induced by receptor inhibition. Assessment of differences in the phosphoproteome induced by drug treatment guided investigations of the mechanisms underlying resistance to an FGFR targeted compound.

The MS method employed identified 6706 phosphopeptides across all samples, with the abundance of 525 of these changed significantly in PD173074 treated samples. Analysis of this subset of phosphopeptides showed the predominant pattern of phosphorylation across the time points in PD173074 treated cells to be the same as DMSO samples at one day treatment, significant down-regulation at seven days drug exposure, and a return to baseline levels at 14 days. Inference of the upstream kinases of these phosphopeptides, garnered from KSEA analysis, revealed that a number of phosphorylation sites known to be downstream of AKT followed the baseline – down-regulation – baseline pattern, over the three time points in PD173074 treated cells. Phosphorylation sites known to be substrates of kinases downstream of AKT, including mTOR, were also found to follow this pattern, further supporting the findings that the change in AKT signalling identified in the MS data was transmitted downstream. The potential role of AKT signalling in overcoming FGFR inhibitor resistance in MFE-296 cells was further highlighted by up-regulation of four phosphopeptides, each implicated in AKT signalling, after 14 days of drug exposure (Chaudhury et al., 2010, Hussey et al., 2011, Ma et al., 2014, Morita et al., 2013, Roux and Topisirovic, 2012, Song et al., 2014, Zhang and Dou, 2014).

The significance of AKT signalling in FGFR inhibitor resistant MFE-296 cells was investigated in our 3D organotypic model, to assess the effects of AKT-targeted small molecule inhibition. MK2206, an inhibitor of AKT 1, 2 and 3 (Hirai et al., 2010), had a more marked effect on cell number and proliferation in MFE-296 cells than AKTVIII, which inhibits AKT 1 and 2 (Lindsley et al., 2005), both alone and in

combination with PD173074, suggesting AKT3 may be particularly important in the compensatory mechanism of MFE-296 cells.

The dramatic reduction in cell number and proliferation exhibited upon dual drug treatment targeting FGFR and AKT1-3 suggested a possible therapeutic regimen for overcoming FGFR inhibitor resistant acquisition. The prospect of treating endometrial cancer with a combination of chemotherapeutic drugs, or small molecule inhibitors and chemotherapeutics, has been outlined previously (Gozgit et al., 2013, Byron et al., 2012). Although these studies investigated the synergistic effects of dual drug therapy, we present the first study to investigate potential resistance mechanisms upon FGFR inhibition in endometrial cancer, and use these data as the rationale for choosing an additional therapeutic target.

Using an MS phosphoproteomic approach, we have demonstrated the changes in signalling networks upon acquisition of FGFR inhibitor resistance in MFE-296 cells. By investigating this, using an unbiased and quantitative approach, we have provided evidence of the importance of AKT signalling in acquisition of FGFR inhibitor resistance. Importantly, the effects of small molecule inhibition outlined in these data are FGFR2 mutation status dependent, as shown by the absence of growth inhibition in the FGFR2 wild-type Ishikawa cell line, in the presence of FGFR inhibitor. The lack of effect of the AKT inhibitors in Ishikawa cells was interesting, given that this cell line was *PTEN* and *PIK3R1* mutant. However, these mutations occur in the context of additional genetic aberrations in this cell line, of which deregulation of the PI3K pathway may not be of critical importance.

Future Directions

The exact phosphorylation sites of the nine of the phosphopeptides identified using MS could not be determined definitively, due to inadequate fragmentation of the peptide. Furthermore, these peptides possessed multiple potential phosphorylation sites and so the specific phosphorylated residues remained elusive. Whilst the

fragmentation method employed in our work (CID-MSA) is used routinely in phosphopeptide analysis (Boersema et al., 2009), more sensitive methods do exist, for example ECD and HCD, which could be used in future to determine the exact phosphorylated residues in these peptides (Olsen et al., 2007, Syka et al., 2004, Zubarev, 2004).

Notably, total protein levels were not assessed in this study. Our work has focused primarily on changes in signalling peptides upon drug exposure, of which phosphopeptides are the most important (Cohen, 2000, Manning et al., 2002). We do, however, acknowledge that analysis of total protein levels adds an additional layer of information to changes within the cell upon drug treatment, and so repetition of this experiment to elucidate such changes may be of interest in the future.

MS generates a large quantity of data, and validation of all potential pathways highlighted in this analysis is outside of the scope of this thesis. Whilst the AKT pathway was associated with the most de-regulated phosphopeptides identified in our study, we are nevertheless mindful that pathways other than AKT could have been selected to target alongside FGFR2.

While *in vivo* studies investigating the role of AKT in development and disease have shown different phenotypes for individual knockout of AKT1, 2 and 3, little is known about the specific functions of these isoforms and how they are regulated (Madhunapantula and Robertson, 2011). However, increased AKT3 activity has been shown to play an important role in the development of melanoma (Stahl et al., 2004). AKT1 and 3 have also been shown to be involved in regulation of splicing of FGFR2 in lung cancer (Sanidas et al., 2014). As such, the role of the individual isoforms of AKT in the FGFR inhibitor resistance mechanism warrants further investigation. One method of analysis would be siRNA-mediated knockdown of AKT3 in MFE-296 cells and subsequent treatment with PD173074, to assess the propensity of this cell line to acquire FGFR inhibitor resistance without AKT3

expression. However, such investigations may prove difficult given the ability of the various AKT isoforms to compensate for one another (Dummler et al., 2006).

6.4 Dissection of drug resistance mechanisms using transcriptomic analysis

To dissect the AKT-related drug resistance mechanism further, an inhibitor resistant population of MFE-296 cells was produced, by continuous exposure to PD173074, and named MFE-296^{PDR}. We addressed the question of possible up-regulation of an alternative RTK pathway to compensate for loss of FGFR signalling, as has been noted elsewhere in the literature (Niederst and Engelman, 2013). As tyrosine phosphorylation events occur at a reduced rate compared to that of serine and threonine (Delom and Chevet, 2006), it was possible that our MS investigations failed to highlight increased phosphorylation of an alternative RTK. However, PathScan analysis showed there to be low level down-regulation of alternative RTKs in MFE-296^{PDR} cells, implying the resistance mechanism was acquired via alternative means.

To gain insight into the differences in the transcriptomes of parental and resistant cells in a global, unbiased manner, microarray gene expression analysis was employed. Transcriptomic analysis of MFE-296^{PDR} cells, along with analysis of an additional inhibitor resistant cell line, MFE-296^{AZR}, showed a distinct gene expression signature common to drug resistant cells, compared to their parental counterparts.

IGFBP5 was significantly up-regulated in both resistant cell lines compared to the parental cells. Expression of this gene is known to be elevated in the absence of FGFR2 in keratinocytes in *in vivo* models (Schlake, 2005) and therefore potentially validating our data. The most significantly down-regulated gene in both resistant cell lines was *PHLDA1*, a negative regulator of AKT signalling.

In light of our data identifying a role for AKT in maintaining FGFR inhibitor resistance in MFE-296 cells, it was of particular interest that a negative regulator of AKT signalling was the most significantly down-regulated of all genes analysed on the microarray. Published work has noted the down-regulation of this gene in patient samples of melanoma and has postulated its use as a biomarker of disease

progression (Nagai et al., 2007, Neef et al., 2002). However, this was the first demonstration of a potential role for PHLDA1 in the acquisition and maintenance of drug resistance in cancers cells.

PHLDA1 expression was validated at the protein level, showing high expression in MFE-296 cells, localised to the membrane, and inhibition of this upon seven days PD173074 treatment. PHLDA1 was not expressed in MFE-296^{PDR} cells. The importance of down-regulation of this protein was shown upon siRNA knockdown of PHLDA1 in the parental MFE-296 cell line, which induced PD173074 inhibitor resistance after just three days of exposure to the drug.

In summary, our work has shown that inhibition of mutant FGFR signalling in the MFE-296 cell line decreased cell growth and proliferation over seven days. Although FGFR2 signalling was blocked, the cells were able to continue signalling at a reduced rate. This most likely occurred via the mutant copy of *PIK3CA* harboured in this cell line. As FGFR2 also induces PI3K signalling, decreased downstream effects of PI3K were observed via MS analysis over seven days exposure to PD173074. This decreased PI3K signalling led subsequently to a decrease in PIP₃ at the membrane. To compensate for the decreased PI3K signalling upon FGFR2 inhibition, PHLDA1 expression was decreased. Therefore, whilst there was reduced PI3K signalling, the AKT available in the cells was able to bind to PIP₃ free of competition with PHLDA1. In this way, AKT signalling could be sustained, even in the absence of mutant FGFR2 signalling.

Future Directions

Future work should focus on identification of the mechanism of PHLDA1 down-regulation in response to FGFR2 signalling inhibition. As PHLDA1 expression was not recovered upon removal of PD173074 from the medium of resistant cells, the down-regulation may be of a permanent nature, potentially induced by epigenetic modulation of the gene. Another intriguing line of enquiry is the potential feedback

loop between AKT and p53 resulting in down-regulation of PHLDA1, as has been noted in signalling of its protein family member, PHLDA3 (Kawase et al., 2009, Liao and Hung, 2010).

Crucial to the proposed mechanism outlined in this work are the differential levels of PIP₂ and PIP₃ levels in MFE-296 and MFE-296^{PDR} cells. Whilst we postulate these are lower in the resistant cell line, requiring PHLDA1 down-regulation in order to maintain AKT signalling, we aim to validate this using a PIP₃ competition assay in our future work.

In an alternative approach, the effect of PHLDA1 over-expression on MFE-296 and MFE-296^{PDR} cells will be assessed. Here we aim to assess whether MFE-296^{PDR} cells can be re-sensitised to PD173074 treatment by reintroduction of PHLDA1 into cells. We also aim to further validate the importance of PHLDA1 in FGFR inhibitor resistance by assessing basal levels in AN3CA cells and, if expressed, knocking down this protein in this cell line to investigate whether drug resistance can be induced.

Whilst this work focuses on endometrial cancer, activating FGFR2 mutations are found in a range of malignancies. As such, an interesting line of enquiry is whether the PHLDA1-associated drug resistance mechanism highlighted in this work is induced in other cancer types, in response to FGFR perturbation – or indeed when other RTKs are inhibited. The validity of the drug combinations highlighted in this work should also be investigated further in *in vivo* models.

6.5 Concluding remarks

Using a combination of MS-based phosphoproteomics, transcriptomics and biochemical methods, we have identified differential signalling in FGFR2 mutant endometrial cancer cells and successfully elucidated a mechanism of its acquisition. We show the first evidence of PHLDA1 down-regulation in response to targeted inhibition of a mutant RTK, and establish its role in maintaining drug resistance. Whether this phenomenon is specific to endometrial cancer cells or is a more global method of acquiring drug resistance remains to be elucidated. Nevertheless, further *in vivo* investigations should be undertaken to establish the potential viability of the FGFR/AKT drug combination outlined in this work in the treatment of endometrial cancer. Although combination trials are not currently underway, initial investigations into neuroblastoma and glioma, amongst others, suggest use of MK2206 alongside other small molecule inhibitors and chemotherapeutics provides an advantage in inducing cancer cell death (Cheng et al., 2012, Li et al., 2012, Agarwal et al., 2013). It is also promising that use of MK2206 alone is currently in clinical trials (Molife et al., 2014), as is the AZD4547 FGFR inhibitor (Xie et al., 2013, Zamora et al., 2014). The combinatorial use of both drugs represents an exciting line of clinical investigation, with the potential to overcome chemoresistance in FGFR2-driven cancers.

Chapter 7

References

- AGARWAL, E., BRATTAIN, M. G. & CHOWDHURY, S. 2013. Cell survival and metastasis regulation by Akt signaling in colorectal cancer. *Cell Signal*, 25, 1711-9.
- AGUAN, K., CARVAJAL, J. A., THOMPSON, L. P. & WEINER, C. P. 2000. Application of a functional genomics approach to identify differentially expressed genes in human myometrium during pregnancy and labour. *Mol Hum Reprod*, 6, 1141-5.
- AHMED, Z., LIN, C. C., SUEN, K. M., MELO, F. A., LEVITT, J. A., SUHLING, K. & LADBURY, J. E. 2013. Grb2 controls phosphorylation of FGFR2 by inhibiting receptor kinase and Shp2 phosphatase activity. *J Cell Biol*, 200, 493-504.
- AHMED, Z., SCHULLER, A. C., SUHLING, K., TREGIDGO, C. & LADBURY, J. E. 2008. Extracellular point mutations in FGFR2 elicit unexpected changes in intracellular signalling.
- ALCOLEA, M. P., CASADO, P., RODRIGUEZ-PRADOS, J. C., VANHAESEBROECK, B. & CUTILLAS, P. R. 2012. Phosphoproteomic analysis of leukemia cells under basal and drug-treated conditions identifies markers of kinase pathway activation and mechanisms of resistance. *Mol Cell Proteomics*, 11, 453-66.
- ALESSI, D. R., JAMES, S. R., DOWNES, C. P., HOLMES, A. B., GAFFNEY, P. R., REESE, C. B. & COHEN, P. 1997. Characterization of a 3-phosphoinositide-dependent protein kinase which phosphorylates and activates protein kinase B α . *Curr Biol*, 7, 261-9.
- AMANT, F., MOERMAN, P., NEVEN, P., TIMMERMAN, D., VAN LIMBERGEN, E. & VERGOTE, I. 2005. Endometrial cancer. *Lancet*, 366, 491-505.
- AMBUDKAR, S. V., DEY, S., HRYCYNA, C. A., RAMACHANDRA, M., PASTAN, I. & GOTTESMAN, M. M. 1999. Biochemical, cellular, and pharmacological aspects of the multidrug transporter. *Annu Rev Pharmacol Toxicol*, 39, 361-98.
- ANDRE, F., BACHELOT, T., CAMPONE, M., DALENC, F., PEREZ-GARCIA, J. M., HURVITZ, S. A., TURNER, N., RUGO, H., SMITH, J. W., DEUDON, S., SHI, M., ZHANG, Y., KAY, A., PORTA, D. G., YOVINE, A. & BASELGA, J. 2013. Targeting FGFR with dovitinib (TKI258): preclinical and clinical data in breast cancer. *Clin Cancer Res*, 19, 3693-702.

- ARAI, Y., TOTOKI, Y., HOSODA, F., SHIROTA, T., HAMA, N., NAKAMURA, H., OJIMA, H., FURUTA, K., SHIMADA, K., OKUSAKA, T., KOSUGE, T. & SHIBATA, T. 2014. Fibroblast growth factor receptor 2 tyrosine kinase fusions define a unique molecular subtype of cholangiocarcinoma. *Hepatology*, 59, 1427-34.
- ATSMA, F., BARTELINK, M. L., GROBBEE, D. E. & VAN DER SCHOUW, Y. T. 2006. Postmenopausal status and early menopause as independent risk factors for cardiovascular disease: a meta-analysis. *Menopause*, 13, 265-79.
- BAI, A., MEETZE, K., VO, N. Y., KOLLIPARA, S., MAZSA, E. K., WINSTON, W. M., WEILER, S., POLING, L. L., CHEN, T., ISMAIL, N. S., JIANG, J., LERNER, L., GYURIS, J. & WENG, Z. 2010. GP369, an FGFR2-IIIb-specific antibody, exhibits potent antitumor activity against human cancers driven by activated FGFR2 signaling. *Cancer Res*, 70, 7630-9.
- BALLA, T. 2013. Phosphoinositides: tiny lipids with giant impact on cell regulation. *Physiol Rev*, 93, 1019-137.
- BANWAIT, J. K. & BASTOLA, D. R. 2014. Contribution of bioinformatics prediction in microRNA-based cancer therapeutics. *Adv Drug Deliv Rev*.
- BEERLI, R. R. & BARBAS, C. F., 3RD 2002. Engineering polydactyl zinc-finger transcription factors. *Nat Biotechnol*, 20, 135-41.
- BEERLI, R. R., DREIER, B. & BARBAS, C. F., 3RD 2000. Positive and negative regulation of endogenous genes by designed transcription factors. *Proc Natl Acad Sci U S A*, 97, 1495-500.
- BEERLI, R. R., SEGAL, D. J., DREIER, B. & BARBAS, C. F., 3RD 1998. Toward controlling gene expression at will: specific regulation of the erbB-2/HER-2 promoter by using polydactyl zinc finger proteins constructed from modular building blocks. *Proc Natl Acad Sci U S A*, 95, 14628-33.
- BELOV, A. A. & MOHAMMADI, M. 2013. Molecular mechanisms of fibroblast growth factor signaling in physiology and pathology. *Cold Spring Harb Perspect Biol*, 5.
- BHAKTA, M. S., HENRY, I. M., OUSTEROUT, D. G., DAS, K. T., LOCKWOOD, S. H., MECKLER, J. F., WALLEN, M. C., ZYKOVICH, A., YU, Y., LEO, H., XU, L., GERSBACH, C. A. & SEGAL, D. J. 2013. Highly active zinc-finger nucleases by extended modular assembly. *Genome Res*, 23, 530-8.

- BIBIKOVA, M., CARROLL, D., SEGAL, D. J., TRAUTMAN, J. K., SMITH, J., KIM, Y. G. & CHANDRASEGARAN, S. 2001. Stimulation of homologous recombination through targeted cleavage by chimeric nucleases. *Mol Cell Biol*, 21, 289-97.
- BIEMANN, K. 1988. Contributions of mass spectrometry to peptide and protein structure. *Biomed Environ Mass Spectrom*, 16, 99-111.
- BOCH, J., SCHOLZE, H., SCHORNACK, S., LANDGRAF, A., HAHN, S., KAY, S., LAHAYE, T., NICKSTADT, A. & BONAS, U. 2009. Breaking the code of DNA binding specificity of TAL-type III effectors. *Science*, 326, 1509-12.
- BODNAR, A. G., OUELLETTE, M., FROLKIS, M., HOLT, S. E., CHIU, C. P., MORIN, G. B., HARLEY, C. B., SHAY, J. W., LICHTSTEINER, S. & WRIGHT, W. E. 1998. Extension of life-span by introduction of telomerase into normal human cells. *Science*, 279, 349-52.
- BOERSEMA, P. J., MOHAMMED, S. & HECK, A. J. 2009. Phosphopeptide fragmentation and analysis by mass spectrometry. *J Mass Spectrom*, 44, 861-78.
- BOGOYEVITCH, M. A., GLENNON, P. E., ANDERSSON, M. B., CLERK, A., LAZOU, A., MARSHALL, C. J., PARKER, P. J. & SUGDEN, P. H. 1994. Endothelin-1 and fibroblast growth factors stimulate the mitogen-activated protein kinase signaling cascade in cardiac myocytes. The potential role of the cascade in the integration of two signaling pathways leading to myocyte hypertrophy. *J Biol Chem*, 269, 1110-9.
- BOLSTAD, B. M., IRIZARRY, R. A., ASTRAND, M. & SPEED, T. P. 2003. A comparison of normalization methods for high density oligonucleotide array data based on variance and bias. *Bioinformatics*, 19, 185-93.
- BOTTCHER, R. T. & NIEHRS, C. 2005. Fibroblast growth factor signaling during early vertebrate development. *Endocr Rev*, 26, 63-77.
- BUDAY, L., WARNE, P. H. & DOWNWARD, J. 1995. Downregulation of the Ras activation pathway by MAP kinase phosphorylation of Sos. *Oncogene*, 11, 1327-31.
- BYRON, S. A., CHEN, H., WORTMANN, A., LOCH, D., GARTSIDE, M. G., DEHKHODA, F., BLAIS, S. P., NEUBERT, T. A., MOHAMMADI, M. & POLLOCK, P. M. 2013. The N550K/H mutations in FGFR2 confer differential

- resistance to PD173074, dovitinib, and ponatinib ATP-competitive inhibitors. *Neoplasia*, 15, 975-88.
- BYRON, S. A., GARTSIDE, M. G., WELLENS, C. L., MALLON, M. A., KEENAN, J. B., POWELL, M. A., GOODFELLOW, P. J. & POLLOCK, P. M. 2008. Inhibition of activated fibroblast growth factor receptor 2 in endometrial cancer cells induces cell death despite PTEN abrogation. *Cancer Res*, 68, 6902-7.
- BYRON, S. A., LOCH, D. C. & POLLOCK, P. M. 2012. Fibroblast growth factor receptor inhibition synergizes with Paclitaxel and Doxorubicin in endometrial cancer cells. *Int J Gynecol Cancer*, 22, 1517-26.
- CAPECCHI, M. R. 2005. Gene targeting in mice: functional analysis of the mammalian genome for the twenty-first century. *Nat Rev Genet*, 6, 507-12.
- CARGNELLO, M. & ROUX, P. P. 2011. Activation and function of the MAPKs and their substrates, the MAPK-activated protein kinases. *Microbiol Mol Biol Rev*, 75, 50-83.
- CARPENTER, G. & JI, Q. 1999. Phospholipase C-gamma as a signal-transducing element. *Exp Cell Res*, 253, 15-24.
- CARROLL, D. 2011. Genome engineering with zinc-finger nucleases. *Genetics*, 188, 773-82.
- CARTER, E. P., FEARON, A. E. & GROSE, R. P. 2014. Careless talk costs lives: fibroblast growth factor receptor signalling and the consequences of pathway malfunction. *Trends Cell Biol*.
- CASADO, P., ALCOLEA, M. P., IORIO, F., RODRIGUEZ-PRADOS, J. C., VANHAESEBROECK, B., SAEZ-RODRIGUEZ, J., JOEL, S. & CUTILLAS, P. R. 2013a. Phosphoproteomics data classify hematological cancer cell lines according to tumor type and sensitivity to kinase inhibitors. *Genome Biol*, 14, R37.
- CASADO, P. & CUTILLAS, P. R. 2011. A self-validating quantitative mass spectrometry method for assessing the accuracy of high-content phosphoproteomic experiments. *Mol Cell Proteomics*, 10, M110 003079.
- CASADO, P., RODRIGUEZ-PRADOS, J. C., COSULICH, S. C., GUICHARD, S., VANHAESEBROECK, B., JOEL, S. & CUTILLAS, P. R. 2013b. Kinase-substrate enrichment analysis provides insights into the heterogeneity of signaling pathway activation in leukemia cells. *Sci Signal*, 6, rs6.

- CATASUS, L., MATIAS-GUIU, X., MACHIN, P., MUNOZ, J. & PRAT, J. 1998. BAX somatic frameshift mutations in endometrioid adenocarcinomas of the endometrium: evidence for a tumor progression role in endometrial carcinomas with microsatellite instability. *Lab Invest*, 78, 1439-44.
- CERBINI, T., FUNAHASHI, R., LUO, Y., LIU, C., PARK, K., RAO, M., MALIK, N. & ZOU, J. 2015. Transcription Activator-Like Effector Nuclease (TALEN)-Mediated CLYBL Targeting Enables Enhanced Transgene Expression and One-Step Generation of Dual Reporter Human Induced Pluripotent Stem Cell (iPSC) and Neural Stem Cell (NSC) Lines. *PLoS One*, 10, e0116032.
- CHAUDHRY, P. & ASSELIN, E. 2009. Resistance to chemotherapy and hormone therapy in endometrial cancer. *Endocr Relat Cancer*, 16, 363-80.
- CHAUDHURY, A., HUSSEY, G. S., RAY, P. S., JIN, G., FOX, P. L. & HOWE, P. H. 2010. TGF-beta-mediated phosphorylation of hnRNP E1 induces EMT via transcript-selective translational induction of Dab2 and ILEI. *Nat Cell Biol*, 12, 286-93.
- CHELL, V., BALMANN, K., LITTLE, A. S., WILSON, M., ANDREWS, S., BLOCKLEY, L., HAMPSON, M., GAVINE, P. R. & COOK, S. J. 2013. Tumour cell responses to new fibroblast growth factor receptor tyrosine kinase inhibitors and identification of a gatekeeper mutation in FGFR3 as a mechanism of acquired resistance. *Oncogene*, 32, 3059-70.
- CHEN, L., LI, D., LI, C., ENGEL, A. & DENG, C. X. 2003. A Ser252Trp [corrected] substitution in mouse fibroblast growth factor receptor 2 (Fgfr2) results in craniosynostosis. *Bone*, 33, 169-78.
- CHEN, R. H., SARNECKI, C. & BLENIS, J. 1992. Nuclear localization and regulation of erk- and rsk-encoded protein kinases. *Mol Cell Biol*, 12, 915-27.
- CHENG, J. K. & ALPER, H. S. 2014. The genome editing toolbox: a spectrum of approaches for targeted modification. *Curr Opin Biotechnol*, 30C, 87-94.
- CHENG, Y., ZHANG, Y., ZHANG, L., REN, X., HUBER-KEENER, K. J., LIU, X., ZHOU, L., LIAO, J., KEIHACK, H., YAN, L., RUBIN, E. & YANG, J. M. 2012. MK-2206, a novel allosteric inhibitor of Akt, synergizes with gefitinib against malignant glioma via modulating both autophagy and apoptosis. *Mol Cancer Ther*, 11, 154-64.
- CHEUNG, L. W., HENNESSY, B. T., LI, J., YU, S., MYERS, A. P., DJORDJEVIC, B., LU, Y., STEMKE-HALE, K., DYER, M. D., ZHANG, F., JU, Z., CANTLEY, L.

- C., SCHERER, S. E., LIANG, H., LU, K. H., BROADDUS, R. R. & MILLS, G. B. 2011. High frequency of PIK3R1 and PIK3R2 mutations in endometrial cancer elucidates a novel mechanism for regulation of PTEN protein stability. *Cancer Discov*, 1, 170-85.
- CHIONI, A. M. & GROSE, R. 2012. FGFR1 cleavage and nuclear translocation regulates breast cancer cell behavior. *J Cell Biol*, 197, 801-17.
- CHOUDHARY, C. & MANN, M. 2010. Decoding signalling networks by mass spectrometry-based proteomics. *Nat Rev Mol Cell Biol*, 11, 427-39.
- CLINICALTRIALS.GOV 2014. FGFR inhibitor clinical trials.
- COHEN, P. 2000. The regulation of protein function by multisite phosphorylation--a 25 year update. *Trends Biochem Sci*, 25, 596-601.
- COLEMAN, S. J., CHIONI, A. M., GHALLAB, M., ANDERSON, R. K., LEMOINE, N. R., KOCHER, H. M. & GROSE, R. P. 2014. Nuclear translocation of FGFR1 and FGF2 in pancreatic stellate cells facilitates pancreatic cancer cell invasion. *EMBO Mol Med*, 6, 467-81.
- CONDON, J., YIN, S., MAYHEW, B., WORD, R. A., WRIGHT, W. E., SHAY, J. W. & RAINEY, W. E. 2002. Telomerase immortalization of human myometrial cells. *Biol Reprod*, 67, 506-14.
- CORBIT, K. C., TRAKUL, N., EVES, E. M., DIAZ, B., MARSHALL, M. & ROSNER, M. R. 2003. Activation of Raf-1 signaling by protein kinase C through a mechanism involving Raf kinase inhibitory protein. *J Biol Chem*, 278, 13061-8.
- COSMIC 2014. FGFR2 point mutations, copy number and gene expression variations in cancer.
- COUGHLIN, S. R., BARR, P. J., COUSENS, L. S., FRETTO, L. J. & WILLIAMS, L. T. 1988. Acidic and basic fibroblast growth factors stimulate tyrosine kinase activity in vivo. *J Biol Chem*, 263, 988-93.
- COULOMBE, P. & MELOCHE, S. 2007. Atypical mitogen-activated protein kinases: structure, regulation and functions. *Biochim Biophys Acta*, 1773, 1376-87.
- CRADICK, T. J., AMBROSINI, G., ISELI, C., BUCHER, P. & MCCAFFREY, A. P. 2011. ZFN-site searches genomes for zinc finger nuclease target sites and off-target sites. *BMC Bioinformatics*, 12, 152.
- CRITCHLEY, H. O., ROBERTSON, K. A., FORSTER, T., HENDERSON, T. A., WILLIAMS, A. R. & GHAZAL, P. 2006. Gene expression profiling of mid to

- late secretory phase endometrial biopsies from women with menstrual complaint. *Am J Obstet Gynecol*, 195, 406 e1-16.
- CRUK. 2014. *Cancer Research UK* [Online]. Available: <http://www.cancerresearchuk.org/cancer-info/cancerstats/types/uterus/incidence/> [Accessed 10th November 2014 2014].
- CUTILLAS, P. R. & VANHAESEBROECK, B. 2007. Quantitative profile of five murine core proteomes using label-free functional proteomics. *Mol Cell Proteomics*, 6, 1560-73.
- DAN, S., TSUNODA, T., KITAHARA, O., YANAGAWA, R., ZEMBUTSU, H., KATAGIRI, T., YAMAZAKI, K., NAKAMURA, Y. & YAMORI, T. 2002. An integrated database of chemosensitivity to 55 anticancer drugs and gene expression profiles of 39 human cancer cell lines. *Cancer Res*, 62, 1139-47.
- DARNELL, J. E., JR. 1997. STATs and gene regulation. *Science*, 277, 1630-5.
- DAS THAKUR, M., SALANGSANG, F., LANDMAN, A. S., SELLERS, W. R., PRYER, N. K., LEVESQUE, M. P., DUMMER, R., MCMAHON, M. & STUART, D. D. 2013. Modelling vemurafenib resistance in melanoma reveals a strategy to forestall drug resistance. *Nature*, 494, 251-5.
- DAVIES, H., BIGNELL, G. R., COX, C., STEPHENS, P., EDKINS, S., CLEGG, S., TEAGUE, J., WOFFENDIN, H., GARNETT, M. J., BOTTOMLEY, W., DAVIS, N., DICKS, E., EWING, R., FLOYD, Y., GRAY, K., HALL, S., HAWES, R., HUGHES, J., KOSMIDOU, V., MENZIES, A., MOULD, C., PARKER, A., STEVENS, C., WATT, S., HOOPER, S., WILSON, R., JAYATILAKE, H., GUSTERSON, B. A., COOPER, C., SHIPLEY, J., HARGRAVE, D., PRITCHARD-JONES, K., MAITLAND, N., CHENEVIX-TRENCH, G., RIGGINS, G. J., BIGNER, D. D., PALMIERI, G., COSSU, A., FLANAGAN, A., NICHOLSON, A., HO, J. W., LEUNG, S. Y., YUEN, S. T., WEBER, B. L., SEIGLER, H. F., DARROW, T. L., PATERSON, H., MARAIS, R., MARSHALL, C. J., WOOSTER, R., STRATTON, M. R. & FUTREAL, P. A. 2002. Mutations of the BRAF gene in human cancer. *Nature*, 417, 949-54.
- DE WEVER, O. & MAREEL, M. 2003. Role of tissue stroma in cancer cell invasion. *J Pathol*, 200, 429-47.
- DEGNORE, J. P. & QIN, J. 1998. Fragmentation of phosphopeptides in an ion trap mass spectrometer. *J Am Soc Mass Spectrom*, 9, 1175-88.

- DELOM, F. & CHEVET, E. 2006. Phosphoprotein analysis: from proteins to proteomes. *Proteome Sci*, 4, 15.
- DENARDO, D. G., ANDREU, P. & COUSSENS, L. M. 2010. Interactions between lymphocytes and myeloid cells regulate pro- versus anti-tumor immunity. *Cancer Metastasis Rev*, 29, 309-16.
- DHALLUIN, C., YAN, K. S., PLOTNIKOVA, O., ZENG, L., GOLDFARB, M. P. & ZHOU, M. M. 2000. ¹H, ¹³C and ¹⁵N resonance assignments of the SNT PTB domain in complex with FGFR1 peptide. *J Biomol NMR*, 18, 371-2.
- DICKSON, M. A., HAHN, W. C., INO, Y., RONFARD, V., WU, J. Y., WEINBERG, R. A., LOUIS, D. N., LI, F. P. & RHEINWALD, J. G. 2000. Human keratinocytes that express hTERT and also bypass a p16(INK4a)-enforced mechanism that limits life span become immortal yet retain normal growth and differentiation characteristics. *Mol Cell Biol*, 20, 1436-47.
- DOUILLARD-GUILLOUX, G., MOULY, V., CAILLAUD, C. & RICHARD, E. 2009. Immortalization of murine muscle cells from lysosomal alpha-glucosidase deficient mice: a new tool to study pathophysiology and assess therapeutic strategies for Pompe disease. *Biochem Biophys Res Commun*, 388, 333-8.
- DOYON, Y., CHOI, V. M., XIA, D. F., VO, T. D., GREGORY, P. D. & HOLMES, M. C. 2010. Transient cold shock enhances zinc-finger nuclease-mediated gene disruption. *Nat Methods*, 7, 459-60.
- DUBRULLE, J. & POURQUIE, O. 2004. fgf8 mRNA decay establishes a gradient that couples axial elongation to patterning in the vertebrate embryo. *Nature*, 427, 419-22.
- DUGGAN, B. D., FELIX, J. C., MUDERSPACH, L. I., TOURGEMAN, D., ZHENG, J. & SHIBATA, D. 1994. Microsatellite instability in sporadic endometrial carcinoma. *J Natl Cancer Inst*, 86, 1216-21.
- DUMMLER, B., TSCHOPP, O., HYNX, D., YANG, Z. Z., DIRNHOFER, S. & HEMMINGS, B. A. 2006. Life with a single isoform of Akt: mice lacking Akt2 and Akt3 are viable but display impaired glucose homeostasis and growth deficiencies. *Mol Cell Biol*, 26, 8042-51.
- DUTT, A., SALVESEN, H. B., CHEN, T. H., RAMOS, A. H., ONOFRIO, R. C., HATTON, C., NICOLETTI, R., WINCKLER, W., GREWAL, R., HANNA, M., WYHS, N., ZIAUGRA, L., RICHTER, D. J., TROVIK, J., ENGELSEN, I. B., STEFANSSON, I. M., FENNELL, T., CIBULSKIS, K., ZODY, M. C., AKSLEN,

- L. A., GABRIEL, S., WONG, K. K., SELLERS, W. R., MEYERSON, M. & GREULICH, H. 2008. Drug-sensitive FGFR2 mutations in endometrial carcinoma. *Proc Natl Acad Sci U S A*, 105, 8713-7.
- EASTON, D. F., POOLEY, K. A., DUNNING, A. M., PHAROAH, P. D., THOMPSON, D., BALLINGER, D. G., STRUEWING, J. P., MORRISON, J., FIELD, H., LUBEN, R., WAREHAM, N., AHMED, S., HEALEY, C. S., BOWMAN, R., MEYER, K. B., HAIMAN, C. A., KOLONEL, L. K., HENDERSON, B. E., LE MARCHAND, L., BRENNAN, P., SANGRAJRANG, S., GABORIEAU, V., ODEFREY, F., SHEN, C. Y., WU, P. E., WANG, H. C., ECCLES, D., EVANS, D. G., PETO, J., FLETCHER, O., JOHNSON, N., SEAL, S., STRATTON, M. R., RAHMAN, N., CHENEVIX-TRENCH, G., BOJESSEN, S. E., NORDESTGAARD, B. G., AXELSSON, C. K., GARCIA-CLOSAS, M., BRINTON, L., CHANOCK, S., LISSOWSKA, J., PEPLONSKA, B., NEVANLINNA, H., FAGERHOLM, R., EEROLA, H., KANG, D., YOO, K. Y., NOH, D. Y., AHN, S. H., HUNTER, D. J., HANKINSON, S. E., COX, D. G., HALL, P., WEDREN, S., LIU, J., LOW, Y. L., BOGDANOVA, N., SCHURMANN, P., DORK, T., TOLLENAAR, R. A., JACOBI, C. E., DEVILEE, P., KLIJN, J. G., SIGURDSON, A. J., DOODY, M. M., ALEXANDER, B. H., ZHANG, J., COX, A., BROCK, I. W., MACPHERSON, G., REED, M. W., COUCH, F. J., GOODE, E. L., OLSON, J. E., MEIJERS-HEIJBOER, H., VAN DEN OUWELAND, A., UITTERLINDEN, A., RIVADENEIRA, F., MILNE, R. L., RIBAS, G., GONZALEZ-NEIRA, A., BENITEZ, J., HOPPER, J. L., MCCREDIE, M., SOUTHEY, M., GILES, G. G., SCHROEN, C., JUSTENHOVEN, C., BRAUCH, H., HAMANN, U., KO, Y. D., SPURDLE, A. B., BEESLEY, J., CHEN, X., MANNERMAA, A., KOSMA, V. M., KATAJA, V., HARTIKAINEN, J., DAY, N. E., et al. 2007. Genome-wide association study identifies novel breast cancer susceptibility loci. *Nature*, 447, 1087-93.
- EBONG, S., YU, C. R., CARPER, D. A., CHEPELINSKY, A. B. & EGWUAGU, C. E. 2004. Activation of STAT signaling pathways and induction of suppressors of cytokine signaling (SOCS) proteins in mammalian lens by growth factors. *Invest Ophthalmol Vis Sci*, 45, 872-8.
- EMENS, L. A. & MIDDLETON, G. 2015. The Interplay of Immunotherapy and Chemotherapy: Harnessing Potential Synergies. *Cancer Immunol Res*, 3, 436-443.

- ENGLISH, J. D. & SWEATT, J. D. 1997. A requirement for the mitogen-activated protein kinase cascade in hippocampal long term potentiation. *J Biol Chem*, 272, 19103-6.
- ENS, W. & STANDING, K. G. 2005. Hybrid quadrupole/time-of-flight mass spectrometers for analysis of biomolecules. *Methods Enzymol*, 402, 49-78.
- ESWARAKUMAR, V. P., HOROWITZ, M. C., LOCKLIN, R., MORRISS-KAY, G. M. & LONAI, P. 2004. A gain-of-function mutation of Fgfr2c demonstrates the roles of this receptor variant in osteogenesis. *Proc Natl Acad Sci U S A*, 101, 12555-60.
- ESWARAKUMAR, V. P., LAX, I. & SCHLESSINGER, J. 2005. Cellular signaling by fibroblast growth factor receptors. *Cytokine Growth Factor Rev*, 16, 139-49.
- FABBRO, D. & MANLEY, P. W. 2001. Su-6668. SUGEN. *Curr Opin Investig Drugs*, 2, 1142-8.
- FACCHINETTI, V., OUYANG, W., WEI, H., SOTO, N., LAZORCHAK, A., GOULD, C., LOWRY, C., NEWTON, A. C., MAO, Y., MIAO, R. Q., SESSA, W. C., QIN, J., ZHANG, P., SU, B. & JACINTO, E. 2008. The mammalian target of rapamycin complex 2 controls folding and stability of Akt and protein kinase C. *EMBO J*, 27, 1932-43.
- FANNING, E. 1992. Simian virus 40 large T antigen: the puzzle, the pieces, and the emerging picture. *J Virol*, 66, 1289-93.
- FARATIAN, D., GOLTSOV, A., LEBEDEVA, G., SOROKIN, A., MOODIE, S., MULLEN, P., KAY, C., UM, I. H., LANGDON, S., GORYANIN, I. & HARRISON, D. J. 2009. Systems biology reveals new strategies for personalizing cancer medicine and confirms the role of PTEN in resistance to trastuzumab. *Cancer Res*, 69, 6713-20.
- FARWELL, D. G., SHERA, K. A., KOOP, J. I., BONNET, G. A., MATTHEWS, C. P., REUTHER, G. W., COLTRERA, M. D., MCDUGALL, J. K. & KLINGELHUTZ, A. J. 2000. Genetic and epigenetic changes in human epithelial cells immortalized by telomerase. *Am J Pathol*, 156, 1537-47.
- FEARON, A. E., GOULD, C. R. & GROSE, R. P. 2013. FGFR signalling in women's cancers. *Int J Biochem Cell Biol*, 45, 2832-42.
- FEARON, A. E. & GROSE, R. P. 2014. Grb-ing receptor activation by the tail. *Nat Struct Mol Biol*, 21, 113-4.

- FELDMAN, B., POUHEYMIROU, W., PAPAIOANNOU, V. E., DECHIARA, T. M. & GOLDFARB, M. 1995. Requirement of FGF-4 for postimplantation mouse development. *Science*, 267, 246-9.
- FENG, Y., NIE, L., THAKUR, M. D., SU, Q., CHI, Z., ZHAO, Y. & LONGMORE, G. D. 2010. A multifunctional lentiviral-based gene knockdown with concurrent rescue that controls for off-target effects of RNAi. *Genomics Proteomics Bioinformatics*, 8, 238-45.
- FINN, O. J. 2014. Vaccines for cancer prevention: a practical and feasible approach to the cancer epidemic. *Cancer Immunol Res*, 2, 708-13.
- FLAHERTY, K. T., PUZANOV, I., KIM, K. B., RIBAS, A., MCARTHUR, G. A., SOSMAN, J. A., O'DWYER, P. J., LEE, R. J., GRIPPO, J. F., NOLOP, K. & CHAPMAN, P. B. 2010. Inhibition of mutated, activated BRAF in metastatic melanoma. *N Engl J Med*, 363, 809-19.
- FONG, L. & SMALL, E. J. 2008. Anti-cytotoxic T-lymphocyte antigen-4 antibody: the first in an emerging class of immunomodulatory antibodies for cancer treatment. *J Clin Oncol*, 26, 5275-83.
- FOTH, M., AHMAD, I., VAN RHIJN, B. W., VAN DER KWAST, T., BERGMAN, A. M., KING, L., RIDGWAY, R., LEUNG, H. Y., FRASER, S., SANSOM, O. J. & IWATA, T. 2014. Fibroblast growth factor receptor 3 activation plays a causative role in urothelial cancer pathogenesis in cooperation with Pten loss in mice. *J Pathol*, 233, 148-58.
- FRANCAVILLA, C., RIGBOLT, K. T., EMDAL, K. B., CARRARO, G., VERNET, E., BEKKER-JENSEN, D. B., STREICHER, W., WIKSTROM, M., SUNDSTROM, M., BELLUSCI, S., CAVALLARO, U., BLAGOEV, B. & OLSEN, J. V. 2013. Functional proteomics defines the molecular switch underlying FGF receptor trafficking and cellular outputs. *Mol Cell*, 51, 707-22.
- FRANK, D., MENDELSON, C. L., CICCONE, E., SVENSSON, K., OHLSSON, R. & TYCKO, B. 1999. A novel pleckstrin homology-related gene family defined by *lpl/Tssc3*, *TDAG51*, and *Tih1*: tissue-specific expression, chromosomal location, and parental imprinting. *Mamm Genome*, 10, 1150-9.
- FRANKE, T. F., YANG, S. I., CHAN, T. O., DATTA, K., KAZLAUSKAS, A., MORRISON, D. K., KAPLAN, D. R. & TSICHLIS, P. N. 1995. The protein kinase encoded by the Akt proto-oncogene is a target of the PDGF-activated phosphatidylinositol 3-kinase. *Cell*, 81, 727-36.

- FREITAS, E. C., NASCIMENTO, S. R., DE MELLO, M. P. & GIL-DA-SILVA-LOPES, V. L. 2006. Q289P mutation in FGFR2 gene causes Saethre-Chotzen syndrome: some considerations about familial heterogeneity. *Cleft Palate Craniofac J*, 43, 142-7.
- FROELING, F. E., MIRZA, T. A., FEAOKINS, R. M., SEEDHAR, A., ELIA, G., HART, I. R. & KOCHER, H. M. 2009. Organotypic culture model of pancreatic cancer demonstrates that stromal cells modulate E-cadherin, beta-catenin, and Ezrin expression in tumor cells. *Am J Pathol*, 175, 636-48.
- FULCHER, M. L., GABRIEL, S. E., OLSEN, J. C., TATREAU, J. R., GENTZSCH, M., LIVANOS, E., SAAVEDRA, M. T., SALMON, P. & RANDELL, S. H. 2009. Novel human bronchial epithelial cell lines for cystic fibrosis research. *Am J Physiol Lung Cell Mol Physiol*, 296, L82-91.
- FURDUI, C. M., LEW, E. D., SCHLESSINGER, J. & ANDERSON, K. S. 2006. Autophosphorylation of FGFR1 kinase is mediated by a sequential and precisely ordered reaction. *Mol Cell*, 21, 711-7.
- FURTHAUER, M., REIFERS, F., BRAND, M., THISSE, B. & THISSE, C. 2001. sprouty4 acts in vivo as a feedback-induced antagonist of FGF signaling in zebrafish. *Development*, 128, 2175-86.
- FUSENIG, N. E., BREITKREUTZ, D., DZARLIEVA, R. T., BOUKAMP, P., BOHNERT, A. & TILGEN, W. 1983. Growth and differentiation characteristics of transformed keratinocytes from mouse and human skin in vitro and in vivo. *J Invest Dermatol*, 81, 168s-75s.
- GAJ, T., GERSBACH, C. A. & BARBAS, C. F., 3RD 2013. ZFN, TALEN, and CRISPR/Cas-based methods for genome engineering. *Trends Biotechnol*, 31, 397-405.
- GAMBARINI, A. G., MIYAMOTO, C. A., LIMA, G. A., NADER, H. B. & DIETRICH, C. P. 1993. Mitogenic activity of acidic fibroblast growth factor is enhanced by highly sulfated oligosaccharides derived from heparin and heparan sulfate. *Mol Cell Biochem*, 124, 121-9.
- GAVINE, P. R., MOONEY, L., KILGOUR, E., THOMAS, A. P., AL-KADHIMI, K., BECK, S., ROONEY, C., COLEMAN, T., BAKER, D., MELLOR, M. J., BROOKS, A. N. & KLINOWSKA, T. 2012. AZD4547: an orally bioavailable, potent, and selective inhibitor of the fibroblast growth factor receptor tyrosine kinase family. *Cancer Res*, 72, 2045-56.

- GEORGOPOULOS, N. T., KIRKWOOD, L. A., VARLEY, C. L., MACLAINE, N. J., AZIZ, N. & SOUTHGATE, J. 2011. Immortalisation of normal human urothelial cells compromises differentiation capacity. *Eur Urol*, 60, 141-9.
- GHABRIAL, A., LUSCHNIG, S., METZSTEIN, M. M. & KRASNOW, M. A. 2003. Branching morphogenesis of the Drosophila tracheal system. *Annu Rev Cell Dev Biol*, 19, 623-47.
- GLIGORIJEVIC, B., BERGMAN, A. & CONDEELIS, J. 2014. Multiparametric Classification Links Tumor Microenvironments with Tumor Cell Phenotype. *PLoS Biol*, 12, e1001995.
- GOLTSOV, A., FARATIAN, D., LANGDON, S. P., BOWN, J., GORYANIN, I. & HARRISON, D. J. 2011. Compensatory effects in the PI3K/PTEN/AKT signaling network following receptor tyrosine kinase inhibition. *Cell Signal*, 23, 407-16.
- GOLTSOV, A., FARATIAN, D., LANGDON, S. P., MULLEN, P., HARRISON, D. J. & BOWN, J. 2012. Features of the reversible sensitivity-resistance transition in PI3K/PTEN/AKT signalling network after HER2 inhibition. *Cell Signal*, 24, 493-504.
- GOMM, J. J., BROWNE, P. J., COOPE, R. C., LIU, Q. Y., BULUWELA, L. & COOMBES, R. C. 1995. Isolation of pure populations of epithelial and myoepithelial cells from the normal human mammary gland using immunomagnetic separation with Dynabeads. *Anal Biochem*, 226, 91-9.
- GONZALEZ, B., SCHWIMMER, L. J., FULLER, R. P., YE, Y., ASAWAPORNMONGKOL, L. & BARBAS, C. F., 3RD 2010. Modular system for the construction of zinc-finger libraries and proteins. *Nat Protoc*, 5, 791-810.
- GOTOH, N. 2008. Regulation of growth factor signaling by FRS2 family docking/scaffold adaptor proteins. *Cancer Sci*, 99, 1319-25.
- GOTTESMAN, M. M., FOJO, T. & BATES, S. E. 2002. Multidrug resistance in cancer: role of ATP-dependent transporters. *Nat Rev Cancer*, 2, 48-58.
- GOZGIT, J. M., SQUILLACE, R. M., WONGCHENKO, M. J., MILLER, D., WARDWELL, S., MOHEMMAD, Q., NARASIMHAN, N. I., WANG, F., CLACKSON, T. & RIVERA, V. M. 2013. Combined targeting of FGFR2 and mTOR by ponatinib and ridaforolimus results in synergistic antitumor activity

- in FGFR2 mutant endometrial cancer models. *Cancer Chemother Pharmacol*, 71, 1315-23.
- GREULICH, H. & POLLOCK, P. M. 2011a. Targeting mutant fibroblast growth factor receptors in cancer.
- GREULICH, H. & POLLOCK, P. M. 2011b. Targeting mutant fibroblast growth factor receptors in cancer. *Trends Mol Med*, 17, 283-92.
- GRIVENNIKOV, S. I., GRETEN, F. R. & KARIN, M. 2010. Immunity, inflammation, and cancer. *Cell*, 140, 883-99.
- GROSE, R., FANTL, V., WERNER, S., CHIONI, A. M., JAROSZ, M., RUDLING, R., CROSS, B., HART, I. R. & DICKSON, C. 2007. The role of fibroblast growth factor receptor 2b in skin homeostasis and cancer development. *EMBO J*, 26, 1268-78.
- GRYGIELEWICZ, P., DYMEK, B., BUJAK, A., GUNERKA, P., STANCZAK, A., LAMPARSKA-PRZYBYSZ, M., WIECZOREK, M., DZWONEK, K. & ZDZALIK, D. 2014. Epithelial-mesenchymal transition confers resistance to selective FGFR inhibitors in SNU-16 gastric cancer cells. *Gastric Cancer*.
- GUAL, P., GIORDANO, S., ANGUSSOLA, S., PARKER, P. J. & COMOGLIO, P. M. 2001. Gab1 phosphorylation: a novel mechanism for negative regulation of HGF receptor signaling. *Oncogene*, 20, 156-66.
- GUIMOND, S. E. & TURNBULL, J. E. 1999. Fibroblast growth factor receptor signalling is dictated by specific heparan sulphate saccharides. *Curr Biol*, 9, 1343-6.
- GUNEY, I., WU, S. & SEDIVY, J. M. 2006. Reduced c-Myc signaling triggers telomere-independent senescence by regulating Bmi-1 and p16(INK4a). *Proc Natl Acad Sci U S A*, 103, 3645-50.
- GYMNOPOULOS, M., ELSLIGER, M. A. & VOGT, P. K. 2007. Rare cancer-specific mutations in PIK3CA show gain of function. *Proc Natl Acad Sci U S A*, 104, 5569-74.
- HACOHEN, N., KRAMER, S., SUTHERLAND, D., HIROMI, Y. & KRASNOW, M. A. 1998. sprouty encodes a novel antagonist of FGF signaling that patterns apical branching of the Drosophila airways. *Cell*, 92, 253-63.
- HAN, S. Y., KATO, H., KATO, S., SUZUKI, T., SHIBATA, H., ISHII, S., SHIIBA, K., MATSUNO, S., KANAMARU, R. & ISHIOKA, C. 2000. Functional evaluation

- of PTEN missense mutations using in vitro phosphoinositide phosphatase assay. *Cancer Res*, 60, 3147-51.
- HANAHAH, D. & WEINBERG, R. A. 2000. The hallmarks of cancer. *Cell*, 100, 57-70.
- HANAHAH, D. & WEINBERG, R. A. 2011. Hallmarks of cancer: the next generation. *Cell*, 144, 646-74.
- HARDING, T. C., LONG, L., PALENCIA, S., ZHANG, H., SADRA, A., HESTIR, K., PATIL, N., LEVIN, A., HSU, A. W., CHARYCH, D., BRENNAN, T., ZANGHI, J., HALENBECK, R., MARSHALL, S. A., QIN, M., DOBERSTEIN, S. K., HOLLENBAUGH, D., KAVANAUGH, W. M., WILLIAMS, L. T. & BAKER, K. P. 2013. Blockade of nonhormonal fibroblast growth factors by FP-1039 inhibits growth of multiple types of cancer. *Sci Transl Med*, 5, 178ra39.
- HATCH, N. E. 2010. FGF signaling in craniofacial biological control and pathological craniofacial development. *Crit Rev Eukaryot Gene Expr*, 20, 295-311.
- HAYFLICK, L. & MOORHEAD, P. S. 1961. The serial cultivation of human diploid cell strains. *Exp Cell Res*, 25, 585-621.
- HERBERT, C., SCHIEBORR, U., SAXENA, K., JURASZEK, J., DE SMET, F., ALCOUFFE, C., BIANCIOTTO, M., SALADINO, G., SIBRAC, D., KUDLINZKI, D., SREERAMULU, S., BROWN, A., RIGON, P., HERAULT, J. P., LASSALLE, G., BLUNDELL, T. L., ROUSSEAU, F., GILS, A., SCHYMKOWITZ, J., TOMPA, P., HERBERT, J. M., CARMELIET, P., GERVASIO, F. L., SCHWALBE, H. & BONO, F. 2013. Molecular mechanism of SSR128129E, an extracellularly acting, small-molecule, allosteric inhibitor of FGF receptor signaling. *Cancer Cell*, 23, 489-501.
- HIRAI, H., SOOTOME, H., NAKATSURU, Y., MIYAMA, K., TAGUCHI, S., TSUJIOKA, K., UENO, Y., HATCH, H., MAJUMDER, P. K., PAN, B. S. & KOTANI, H. 2010. MK-2206, an allosteric Akt inhibitor, enhances antitumor efficacy by standard chemotherapeutic agents or molecular targeted drugs in vitro and in vivo. *Mol Cancer Ther*, 9, 1956-67.
- HOJJAT-FARSANGI, M. 2014. Small-molecule inhibitors of the receptor tyrosine kinases: promising tools for targeted cancer therapies. *Int J Mol Sci*, 15, 13768-801.
- HOLOHAN, C., VAN SCHAEYBROECK, S., LONGLEY, D. B. & JOHNSTON, P. G. 2013. Cancer drug resistance: an evolving paradigm. *Nat Rev Cancer*, 13, 714-26.

- HOMBRINK, P., HASSAN, C., KESTER, M. G., JAHN, L., PONT, M. J., DE RU, A. H., VAN BERGEN, C. A., GRIFFIOEN, M., FALKENBURG, J. H., VAN VEELLEN, P. A. & HEEMSKERK, M. H. 2015. Identification of biological relevant minor histocompatibility antigens within the B-lymphocyte derived HLA-ligandome using a reverse immunology approach. *Clin Cancer Res*.
- HONG, L., HAN, Y., LIU, J. & BRAIN, L. 2013. Fibroblast growth factor receptor 2: a therapeutic target in gastric cancer. *Expert Rev Gastroenterol Hepatol*, 7, 759-65.
- HOSSAIN, G. S., VAN THIENEN, J. V., WERSTUCK, G. H., ZHOU, J., SOOD, S. K., DICKHOUT, J. G., DE KONING, A. B., TANG, D., WU, D., FALK, E., PODDAR, R., JACOBSEN, D. W., ZHANG, K., KAUFMAN, R. J. & AUSTIN, R. C. 2003. TDAG51 is induced by homocysteine, promotes detachment-mediated programmed cell death, and contributes to the development of atherosclerosis in hyperhomocysteinemia. *J Biol Chem*, 278, 30317-27.
- HU, W., JIN, L., JIANG, C. C., LONG, G. V., SCOLYER, R. A., WU, Q., ZHANG, X. D., MEI, Y. & WU, M. 2013. AEBP1 upregulation confers acquired resistance to BRAF (V600E) inhibition in melanoma. *Cell Death Dis*, 4, e914.
- HUANG, P. & STERN, M. J. 2005. FGF signaling in flies and worms: more and more relevant to vertebrate biology. *Cytokine Growth Factor Rev*, 16, 151-8.
- HUNTER, D. J., KRAFT, P., JACOBS, K. B., COX, D. G., YEAGER, M., HANKINSON, S. E., WACHOLDER, S., WANG, Z., WELCH, R., HUTCHINSON, A., WANG, J., YU, K., CHATTERJEE, N., ORR, N., WILLETT, W. C., COLDITZ, G. A., ZIEGLER, R. G., BERG, C. D., BUYS, S. S., MCCARTY, C. A., FEIGELSON, H. S., CALLE, E. E., THUN, M. J., HAYES, R. B., TUCKER, M., GERHARD, D. S., FRAUMENI, J. F., JR., HOOVER, R. N., THOMAS, G. & CHANOCK, S. J. 2007. A genome-wide association study identifies alleles in FGFR2 associated with risk of sporadic postmenopausal breast cancer. *Nat Genet*, 39, 870-4.
- HUSSEY, G. S., CHAUDHURY, A., DAWSON, A. E., LINDNER, D. J., KNUDSEN, C. R., WILCE, M. C., MERRICK, W. C. & HOWE, P. H. 2011. Identification of an mRNP complex regulating tumorigenesis at the translational elongation step. *Mol Cell*, 41, 419-31.
- IBRAHIMI, O. A., ELISEENKOVA, A. V., PLOTNIKOV, A. N., YU, K., ORNITZ, D. M. & MOHAMMADI, M. 2001. Structural basis for fibroblast growth factor

- receptor 2 activation in Apert syndrome. *Proc Natl Acad Sci U S A*, 98, 7182-7.
- INOKI, K., LI, Y., ZHU, T., WU, J. & GUAN, K. L. 2002. TSC2 is phosphorylated and inhibited by Akt and suppresses mTOR signalling. *Nat Cell Biol*, 4, 648-57.
- ISHIHAMA, Y., ODA, Y., TABATA, T., SATO, T., NAGASU, T., RAPPSILBER, J. & MANN, M. 2005. Exponentially modified protein abundance index (emPAI) for estimation of absolute protein amount in proteomics by the number of sequenced peptides per protein. *Mol Cell Proteomics*, 4, 1265-72.
- ISHIWATA, T., MATSUDA, Y., YAMAMOTO, T., UCHIDA, E., KORC, M. & NAITO, Z. 2012. Enhanced expression of fibroblast growth factor receptor 2 IIIc promotes human pancreatic cancer cell proliferation. *Am J Pathol*, 180, 1928-41.
- JEMAL, A., BRAY, F., CENTER, M. M., FERLAY, J., WARD, E. & FORMAN, D. 2011. Global cancer statistics. *CA Cancer J Clin*, 61, 69-90.
- JIANG, Q., MENG, X., MENG, L., CHANG, N., XIONG, J., CAO, H. & LIANG, Z. 2015. Small indels induced by CRISPR/Cas9 in the 5' region of microRNA lead to its depletion and Drosha processing retardance. *RNA Biol*, 0.
- JOHANNESSEN, C. M., BOEHM, J. S., KIM, S. Y., THOMAS, S. R., WARDWELL, L., JOHNSON, L. A., EMERY, C. M., STRANSKY, N., COGDILL, A. P., BARRETINA, J., CAPONIGRO, G., HIERONYMUS, H., MURRAY, R. R., SALEHI-ASHTIANI, K., HILL, D. E., VIDAL, M., ZHAO, J. J., YANG, X., ALKAN, O., KIM, S., HARRIS, J. L., WILSON, C. J., MYER, V. E., FINAN, P. M., ROOT, D. E., ROBERTS, T. M., GOLUB, T., FLAHERTY, K. T., DUMMER, R., WEBER, B. L., SELLERS, W. R., SCHLEGEL, R., WARGO, J. A., HAHN, W. C. & GARRAWAY, L. A. 2010. COT drives resistance to RAF inhibition through MAP kinase pathway reactivation. *Nature*, 468, 968-72.
- JOHNSON, D. E., LU, J., CHEN, H., WERNER, S. & WILLIAMS, L. T. 1991. The human fibroblast growth factor receptor genes: a common structural arrangement underlies the mechanisms for generating receptor forms that differ in their third immunoglobulin domain. *Mol Cell Biol*, 11, 4627-34.
- JOHNSON, D. E. & WILLIAMS, L. T. 1993. Structural and functional diversity in the FGF receptor multigene family.
- JUANPERE, N., AGELL, L., LORENZO, M., DE MUGA, S., LOPEZ-VILARO, L., MURILLO, R., MOJAL, S., SERRANO, S., LORENTE, J. A., LLORETA, J. &

- HERNANDEZ, S. 2012. Mutations in FGFR3 and PIK3CA, singly or combined with RAS and AKT1, are associated with AKT but not with MAPK pathway activation in urothelial bladder cancer. *Hum Pathol*, 43, 1573-82.
- KAHN, J., TOFILON, P. J. & CAMPHAUSEN, K. 2012. Preclinical models in radiation oncology. *Radiat Oncol*, 7, 223.
- KALININA, J., DUTTA, K., ILGHARI, D., BEENKEN, A., GOETZ, R., ELISEENKOVA, A. V., COWBURN, D. & MOHAMMADI, M. 2012. The alternatively spliced acid box region plays a key role in FGF receptor autoinhibition. *Structure*, 20, 77-88.
- KAULICH, M., LEE, Y. J., LONN, P., SPRINGER, A. D., MEADE, B. R. & DOWDY, S. F. 2015. Efficient CRISPR-rAAV engineering of endogenous genes to study protein function by allele-specific RNAi. *Nucleic Acids Res*.
- KAWASE, R., ISHIWATA, T., MATSUDA, Y., ONDA, M., KUDO, M., TAKESHITA, T. & NAITO, Z. 2010. Expression of fibroblast growth factor receptor 2 IIIc in human uterine cervical intraepithelial neoplasia and cervical cancer. *Int J Oncol*, 36, 331-40.
- KAWASE, T., OHKI, R., SHIBATA, T., TSUTSUMI, S., KAMIMURA, N., INAZAWA, J., OHTA, T., ICHIKAWA, H., ABURATANI, H., TASHIRO, F. & TAYA, Y. 2009. PH domain-only protein PHLDA3 is a p53-regulated repressor of Akt. *Cell*, 136, 535-50.
- KIM, J., SHEN, B. & DORSETT, D. 1993. The *Drosophila melanogaster* suppressor of Hairy-wing zinc finger protein has minimal effects on gene expression in *Saccharomyces cerevisiae*. *Genetics*, 135, 343-55.
- KIM, S., LEE, M. J., KIM, H., KANG, M. & KIM, J. S. 2011. Preassembled zinc-finger arrays for rapid construction of ZFNs. *Nat Methods*, 8, 7.
- KIM, Y. G., CHA, J. & CHANDRASEGARAN, S. 1996. Hybrid restriction enzymes: zinc finger fusions to Fok I cleavage domain. *Proc Natl Acad Sci U S A*, 93, 1156-60.
- KLINT, P. & CLAEISSON-WELSH, L. 1999. Signal transduction by fibroblast growth factor receptors. *Front Biosci*, 4, D165-77.
- KNIGHTS, V. & COOK, S. J. 2010. De-regulated FGF receptors as therapeutic targets in cancer. *Pharmacol Ther*, 125, 105-17.

- KOBRIN, M. S., YAMANAKA, Y., FRIESS, H., LOPEZ, M. E. & KORC, M. 1993. Aberrant expression of type I fibroblast growth factor receptor in human pancreatic adenocarcinomas.
- KONECNY, G. E., KOLAROVA, T., O'BRIEN, N. A., WINTERHOFF, B., YANG, G., QI, J., QI, Z., VENKATESAN, N., AYALA, R., LUO, T., FINN, R. S., KRISTOF, J., GALDERISI, C., PORTA, D. G., ANDERSON, L., SHI, M. M., YOVINE, A. & SLAMON, D. J. 2013. Activity of the fibroblast growth factor receptor inhibitors dovitinib (TKI258) and NVP-BGJ398 in human endometrial cancer cells. *Mol Cancer Ther*, 12, 632-42.
- KONG, D., YAGUCHI, S. & YAMORI, T. 2009. Effect of ZSTK474, a novel phosphatidylinositol 3-kinase inhibitor, on DNA-dependent protein kinase. *Biol Pharm Bull*, 32, 297-300.
- KONSTANTINOVA, D., KANEVA, R., DIMITROV, R., SAVOV, A., IVANOV, S., DYANKOVA, T., KREMENSKY, I. & MITEV, V. 2010. Rare mutations in the PIK3CA gene contribute to aggressive endometrial cancer. *DNA Cell Biol*, 29, 65-70.
- KOUHARA, H., HADARI, Y. R., SPIVAK-KROIZMAN, T., SCHILLING, J., BARSAGI, D., LAX, I. & SCHLESSINGER, J. 1997. A lipid-anchored Grb2-binding protein that links FGF-receptor activation to the Ras/MAPK signaling pathway. *Cell*, 89, 693-702.
- KOVALENKO, D., YANG, X., NADEAU, R. J., HARKINS, L. K. & FRIESEL, R. 2003. Sef inhibits fibroblast growth factor signaling by inhibiting FGFR1 tyrosine phosphorylation and subsequent ERK activation.
- KUMAR, P. & WOON-KHIONG, C. 2011. Optimization of lentiviral vectors generation for biomedical and clinical research purposes: contemporary trends in technology development and applications. *Curr Gene Ther*, 11, 144-53.
- KURMAN, R. J. & SHIH IE, M. 2011. Molecular pathogenesis and extraovarian origin of epithelial ovarian cancer--shifting the paradigm. *Hum Pathol*, 42, 918-31.
- KYO, S., NAKAMURA, M., KIYONO, T., MAIDA, Y., KANAYA, T., TANAKA, M., YATABE, N. & INOUE, M. 2003. Successful immortalization of endometrial glandular cells with normal structural and functional characteristics. *Am J Pathol*, 163, 2259-69.
- LAJEUNIE, E., HEUERTZ, S., EL GHOZZI, V., MARTINOVIC, J., RENIER, D., LE MERRER, M. & BONAVENTURE, J. 2006. Mutation screening in patients with

- syndromic craniosynostoses indicates that a limited number of recurrent FGFR2 mutations accounts for severe forms of Pfeiffer syndrome. *Eur J Hum Genet*, 14, 289-98.
- LAMOUILLE, S., XU, J. & DERYNCK, R. 2014. Molecular mechanisms of epithelial-mesenchymal transition. *Nat Rev Mol Cell Biol*, 15, 178-96.
- LANGLEY, R. R. & FIDLER, I. J. 2011. The seed and soil hypothesis revisited--the role of tumor-stroma interactions in metastasis to different organs. *Int J Cancer*, 128, 2527-35.
- LAU, H. Y., TWU, N. F., YEN, M. S., TSAI, H. W., WANG, P. H., CHUANG, C. M., WU, H. H., CHAO, K. C. & CHEN, Y. J. 2014. Impact of ovarian preservation in women with endometrial cancer. *J Chin Med Assoc*, 77, 379-84.
- LAWRENCE, M. S., STOJANOV, P., MERMEL, C. H., ROBINSON, J. T., GARRAWAY, L. A., GOLUB, T. R., MEYERSON, M., GABRIEL, S. B., LANDER, E. S. & GETZ, G. 2014. Discovery and saturation analysis of cancer genes across 21 tumour types. *Nature*, 505, 495-501.
- LENORMAND, P., SARDET, C., PAGES, G., L'ALLEMAIN, G., BRUNET, A. & POUYSSEGUR, J. 1993. Growth factors induce nuclear translocation of MAP kinases (p42mapk and p44mapk) but not of their activator MAP kinase kinase (p45mapkk) in fibroblasts. *J Cell Biol*, 122, 1079-88.
- LI, C., SCOTT, D. A., HATCH, E., TIAN, X. & MANSOUR, S. L. 2007. Dusp6 (Mkp3) is a negative feedback regulator of FGF-stimulated ERK signaling during mouse development. *Development*, 134, 167-76.
- LI, H., SONG, F., CHEN, X., LI, Y., FAN, J. & WU, X. 2014. Bmi-1 regulates epithelial-to-mesenchymal transition to promote migration and invasion of breast cancer cells. *Int J Clin Exp Pathol*, 7, 3057-64.
- LI, L., WU, L. P. & CHANDRASEGARAN, S. 1992. Functional domains in Fok I restriction endonuclease. *Proc Natl Acad Sci U S A*, 89, 4275-9.
- LI, Z., YAN, S., ATTAYAN, N., RAMALINGAM, S. & THIELE, C. J. 2012. Combination of an allosteric Akt Inhibitor MK-2206 with etoposide or rapamycin enhances the antitumor growth effect in neuroblastoma. *Clin Cancer Res*, 18, 3603-15.
- LIAO, Y. & HUNG, M. C. 2010. Physiological regulation of Akt activity and stability. *Am J Transl Res*, 2, 19-42.

- LIN, C. C., MELO, F. A., GHOSH, R., SUEN, K. M., STAGG, L. J., KIRKPATRICK, J., AROLD, S. T., AHMED, Z. & LADBURY, J. E. 2012. Inhibition of basal FGF receptor signaling by dimeric Grb2. *Cell*, 149, 1514-24.
- LINDAHL, U. & HOOK, M. 1978. Glycosaminoglycans and their binding to biological macromolecules.
- LINDSLEY, C. W., ZHAO, Z., LEISTER, W. H., ROBINSON, R. G., BARNETT, S. F., DEFEO-JONES, D., JONES, R. E., HARTMAN, G. D., HUFF, J. R., HUBER, H. E. & DUGGAN, M. E. 2005. Allosteric Akt (PKB) inhibitors: discovery and SAR of isozyme selective inhibitors. *Bioorg Med Chem Lett*, 15, 761-4.
- LIOTTA, L. A. & KOHN, E. C. 2001. The microenvironment of the tumour-host interface. *Nature*, 411, 375-9.
- LITO, P., ROSEN, N. & SOLIT, D. B. 2013. Tumor adaptation and resistance to RAF inhibitors. *Nat Med*, 19, 1401-9.
- LIU, Q., SEGAL, D. J., GHIARA, J. B. & BARBAS, C. F., 3RD 1997. Design of polydactyl zinc-finger proteins for unique addressing within complex genomes. *Proc Natl Acad Sci U S A*, 94, 5525-30.
- LIU, X., ZHANG, W., GENG, D., HE, J., ZHAO, Y. & YU, L. 2014. Clinical significance of fibroblast growth factor receptor-3 mutations in bladder cancer: a systematic review and meta-analysis. *Genet Mol Res*, 13, 1109-20.
- MA, L., WANG, J., LIN, J., PAN, Q., YU, Y. & SUN, F. 2014. Cluster of differentiation 166 (CD166) regulated by phosphatidylinositide 3-Kinase (PI3K)/AKT signaling to exert its anti-apoptotic role via yes-associated protein (YAP) in liver cancer. *J Biol Chem*, 289, 6921-33.
- MADHUNAPANTULA, S. V. & ROBERTSON, G. P. 2011. Therapeutic Implications of Targeting AKT Signaling in Melanoma. *Enzyme Res*, 2011, 327923.
- MAKKER, A., GOEL, M. M. & MAHDI, A. A. 2014. PI3K/PTEN/Akt and TSC/mTOR signaling pathways, ovarian dysfunction, and infertility: an update. *J Mol Endocrinol*, 53, R103-R118.
- MALLICK, P., SCHIRLE, M., CHEN, S. S., FLORY, M. R., LEE, H., MARTIN, D., RANISH, J., RAUGHT, B., SCHMITT, R., WERNER, T., KUSTER, B. & AEBERSOLD, R. 2007. Computational prediction of proteotypic peptides for quantitative proteomics. *Nat Biotechnol*, 25, 125-31.
- MANI, M., SMITH, J., KANDAVELOU, K., BERG, J. M. & CHANDRASEGARAN, S. 2005. Binding of two zinc finger nuclease monomers to two specific sites is

- required for effective double-strand DNA cleavage. *Biochem Biophys Res Commun*, 334, 1191-7.
- MANNING, G., WHYTE, D. B., MARTINEZ, R., HUNTER, T. & SUDARSANAM, S. 2002. The protein kinase complement of the human genome. *Science*, 298, 1912-34.
- MANSSON, P. E., ADAMS, P., KAN, M. & MCKEEHAN, W. L. 1989. Heparin-binding growth factor gene expression and receptor characteristics in normal rat prostate and two transplantable rat prostate tumors.
- MARDAKHEH, F. K., YEKEZARE, M., MACHESKY, L. M. & HEATH, J. K. 2009. Spred2 interaction with the late endosomal protein NBR1 down-regulates fibroblast growth factor receptor signaling.
- MARSHALL, C. J. 1995. Specificity of receptor tyrosine kinase signaling: transient versus sustained extracellular signal-regulated kinase activation. *Cell*, 80, 179-85.
- MATHUPALA, S. & SLOAN, A. A. 2009. An agarose-based cloning-ring anchoring method for isolation of viable cell clones. *Biotechniques*, 46, 305-7.
- MATSUBARA, Y., KATO, T., KASHIMADA, K., TANAKA, H., ZHI, Z., ICHINOSE, S., MIZUTANI, S., MORIO, T., CHIBA, T., ITO, Y., SAGA, Y., TAKADA, S. & ASAHARA, H. 2015. TALEN-mediated gene disruption on Y Chromosome reveals Critical Role of EIF2S3Y in Mouse Spermatogenesis. *Stem Cells Dev.*
- MAUCHAMP, J., MIRRIONE, A., ALQUIER, C. & ANDRE, F. 1998. Follicle-like structure and polarized monolayer: role of the extracellular matrix on thyroid cell organization in primary culture. *Biol Cell*, 90, 369-80.
- MCFARLAND, C. D., MIRNY, L. A. & KOROLEV, K. S. 2014. Tug-of-war between driver and passenger mutations in cancer and other adaptive processes. *Proc Natl Acad Sci U S A*, 111, 15138-43.
- MCMANUS, M. T. & SHARP, P. A. 2002. Gene silencing in mammals by small interfering RNAs. *Nat Rev Genet*, 3, 737-47.
- MEJA, K., STENGEL, C., SELLAR, R., HUSZAR, D., DAVIES, B. R., GALE, R. E., LINCH, D. C. & KHWAJA, A. 2014. PIM and AKT kinase inhibitors show synergistic cytotoxicity in acute myeloid leukaemia that is associated with convergence on mTOR and MCL1 pathways. *Br J Haematol*, 167, 69-79.

- MELERO, I., HERVAS-STUBBS, S., GLENNIE, M., PARDOLL, D. M. & CHEN, L. 2007. Immunostimulatory monoclonal antibodies for cancer therapy. *Nat Rev Cancer*, 7, 95-106.
- MELNIK, S., DENG, B., PAPANTONIS, A., BABOO, S., CARR, I. M. & COOK, P. R. 2011. The proteomes of transcription factories containing RNA polymerases I, II or III. *Nat Methods*, 8, 963-8.
- MILLER, J. C., HOLMES, M. C., WANG, J., GUSCHIN, D. Y., LEE, Y. L., RUPNIEWSKI, I., BEAUSEJOUR, C. M., WAITE, A. J., WANG, N. S., KIM, K. A., GREGORY, P. D., PABO, C. O. & REBAR, E. J. 2007. An improved zinc-finger nuclease architecture for highly specific genome editing. *Nat Biotechnol*, 25, 778-85.
- MOHAMMADI, M., DIKIC, I., SOROKIN, A., BURGESS, W. H., JAYE, M. & SCHLESSINGER, J. 1996. Identification of six novel autophosphorylation sites on fibroblast growth factor receptor 1 and elucidation of their importance in receptor activation and signal transduction. *Mol Cell Biol*, 16, 977-89.
- MOHAMMADI, M., DIONNE, C. A., LI, W., LI, N., SPIVAK, T., HONEGGER, A. M., JAYE, M. & SCHLESSINGER, J. 1992. Point mutation in FGF receptor eliminates phosphatidylinositol hydrolysis without affecting mitogenesis. *Nature*, 358, 681-4.
- MOHAMMADI, M., FROUM, S., HAMBY, J. M., SCHROEDER, M. C., PANEK, R. L., LU, G. H., ELISEENKOVA, A. V., GREEN, D., SCHLESSINGER, J. & HUBBARD, S. R. 1998. Crystal structure of an angiogenesis inhibitor bound to the FGF receptor tyrosine kinase domain. *EMBO J*, 17, 5896-904.
- MOHAMMADI, M., HONEGGER, A. M., ROTIN, D., FISCHER, R., BELLOT, F., LI, W., DIONNE, C. A., JAYE, M., RUBINSTEIN, M. & SCHLESSINGER, J. 1991. A tyrosine-phosphorylated carboxy-terminal peptide of the fibroblast growth factor receptor (Fg) is a binding site for the SH2 domain of phospholipase C-gamma 1. *Mol Cell Biol*, 11, 5068-78.
- MOLIFE, L. R., YAN, L., VITFELL-RASMUSSEN, J., ZERNHELT, A. M., SULLIVAN, D. M., CASSIER, P. A., CHEN, E., BIONDO, A., TETTEH, E., SIU, L. L., PATNAIK, A., PAPADOPOULOS, K. P., DE BONO, J. S., TOLCHER, A. W. & MINTON, S. 2014. Phase 1 trial of the oral AKT inhibitor MK-2206 plus carboplatin/paclitaxel, docetaxel, or erlotinib in patients with advanced solid tumors. *J Hematol Oncol*, 7, 1.

- MONTAGUT, C., SHARMA, S. V., SHIODA, T., MCDERMOTT, U., ULMAN, M., ULKUS, L. E., DIAS-SANTAGATA, D., STUBBS, H., LEE, D. Y., SINGH, A., DREW, L., HABER, D. A. & SETTLEMAN, J. 2008. Elevated CRAF as a potential mechanism of acquired resistance to BRAF inhibition in melanoma. *Cancer Res*, 68, 4853-61.
- MORADIAN, A., KALLI, A., SWEREDOSKI, M. J. & HESS, S. 2014. The top-down, middle-down, and bottom-up mass spectrometry approaches for characterization of histone variants and their post-translational modifications. *Proteomics*, 14, 489-97.
- MORALES, C. P., HOLT, S. E., OUELLETTE, M., KAUR, K. J., YAN, Y., WILSON, K. S., WHITE, M. A., WRIGHT, W. E. & SHAY, J. W. 1999. Absence of cancer-associated changes in human fibroblasts immortalized with telomerase. *Nat Genet*, 21, 115-8.
- MORITA, M., GRAVEL, S. P., CHENARD, V., SIKSTROM, K., ZHENG, L., ALAIN, T., GANDIN, V., AVIZONIS, D., ARGUELLO, M., ZAKARIA, C., MCLAUGHLAN, S., NOUET, Y., PAUSE, A., POLLAK, M., GOTTLIEB, E., LARSSON, O., ST-PIERRE, J., TOPISIROVIC, I. & SONENBERG, N. 2013. mTORC1 controls mitochondrial activity and biogenesis through 4E-BP-dependent translational regulation. *Cell Metab*, 18, 698-711.
- MOSCOU, M. J. & BOGDANOVE, A. J. 2009. A simple cipher governs DNA recognition by TAL effectors. *Science*, 326, 1501.
- MUELLER, M. M. & FUSENIG, N. E. 2002. Tumor-stroma interactions directing phenotype and progression of epithelial skin tumor cells. *Differentiation*, 70, 486-97.
- MURATA, T., SATO, T., KAMODA, T., MORIYAMA, H., KUMAZAWA, Y. & HANADA, N. 2014. Differential susceptibility to hydrogen sulfide-induced apoptosis between PHLDA1-overexpressing oral cancer cell lines and oral keratinocytes: role of PHLDA1 as an apoptosis suppressor. *Exp Cell Res*, 320, 247-57.
- NAGAI, M. A., FREGNANI, J. H., NETTO, M. M., BRENTANI, M. M. & SOARES, F. A. 2007. Down-regulation of PHLDA1 gene expression is associated with breast cancer progression. *Breast Cancer Res Treat*, 106, 49-56.
- NARLIK-GRASSOW, M., BLANCO-APARICIO, C., CECILIA, Y., PEREZ, M., MUNOZ-GALVAN, S., CANAMERO, M., RENNER, O. & CARNERO, A. 2013.

- Conditional transgenic expression of PIM1 kinase in prostate induces inflammation-dependent neoplasia. *PLoS One*, 8, e60277.
- NAZARIAN, R., SHI, H., WANG, Q., KONG, X., KOYA, R. C., LEE, H., CHEN, Z., LEE, M. K., ATTAR, N., SAZEGAR, H., CHODON, T., NELSON, S. F., MCARTHUR, G., SOSMAN, J. A., RIBAS, A. & LO, R. S. 2010. Melanomas acquire resistance to B-RAF(V600E) inhibition by RTK or N-RAS upregulation. *Nature*, 468, 973-7.
- NEEF, R., KUSKE, M. A., PROLS, E. & JOHNSON, J. P. 2002. Identification of the human PHLDA1/TDAG51 gene: down-regulation in metastatic melanoma contributes to apoptosis resistance and growth deregulation. *Cancer Res*, 62, 5920-9.
- NIEDERST, M. J. & ENGELMAN, J. A. 2013. Bypass mechanisms of resistance to receptor tyrosine kinase inhibition in lung cancer. *Sci Signal*, 6, re6.
- NYSTROM, M. L., THOMAS, G. J., STONE, M., MACKENZIE, I. C., HART, I. R. & MARSHALL, J. F. 2005. Development of a quantitative method to analyse tumour cell invasion in organotypic culture. *J Pathol*, 205, 468-75.
- O'DAY, S. J., HAMID, O. & URBA, W. J. 2007. Targeting cytotoxic T-lymphocyte antigen-4 (CTLA-4): a novel strategy for the treatment of melanoma and other malignancies. *Cancer*, 110, 2614-27.
- O'DAY, S. J., MAIO, M., CHIARION-SILENI, V., GAJEWSKI, T. F., PEHAMBERGER, H., BONDARENKO, I. N., QUEIROLO, P., LUNDGREN, L., MIKHAILOV, S., ROMAN, L., VERSCHRAEGEN, C., HUMPHREY, R., IBRAHIM, R., DE PRIL, V., HOOS, A. & WOLCHOK, J. D. 2010. Efficacy and safety of ipilimumab monotherapy in patients with pretreated advanced melanoma: a multicenter single-arm phase II study. *Ann Oncol*, 21, 1712-7.
- OHGINO, K., SOEJIMA, K., YASUDA, H., HAYASHI, Y., HAMAMOTO, J., NAOKI, K., ARAI, D., ISHIOKA, K., SATO, T., TERAJ, H., IKEMURA, S., YODA, S., TANI, T., KURODA, A. & BETSUYAKU, T. 2014. Expression of fibroblast growth factor 9 is associated with poor prognosis in patients with resected non-small cell lung cancer. *Lung Cancer*, 83, 90-6.
- OHKI, R., SAITO, K., CHEN, Y., KAWASE, T., HIRAOKA, N., SAIGAWA, R., MINEGISHI, M., AITA, Y., YANAI, G., SHIMIZU, H., YACHIDA, S., SAKATA, N., DOI, R., KOSUGE, T., SHIMADA, K., TYCKO, B., TSUKADA, T., KANAI, Y., SUMI, S., NAMIKI, H., TAYA, Y., SHIBATA, T. & NAKAGAMA, H. 2014.

- PHLDA3 is a novel tumor suppressor of pancreatic neuroendocrine tumors. *Proc Natl Acad Sci U S A*, 111, E2404-13.
- OLD, W. M., MEYER-ARENDR, K., AVELINE-WOLF, L., PIERCE, K. G., MENDOZA, A., SEVINSKY, J. R., RESING, K. A. & AHN, N. G. 2005. Comparison of label-free methods for quantifying human proteins by shotgun proteomics. *Mol Cell Proteomics*, 4, 1487-502.
- OLDRIDGE, M., LUNT, P. W., ZACKAI, E. H., MCDONALD-MCGINN, D. M., MUENKE, M., MOLONEY, D. M., TWIGG, S. R., HEATH, J. K., HOWARD, T. D., HOGANSON, G., GAGNON, D. M., JABS, E. W. & WILKIE, A. O. 1997. Genotype-phenotype correlation for nucleotide substitutions in the IgII-IgIII linker of FGFR2. *Hum Mol Genet*, 6, 137-43.
- OLIVERA-MARTINEZ, I., SCHURCH, N., LI, R. A., SONG, J., HALLEY, P. A., DAS, R. M., BURT, D. W., BARTON, G. J. & STOREY, K. G. 2014. Major transcriptome re-organisation and abrupt changes in signalling, cell cycle and chromatin regulation at neural differentiation in vivo. *Development*, 141, 3266-76.
- OLIVIER, J. P., RAABE, T., HENKEMEYER, M., DICKSON, B., MBAMALU, G., MARGOLIS, B., SCHLESSINGER, J., HAFEN, E. & PAWSON, T. 1993. A Drosophila SH2-SH3 adaptor protein implicated in coupling the sevenless tyrosine kinase to an activator of Ras guanine nucleotide exchange, Sos. *Cell*, 73, 179-91.
- OLSEN, J. V., MACEK, B., LANGE, O., MAKAROV, A., HORNING, S. & MANN, M. 2007. Higher-energy C-trap dissociation for peptide modification analysis. *Nat Methods*, 4, 709-12.
- OLSEN, S. K., IBRAHIMI, O. A., RAUCCI, A., ZHANG, F., ELISEENKOVA, A. V., YAYON, A., BASILICO, C., LINHARDT, R. J., SCHLESSINGER, J. & MOHAMMADI, M. 2004. Insights into the molecular basis for fibroblast growth factor receptor autoinhibition and ligand-binding promiscuity.
- ONG, S. E., BLAGOEV, B., KRATCHMAROVA, I., KRISTENSEN, D. B., STEEN, H., PANDEY, A. & MANN, M. 2002. Stable isotope labeling by amino acids in cell culture, SILAC, as a simple and accurate approach to expression proteomics. *Mol Cell Proteomics*, 1, 376-86.
- ONG, S. H., DILWORTH, S., HAUCK-SCHMALENBERGER, I., PAWSON, T. & KIEFER, F. 2001. ShcA and Grb2 mediate polyoma middle T antigen-induced

- endothelial transformation and Gab1 tyrosine phosphorylation. *EMBO J*, 20, 6327-36.
- ONG, S. H., GUY, G. R., HADARI, Y. R., LAKS, S., GOTOH, N., SCHLESSINGER, J. & LAX, I. 2000. FRS2 proteins recruit intracellular signaling pathways by binding to diverse targets on fibroblast growth factor and nerve growth factor receptors. *Mol Cell Biol*, 20, 979-89.
- ONUIGBO, W. I. 1975. Human model for studying seed-soil factors in blood-borne metastasis. *Arch Pathol*, 99, 342-3.
- ORNITZ, D. M., HERR, A. B., NILSSON, M., WESTMAN, J., SVAHN, C. M. & WAKSMAN, G. 1995. FGF binding and FGF receptor activation by synthetic heparan-derived di- and trisaccharides. *Science*, 268, 432-6.
- ORNITZ, D. M. & ITOH, N. 2001. Fibroblast growth factors. *Genome Biol*, 2, REVIEWS3005.
- ORNITZ, D. M., XU, J., COLVIN, J. S., MCEWEN, D. G., MACARTHUR, C. A., COULIER, F., GAO, G. & GOLDFARB, M. 1996. Receptor specificity of the fibroblast growth factor family. *J Biol Chem*, 271, 15292-7.
- ORNITZ, D. M., YAYON, A., FLANAGAN, J. G., SVAHN, C. M., LEVI, E. & LEDER, P. 1992. Heparin is required for cell-free binding of basic fibroblast growth factor to a soluble receptor and for mitogenesis in whole cells. *Mol Cell Biol*, 12, 240-7.
- ORR-URTREGER, A., BEDFORD, M. T., BURAKOVA, T., ARMAN, E., ZIMMER, Y., YAYON, A., GIVOL, D. & LONAI, P. 1993. Developmental localization of the splicing alternatives of fibroblast growth factor receptor-2 (FGFR2). *Dev Biol*, 158, 475-86.
- PARDOLL, D. M. 2012. The blockade of immune checkpoints in cancer immunotherapy. *Nat Rev Cancer*, 12, 252-64.
- PASSOS-BUENO, M. R., RICHIERI-COSTA, A., SERTIE, A. L. & KNEPPERS, A. 1998. Presence of the Apert canonical S252W FGFR2 mutation in a patient without severe syndactyly. *J Med Genet*, 35, 677-9.
- PENG, W. X., KUDO, M., FUJII, T., TEDUKA, K. & NAITO, Z. 2014. Altered expression of fibroblast growth factor receptor 2 isoform IIIc: relevance to endometrioid adenocarcinoma carcinogenesis and histological differentiation. *Int J Clin Exp Pathol*, 7, 1069-76.

- PERICA, K., VARELA, J. C., OELKE, M. & SCHNECK, J. 2015. Adoptive T cell immunotherapy for cancer. *Rambam Maimonides Med J*, 6, e0004.
- PERKINS, D. N., PAPPIN, D. J., CREASY, D. M. & COTTRELL, J. S. 1999. Probability-based protein identification by searching sequence databases using mass spectrometry data. *Electrophoresis*, 20, 3551-67.
- PHANG, R. Z., TAY, F. C., GOH, S. L., LAU, C. H., ZHU, H., TAN, W. K., LIANG, Q., CHEN, C., DU, S., LI, Z., TAY, J. C., WU, C., ZENG, J., FAN, W., TOH, H. C. & WANG, S. 2013. Zinc finger nuclease-expressing baculoviral vectors mediate targeted genome integration of reprogramming factor genes to facilitate the generation of human induced pluripotent stem cells. *Stem Cells Transl Med*, 2, 935-45.
- PIRKMAJER, S. & CHIBALIN, A. V. 2011. Serum starvation: caveat emptor. *Am J Physiol Cell Physiol*, 301, C272-9.
- PLOTNIKOV, A. N., SCHLESSINGER, J., HUBBARD, S. R. & MOHAMMADI, M. 1999. Structural basis for FGF receptor dimerization and activation. *Cell*, 98, 641-50.
- POLANSKA, U. M., FERNIG, D. G. & KINNUNEN, T. 2009. Extracellular interactome of the FGF receptor-ligand system: complexities and the relative simplicity of the worm. *Dev Dyn*, 238, 277-93.
- POLLOCK, P. M., GARTSIDE, M. G., DEJEZA, L. C., POWELL, M. A., MALLON, M. A., DAVIES, H., MOHAMMADI, M., FUTREAL, P. A., STRATTON, M. R., TRENT, J. M. & GOODFELLOW, P. J. 2007. Frequent activating FGFR2 mutations in endometrial carcinomas parallel germline mutations associated with craniosynostosis and skeletal dysplasia syndromes. *Oncogene*, 26, 7158-62.
- POTTER, C. J., PEDRAZA, L. G. & XU, T. 2002. Akt regulates growth by directly phosphorylating Tsc2. *Nat Cell Biol*, 4, 658-65.
- POWNALL, M. E. & ISAACS, H. V. 2010. *FGF Signalling in Vertebrate Development*, San Rafael CA, 2010 by Morgan & Claypool Life Sciences.
- PRIMER3PLUS 2015. Primer3Plus software.
- QIAN, B. Z. & POLLARD, J. W. 2010. Macrophage diversity enhances tumor progression and metastasis. *Cell*, 141, 39-51.
- QIAN, X., BA, Y., ZHUANG, Q. & ZHONG, G. 2014. RNA-Seq technology and its application in fish transcriptomics. *OMICS*, 18, 98-110.

- RAFFIONI, S., THOMAS, D., FOEHR, E. D., THOMPSON, L. M. & BRADSHAW, R. A. 1999. Comparison of the intracellular signaling responses by three chimeric fibroblast growth factor receptors in PC12 cells.
- RAMEH, L. E., RHEE, S. G., SPOKES, K., KAZLAUSKAS, A., CANTLEY, L. C. & CANTLEY, L. G. 1998. Phosphoinositide 3-kinase regulates phospholipase Cgamma-mediated calcium signaling. *J Biol Chem*, 273, 23750-7.
- REINTJES, N., LI, Y., BECKER, A., ROHMANN, E., SCHMUTZLER, R. & WOLLNIK, B. 2013. Activating somatic FGFR2 mutations in breast cancer. *PLoS One*, 8, e60264.
- REPORT 2014. In brief: ponatinib (Inclusig) returns. *Med Lett Drugs Ther*, 56, 8.
- RIECKMANN, T., ZHUANG, L., FLUCK, C. E. & TRUEB, B. 2009. Characterization of the first FGFR1 mutation identified in a craniosynostosis patient. *Biochim Biophys Acta*, 1792, 112-21.
- ROBBEZ-MASSON, L. J., BODOR, C., JONES, J. L., HURST, H. C., FITZGIBBON, J., HART, I. R. & GROSE, R. P. 2013. Functional analysis of a breast cancer-associated FGFR2 single nucleotide polymorphism using zinc finger mediated genome editing. *PLoS One*, 8, e78839.
- ROBERT, C. & GHIRINGHELLI, F. 2009. What is the role of cytotoxic T lymphocyte-associated antigen 4 blockade in patients with metastatic melanoma? *Oncologist*, 14, 848-61.
- ROEPSTORFF, P. & FOHLMAN, J. 1984. Proposal for a common nomenclature for sequence ions in mass spectra of peptides. *Biomed Mass Spectrom*, 11, 601.
- ROSS, P. L., HUANG, Y. N., MARCHESE, J. N., WILLIAMSON, B., PARKER, K., HATTAN, S., KHAINOVSKI, N., PILLAI, S., DEY, S., DANIELS, S., PURKAYASTHA, S., JUHASZ, P., MARTIN, S., BARTLET-JONES, M., HE, F., JACOBSON, A. & PAPPIN, D. J. 2004. Multiplexed protein quantitation in *Saccharomyces cerevisiae* using amine-reactive isobaric tagging reagents. *Mol Cell Proteomics*, 3, 1154-69.
- ROUX, P. P. & TOPISIROVIC, I. 2012. Regulation of mRNA translation by signaling pathways. *Cold Spring Harb Perspect Biol*, 4.
- SAKAMOTO, T., HIRANO, K., MORISHIMA, Y., MASUYAMA, K., ISHII, Y., NOMURA, A., UCHIDA, Y., OHTSUKA, M. & SEKIZAWA, K. 2001. Maintenance of the differentiated type II cell characteristics by culture on an acellular human amnion membrane. *In Vitro Cell Dev Biol Anim*, 37, 471-9.

- SANDERSON, I. R., EZZELL, R. M., KEDINGER, M., ERLANGER, M., XU, Z. X., PRINGAULT, E., LEON-ROBINE, S., LOUVARD, D. & WALKER, W. A. 1996. Human fetal enterocytes in vitro: modulation of the phenotype by extracellular matrix. *Proc Natl Acad Sci U S A*, 93, 7717-22.
- SANIDAS, I., POLYTARCHOU, C., HATZIAPOSTOLOU, M., EZZELL, S. A., KOTTAKIS, F., HU, L., GUO, A., XIE, J., COMB, M. J., ILIOPOULOS, D. & TSICHLIS, P. N. 2014. Phosphoproteomics screen reveals akt isoform-specific signals linking RNA processing to lung cancer. *Mol Cell*, 53, 577-90.
- SARBASSOV, D. D., GUERTIN, D. A., ALI, S. M. & SABATINI, D. M. 2005. Phosphorylation and regulation of Akt/PKB by the rictor-mTOR complex. *Science*, 307, 1098-101.
- SASAKI, A., TAKETOMI, T., KATO, R., SAEKI, K., NONAMI, A., SASAKI, M., KURIYAMA, M., SAITO, N., SHIBUYA, M. & YOSHIMURA, A. 2003. Mammalian Sprouty4 suppresses Ras-independent ERK activation by binding to Raf1.
- SCHLAKE, T. 2005. FGF signals specifically regulate the structure of hair shaft medulla via IGF-binding protein 5. *Development*, 132, 2981-90.
- SCHLESSINGER, J., PLOTNIKOV, A. N., IBRAHIMI, O. A., ELISEENKOVA, A. V., YEH, B. K., YAYON, A., LINHARDT, R. J. & MOHAMMADI, M. 2000. Crystal structure of a ternary FGF-FGFR-heparin complex reveals a dual role for heparin in FGFR binding and dimerization. *Mol Cell*, 6, 743-50.
- SCHROEDER, M. J., SHABANOWITZ, J., SCHWARTZ, J. C., HUNT, D. F. & COON, J. J. 2004. A neutral loss activation method for improved phosphopeptide sequence analysis by quadrupole ion trap mass spectrometry. *Anal Chem*, 76, 3590-8.
- SHARMA, S. V. & SETTLEMAN, J. 2007. Oncogene addiction: setting the stage for molecularly targeted cancer therapy. *Genes Dev*, 21, 3214-31.
- SHIRAKIHARA, T., HORIGUCHI, K., MIYAZAWA, K., EHATA, S., SHIBATA, T., MORITA, I., MIYAZONO, K. & SAITOH, M. 2011. TGF-beta regulates isoform switching of FGF receptors and epithelial-mesenchymal transition. *EMBO J*, 30, 783-95.
- SILVA, J., GARCIA, J. M., PENA, C., GARCIA, V., DOMINGUEZ, G., SUAREZ, D., CAMACHO, F. I., ESPINOSA, R., PROVENCIO, M., ESPANA, P. & BONILLA, F. 2006. Implication of polycomb members Bmi-1, Mel-18, and

- Hpc-2 in the regulation of p16INK4a, p14ARF, h-TERT, and c-Myc expression in primary breast carcinomas. *Clin Cancer Res*, 12, 6929-36.
- SILVA, P. N., ALTAMENTOVA, S. M., KILKENNY, D. M. & ROCHELEAU, J. V. 2013. Fibroblast growth factor receptor like-1 (FGFRL1) interacts with SHP-1 phosphatase at insulin secretory granules and induces beta-cell ERK1/2 protein activation. *J Biol Chem*, 288, 17859-70.
- SINGH, D., CHAN, J. M., ZOPPOLI, P., NIOLA, F., SULLIVAN, R., CASTANO, A., LIU, E. M., REICHEL, J., PORRATI, P., PELLEGGATTA, S., QIU, K., GAO, Z., CECCARELLI, M., RICCARDI, R., BRAT, D. J., GUHA, A., ALDAPE, K., GOLFINOS, J. G., ZAGZAG, D., MIKKELSEN, T., FINOCCHIARO, G., LASORELLA, A., RABADAN, R. & IAVARONE, A. 2012. Transforming fusions of FGFR and TACC genes in human glioblastoma. *Science*, 337, 1231-5.
- SLEEMAN, M., FRASER, J., MCDONALD, M., YUAN, S., WHITE, D., GRANDISON, P., KUMBLE, K., WATSON, J. D. & MURISON, J. G. 2001. Identification of a new fibroblast growth factor receptor, FGFR5. *Gene*, 271, 171-82.
- SMALLWOOD, P. M., MUNOZ-SANJUAN, I., TONG, P., MACKE, J. P., HENDRY, S. H., GILBERT, D. J., COPELAND, N. G., JENKINS, N. A. & NATHANS, J. 1996. Fibroblast growth factor (FGF) homologous factors: new members of the FGF family implicated in nervous system development. *Proc Natl Acad Sci U S A*, 93, 9850-7.
- SMITH, J., BIBIKOVA, M., WHITBY, F. G., REDDY, A. R., CHANDRASEGARAN, S. & CARROLL, D. 2000. Requirements for double-strand cleavage by chimeric restriction enzymes with zinc finger DNA-recognition domains. *Nucleic Acids Res*, 28, 3361-9.
- SMYTH, G. K. 2004. Linear models and empirical bayes methods for assessing differential expression in microarray experiments. *Stat Appl Genet Mol Biol*, 3, Article3.
- SONG, Q., SHENG, W., ZHANG, X., JIAO, S. & LI, F. 2014. ILEI drives epithelial to mesenchymal transition and metastatic progression in the lung cancer cell line A549. *Tumour Biol*, 35, 1377-82.
- SORIA, J. C., DEBRAUD, F., BAHLEDA, R., ADAMO, B., ANDRE, F., DIENTSMANN, R., DELMONTE, A., CEREDA, R., ISAACSON, J., LITTEN, J., ALLEN, A., DUBOIS, F., SABA, C., ROBERT, R., D'INCALCI, M., ZUCCHETTI, M., CAMBONI, M. G. & TABERNERO, J. 2014. Phase I/IIa

- study evaluating the safety, efficacy, pharmacokinetics, and pharmacodynamics of lucitanib in advanced solid tumors. *Ann Oncol*, 25, 2244-51.
- STAHL, J. M., SHARMA, A., CHEUNG, M., ZIMMERMAN, M., CHENG, J. Q., BOSENBERG, M. W., KESTER, M., SANDIRASEGARANE, L. & ROBERTSON, G. P. 2004. Deregulated Akt3 activity promotes development of malignant melanoma. *Cancer Res*, 64, 7002-10.
- STAUBER, D. J., DIGABRIELE, A. D. & HENDRICKSON, W. A. 2000. Structural interactions of fibroblast growth factor receptor with its ligands. *Proc Natl Acad Sci U S A*, 97, 49-54.
- STEELE, I. A., EDMONDSON, R. J., BULMER, J. N., BOLGER, B. S., LEUNG, H. Y. & DAVIES, B. R. 2001. Induction of FGF receptor 2-IIIb expression and response to its ligands in epithelial ovarian cancer. *Oncogene*, 20, 5878-87.
- STEINBERG, F., ZHUANG, L., BEYELER, M., KALIN, R. E., MULLIS, P. E., BRANDLI, A. W. & TRUEB, B. 2010. The FGFR1 receptor is shed from cell membranes, binds fibroblast growth factors (FGFs), and antagonizes FGF signaling in *Xenopus* embryos. *J Biol Chem*, 285, 2193-202.
- SU, X., ZHAN, P., GAVINE, P. R., MORGAN, S., WOMACK, C., NI, X., SHEN, D., BANG, Y. J., IM, S. A., HO KIM, W., JUNG, E. J., GRABSCH, H. I. & KILGOUR, E. 2014. FGFR2 amplification has prognostic significance in gastric cancer: results from a large international multicentre study. *Br J Cancer*, 110, 967-75.
- SUH, D. H., KIM, H. S., KIM, B. & SONG, Y. S. 2014. Metabolic orchestration between cancer cells and tumor microenvironment as a co-evolutionary source of chemoresistance in ovarian cancer: A therapeutic implication. *Biochem Pharmacol*.
- SUN, X., MEYERS, E. N., LEWANDOSKI, M. & MARTIN, G. R. 1999. Targeted disruption of *Fgf8* causes failure of cell migration in the gastrulating mouse embryo. *Genes Dev*, 13, 1834-46.
- SYKA, J. E., COON, J. J., SCHROEDER, M. J., SHABANOWITZ, J. & HUNT, D. F. 2004. Peptide and protein sequence analysis by electron transfer dissociation mass spectrometry. *Proc Natl Acad Sci U S A*, 101, 9528-33.
- TARCA, A. L., ROMERO, R. & DRAGHICI, S. 2006. Analysis of microarray experiments of gene expression profiling. *Am J Obstet Gynecol*, 195, 373-88.

- TCHAICHA, J. H., AKBAY, E. A., ALTABEF, A., MIKSE, O. R., KIKUCHI, E., RHEE, K., LIAO, R. G., BRONSON, R. T., SHOLL, L. M., MEYERSON, M., HAMMERMAN, P. S. & WONG, K. K. 2014. Kinase domain activation of FGFR2 yields high-grade lung adenocarcinoma sensitive to a Pan-FGFR inhibitor in a mouse model of NSCLC. *Cancer Res*, 74, 4676-84.
- THISSE, B. & THISSE, C. 2005. Functions and regulations of fibroblast growth factor signaling during embryonic development.
- THOLEY, A., REED, J. & LEHMANN, W. D. 1999. Electrospray tandem mass spectrometric studies of phosphopeptides and phosphopeptide analogues. *J Mass Spectrom*, 34, 117-23.
- THORPE, L. M., YUZUGULLU, H. & ZHAO, J. J. 2014. PI3K in cancer: divergent roles of isoforms, modes of activation and therapeutic targeting. *Nat Rev Cancer*, 15, 7-24.
- TIMSAH, Z., AHMED, Z., LIN, C. C., MELO, F. A., STAGG, L. J., LEONARD, P. G., JEYABAL, P., BERROUT, J., O'NEIL, R. G., BOGDANOV, M. & LADBURY, J. E. 2014. Competition between Grb2 and Plcgamma1 for FGFR2 regulates basal phospholipase activity and invasion. *Nat Struct Mol Biol*, 21, 180-8.
- TORII, S., KUSAKABE, M., YAMAMOTO, T., MAEKAWA, M. & NISHIDA, E. 2004. Sef is a spatial regulator for Ras/MAP kinase signaling.
- TORTI, D. & TRUSOLINO, L. 2011. Oncogene addiction as a foundational rationale for targeted anti-cancer therapy: promises and perils. *EMBO Mol Med*, 3, 623-36.
- TOYOSHIMA, Y., KARAS, M., YAKAR, S., DUPONT, J., LEE, H. & LEROITH, D. 2004. TDAG51 mediates the effects of insulin-like growth factor I (IGF-I) on cell survival. *J Biol Chem*, 279, 25898-904.
- TRUDEL, S., STEWART, A. K., ROM, E., WEI, E., LI, Z. H., KOTZER, S., CHUMAKOV, I., SINGER, Y., CHANG, H., LIANG, S. B. & YAYON, A. 2006. The inhibitory anti-FGFR3 antibody, PRO-001, is cytotoxic to t(4;14) multiple myeloma cells. *Blood*, 107, 4039-46.
- TRUEB, B., ZHUANG, L., TAESCHLER, S. & WIEDEMANN, M. 2003. Characterization of FGFR1, a novel fibroblast growth factor (FGF) receptor preferentially expressed in skeletal tissues. *J Biol Chem*, 278, 33857-65.
- TSAI, J., LEE, J. T., WANG, W., ZHANG, J., CHO, H., MAMO, S., BREMER, R., GILLETTE, S., KONG, J., HAASS, N. K., SPROESSER, K., LI, L., SMALLEY,

- K. S., FONG, D., ZHU, Y. L., MARIMUTHU, A., NGUYEN, H., LAM, B., LIU, J., CHEUNG, I., RICE, J., SUZUKI, Y., LUU, C., SETTACHATGUL, C., SHELLOOE, R., CANTWELL, J., KIM, S. H., SCHLESSINGER, J., ZHANG, K. Y., WEST, B. L., POWELL, B., HABETS, G., ZHANG, C., IBRAHIM, P. N., HIRTH, P., ARTIS, D. R., HERLYN, M. & BOLLAG, G. 2008. Discovery of a selective inhibitor of oncogenic B-Raf kinase with potent antimelanoma activity. *Proc Natl Acad Sci U S A*, 105, 3041-6.
- TSANG, M., FRIESEL, R., KUDOH, T. & DAWID, I. B. 2002. Identification of Sef, a novel modulator of FGF signalling.
- TURNER, N. & GROSE, R. 2010. Fibroblast growth factor signalling: from development to cancer. *Nat Rev Cancer*, 10, 116-29.
- UEKI, K., MATSUDA, S., TOBE, K., GOTOH, Y., TAMEMOTO, H., YACHI, M., AKANUMA, Y., YAZAKI, Y., NISHIDA, E. & KADOWAKI, T. 1994. Feedback regulation of mitogen-activated protein kinase kinase activity of c-Raf-1 by insulin and phorbol ester stimulation. *J Biol Chem*, 269, 15756-61.
- URNOV, F. D., MILLER, J. C., LEE, Y. L., BEAUSEJOUR, C. M., ROCK, J. M., AUGUSTUS, S., JAMIESON, A. C., PORTEUS, M. H., GREGORY, P. D. & HOLMES, M. C. 2005. Highly efficient endogenous human gene correction using designed zinc-finger nucleases. *Nature*, 435, 646-51.
- URNOV, F. D., REBAR, E. J., HOLMES, M. C., ZHANG, H. S. & GREGORY, P. D. 2010. Genome editing with engineered zinc finger nucleases. *Nat Rev Genet*, 11, 636-46.
- VAINIKKA, S., PARTANEN, J., BELLOSTA, P., COULIER, F., BIRNBAUM, D., BASILICO, C., JAYE, M. & ALITALO, K. 1992. Fibroblast growth factor receptor-4 shows novel features in genomic structure, ligand binding and signal transduction.
- VAN ALLEN, E. M., FOYE, A., WAGLE, N., KIM, W., CARTER, S. L., MCKENNA, A., SIMKO, J. P., GARRAWAY, L. A. & FEBBO, P. G. 2014. Successful whole-exome sequencing from a prostate cancer bone metastasis biopsy. *Prostate Cancer Prostatic Dis*, 17, 23-7.
- VANHAESEBROECK, B., GUILLERMET-GUIBERT, J., GRAUPERA, M. & BILANGES, B. 2010. The emerging mechanisms of isoform-specific PI3K signalling. *Nat Rev Mol Cell Biol*, 11, 329-41.

- VARNAI, P., BONDEVA, T., TAMAS, P., TOTH, B., BUDAY, L., HUNYADY, L. & BALLA, T. 2005. Selective cellular effects of overexpressed pleckstrin-homology domains that recognize PtdIns(3,4,5)P₃ suggest their interaction with protein binding partners. *J Cell Sci*, 118, 4879-88.
- VAZIRI, H., SQUIRE, J. A., PANDITA, T. K., BRADLEY, G., KUBA, R. M., ZHANG, H., GULYAS, S., HILL, R. P., NOLAN, G. P. & BENCHIMOL, S. 1999. Analysis of genomic integrity and p53-dependent G1 checkpoint in telomerase-induced extended-life-span human fibroblasts. *Mol Cell Biol*, 19, 2373-9.
- VOGELSTEIN, B., PAPADOPOULOS, N., VELCULESCU, V. E., ZHOU, S., DIAZ, L. A., JR. & KINZLER, K. W. 2013. Cancer genome landscapes. *Science*, 339, 1546-58.
- VUKICEVIC, S., LUYTEN, F. P., KLEINMAN, H. K. & REDDI, A. H. 1990. Differentiation of canalicular cell processes in bone cells by basement membrane matrix components: regulation by discrete domains of laminin. *Cell*, 63, 437-45.
- WAGLE, N., EMERY, C., BERGER, M. F., DAVIS, M. J., SAWYER, A., POCHANARD, P., KEHOE, S. M., JOHANNESSEN, C. M., MACCONAILL, L. E., HAHN, W. C., MEYERSON, M. & GARRAWAY, L. A. 2011. Dissecting therapeutic resistance to RAF inhibition in melanoma by tumor genomic profiling. *J Clin Oncol*, 29, 3085-96.
- WAKIOKA, T., SASAKI, A., KATO, R., SHOUDA, T., MATSUMOTO, A., MIYOSHI, K., TSUNEOKA, M., KOMIYA, S., BARON, R. & YOSHIMURA, A. 2001. Spred is a Sprouty-related suppressor of Ras signalling. *Nature*, 412, 647-51.
- WALTHER, T. C. & MANN, M. 2010. Mass spectrometry-based proteomics in cell biology. *J Cell Biol*, 190, 491-500.
- WAN, X., LI, J., XIE, X. & LU, W. 2007. PTEN augments doxorubicin-induced apoptosis in PTEN-null Ishikawa cells. *Int J Gynecol Cancer*, 17, 808-12.
- WANG, J., MIKSE, O., LIAO, R. G., LI, Y., TAN, L., JANNE, P. A., GRAY, N. S., WONG, K. K. & HAMMERMAN, P. S. 2014a. Ligand-associated ERBB2/3 activation confers acquired resistance to FGFR inhibition in FGFR3-dependent cancer cells. *Oncogene*.

- WANG, L., RHODES, C. J. & LAWRENCE, J. C., JR. 2006. Activation of mammalian target of rapamycin (mTOR) by insulin is associated with stimulation of 4EBP1 binding to dimeric mTOR complex 1. *J Biol Chem*, 281, 24293-303.
- WANG, L., RUDERT, W. A., LOUTAIEV, I., ROGINSKAYA, V. & COREY, S. J. 2002. Repression of c-Cbl leads to enhanced G-CSF Jak-STAT signaling without increased cell proliferation. *Oncogene*, 21, 5346-55.
- WANG, R., WANG, L., LI, Y., HU, H., SHEN, L., SHEN, X., PAN, Y., YE, T., ZHANG, Y., LUO, X., PAN, B., LI, B., LI, H., ZHANG, J., PAO, W., JI, H., SUN, Y. & CHEN, H. 2014b. FGFR1/3 tyrosine kinase fusions define a unique molecular subtype of non-small cell lung cancer. *Clin Cancer Res*, 20, 4107-14.
- WANG, Y., XIAO, R., YANG, F., KARIM, B. O., IACOVELLI, A. J., CAI, J., LERNER, C. P., RICHTSMEIER, J. T., LESZL, J. M., HILL, C. A., YU, K., ORNITZ, D. M., ELISSEEFF, J., HUSO, D. L. & JABS, E. W. 2005. Abnormalities in cartilage and bone development in the Apert syndrome FGFR2(+S252W) mouse. *Development*, 132, 3537-48.
- WEBER, J. 2009. Ipilimumab: controversies in its development, utility and autoimmune adverse events. *Cancer Immunol Immunother*, 58, 823-30.
- WEBER, J., THOMPSON, J. A., HAMID, O., MINOR, D., AMIN, A., RON, I., RIDOLFI, R., ASSI, H., MARAVEYAS, A., BERMAN, D., SIEGEL, J. & O'DAY, S. J. 2009. A randomized, double-blind, placebo-controlled, phase II study comparing the tolerability and efficacy of ipilimumab administered with or without prophylactic budesonide in patients with unresectable stage III or IV melanoma. *Clin Cancer Res*, 15, 5591-8.
- WEBSTER, M. K. & DONOGHUE, D. J. 1997. FGFR activation in skeletal disorders: too much of a good thing. *Trends Genet*, 13, 178-82.
- WEIGELT, B., WARNE, P. H., LAMBROS, M. B., REIS-FILHO, J. S. & DOWNWARD, J. 2013. PI3K pathway dependencies in endometrioid endometrial cancer cell lines. *Clin Cancer Res*, 19, 3533-44.
- WHELDON, L. M., KHODABUKUS, N., PATEY, S. J., SMITH, T. G., HEATH, J. K. & HAJIHOSSEINI, M. K. 2011. Identification and characterization of an inhibitory fibroblast growth factor receptor 2 (FGFR2) molecule, up-regulated in an Apert Syndrome mouse model.
- WIEDEMANN, M. & TRUEB, B. 2000. Characterization of a novel protein (FGFRL1) from human cartilage related to FGF receptors. *Genomics*, 69, 275-9.

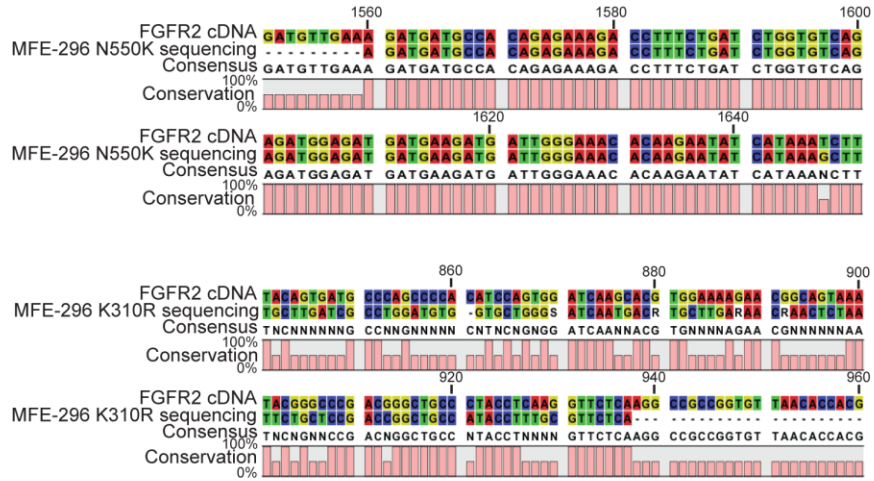
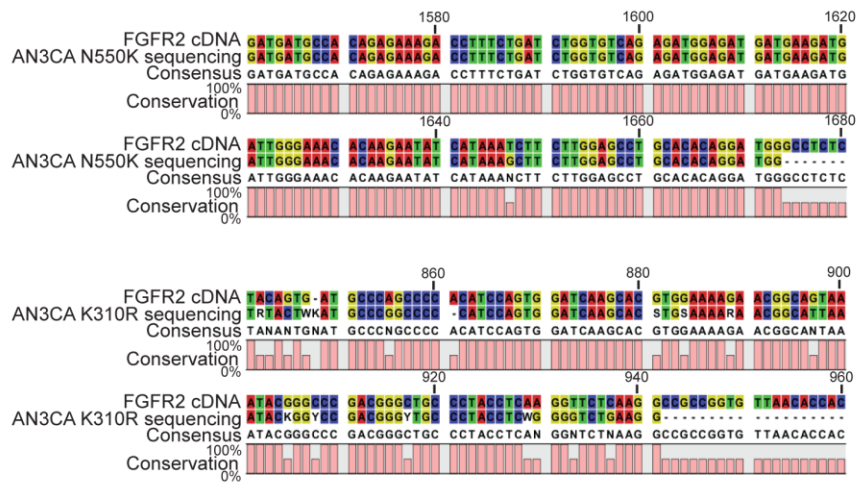
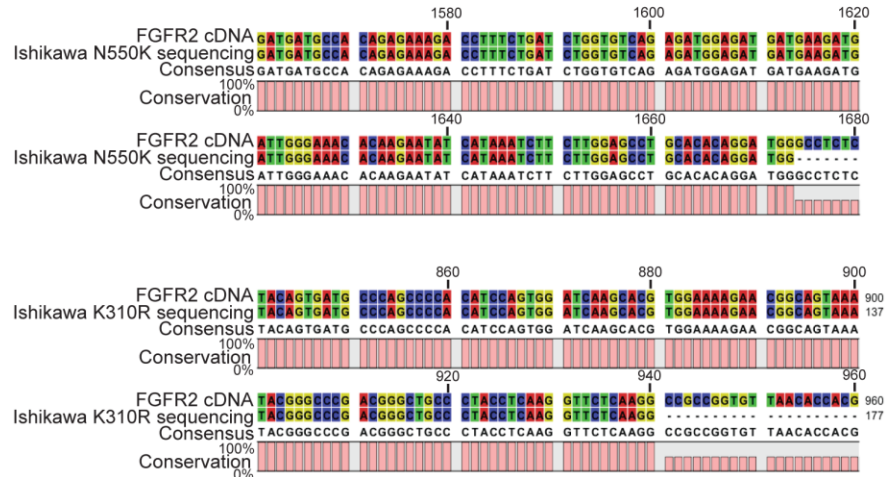
- WILKIE, A. O. 2005. Bad bones, absent smell, selfish testes: the pleiotropic consequences of human FGF receptor mutations. *Cytokine Growth Factor Rev*, 16, 187-203.
- WILLIAMS, S. V., HURST, C. D. & KNOWLES, M. A. 2013. Oncogenic FGFR3 gene fusions in bladder cancer. *Hum Mol Genet*, 22, 795-803.
- WITZ, I. P. & LEVY-NISSENBAUM, O. 2006. The tumor microenvironment in the post-PAGET era. *Cancer Lett*, 242, 1-10.
- WOLCHOK, J. D., NEYNS, B., LINETTE, G., NEGRIER, S., LUTZKY, J., THOMAS, L., WATERFIELD, W., SCHADENDORF, D., SMYLIE, M., GUTHRIE, T., JR., GROB, J. J., CHESNEY, J., CHIN, K., CHEN, K., HOOS, A., O'DAY, S. J. & LEBBE, C. 2010. Ipilimumab monotherapy in patients with pretreated advanced melanoma: a randomised, double-blind, multicentre, phase 2, dose-ranging study. *Lancet Oncol*, 11, 155-64.
- WRIGHT, J. D., BUCK, A. M., SHAH, M., BURKE, W. M., SCHIFF, P. B. & HERZOG, T. J. 2009. Safety of ovarian preservation in premenopausal women with endometrial cancer. *J Clin Oncol*, 27, 1214-9.
- WU, Y. M., SU, F., KALYANA-SUNDARAM, S., KHAZANOV, N., ATEEQ, B., CAO, X., LONIGRO, R. J., VATS, P., WANG, R., LIN, S. F., CHENG, A. J., KUNJU, L. P., SIDDIQUI, J., TOMLINS, S. A., WYNGAARD, P., SADIS, S., ROYCHOWDHURY, S., HUSSAIN, M. H., FENG, F. Y., ZALUPSKI, M. M., TALPAZ, M., PIENTA, K. J., RHODES, D. R., ROBINSON, D. R. & CHINNAIYAN, A. M. 2013. Identification of targetable FGFR gene fusions in diverse cancers. *Cancer Discov*, 3, 636-47.
- XIE, L., SU, X., ZHANG, L., YIN, X., TANG, L., ZHANG, X., XU, Y., GAO, Z., LIU, K., ZHOU, M., GAO, B., SHEN, D., JI, J., GAVINE, P. R., ZHANG, J., KILGOUR, E. & JI, Q. 2013. FGFR2 gene amplification in gastric cancer predicts sensitivity to the selective FGFR inhibitor AZD4547. *Clin Cancer Res*, 19, 2572-83.
- XIONG, S., ZHAO, Q., RONG, Z., HUANG, G., HUANG, Y., CHEN, P., ZHANG, S., LIU, L. & CHANG, Z. 2003. hSef inhibits PC-12 cell differentiation by interfering with Ras-mitogen-activated protein kinase MAPK signaling.
- YAN, G., FUKABORI, Y., MCBRIDE, G., NIKOLAROPOLOUS, S. & MCKEEHAN, W. L. 1993. Exon switching and activation of stromal and embryonic fibroblast growth factor (FGF)-FGF receptor genes in prostate epithelial cells

- accompany stromal independence and malignancy. *Mol Cell Biol*, 13, 4513-22.
- YANG, R. B., NG, C. K., WASSERMAN, S. M., KOMUVES, L. G., GERRITSEN, M. E. & TOPPER, J. N. 2003. A novel interleukin-17 receptor-like protein identified in human umbilical vein endothelial cells antagonizes basic fibroblast growth factor-induced signaling. *J Biol Chem*, 278, 33232-8.
- YAYON, A., KLAGSBRUN, M., ESKO, J. D., LEDER, P. & ORNITZ, D. M. 1991. Cell surface, heparin-like molecules are required for binding of basic fibroblast growth factor to its high affinity receptor. *Cell*, 64, 841-8.
- YERAMIAN, A., MORENO-BUENO, G., DOLCET, X., CATASUS, L., ABAL, M., COLAS, E., REVENTOS, J., PALACIOS, J., PRAT, J. & MATIAS-GUIU, X. 2013. Endometrial carcinoma: molecular alterations involved in tumor development and progression. *Oncogene*, 32, 403-13.
- YOKOTA, M., KOBAYASHI, Y., MORITA, J., SUZUKI, H., HASHIMOTO, Y., SASAKI, Y., AKIYOSHI, K. & MORIYAMA, K. 2014. Therapeutic effect of nanogel-based delivery of soluble FGFR2 with S252W mutation on craniosynostosis. *PLoS One*, 9, e101693.
- YU, K., HERR, A. B., WAKSMAN, G. & ORNITZ, D. M. 2000. Loss of fibroblast growth factor receptor 2 ligand-binding specificity in Apert syndrome. *Proc Natl Acad Sci U S A*, 97, 14536-41.
- ZACHAREK, S. J., FILLMORE, C. M., LAU, A. N., GLUDISH, D. W., CHOU, A., HO, J. W., ZAMPONI, R., GAZIT, R., BOCK, C., JAGER, N., SMITH, Z. D., KIM, T. M., SAUNDERS, A. H., WONG, J., LEE, J. H., ROACH, R. R., ROSSI, D. J., MEISSNER, A., GIMELBRANT, A. A., PARK, P. J. & KIM, C. F. 2011. Lung stem cell self-renewal relies on BMI1-dependent control of expression at imprinted loci. *Cell Stem Cell*, 9, 272-81.
- ZACK, T. I., SCHUMACHER, S. E., CARTER, S. L., CHERNIACK, A. D., SAKSENA, G., TABAK, B., LAWRENCE, M. S., ZHANG, C. Z., WALA, J., MERMEL, C. H., SOUGNEZ, C., GABRIEL, S. B., HERNANDEZ, B., SHEN, H., LAIRD, P. W., GETZ, G., MEYERSON, M. & BEROUKHIM, R. 2013. Pan-cancer patterns of somatic copy number alteration. *Nat Genet*, 45, 1134-1140.
- ZALATAN, J. G., LEE, M. E., ALMEIDA, R., GILBERT, L. A., WHITEHEAD, E. H., LA RUSSA, M., TSAI, J. C., WEISSMAN, J. S., DUEBER, J. E., QI, L. S. & LIM,

- W. A. 2014. Engineering Complex Synthetic Transcriptional Programs with CRISPR RNA Scaffolds. *Cell*.
- ZAMORA, E., MUÑOZ-COUSELO, E., CORTES, J. & PEREZ-GARCIA, J. 2014. The Fibroblast Growth Factor Receptor: A New Potential Target for the Treatment of Breast Cancer. *Current Breast Cancer Reports*, 6, 51-58.
- ZHANG, H. Y. & DOU, K. F. 2014. PCBP1 is an important mediator of TGF-beta-induced epithelial to mesenchymal transition in gall bladder cancer cell line GBC-SD. *Mol Biol Rep*, 41, 5519-24.
- ZHANG, J., YANG, P. L. & GRAY, N. S. 2009. Targeting cancer with small molecule kinase inhibitors. *Nat Rev Cancer*, 9, 28-39.
- ZHANG, Y., PAN, T., ZHONG, X. & CHENG, C. 2014. Resistance to cetuximab in EGFR-overexpressing esophageal squamous cell carcinoma xenografts due to FGFR2 amplification and overexpression. *J Pharmacol Sci*, 126, 77-83.
- ZHUANG, L., KAROTKI, A. V., BRUECKER, P. & TRUEB, B. 2009. Comparison of the receptor FGFR1 from sea urchins and humans illustrates evolution of a zinc binding motif in the intracellular domain. *BMC Biochem*, 10, 33.
- ZUBAREV, R. A. 2004. Electron-capture dissociation tandem mass spectrometry. *Curr Opin Biotechnol*, 15, 12-6.

Appendix 1

Supplementary figures

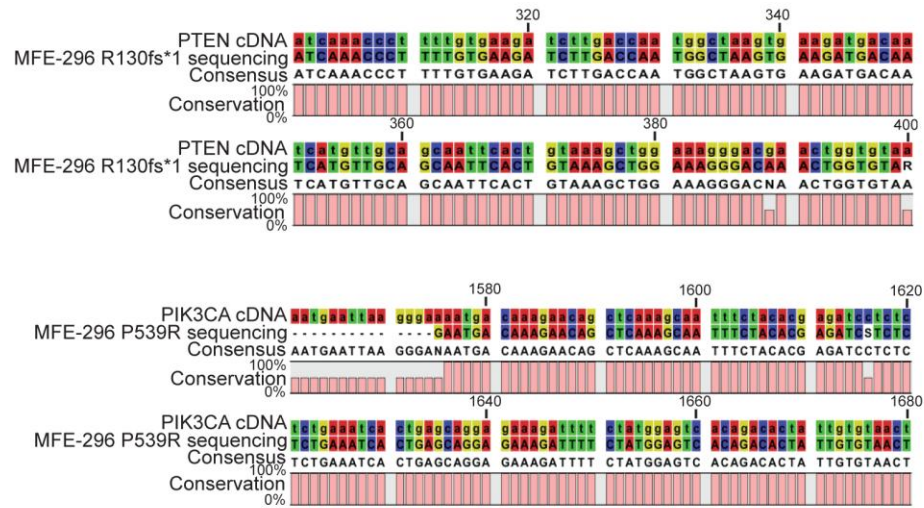
A**B****C**

Appendix Figure 1.1. *FGFR2* mutation sequencing of endometrial cancer cell lines.

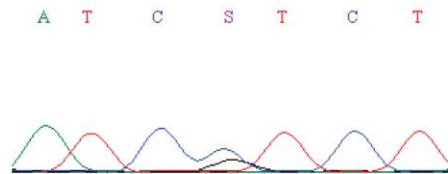
PCR was performed on cDNA from each cell line using primers designed to amplify the region containing the two *FGFR2* mutations of interest. Cycle sequencing was then performed on the PCR products and the resulting sequences compared to wild type *FGFR2* cDNA using CLC Sequence Viewer (v6). (A) Substitution of a thymine residue to guanine at

FGFR2 cDNA position 1647 results in the N550K amino acid mutation. The MFE-296 cell line contains this mutation, as shown by the mismatch between wild type and MFE-296 cDNA in the alignment (top panel). Conversion of residue 929 from adenosine to guanine results in the K310R FGFR2 mutation. The MFE-296 cell line contains this mismatch, as shown by the mismatch in sequence alignment with wild type FGFR2 cDNA (bottom panel). There are also many additional mismatches between MFE-296 and wild type cDNA in this region. These are not noted in the literature. (B) The AN3CA cell line harbours both the N550K and K310R FGFR2 mutations (top and bottom panels, respectively). (C) The Ishikawa cell line is wild type for both the N550K and K310R mutations.

A

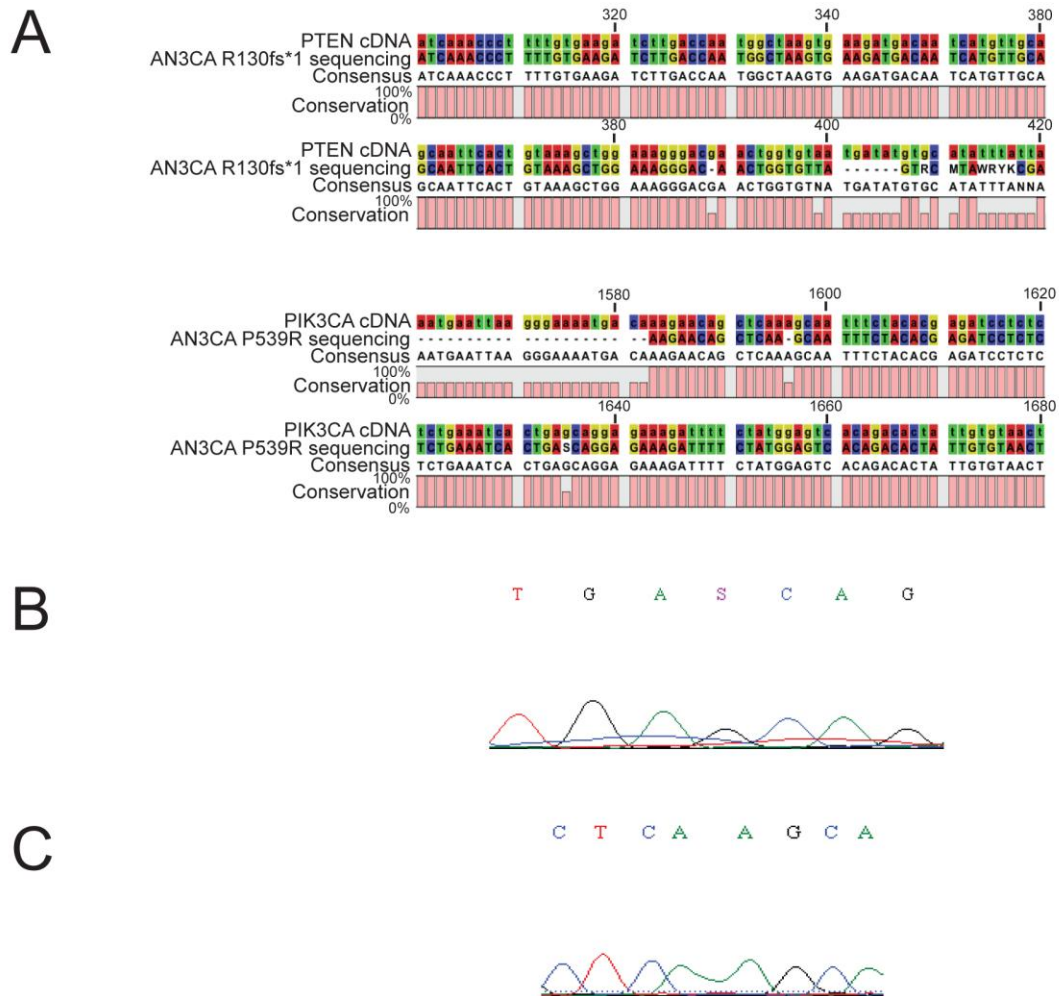


B



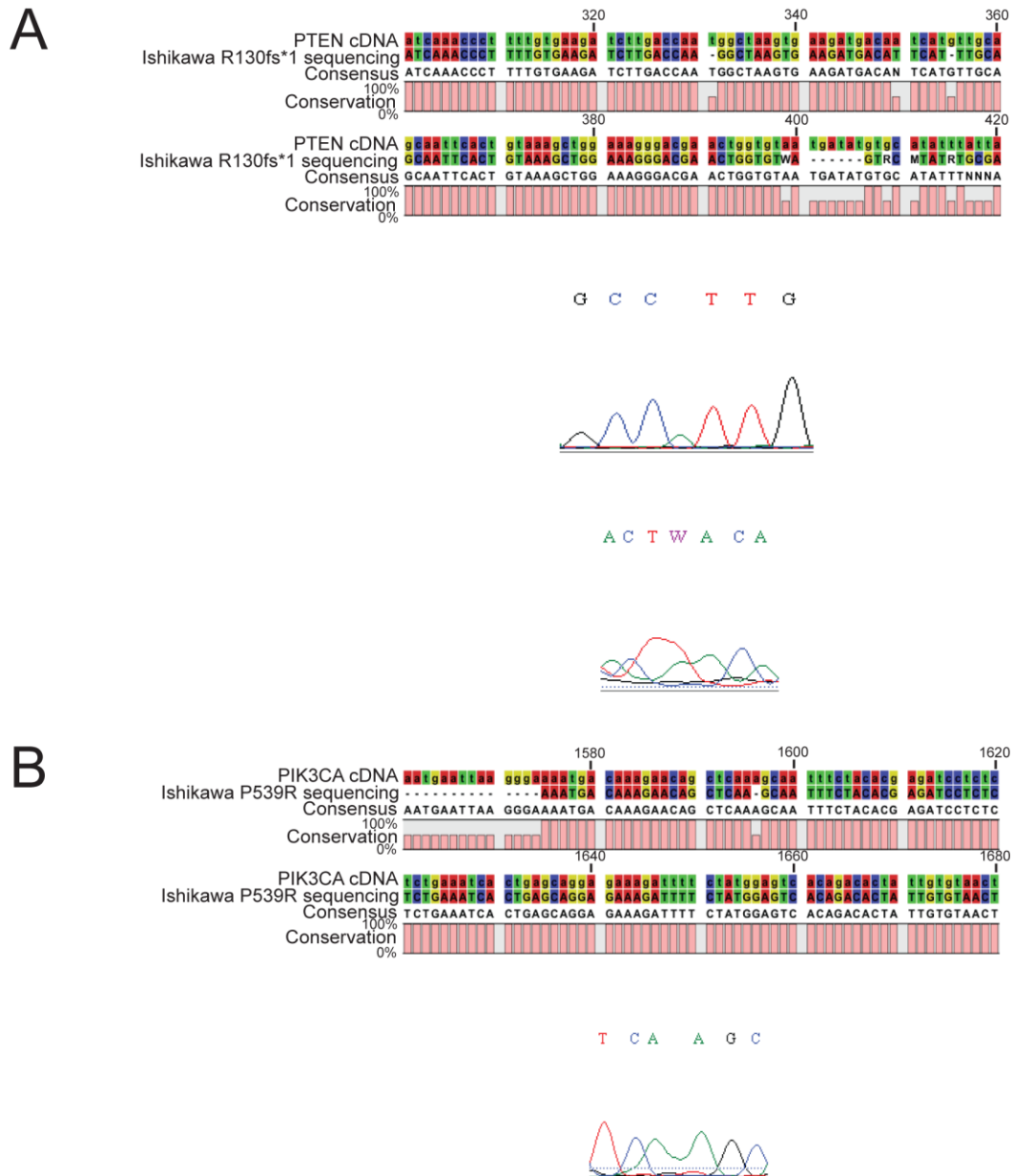
Appendix Figure 1.2. *PTEN* and *PIK3CA* mutation sequencing of MFE-296 cells.

MFE-296 cells were sequenced for the *PTEN* R130Q and R130fs*1 mutations, as well as the *PIK3CA* P539R mutations using cycle sequencing; resulting sequences were analysed using BioEdit and CLC Sequence Viewer (v6). (A) MFE-296 cells are *PTEN* R130Q mutant (top panel). The R130fs*1 frame shift is not present in the MFE-296 cell line. The PI3Ka P539R sequencing data gave an ‘S’ in the 1616 residue position, indicating that the software could not distinguish between cytosine or guanine (bottom panel). (B) BioEdit visualisation of the sequencing trace revealed two peaks at the 1616 position of cytosine and guanine, indicating the cell line harbours copies of both of these residues. The MFE-296 cell line is therefore heterozygous for this mutation, as noted in the literature.



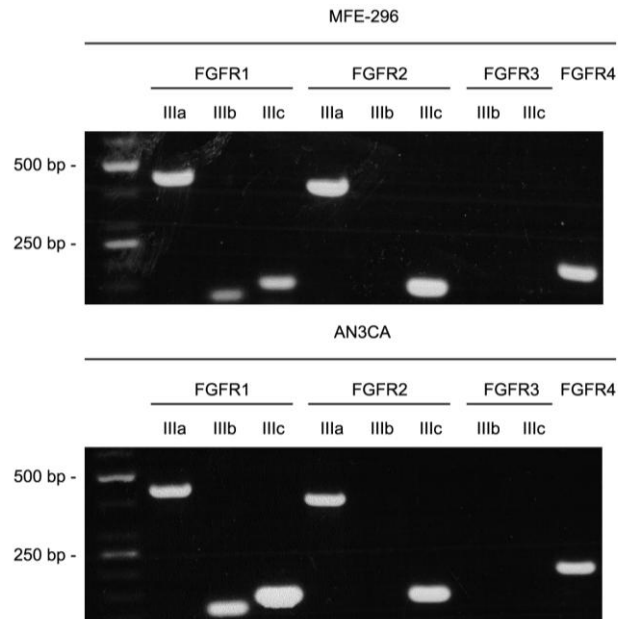
Appendix Figure 1.3. *PTEN* and *PIK3CA* mutation sequencing of AN3CA cells.

AN3CA cells were sequenced for the *PTEN* R130Q and R130fs*1 mutations, as well as the *PIK3CA* P539R mutation using cycle sequencing; resulting sequences were analysed using BioEdit and CLC Sequence Viewer (v6). (A) AN3CA cells are R130fs*1 *PTEN* mutant (top panel). Sequencing for P539R shows AN3CA cells are *PIK3CA* wild type (bottom panel). (B) BioEdit analysis of the missing base at position 1635 shows the residue is most likely guanine (listed as 'S' in the trace) but is shown as the trace around the base is not clear and so the base can not be definitively assigned. (C) The missing base at position 1586 is most likely adenine, as shown in the BioEdit trace where the adenine triplicate appears as an indefinable smear in the BioEdit trace.



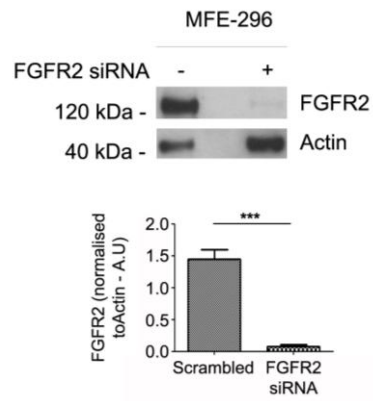
Appendix Figure 1.4. *PTEN* and *PIK3CA* mutation sequencing of Ishikawa cells.

Ishikawa cells were sequenced for both R130Q and R130fs*1 *PTEN* mutations, as well as P539R *PIK3CA* mutations using cycle sequencing; the resulting data were analysed using BioEdit and CLC Sequence Viewer (v6). (A) Ishikawa cells are *PTEN* R130fs*1 and R130Q wild type (top panel). BioEdit analysis of the missing thymine residue at position 331 shows this base is present, however, owing to a poor sequencing trace at this base, the software was not able to definitively assign thymine to this position (middle panel). Thymine appears as adenine in the trace as the sequence has been reversed. The 'W' residue at position 399 is most likely an adenine, as shown in the BioEdit trace (bottom panel). (B) Ishikawa cells are *PIK3CA* wild type (top panel). The missing base at position 1596 is most likely adenine, as shown in the BioEdit trace (bottom panel).



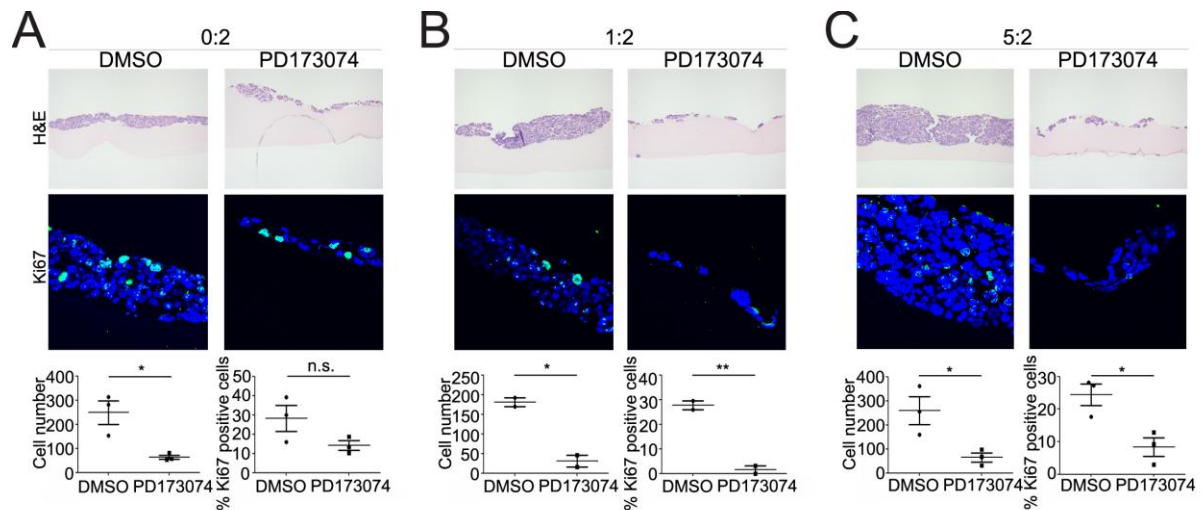
Appendix Figure 1.5. FGFR isoform expression in MFE-296 and AN3CA.

PCR was performed on MFE-296 and AN3CA cell lines to establish expression of each of the FGFR1-4 isoforms. MFE-296 and AN3CA cells expressed FGFR1IIIa, b and c, FGFR2IIIa and c and FGFR4. Neither cell line expressed FGFR3. III represents the isoform produced as a result of alternative splicing of the third Ig loop. There are three potential isoforms of FGFR1 and 2 (IIIa, b and c), two of FGFR3 (IIIb and c) and one of FGFR4.



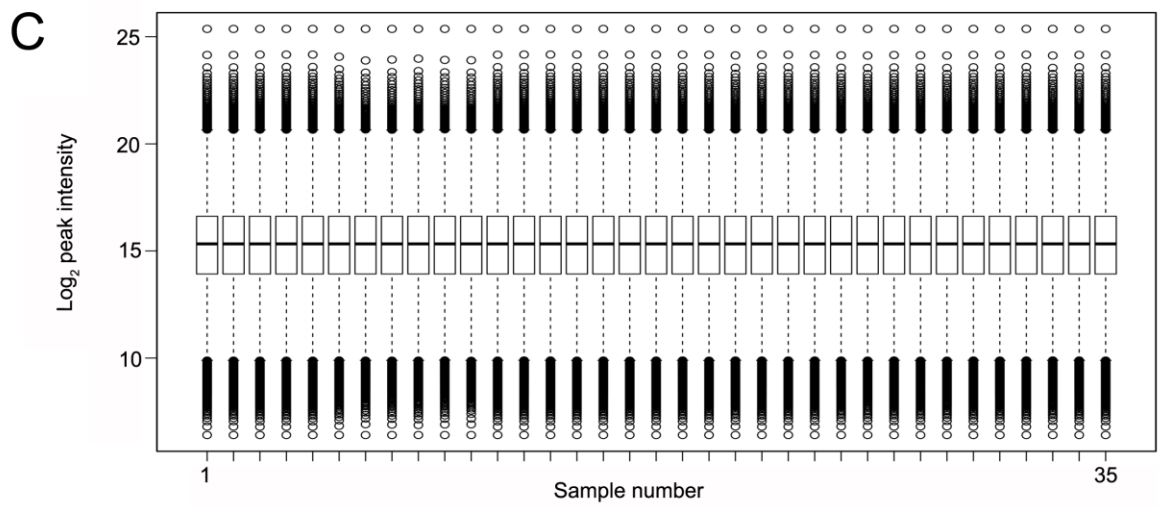
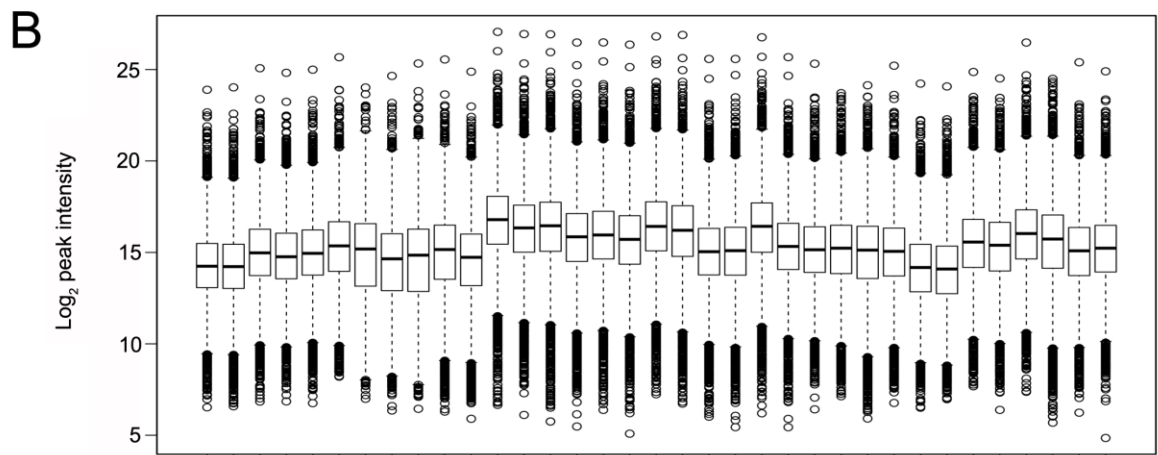
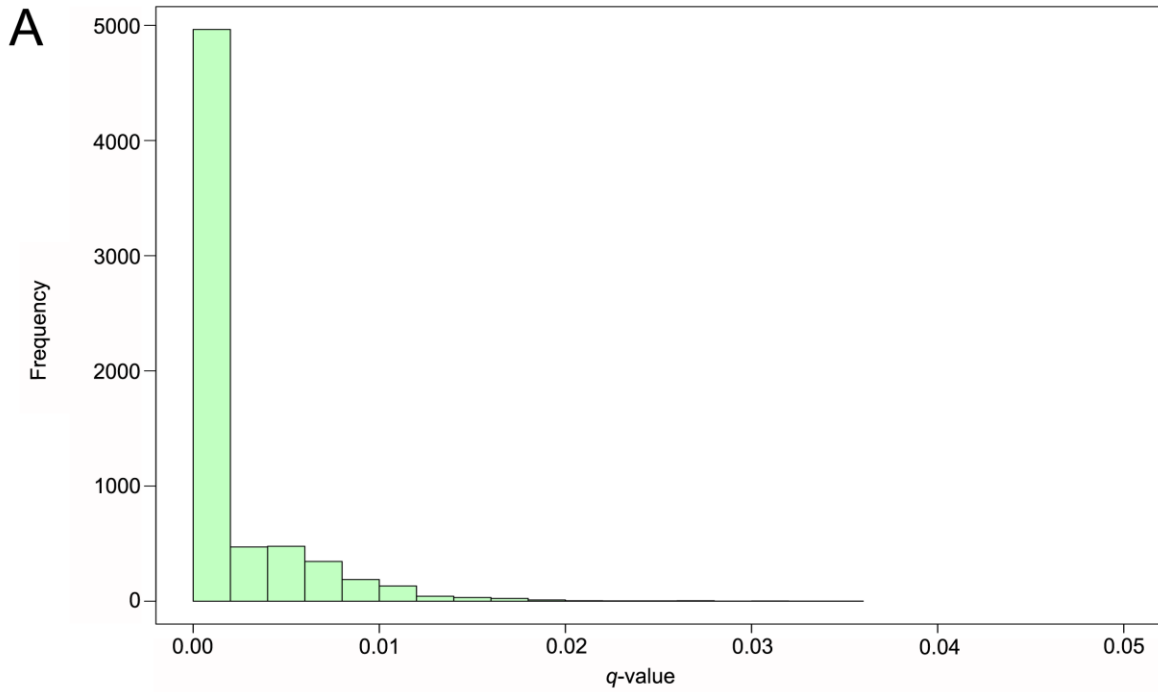
Appendix Figure 1.6. FGFR2 antibody validation.

Specificity and efficiency of the FGFR2 antibody used throughout this work was validated via siRNA knockdown of FGFR2 for 48 hours in MFE-296 cells. 15 µg protein was used for each blot. Error bars show means ± SEM of three replicates.



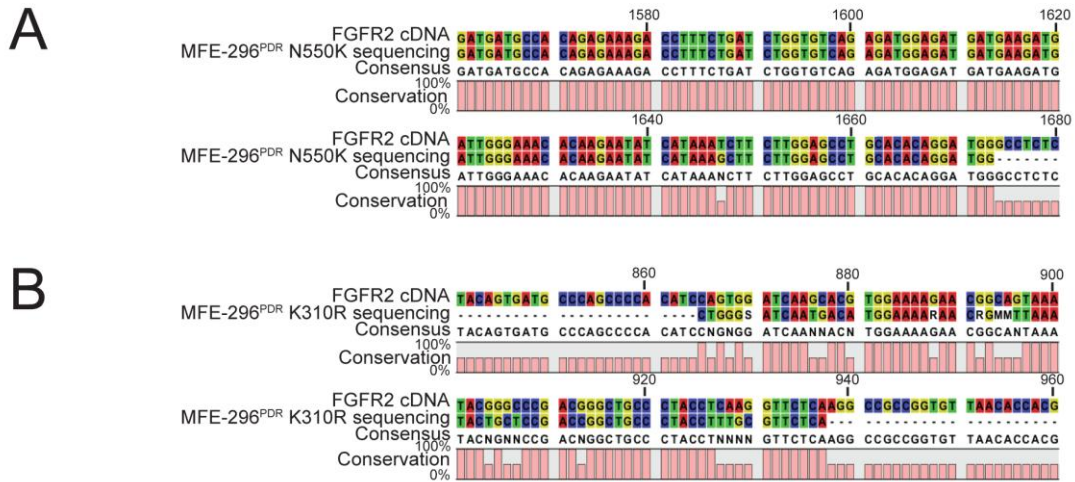
Appendix Figure 1.7. Effect of varying HFF2:MFE-296 ratio in a 3D organotypic model of endometrial cancer.

An endometrial cancer cell model was designed using a collagen/Matrigel mix containing human foreskin fibroblasts (HFF2) cells as a stromal equivalent, overlaid with MFE-296 cells in a Transwell insert, respecting the cell ratios previously outlined. Cells were cultured at an air-liquid interface for seven days in the presence of an FGFR inhibitor or DMSO control. Ratios refer to HFF2:MFE-296 cell ratios. (A) Cell number was decreased significantly after seven days FGFR inhibition using PD173074, when cells were cultured in the absence of fibroblasts. However, there was no change in the percentage of cells capable of proliferation, as shown by Ki67 staining (green). (B and C) Both cell number and proliferation was decreased significantly upon inclusion of HFF2 cells in the organotypic model. Original magnification of H&E images, 10X objective; bar, 100 μ m. Original magnification of confocal images, 40X objective; bar, 25 μ m. Error bars show means \pm SEM. Data points represent the average cell number/Ki67 positive cells of six fields of view of one to three technical replicates of three biological replicates. Cell number and percent Ki67 positive cells represents average values per field of view.



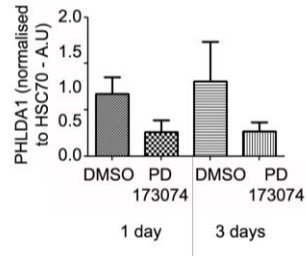
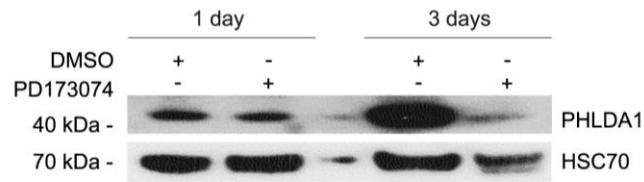
Appendix Figure 1.8. False discovery rate (FDR) and quantile normalisation of phosphopeptide ions.

Statistical normalisation of MS data. (A) The false discovery rate (FDR) of phosphopeptides was <1% for 95% of identifications and <5% for the remainder. (B) Log_2 peak intensity of phosphopeptides in each sample. (C) Quantile normalized Log_2 peak intensity of phosphopeptides (Bolstad et al., 2003).



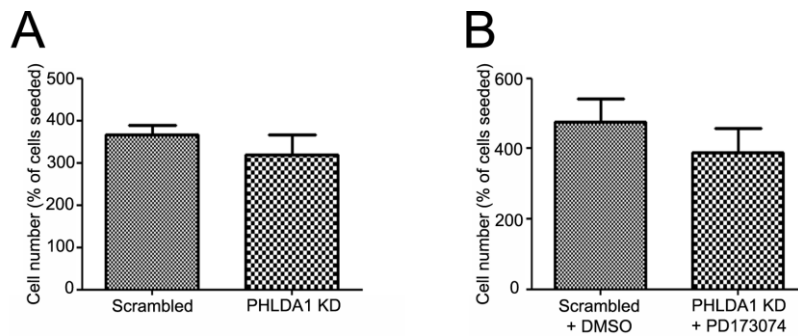
Appendix Figure 1.9. *FGFR2* mutation sequencing of MFE-296^{PDR} cells.

PCR was performed on cDNA from each cell line using primers designed to amplify the region containing the two *FGFR2* mutations of interest. Cycle sequencing was then performed on the PCR products and the resulting sequences compared to wild type *FGFR2* cDNA using CLC Sequence Viewer (v6). Substitution of a thymine residue to guanine at *FGFR2* cDNA position 1647 results in the N550K amino acid mutation. The MFE-296 cell line contains this mutation, as shown by the mismatch between wild type and MFE-296 cDNA in the alignment (top panel). Conversion of residue 929 from adenine to guanine results in the K310R *FGFR2* mutation. The MFE-296 cell line contains this mismatch, as shown by the mismatch in sequence alignment with wild type *FGFR2* cDNA (bottom panel). MFE-296^{PDR} cells contain the same *FGFR2* mutations as the parental MFE-296 cell line. The resulting sequences were analysed in BioEdit Sequence Alignment Editor and CLC Sequence Viewer (v.6).



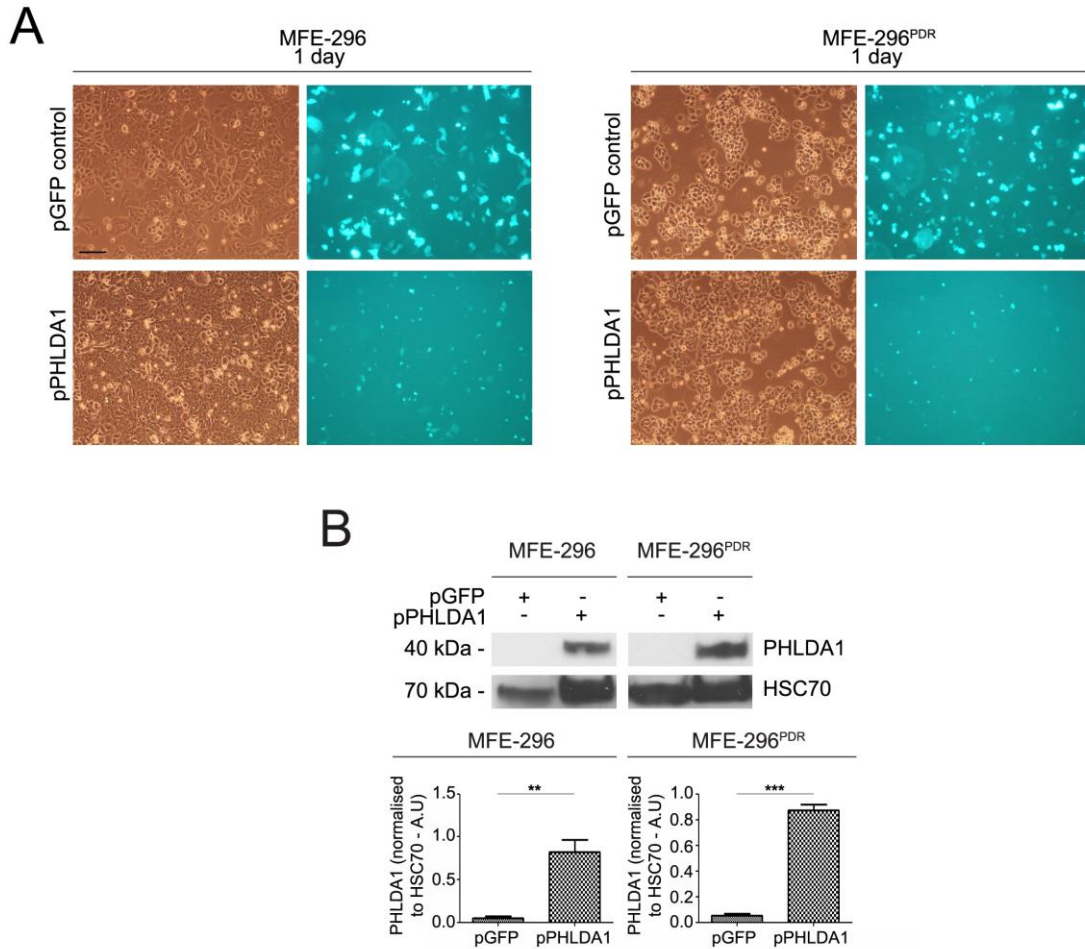
Appendix Figure 1.10. Effect of PD173074 on PHLDA1 levels in MFE-296 cells.

MFE-296 cells were treated with 2 μ M PD173074 or DMSO as a vehicle control for one and three days and PHLDA1 levels assessed. There was no significant difference in PHLDA1 levels after 1 or 3 days PD173074 treatment in MFE-296 cells (Student's *t* test, $P > 0.05$). 40 μ g protein was used for each blot. Error bars show means \pm SEM of two replicates.



Appendix Figure 1.11. PHLDA1 knockdown does not affect MFE-296^{PDR} cell number.

The effect of PHLDA1 knockdown (KD) on MFE-296^{PDR} cells in the presence and absence of PD173074 was assessed in 2D culture. (A) MFE-296^{PDR} cells were treated with PHLDA1 siRNA (PHLDA1 KD) or a non-targeting control (scrambled) for two days, after which cell number was counted using a haemocytometer. There was no significant difference in cell number when MFE-296^{PDR} cells were treated with PHLDA1 siRNA. (B) Cells were treated with PHLDA1 siRNA or a scrambled control for two days. PHLDA1 siRNA treated cells were subsequently treated with 5 μ M PD173074 for three days, while scrambled siRNA treated cells were treated with DMSO as a control. The number of cells remaining after each treatment was calculated by counting cells using a haemocytometer. siRNA knockdown of PHLDA1 followed by treatment with PD173074 did not affect cell number compared to the control. Cell number is displayed as the percentage of cells seeded. Error bars show means \pm SEM of three replicates.



Appendix Figure 1.12. PHLDA1 over-expression in MFE-296 and MFE-296^{PDR} cells.

MFE-296 and MFE-296^{PDR} cells were transfected with a GFP-tagged PHLDA1 plasmid or a GFP only plasmid as a control. (A) After one day, cells were visualised under a light microscope as well as under UV light. Transfection of both plasmids was successful in both cell lines. (B) Western blot analysis of control and PHLDA1 transfected cells showed PHLDA1 expression in both MFE-296 and MFE-296^{PDR} cell lines. Brightfield and UV light images of each transfection are of the same field of view. Original magnification of bright field and UV images, 10X objective; bar 100 μ m. Images are representative of three biological replicates. **, $P \leq 0.01$; ***, $P \leq 0.001$ (Student's *t* test). 40 μ g protein was used for each lane. Error bars show means \pm SEM of three replicates.

Appendix 2

Genomic editing of *FGFR2* mutation status using ZFN technology

Appendix 2.1 Introduction

Advances in high throughput screening have greatly increased our knowledge of potentially important genes of interest in the initiation and progression of cancer. While our ability to identify these targets has advanced, our capacity to assess their function in a physiologically relevant context has been lacking. Historically, use of RNA interference (RNAi) and pharmacological inhibitors have been used to assess genes and proteins of interest (McManus and Sharp, 2002). Whilst this has produced relevant and important results, such methods often have off-target effects, occasionally making phenotypic consequences hard to decipher. To combat this, a variety of genomic editing tools have been developed, allowing for more precise targeting of the gene of interest. Whilst these tools, for example zinc finger nucleases (ZFNs), transcription activator-like effector nucleases (TALENs) and clustered regulatory interspaced short palindromic repeats (CRISPRs), are still relatively novel, their potential to aid understanding of cell behaviour is profound.

ZFNs and TALENs allow targeted genome editing via introduction of double strand breaks (DSBs) and subsequent DNA repair (Capecchi, 2005). These tools comprise a nuclease component, engineered to target and bind to a specific DNA sequence, and a non-specific DNA cleavage domain, most commonly derived from the FokI endonuclease (Carroll, 2011, Cheng and Alper, 2014, Urnov et al., 2010) (Appendix Figure 2.1 A). Importantly, these chimeric nucleases act in pairs, forming precise molecular scissors. This enables site-specific localisation of the FokI dimer and subsequent editing of the endogenous gene sequence by induction of the cellular DNA repair mechanisms; non-homologous end joining (NHEJ) and homologous repair (HR) (Gaj et al., 2013). The pioneering work on these tools was performed using ZFNs, while the recent discovery of TALE proteins has led to the expansion of these genome editing technologies (Boch et al., 2009, Moscou and Bogdanove, 2009). As the latest agent in this repertoire, CRISPR technology is still in relative infancy. However, recent work has shown how this RNA-guided DNA endonuclease system affords excellent specificity to its targets and can allow for complex manipulation of multiple genes in a pathway (Zalatan et al., 2014).

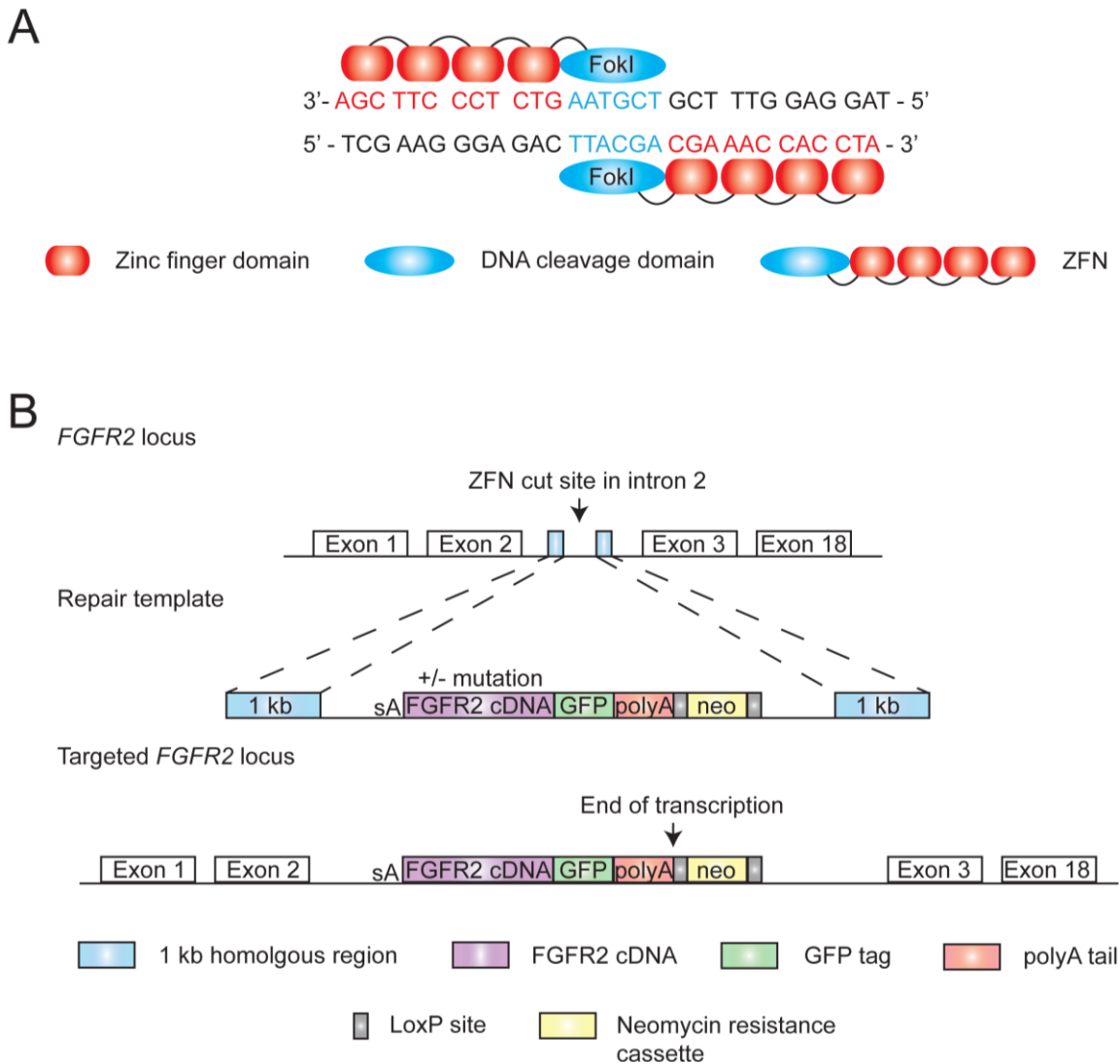
ZFN technology

The DNA recognition portion of ZFNs consists of Cys2-His2 zinc finger domains, the most common DNA-binding motif in eukaryotes (Gaj et al., 2013). Each zinc finger protein exists in an highly conserved β -sheet, β -sheet, α -helix conformation with a single zinc atom; the α portion is able to engage three base pairs of DNA (Beerli and Barbas, 2002, Kim et al., 1993). Chains of zinc finger proteins can be produced utilising a conserved linker sequence, forming a synthetic protein engineered to target a specific DNA motif (Liu et al., 1997). Zinc finger modules recognising nearly all 64 nucleotide triplets have been developed, allowing production of assemblies up to 18 base pairs long, engineered to the gene of interest (Beerli et al., 1998, Beerli and Barbas, 2002, Bhakta et al., 2013, Gonzalez et al., 2010, Kim et al., 2011). Therefore, ZFN technology allows for targeting of virtually any DNA sequence.

These ZFN assemblies are bound to the catalytic domain of the FokI endonuclease (Bibikova et al., 2001, Mani et al., 2005, Smith et al., 2000). Type IIS FokI consists of two domains with separable DNA recognition and cleavage functions (Li et al., 1992). This protein is utilised in ZFN technology by replacing the DNA recognition domain with the zinc finger chain (Kim et al., 1996). Since DNA cleavage is only achieved upon FokI dimerisation, the action of each ZFN can only be achieved when acting in a pair, therefore increasing target specificity (Mani et al., 2005, Miller et al., 2007).

The range of uses of ZFN technology is broad, from gene knockout, tagging of an endogenous gene or site-directed mutagenesis with an alternative repair construct (Beerli et al., 2000). For example, manipulation of gene expression can be achieved by flooding cells with an engineered repair construct in combination with ZFN transfection (Appendix Figure 2.1 B). In a proportion of cells, this construct will be incorporated into the genome, during the DSB repair process induced by the ZFN, resulting in transcription of the construct under the endogenous promoter. This technology is particularly useful in assessing the effect of specific mutations in, for example, a wild type background, by incorporation of a mutant construct at the ZFN

cut site. The validity of this technology for use in *FGFR2* has been shown in breast cancer cells (Robbez-Masson et al., 2013). Constructs with varying small nucleotide polymorphisms (SNPs) in intron 2 of *FGFR2*, shown in genome wide association studies (GWAS) to associate with increased breast cancer risk (Easton et al., 2007, Hunter et al., 2007), were introduced into cells. While this did not produce any obvious phenotype, proof of concept of this genome editing tool was confirmed.



Appendix Figure 2.1. ZFN-mediated genome editing.

(A) Organisation of the ZFN pair at the *FGFR2* target site. Each ZFN consists of two functional domains: a DNA-binding domain, comprised of a chain of four zinc finger subunits (red), and a DNA-cleaving domain, consisting of two FokI endonuclease domains (blue), which act as a specific pair of 'genomic scissors'. The DNA sequence shown is specific to intron 2 of *FGFR2*. (B) Schematic representation of ZFN-mediated insertion of the *FGFR2* gene into cells. The ZFN pair is targeted to intron 2 of the *FGFR2* gene, inducing a double strand break. Transfection of an alternative repair construct results in its incorporation in place of the normal cellular homologous recombination DNA repair, aided by inclusion of 1 kb homologous arms at either end of the construct. Inclusion of a poly-adenylation sequence ensures transcription terminates at the end of the construct, preventing transcription of the endogenous *FGFR2* locus downstream of the ZFN cut site. The GFP tag and neomycin resistance cassette allow effective screening of transfected cells for successful targeting.

The neomycin resistance box is flanked by two LoxP sites, allowing for removal of the neomycin cassette upon expression of Cre recombinase.

Appendix 2.2 Materials and Methods

2.2.1 Custom-made *FGFR2* ZFN

The CompoZr custom made *FGFR2* ZFNs were purchased from Sigma-Aldrich (Sequence shown in Appendix Figure 2.1 A). Vials of ZFN mRNA sufficient for 10 transfections were also supplied by Sigma-Aldrich, as were the two ZFN plasmids from which additional mRNA was generated.

2.2.2 Bacterial transformation

1-10 ng ZFN plasmid DNA was added to 50 μ L chemically competent bacteria (Bioline) and placed on ice for 15 min, followed by heat shock for 30 s at 42°C and returned to ice for a further 2 min. Bacteria were re-suspended in 500 μ L antibiotic-free Luria Broth (LB) and incubated at 37°C with constant agitation at 225 rpm for 1 h. 100 μ L cells were plated on LB agar plates containing 100 μ g/mL kanamycin for antibiotic selection and incubated overnight at 37°C. Small scale and large scale plasmid DNA preparations were carried out using QIAprep Spin Miniprep (QIAGEN) and QIAfilter Maxiprep (QIAGEN) kits, respectively. DNA concentrations were measured using a Nanodrop spectrophotometer.

2.2.3 ZFN mRNA synthesis

ZFN mRNA was prepared using the MessageMax T7 mRNA transcription kit (Cellscript Inc.) according to the manufacturer's instructions. A polyA tail was then added to the mRNA using the A-Plus poly(A) polymerase tailing kit (Epicentre) according to the manufacturer's instructions.

2.2.4 Alternative repair construct

The *FGFR2IIIb*-GFP construct with 1 kb homologous regions in the pJET1.2 ampicillin resistant plasmid was a gift from John Ladbury (University of Leeds). Cells transfected with the construct were screened for GFP expression under UV light to

confirm successful transfection. As an additional selection method, a neomycin resistance cassette was inserted (FGFR2IIIb-GFP-neo). This cassette was flanked by LoxP sites to enable removal of the cassette from selected cells via expression of Cre recombinase.

2.2.5 Site directed mutagenesis

FGFR2IIIb-GFP constructs containing two common FGFR2 mutations found in endometrial cancer were generated via site directed mutagenesis (SDM). Two mutant constructs were generated: N550K and K310R. SDM can be used to introduce point mutations into double stranded plasmid DNA. Using complimentary primers that contain the mutation of interest, KOD DNA Polymerase (Novagen) was used according to the manufacturer's instructions. Briefly, PCR was performed to introduce the mutation and amplify the PCR product. DpnI endonuclease was then used to digest the methylated, wild type DNA, leaving the newly synthesised mutant DNA intact. The final product was cloned into competent bacteria to be re-circularised and amplified. Plasmid DNA was amplified as outline in section 2.2.2. Primers for SDM were generated using the QuikChange Primer Design Programme (Agilent Technologies) (Appendix Table 2.1).

To validate the mutation status, HotStarTaq Plus DNA Polymerase (QIAGEN) was used, utilising the primers detailed in Appendix Table 2.2 and the PCR cycle in Appendix Table 2.3. PCR products were run on an agarose (Life Technologies) gel containing Gel Red (Biotium) and visualised under UV light to ensure a single, strong band was produced from the PCR. The PCR product was then sent to Barts Genome Centre for cycle sequencing. The resulting sequence was analysed using BioEdit and CLC Sequence Viewer (v6) software.

Appendix Table 2.1. Primers used to produce mutant FGFR2IIIb-GFP constructs via SDM

Primer name	Sequence	Source
a102g (K310R mutation)	GGG CTG CCC TAC CTC AGG GTT CTC AAG C	Eurogentec
a102g antisense (K310R mutation)	GCT TGA GAA CCC TGA GGT AGG GCA GCC C	Eurogentec
t103g (N550K mutation)	GAT TGG GAA ACA CAA GAA TAT CAT AAA GCT TCT TGG AGC CTG C	Eurogentec
t103g antisense (N550K mutation)	GCA GGC TCC AAG AAG CTT TAT GAT ATT CTT GTG TTT CCC AAT C	Eurogentec

Appendix Table 2.2. Primers used to sequence endometrial cancer cells for point mutations

Primer name	Sequence	Source
N550K F	GCT GCC CAT GAG TTA GAG GA	Eurogentec
N550K R	GGA AGC CCA GCC ATT TCT A	Eurogentec
K310R F	TCT TCC CTC TCT CCA CCA GA	Eurogentec
K310R R	CAT GAA GGA GAC CCC AGT TG	Eurogentec

Appendix Table 2.3. HotStarTaq Plus DNA polymerase PCR programme

Step	Temperature (°C)	Time (min)	Cycles
Initial denaturation	94	3	1
Denaturation	94	0.5	35
Annealing	58	0.5	
Extension	72	0.5	
Final extension	72	7	1
Hold	4	Indefinitely	

2.2.6 ZFN transfection – lipofection

Cells were seeded in a six well plate at 40% confluency in standard medium. The following day, medium was removed and cells were washed with PBS. OptiMEM (Life Technologies) was warmed to 37°C and 1 mL added to each well. For ZFN transfection control wells, 2 µg/µL ZFN mRNA was added to 250 µL OptiMEM in an eppendorf tube. A second eppendorf tube containing 5 µL Lipofectamine 2000 (Invitrogen) with 250 µL OptiMEM was prepared and both solutions incubated at room temperature for 5 min. The contents of both tubes were then mixed and incubated at room temperature for 20 min. The total volume was then added to control wells and incubated at 30°C for 4 hours. Medium was then removed and replaced with standard culture medium and cells incubated for three days at 30°C.

For pmaxGFP (pGFP) (Lonza) control wells, 2 µg/µL pGFP was added to 250 µL OptiMEM in an eppendorf tube and the method above followed.

For FGFR2IIIb-GFP-neo construct transfection, 2 µg/µL of construct, in addition to 2 µg/µL ZFN mRNA, was added to 250 µL OptiMEM and mixed with the Lipofectamine 2000 preparation as above and added to the cells.

Wells were inspected under UV light for GFP expression over the three days incubation period. Genomic DNA (gDNA) was then extracted from the cells using GenElute Mammalian Genomic DNA miniprep kit (Sigma-Aldrich) according to the manufacturer's instructions. FGFR2IIIb-GFP-neo construct transfected samples were cultured in six well plates and transferred to T75 tissue culture flasks when approximately 80% confluent.

2.2.7 ZFN transfection – nucleofection

Cells were seeded in a 75 cm² tissue culture flask. When cells were approximately 80% confluent, medium was removed and cells were incubated with trypsin/EDTA (Sigma-Aldrich) at 37°C to detach cells from the surface of the flask. Trypsin was inactivated by adding standard medium. The cell suspension was centrifuged at 1500 x g for 3 min. The supernatant was removed and cells were resuspended in 10 mL of fresh culture medium. Cells were counted using a haemocytometer under a light microscope. The required number of cells for the total number of experiments (2 x 10⁶ cells per experiment) was then centrifuged at 90 x g for 10 min at room temperature in a 1.5 mL eppendorf. The supernatant was removed and the cell pellet resuspended in the required volume of Nucleofector solution and supplement (Lonza) for the total number of experiments (100 µL per experiment).

For ZFN controls, 2 µg/µL ZFN mRNA was added to 100 µL of cell suspension in a cuvette (supplied in Nucleofector kit). For GFP controls, 2 µg/µL pGFP was added to 100 µL of cell suspension in a cuvette.

Each cuvette was then inserted into the Nucleofector (Lonza) and the selected programme, specified per kit, applied. The cuvette was then removed and 500 µL of pre-equilibrated culture medium added to the cuvette. The total sample suspension was added to a T75 flask in 12 mL standard medium. Cells were incubated at 30°C for three days, after which gDNA was isolated from control samples. Flasks were inspected under UV light for GFP expression over the three day incubation period.

2.2.8 ZFN-induced mutation detection PCR

To establish the efficiency of the ZFN, an assay was performed using the SURVEYOR Mutation Detection Kit (Transgenomic) on ZFN and pGFP control samples, according to the manufacturer's instructions. Extracted genomic DNA was amplified using ZFN forward and reverse primers in Appendix Table 2.4 and the PCR programme detailed in Appendix Table 2.5. PCR products were denatured and

re-annealed to create mismatch duplexes using the cyclor conditions in Appendix Table 2.6.

Appendix Table 2.4. Sequencing and ZFN-induced mutation detection PCR primers

Primer name	Sequence	Source
ZFN primer F	GCA GAG TTT CTT GCC AGG TC	Sigma-Aldrich
ZFN primer R	ACA TTC CAC GTT AAG AGC CG	Sigma-Aldrich

**Appendix Table 2.5. ZFN-induced mutation detection PCR
primers**

Step	Temperature (°C)	Time (min)	Cycles
Initial denaturation	95	3	1
Denaturation	95	0.5	30
Annealing	57	0.5	
Extension	72	0.5	
Final extension	72	7	1
Hold	4	Indefinitely	

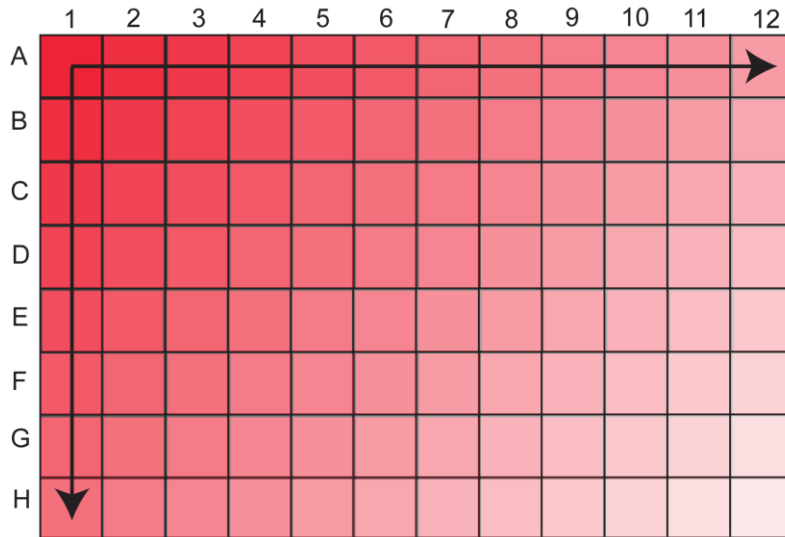
Appendix Table 2.6. Cycler conditions for re-annealing of PCR products in ZFN-induced mutation detection PCR

Temperature (°C)	Time (min)
95	10
85	Cool at 2°C/s
25	Cool at 0.1°C/s
4	Indefinitely

2.2.9 Single cell cloning

To establish monoclonal cell lines of FGFR2IIIb-GFP-neo construct transfected cells, a single cell cloning approach was used (Appendix Figure 2.2). 100 μ L of standard medium supplemented with 100 ng/mL G418 was added to each well of a 96 well plate except well A1. A 200 μ L cell suspension containing 4×10^4 cells/mL was plated in well A1. A serial dilution of this suspension was then achieved by sequentially adding 100 μ L of cell suspension from well A1 to H1. 100 μ L of standard medium was added to each well of column 1 and a serial dilution of each well across the plate achieved in a final volume of 200 μ L/well.

G418-containing medium was changed every two to three days and wells inspected under a light microscope. Wells with single cell colonies were noted and expanded as necessary. Monoclonal cell lines were plated in 25 cm² flasks and six well plates and gDNA extracted, as detailed in section 2.2.6.



Appendix Figure 2.2. Schematic representation of single cell cloning by serial dilution.

Well A1 of a 96 well plate was seeded with 4×10^4 cells, after which 1:1 serial dilution were performed from well A1 to H1 (vertical arrow). Serial dilutions of 1:1 of A1-H1 were then performed across the plate (horizontal arrow), leaving well H12 with the lowest seeding cell number.

2.2.10 FGFR2 N550K mutation sequencing

To establish the mutation status of cells transfected with the FGFR2IIIb-GFP-neo wild type construct, HotStarTaq Plus DNA Polymerase (QIAGEN) was used, utilising the N550K primers detailed in Appendix Table 2.2 and the PCR cycle in Appendix Table 2.3. PCR products were run on an agarose gel containing Gel Red and visualised under UV light to ensure a single, strong band was produced from the PCR. The PCR product was then sent to Barts Genome Centre for cycle sequencing and the resulting data analysed using BioEdit and CLC Sequence Viewer software.

2.2.11 Amplification of the neomycin resistance gene

To assess whether the alternative repair template containing a neomycin resistance cassette was incorporated into the genome after transfection, PCR using primers which recognise this cassette (Appendix Table 2.7) was performed. The PCR cycle outlined in Appendix Table 2.8 was performed and the resulting products were run on an agarose gel containing gel red and visualised under UV light.

Appendix Table 2.7. Neomycin resistance gene primers

Primer name	Sequence	Source
Neomycin primer F	CAA GAT GGA TTG CAC GCA G	Eurogentec
Neomycin primer R	CAT CCT GAT CGA CAA GAC	Eurogentec

Appendix Table 2.8. PCR conditions for amplification of neomycin resistance gene product

Step	Temperature (°C)	Time (min)	Cycles
Initial denaturation	94	5	1
Denaturation	94	0.5	35
Annealing	58	0.5	
Extension	72	0.5	
Final extension	72	7	1
Hold	16	Indefinitely	

Appendix 2.3 ZFN cleavage in endometrial cancer cell lines

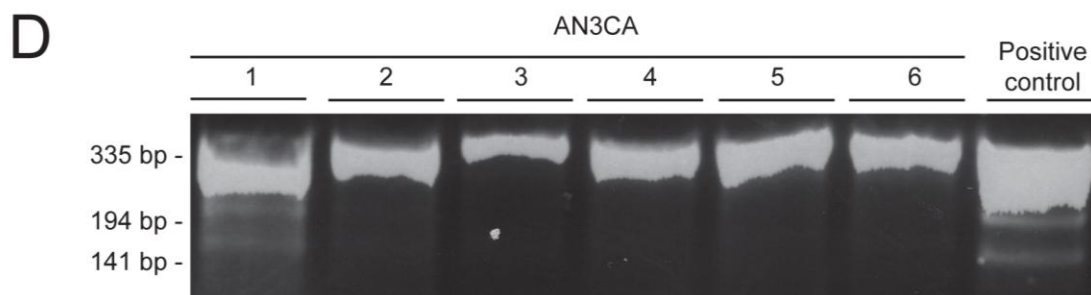
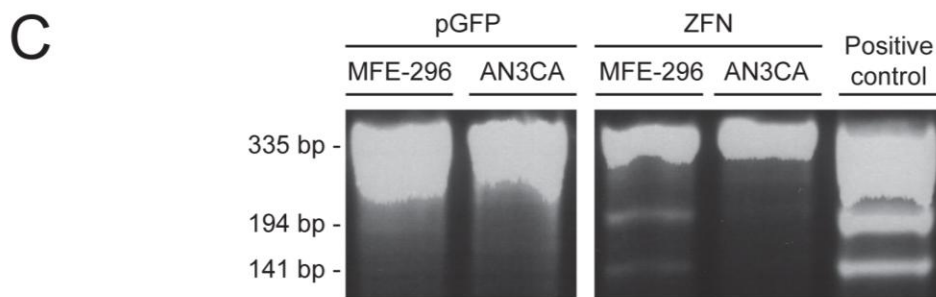
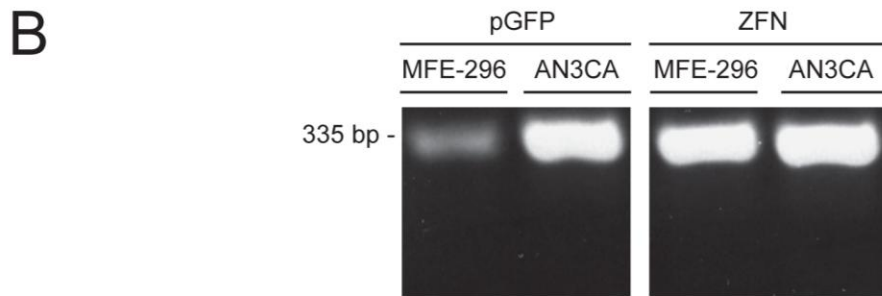
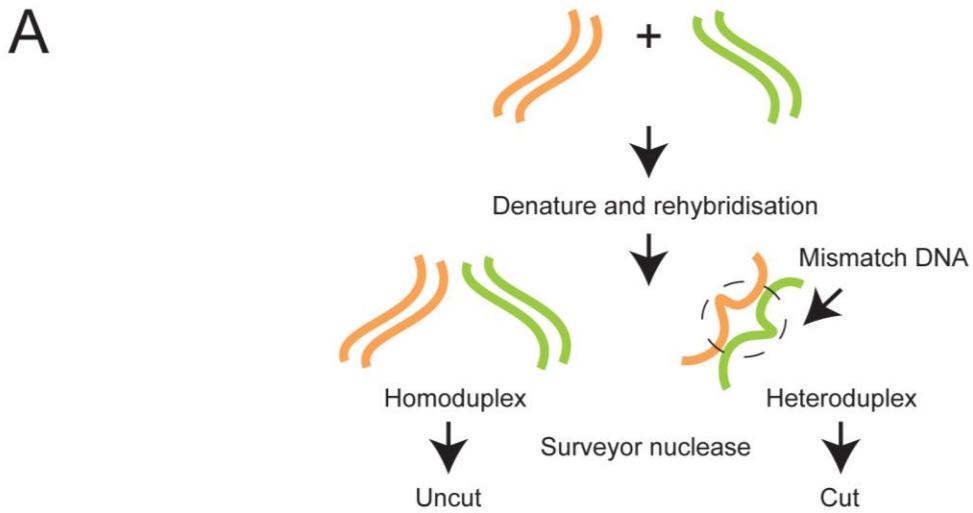
The specificity of the *FGFR2* targeted ZFN was assessed using the ZFN-site database (Cradick et al., 2011). This resource identifies any possible off target cleavage sites of a given ZFN. This algorithm did not identify any other perfect match than *FGFR2*. The other potential non-specific DNA binding regions were two intergenic regions of the genome, four non-coding regions (introns and promoters) and tetraspanin 11 (*TSPAN11*), a membrane scaffolding protein. All of the DNA regions identified only allow for a five nucleotide long spacer region, compared to the six nucleotides in the *FGFR2* site. This makes binding and subsequent cutting of the ZFN at these sites unlikely. All of these potential off target sites also had mismatches with the ZFN in the ZFN binding region, further reducing the likelihood of off target effects.

The efficiency of the ZFN activity in the endometrial cancer cell lines was determined using the surveyor nuclease assay (Appendix Figure 2.3). Cells were transfected using either the ZFN or pGFP as a control. Upon transfection of the ZFN into cells, a proportion of the DNA is cut at the target site. In the absence of a user introduced alternative repair construct, the cellular machinery resolves the double strand break, usually resulting in loss of a few base pairs. After transfection, gDNA was extracted and PCR performed, using primers to amplify the region surrounding the ZFN binding domain. This subsequently generated a combination of PCR products containing the uncut amplicon and the ZFN-cut DNA. A further round of PCR was performed on these PCR products, whereby the DNA was denatured and re-annealed, resulting in the formation of homoduplexes, where two strands of uncut or cut DNA re-annealed, and heteroduplexes, where one strand of each cut and uncut DNA annealed together (Appendix Figure 2.3 A, left and right respectively). In the case of the latter, a mismatch repair bubble is formed. The PCR products were treated with Cell, an endonuclease which cuts the mismatch repair bubble, resulting in two fragments of 194 base pairs (bp) and 141 bp. When resolved on a polyacrylamide gel, the homoduplexes run as a single 335 bp band. The presence of the two 194 bp and 141 bp bands on a gel were indicative of successful ZFN DNA

cleavage. The intensity of the three bands was proportional to the ZFN DNA cleavage efficiency.

Lipid-based transfection of the ZFN and subsequent incubation at 37°C for three days before gDNA extraction was unsuccessful, as indicated by a lack of 194 bp and 141 bp bands upon UV visualisation of the surveyor assay PCR products (Appendix Figure 2.3 B). The lipofection method was attempted again, this time followed by cold shock treatment of cells at 30°C. Transient incubation of ZFN transfected cells at this temperature has been shown to increase the genomic editing capabilities of ZFNs (Doyon et al., 2010). This resulted in successful transfection and subsequent DNA modification by the ZFN in MFE-296 cells (Appendix Figure 2.3 C).

However, lipid-based transfection was insufficient to introduce the ZFN into AN3CA cells. Because of this, nucleofection was attempted. The Lonza nucleofection optimisation kit was used, therefore a range of nucleofection solutions and Nucleofector programmes were utilised (Appendix Figure 2.3 D, 1-6). Nucleofection condition 1, followed by incubation of transfected cells at 30°C for three days, resulted in successful transfection of the ZFN (Appendix Figure 2.3 D).



Appendix Figure 2.3. Utilisation of the surveyor nuclease assay to assess the efficiency of ZFN genomic DNA editing.

(A) Schematic representation of the surveyor nuclease assay. Upon transfection of the ZFN into cells, a proportion of the DNA is cut at the target site. In the absence of a user introduced alternative repair construct, the cellular machinery resolves the double strand break, usually resulting in the loss of a few base pairs. PCR is performed to amplify the region around the ZFN target site, generating a combination of PCR products containing the uncut amplicon and the ZFN-cut DNA. A further round of PCR is performed to denature and re-anneal the DNA, resulting in formation of homoduplexes (left), whereby two strands of uncut DNA or cut DNA are annealed together, and heteroduplexes (right), where one cut and one uncut strand of DNA is re-annealed. In the case of the latter, a mismatch repair bubble is formed. This is cut upon introduction of the Cell endonuclease, resulting in generation of two fragments of 194 bp and 141 bp in size. When resolved on a polyacrylamide gel, the homoduplexes run as a single 335 bp band. The presence of the two 194 bp and 141 bp bands on a gel are indicative of successful ZFN DNA cleavage. The intensity of the three bands is proportional to the ZFN DNA cleavage efficiency. (B) Transfection of ZFN followed by the three days incubation at 37°C did not result in genomic modification by the ZFN as exhibited by only one 335 bp band on the gel. (C) Lipid-based transfection followed by incubation at 30°C for three days prior to gDNA extraction led to successful integration of the ZFN into the MFE-296 cell line and resulted in DNA modification, as indicated by the presence of 194 bp and 141 bp bands on the polyacrylamide gel. Lipofection of the ZFN mRNA followed by cold shock did was unsuccessful in the AN2CA cell line. (D) Nucleofection of ZFN mRNA was trialled on AN3CA cells as an alternative to lipofection. A nucleofection optimisation kit was used. 1-6 refers to sample number as detailed in the nucleofection optimisation kit; each sample used a different Nucleofector programme. Use of programme 1 followed by incubation at 30°C for three days resulted in successful transfection of the ZFN into the AN3CA cell line. PCR products from a successful transfection of the ZFN into MCF-7 cells was used as a positive control. Samples were resolved on 10% non-denaturing polyacrylamide gels.

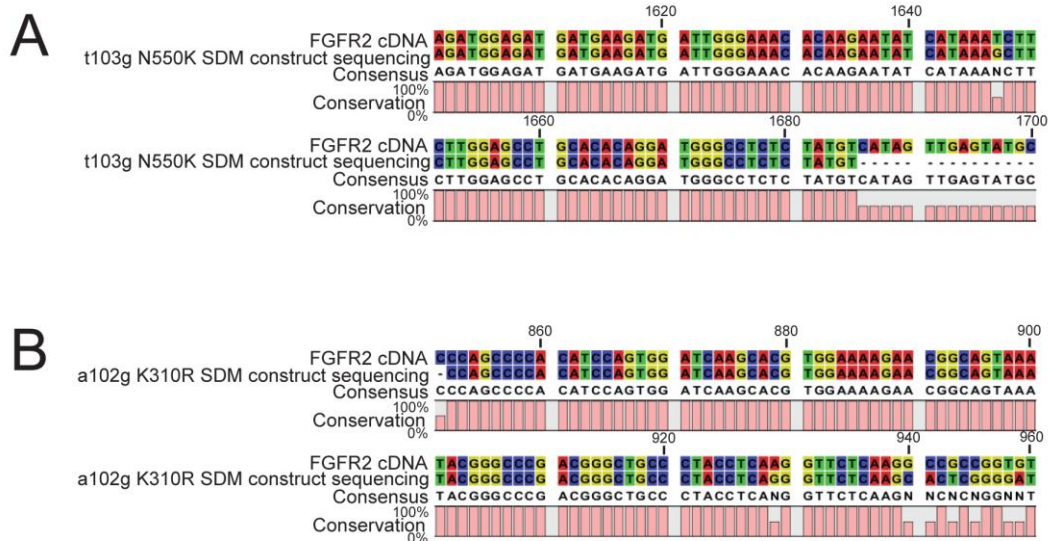
Appendix 2.4 Generation of FGFR2 mutant alternative repair templates

Upon ZFN transfection and subsequent introduction of a double strand break into the user-defined target site, HR machinery is directed to the ZFN cut site (Urnov et al., 2005). ZFN technology can be utilised to introduce a change in the genome at the specified locus by flooding the cells with an alternative repair construct alongside ZFN transfection (Appendix Figure 2.1 B). In this case, the alternative repair template can be used in the DNA repair process, replacing the sister chromatid routinely used in HR. The inclusion of 1 kb lengths of DNA, which are homologous to the 1 kb regions either side of the ZFN cut site, allows for the cellular machinery to use this construct in place of the sister chromatid. This results in a genomic change in the proportion of the cells which are cut by the ZFN and subsequently use the alternative repair template. Indeed, as the concentration of the alternative repair construct transfected into cells is increased, the DNA HR machinery is more likely to use this in place of the sister chromatid, therefore increasing the proportion of cells with altered gene expression.

As the ZFN used in this study cuts in intron 2 of *FGFR2*, an alternative repair construct consisting of wild type *FGFR2* cDNA from exon 3 onwards was designed, with the aim of converting the *FGFR2* mutation status of endometrial cancer cells from mutant to wild type. This cDNA was tagged with a GFP construct, for selection of transfected cells, as well as a polyA sequence. Inclusion of this polyA sequence ensured transcription ended at this point; therefore the endogenous gene downstream of intron 2 was not transcribed (Appendix Figure 2.1 B). A neomycin resistance cassette was added to the construct to act as an additional selectable marker. This box was flanked by loxP sites to enable removal of the cassette upon expression of Cre recombinase.

As well as reverting the mutation status of endometrial cancer cells back to the wild type version of *FGFR2*, we generated mutant versions of the construct for use in *FGFR2* wild type cells (Appendix Figure 2.4). Using SDM, two constructs were generated, each containing the two *FGFR2* mutations harboured in the endometrial

cancer cell lines under investigation: N550K and K310R. Cycle sequencing and subsequent analysis of the resulting data using CLC sequence Viewer of the constructs showed the SDM was successful (Appendix Figure 2.4).

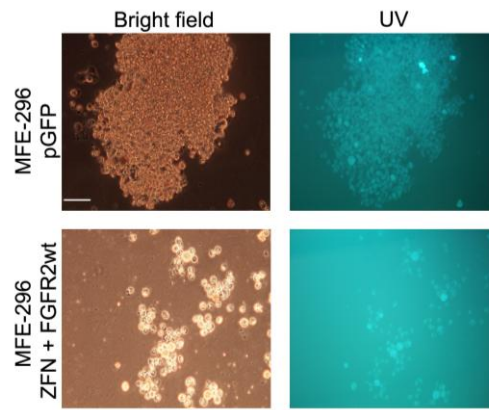


Appendix Figure 2.4. Sequence alignment of FGFR2 wild type and mutant constructs generated via SDM.

Using complimentary primers that contain the mutation of interest, PCR was performed to introduce the mutation and amplify the PCR product. DpnI endonuclease was then used to digest the methylated, wild type DNA, leaving the newly synthesised mutant DNA intact. The final product was cloned into competent bacteria to be re-circularised and amplified. Cycle sequencing on the resulting construct was performed and compared to wild type FGFR2 cDNA using CLC Sequence Viewer (v6). (A) The conversion of a thymine residue to guanine at FGFR2 cDNA position 1647 results in the N550K amino acid mutation. SDM performed on the *FGFR2* alternative repair construct was successful, as shown by the mismatch between wild type and SDM cDNA in the alignment. (B) Conversion of residue 929 from adenosine to guanine, resulting in the K310R mutation, in the *FGFR2* alternative repair construct was successful.

Appendix 2.5 Transfection and screening of MFE-296 cells following ZFN and FGFR2IIIb-GFP-neo construct transfection

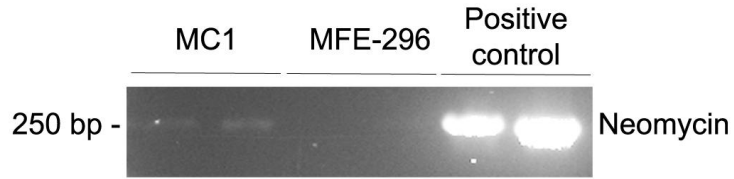
MFE-296 cells were transfected with the ZFN mRNA and simultaneously flooded with the FGFR2IIIb-GFP-neo alternative repair construct. An additional transfection was also performed using pGFP as a positive control. Cells were incubated at 30°C for three days, after which they were cultured at 37°C. From this point onwards, cells transfected with the FGFR2IIIb-GFP-neo construct were grown in medium supplemented with 100 ng/mL G418. Inspection under UV light after three days showed both positive GFP expression in polyclonal population of cells transfected with the pGFP alone as well as in ZFN and FGFR2IIIb-GFP-neo construct transfected cells (Appendix Figure 2.5). This was indicative of integration of the transfected plasmids into the cellular genome.



Appendix Figure 2.5. GFP expression in a polyclonal population of MFE-296 cells transfected with pGFP or ZFN in combination with the FGFR2IIIb-GFP-neo construct.

MFE-296 cells were transfected with pGFP or ZFN in combination with the FGFR2IIIb-GFP-neo construct via lipofection and were incubated at 30°C for three days, after which cells were returned to 37°C and cultured. FGFR2IIIb-GFP-neo transfected cells were grown in G418-supplemented medium. Cells were assessed for GFP expression using UV light after the initial three day cold shock treatment. Both the pGFP and ZFN/FGFR2IIIb-GFP-neo MFE-296 transfected cells showed a proportion of cells positive for GFP expression, indicative of plasmid uptake. Original magnification of images, 20X objective; bar, 50 μ m.

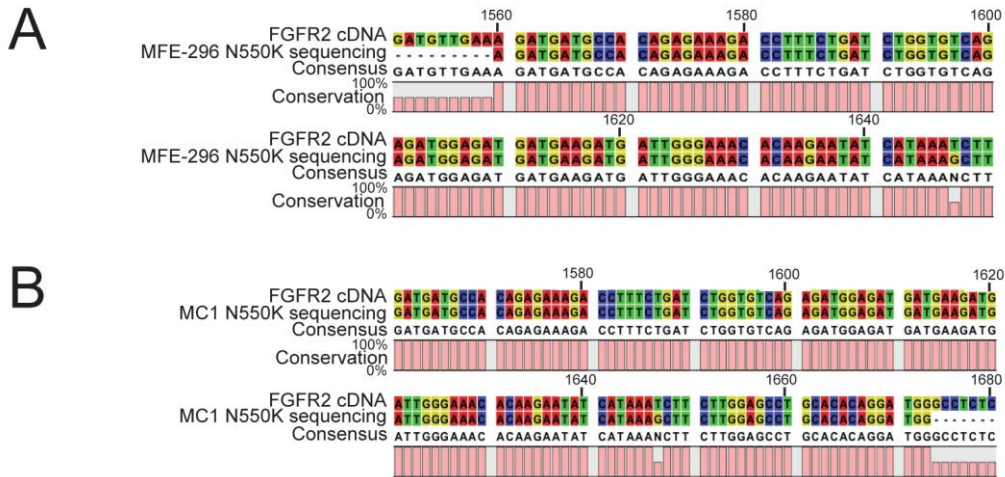
Upon reaching confluence, single cell cloning of the polyclonal population of the FGFR2IIIb-GFP-neo transfected cells was employed to generate a monoclonal cell line (Appendix Figure 2.2). One monoclonal population was established and labelled MC1. MC1 cells were cultured in G418-supplemented medium. PCR using primers designed to recognise the neomycin resistance cassette was subsequently performed on MC1 cells, as well as un-transfected MFE-296 cells and a neomycin plasmid as negative and positive controls, respectively (Appendix Figure 2.6). UV visualisation of the PCR products run on a polyacrylamide gel show the MC1 cell line was positive for neomycin, implying integration of the FGFR2IIIb-GFP-neo construct into the genome.



Appendix Figure 2.6. Neomycin gene amplification in MC1 cells after ZFN and FGFR2IIIb-GFP-neo transfection.

ZFN and FGFR2IIIb-GFP-neo transfected cells were subject to single cell cloning, resulting in establishment of a monoclonal cell line (MC1). The MC1 cell line was cultured and gDNA extracted for PCR with primers specific to the neomycin resistance cassette. MC1 cells expressed the neomycin resistance cassette. Samples were run in duplicate. Un-transfected MFE-296 cells and a neomycin-containing plasmid were used as negative and positive controls, respectively.

To definitively establish whether ZFN-mediated genome editing of the *FGFR2* locus was successful, cycle sequencing was employed to assess the N550K *FGFR2* mutation status (Appendix Figure 2.7). Both untransfected MFE-296 and MC1 cell lines were sequenced, using primers designed to amplify the region surrounding the N550K mutation site. This sequencing revealed the MC1 cell line was N550K mutant, indicating the *FGFR2*IIIb-GFP-neo construct had not been integrated into the genome of MC1 cells.



Appendix Figure 2.7. MC1 cells are N550K FGFR2 mutant.

Cycle sequencing of un-transfected MFE-296 and MC1 cells was performed to assess the N550K mutation status. (A) MFE-296 cells are N550K mutant, as shown by the T-G mismatch with wild type FGFR2 cDNA at position 1647. (B) MC1 cells are also N550K mutant. The MC1 cell line did not express the wild type FGFR2IIIb-GFP-neo construct.

Appendix 2.6 Summary of results

- The *FGFR2*-directed ZFN successfully cuts gDNA in the MFE-296 and AN3CA cell line
- Further work is required to increase transfection efficiency and establish a viable monoclonal cell line in an efficient manner

Appendix 2.7 Discussion

Targeted editing of a genomic locus using ZFN technology enables investigation of the functional significance of a plethora of genes and their mutations (Beerli and Barbas, 2002, Robbez-Masson et al., 2013). In this project, we aimed to utilise a custom made FGFR2-targeted ZFN to investigate the functional significance of FGFR2 mutations in endometrial cancer.

After optimisation of the transfection conditions, we were able to establish that the FGFR2 ZFN successfully introduced a double strand break in two endometrial cancer cell lines, MFE-296 and AN3CA. We proceeded to transfect MFE-296 cells with the ZFN in combination with an FGFR2IIIb-GFP-neo construct, aiming to revert the mutation status from mutant to wild type. Previous studies have speculated that FGFR2 mutations may drive the subset of endometrial cancers they are found in (Byron et al., 2013, Greulich and Pollock, 2011b, Pollock et al., 2007). As such, use of the FGFR2 ZFN is particularly interesting, as it offers a method of investigating the phenotypic consequences of FGFR2 mutations in endometrial cancer by expression of the wild type receptor under the control of the endogenous promoter, in the context of other mutations present in these cells. This therefore has the potential to answer the question of the nature of mutant FGFR2 as a driver in endometrial cancer.

Upon transfection of these cells with the construct, the polyclonal population was assessed for GFP expression by visualisation under UV light. A subset of cells was GFP positive, implying integration of the construct into the genome. To fully understand the consequences of the FGFR2 mutation reversion, single cell cloning was employed with the aim of establishing a monoclonal cell line. This would therefore remove the effects of mutant cells that may prevent the phenotypic consequences of the mutation status reversion being evident. It is also probable that the mutant cells would out-compete the FGFR2 wild type population, further increasing the need for establishment of a monoclonal cell line.

The single cell cloning technique employed has enjoyed success in some studies (Hombrink et al., 2015). However, the effectiveness of this technique is cell type specific. For example, cells which rely heavily on paracrine signalling do not survive well when cultured on their own. Also, monoclonal cell lines were identified by eye following daily inspection of the wells of a 96 well plate under a light microscope. This method has the potential for errors, whereby a polyclonal population may be incorrectly labelled monoclonal. Nevertheless, this method of selection was trialled in FGFR2IIIb-GFP-neo transfected MFE-296 cells and the MC1 monoclonal cell line generated.

Transfected cells were also grown in G418-supplemented medium as an additional selective marker. This neomycin resistance cassette included in the construct was also used as a PCR target; gDNA amplification was evident in MC1 cells. While this indicated that the FGFR2IIIb-GFP-neo construct had been taken up by the cells and integrated into the genome, cycle sequencing revealed the MC1 cells did in fact harbour the N550K FGFR2 mutation.

As PCR analysis indicated integration of the neomycin resistance cassette into the genome, it is possible that the MC1 cell line was not in fact a true monoclonal cell line. A mixed population would result in some neomycin expression but these cells would likely be out-competed by the mutant cells over further culture. Alternative methods, such as ring cloning (Mathupala and Sloan, 2009), could be employed in future attempts of FGFR2-targeted genome editing of endometrial cancer cells which may increase the effectiveness of this technique in yielding results. While MC1 cells were grown in G418-supplemented medium, it is possible a subpopulation of FGFR2 mutant MFE-296 cells in the polyclonal population acquired resistance to neomycin treatment and were therefore able to grow in the supplemented medium. In addition, while the chances are low, it is also possible that the construct was integrated into the genome via random insertion and was expressed at low levels under the control of a weak promoter (Phang et al., 2013).

This attempt at reversion of the FGFR2 mutation status of MFE-296 cells using ZFN technology was unsuccessful. However, the modifications of various elements of the procedure discussed could be employed to increase the chances of successfully integrating the FGFR2IIIb-GFP-neo construct into endometrial cancer cells. We have established the ability of the ZFN to cut in the AN3CA cells and so this cell line could also be utilised for investigation in the future.

Since purchasing the FGFR2 targeted ZFN, TALEN and CRISPR technology has been optimised and now represent a better alternative to ZFNs for genomic editing (Cerbini et al., 2015, Jiang et al., 2015, Kaulich et al., 2015, Matsubara et al., 2015). Use of these alternatives should be considered in future work.

During the course of this project, we have successfully generated N550K and K310R mutant FGFR2 constructs and so these could be used to investigate the importance of these mutations on cell transformation by transfection into an FGFR2 wild type cell line.

Appendix 3

International Journal of Biochemistry and Cell Biology review: FGFR signalling in women's cancers



Contents lists available at ScienceDirect

The International Journal of Biochemistry & Cell Biology

journal homepage: www.elsevier.com/locate/biociel

Signalling networks in focus

FGFR signalling in women's cancers

Abbie E. Fearon , Charlotte R. Gould, Richard P. Grose 

Centre for Tumour Biology, Barts Cancer Institute – A Cancer Research UK Centre of Excellence, Queen Mary University of London, John Vane Science Centre, Charterhouse Square, London EC1M 6BQ, United Kingdom

article info

Article history:

Received 23 August 2013
 Accepted 30 September 2013
 Available online xxx

Keywords:

Fibroblast growth factor (FGF)
 Fibroblast growth factor receptor (FGFR)
 Cancer
 Signalling
 Therapy

abstract

FGFs, in a complex with their receptors (FGFRs) and heparan sulfate (HS), are responsible for a range of cellular functions, from embryogenesis to metabolism. Both germ line and somatic FGFR mutations are known to play a role in a range of diseases, most notably craniosynostosis dysplasias, dwarfism and cancer. Because of the ability of FGFR signalling to induce cell proliferation, migration and survival, FGFRs are readily co-opted by cancer cells. Mutations in, and amplifications of, these receptors are found in a range of cancers with some of the most striking clinical findings relating to their contribution to pathogenesis and progression of female cancers. Here, we outline the molecular mechanisms of FGFR signalling and discuss the role of this pathway in women's cancers, focusing on breast, endometrial, ovarian and cervical carcinomas, and their associated preclinical and clinical data. We also address the rationale for therapeutic intervention and the need for FGFR-targeted therapy to selectively target cancer cells in view of the fundamental roles of FGF signalling in normal physiology.

© 2013 Elsevier Ltd. All rights reserved.

1. Introduction

Fibroblast growth factors (FGFs) are responsible for a plethora of cellular functions, from embryogenesis to metabolism (Belov and Mohammadi, 2013; Bottcher and Niehrs, 2005; Consortium, 2000; Dorey and Amaya, 2010; Dubrulle and Pourquie, 2004; Feldman et al., 1995; Ghabrial et al., 2003; Huang and Stern, 2005; Polanska et al., 2009; Sun et al., 1999). FGFs exert their cellular effects by interacting with FGF receptors (FGFRs) in a complex with heparan sulfate (HS) (Yayon et al., 1991). FGFRs, a class of receptor tyrosine kinase (RTK), dimerise and undergo transphosphorylation of the kinase domain upon ligand binding (Coughlin et al., 1988), leading to the recruitment of adaptor proteins and initiating downstream signalling (Fig. 1). Both germ line and somatic FGFR mutations are


known to play a role in a range of diseases, most notably craniosynostosis dysplasia, dwarfism and cancer (Naski et al., 1996; Wesche et al., 2011; Wilkie, 2005; Wilkie et al., 2002). Given the ability of the FGFR signalling pathway to facilitate cell survival and proliferation, it is readily co-opted by cancer cells. Mutations in, and amplifications of, FGFRs are found in a variety of cancers, notably bladder cancer, and are generally indicative of a more malignant phenotype (van Rhijn et al., 2002). The vast majority of these mutations are activating, resulting in increased proliferation, migration and angiogenesis.

Some of the most striking clinical findings regarding FGFRs relate to how these receptors are implicated in women's cancers. Here, we focus on breast, endometrial, ovarian and cervical carcinomas, presenting preclinical and clinical data outlining how altered FGFRs influence pathogenesis and prognosis. The molecular mechanisms of FGFR signalling are reviewed and discussed as the rationale for therapeutic intervention. We also explore the need for novel biomarkers and the way in which targeted therapy can be further tailored so as to selectively target cancer cells in view of the fundamental roles of FGF signalling in normal physiology.

2. FGFR signalling

The extended FGF family is composed of 22 members, varying in size from 17 to 34 kDa. All members share a conserved 120 amino acid sequence and show 16–65% sequence homology (Ornitz and Itoh, 2001). However, only eighteen FGFs signal via FGFR interactions (FGF1-10 and 16-23), thus many consider the FGF family to comprise only 18 members. Each ligand binds to FGFRs with

Abbreviations: FGF, fibroblast growth factor; FGFR, fibroblast growth factor receptor; HS, heparan sulfate; RTK, receptor tyrosine kinase; ER, oestrogen receptor; PR, progesterone receptor; IDC, invasive ductal carcinoma; FISH, fluorescence in situ hybridisation; TMA, tissue microarray; CISH, chromogenic in situ hybridisation; CLC, classic lobular carcinoma; DCIS, ductal carcinoma in situ; GWAS, Genome Wide Association Study; SNP, small nucleotides polymorphism; TIC, tumour initiating cell; IHC, immunohistochemistry; SC, Saethre Chotzen; EEC, endometrioid endometrial carcinoma; NEEC, non-endometrioid endometrial carcinoma; MSI, microsatellite instability; CCC, clear cell carcinoma; HPV, human papilloma virus; CIN, cervical intraepithelial neoplasia; VEGFR, vascular endothelial growth factor receptor; PDGFR, platelet-derived growth factor receptor; TKI, tyrosine kinase inhibitor; mAb, monoclonal antibody; AuNP, gold nanoparticle.

 Corresponding authors.

E-mail addresses: a.e.fearon@qmul.ac.uk (A.E. Fearon), r.p.grose@qmul.ac.uk (R.P. Grose).

1357-2725/\$ – see front matter © 2013 Elsevier Ltd. All rights reserved.
<http://dx.doi.org/10.1016/j.biociel.2013.09.017>

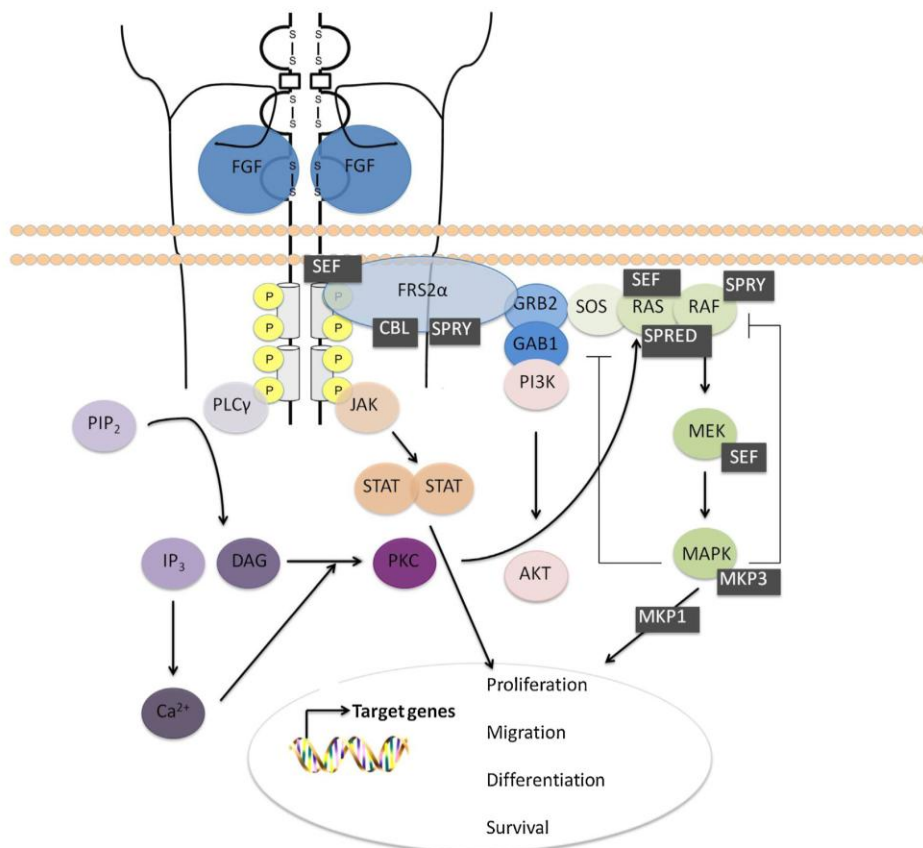


Fig. 1. FGF:FGFR induced downstream signalling. Ligand-receptor binding induces four signalling cascades: MAPK, PLC γ , PI3K/AKT and STAT. These pathways comprise a series of phosphorylation events, culminating in regulation of target genes, which dictate cellular processes, for example proliferation and migration. Negative regulators of the pathways are shown in grey boxes.

varying specificity; some are promiscuous, for example FGF1, and bind to multiple receptors, while others, like FGF7, bind only to one receptor isoform (Ornitz et al., 1996).

There are seven signalling receptors, encoded by four FGFR genes, FGFR1-4 (Johnson and Williams, 1993). Alternative splicing of exons 8 and 9, encoding IgIII of FGFR1-3, results in translation of two distinct isoforms capable of signal transduction (Fig. 2). These isoforms are termed IIIb and IIIc, depending on which exons are spliced out and alternative splicing of this region is responsible for ligand binding specificity. A third isoform exists for FGFR1 and 2, termed IIIa. This variant results in a truncated, secreted protein, which is unable to transduce a signal and may have an auto-inhibitory role in FGF signalling, possibly by sequestering ligands (Wheldon et al., 2011). FGFR4 is distinct in that it has only one isoform, homologous to the IIIc variant of FGFR1-3 (Vainikka et al., 1992). Receptor expression is generally cell type specific, for example IIIb and IIIc isoforms of FGFR1 and 2 are expressed in epithelial and mesenchymal cells, respectively (Orr-Urtreger et al., 1993; Yan et al., 1993). However, as shall be discussed later, this cell type specificity can change when FGFRs are associated with cancer.

Upon ligand binding and receptor dimerisation, the tyrosine kinase domains undergo reciprocal phosphorylation. Phosphotyrosine residues are then able to act as docking sites for intracellular proteins, leading to activation of signalling cascades (Furdui et al.,

2006; Mohammadi et al., 1992, 1996) (Fig. 1). From this, four key signalling pathways can be activated: MAPK, PI3K/AKT, PLC γ and STAT (Furdui et al., 2006). Activation of the MAPK pathway leads to translocation of transcription factors to the nucleus, e.g. c-MYC, influencing the cell cycle, while PI3K/AKT signalling results in initiation of anti-apoptotic signalling, as well as cell growth and proliferation (Gotoh, 2008). Enhanced MAPK signalling occurs via PLC γ activation. Furthermore, STAT-dimers translocate to the nucleus to activate or repress gene transcription (Darnell, 1997).

Regulation of FGF signalling is critical to ensure a balanced response to receptor stimulation. This occurs largely through negative feedback mechanisms, including receptor internalisation via ubiquitination (Wang et al., 2002) and induction of negative regulators, for example SPRY, SPRED 1 and 2 and SEF (Hacohen et al., 1998; Kovalenko et al., 2003; Torii et al., 2004; Wakioka et al., 2001; Yang et al., 2003) (Fig. 1). A further level of control exists in the form of receptor autoinhibition (Plotnikov et al., 1999; Schlessinger et al., 2000; Stauber et al., 2000). Electrostatic bonding between the acid box and the HS-binding site induces a closed, autoinhibited conformation (Kalinina et al., 2012; Olsen et al., 2004) (Fig. 2). This mechanism of autoinhibition supports FGF binding specificity of receptors; only specific ligands with high affinity for the receptors will overcome the inhibition and bind to the receptor.

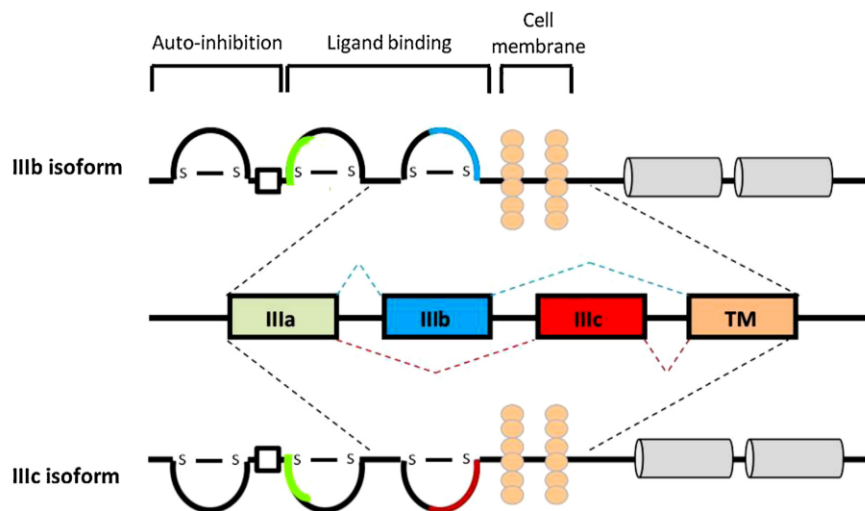


Fig. 2. FGFR structure and control of ligand specificity and receptor autoinhibition via alternative splicing. Each receptor monomer is comprised of an extracellular domain including three Ig loops named Igl, IglI and IglII (also referred to as D1, D2 and D3 respectively), an acid box in the Igl–IglI linker region (represented by a white box), a transmembrane domain and an intracellular split kinase domain. Disulfide bonds are present in each Ig loop. Igl and the acid box are involved in auto-inhibition of the receptor while IglI and IglII are involved in ligand binding. The heparan sulfate binding site is indicated in green. Ligand binding specificity is generated by alternative splicing of the IglII domain. The first half of IglII is encoded by an invariant exon (IIIa), which is spliced to either exon IIIb or IIIc (represented in blue and red respectively), both of which splice to the exon that encodes the transmembrane domain (TM) region. An additional alternative splicing event can occur, leading to the deletion of exons coding for Igl and/or the acid box/linker region. This leads to loss of receptor autoinhibition (Kalinina et al., 2012).

3. FGFR signalling in cancer

3.1. Breast cancer

Breast cancer is the most common female cancer worldwide, comprising 16% of all cancers affecting women, and the most prevalent of all cancers in the UK, despite its rare incidence amongst men (Jemal et al., 2011). Approximately 70% of all deaths from breast cancer occur in developing countries. Incidence of female breast cancer in both developing and developed countries continues to rise (Jemal et al., 2011).

Breast cancer collectively describes neoplasms arising from epithelial cells lining the mammary ducts and lobules, termed ductal carcinoma or lobular carcinoma, respectively. There are three major molecular subtypes of this cancer: 1. Luminal, which accounts for 70% of invasive breast cancer and is oestrogen receptor (ER)/progesterone receptor (PR) positive; 2. HER2, which is ER/PR negative and represents approximately 15% of invasive breast cancer; 3. Basal, accounting for approximately 15% of invasive breast cancer, is ER/PR/HER2 negative (referred to as triple negative) and is associated with BRCA1 dysfunction (Schnitt, 2010). These subtypes can be further classified according to additional molecular alterations (Perou et al., 2000).

A variety of FGFR abnormalities have been identified in breast cancer. FGFR1 amplification is found in 8–15% of all breast carcinomas (Andre et al., 2009; Elbauomy Elsheikh et al., 2007; Reis-Filho et al., 2006) and 16–27% of luminal type B breast cancer (Turner et al., 2010b). In addition, both cytoplasmic and nuclear expression of FGFR2 are elevated in invasive ductal carcinoma (IDC) compared to normal tissue, predicting worse outcomes in terms of overall survival and disease free survival (Sun et al., 2012). Thus, FGFR amplification and mutations in breast cancer are associated with poor prognosis (Elbauomy Elsheikh et al., 2007; Reis-Filho et al., 2006; Turner et al., 2010b).

Amplifications of the chromosomal region harbouring FGFR1 (8p11–12) have been detected in 10–15% of breast cancers

(Jacquemier et al., 1994). High resolution comparative genome hybridisation analysis delineated the structure of the 8p11–12 amplicon and revealed a complex region, comprising four separate cores, each of which could be independently amplified (Gelsi-Boyer et al., 2005). FGFR1 maps to the proximal A2 core, amplification of which correlates robustly to increased FGFR1 expression in both cell lines and tumour samples. A2 core amplification determined by fluorescence in situ hybridisation (FISH) on breast cancer tissue microarrays (TMAs) was associated with reduced metastasis-free survival (Gelsi-Boyer et al., 2005).

The effects of FGFR1 amplification on prognosis were confirmed by chromogenic in situ hybridisation (CISH) analysis of TMAs and subsequent correlation of FGFR1 overexpression to survival statistics (Elbauomy Elsheikh et al., 2007). FGFR1 overexpression was shown to be an independent predictor of poor overall survival in ER positive tumours (Elbauomy Elsheikh et al., 2007). These FGFR1 amplified ER positive tumours are commonly endocrine therapy resistant, a result of increased ligand dependent and independent signalling, with enhanced MAPK activation promoting upregulation of the gene encoding cyclin D1 (CCND1) (Turner et al., 2010b).

FGFR1 amplification and overexpression has been detected in 43% of classic lobular carcinomas (CLCs), a subtype accounting for 5–15% of invasive breast cancers (Reis-Filho et al., 2006). In vitro analysis has shown abrogation of FGFR1 signalling reduces cell viability, suggesting that FGFR1 amplification leads to oncogene addiction (Reis-Filho et al., 2006). In vivo inducible FGFR1 models have shown invasive cell behaviours are attributed to the induction of matrix metalloproteinase 3 (MMP-3) and subsequent cleavage of E-cadherin (Xian et al., 2009). These observations suggest that down regulation of E-cadherin, typical of CLC, may be mediated by FGFR1 overexpression. CLCs are often devoid of the necessary biomarkers for current chemotherapy and targeted regimes. As FGFR1 amplification occurs in a subset of these tumours, FGFR1 overexpression may represent a new definitive identifier for treatment (Brunello et al., 2012).

The role of FGFR1 amplification in ductal carcinoma in situ (DCIS) progression has also been considered (Jang et al., 2012). Using FISH probes on TMAs, FGFR1 amplification was shown to be more frequent in invasive breast cancer than DCIS, and these amplifications were more commonly located in the invasive components of tumours (Jang et al., 2012). As such, it is proposed that activation of FGFR1 may drive the transition of localised to intrusive disease (Jang et al., 2012).

Genome wide association studies (GWAS), powered to elucidate susceptibility loci in breast cancer, identified small nucleotide polymorphisms (SNPs) in intron 2 of FGFR2 with the strongest significant breast cancer association (Easton et al., 2007; Hunter et al., 2007). Similar findings have been replicated in several populations including those of Ashkenazi, Chinese and Siberian descent (Boyarskikh et al., 2009; Chen et al., 2012; Long et al., 2010; Raskin et al., 2008; Rinella et al., 2013). The minor, disease causing, allele only marginally increases the likelihood of developing breast cancer but is, however, present at high frequency (0.4) in the population and, as such, is likely to influence risk in many individuals (Fanale et al., 2012; Huijts et al., 2011). Interestingly, the minor allele seems to exhibit a strong association with the development of ER positive breast cancer, with little effect on ER negative disease (Fanale et al., 2012).

Further studies have elucidated which polymorphisms within the linkage disequilibrium block are functionally important (Meyer et al., 2008). The SNPs rs2981582 and rs7895676 lie close to binding sites for two transcription factors, Oct1 and Runx2; these binding sites have been shown to be occupied in vivo (Meyer et al., 2008). This suggests the presence of these SNPs leads to increased FGFR2 expression as a result of Oct1 and Runx2 binding to their respective sites on the DNA, thereby driving transcription. The ER binding site often clusters with Oct1 and so, in conjunction with Oct1/Runx2, ER may act to upregulate FGFR2 gene expression, potentially augmenting FGFR signalling and hence breast cancer predisposition (Meyer et al., 2008). Indeed, the expression of FGFR2 is significantly higher in breast tumour samples homozygous for the minor allele (Meyer et al., 2008).

A recent study proposed a novel mechanism of FGFR2 mediated cancer growth in which its expression is upregulated in tumour initiating cells (TICs) (Kim et al., 2013). TICs, a minority subpopulation with an enriched ability to proliferate, are resistant to conventional cancer treatment and able to re-initiate tumour growth, generating similar heterogeneity to that of the original tumour (Zhou et al., 2009). As such they are considered to be the source of metastasis and cause of patient relapse (Zhou et al., 2009). Isolation of TICs from mammary tumours of transgenic mice demonstrated upregulation and expression of FGFR2 compared to lineage-restricted non-TICs. Targeting FGFR2 with shRNA inhibited cell proliferation and anchorage independent growth in vitro and was associated with attenuated MAPK signalling (Sun et al., 2012). Suppression of tumour cell growth was shown in mice injected with shFGFR2-transduced tumour cells; tumour growth was restored by rescue treatment with shRNA-resistant FGFR2 (Sun et al., 2012). Further analysis showed that the fraction of TICs in shFGFR2-transduced tumours had diminished, whilst the opposite was true of the non-TIC subpopulation (Kim et al., 2013). Furthermore, inhibition of FGFR2 using TKI258 (dovitinib) reduced the TIC population and led to suppression of mammary tumour growth (Kim et al., 2013). In patient tumour samples, FGFR2 enriched TICs were shown to be capable of initiating tumour growth in immunocompromised mice (Kim et al., 2013).

It is proposed that FGFR2 signalling may form a vital part of the TIC niche environment, facilitating the persistence of TICs. Inhibition of this growth factor survival pathway may block the self-renewing capacity of TICs, suppressing not only the subpopulation of cells controlling proliferation but also the reservoir for

disease recurrence. However, one should bear in mind the debate regarding the validity of biomarkers used to identify TIC subpopulations and, additionally, whether or not these biomarkers differ between breast cancer subtypes. As the tumour microenvironment plays a critical role in the regulation and maintenance of TICs, for example via growth signalling pathways, it too should be considered in design of targeted therapy.

FGFR2 amplification and enrichment also occurs in approximately 4% of triple negative breast tumours (Turner et al., 2010a). In two triple negative FGFR2 amplified cell lines, constitutive signalling appeared to confer a survival advantage over non-amplified cell lines (Turner et al., 2010a). The role of FGFR2 in these cancers has been confirmed by in vitro studies using a FGFR-targeted small molecule tyrosine kinase inhibitor (PD173074) or RNAi treatment, which reduced cell survival, blocked PI3K/AKT signalling and induced apoptosis (Turner et al., 2010a).

The presence of elevated levels of FGFR3 in malignant breast tissues has been demonstrated in a number of studies (Glenisson et al., 2012), and a significant correlation between elevated levels and poor survival has been made (Kuroso et al., 2010). In a recent study, where 58 breast tumours were assessed for FGFR3 expression, almost all expressed moderate or high levels, with approximately 30% exhibiting nuclear localisation of the receptor (Cerliani et al., 2012). The function of nuclear FGFR3 is uncertain, but proteolytically cleaved FGFR3 has been reported to traffic to the nucleus (Degnin et al., 2011) and nuclear FGFR1 has recently been reported to drive invasive behaviour of breast cancer cells (Chioni and Grose, 2012).

FGFR3 immunohistochemistry (IHC) on TMAs from patients treated with tamoxifen showed differential expression of FGFR3 between patients who responded well to treatment and those that did not with significantly stronger staining in endocrine therapy resistant tumours (Tomlinson et al., 2011). Furthermore, after cloning an inducible FGFR3 construct into MCF-7 cells, resistance to tamoxifen was demonstrated. The mechanism of resistance and increased cell viability is thought to be due to enhanced activation of PLC γ signalling (Tomlinson et al., 2011).

Germline mutations in FGFR3 are known to cause developmental abnormalities, such as the craniosynostosis syndrome Saethre Chotzen (SC) (Bergman et al., 2009). Intriguingly, a higher incidence of breast cancer has been reported in individuals with this syndrome. A missense germline SNP in exon 7 of FGFR3 in one individual with SC who developed breast cancer was demonstrated via DNA sequencing (Sahlin et al., 2009). The gain of function polymorphism occurs in the region of the extracellular ligand-binding domain, conferring enhanced FGF binding (Sahlin et al., 2009). These observations suggest FGFR3 may be a breast cancer susceptibility gene. It is of note, however, that although the majority of germline mutations in FGFR2 and FGFR3 responsible for developmental disorders are the same as somatic mutations causing cancer, patients suffering from these developmental defects do not have a higher incidence of cancer, with the exception of SC. However, the reduced life span of these individuals means the effects of these mutations on cancer incidence are difficult to study.

A germ-line SNP in FGFR4 results in a missense polymorphism occurring at codon 388, where glycine is substituted for arginine (G388R) (Bange et al., 2002). The sequence variant is common, occurring in approximately half of the population (Bange et al., 2002). On analysing the impact of the polymorphism in patients with breast cancer, both homo- and heterozygous carriers were shown to be overrepresented in a subset of patients with lymph node positive breast cancer; the presence of G388R was linked to early disease relapse (Bange et al., 2002). In vitro molecular studies were unable to attribute the more aggressive disease to increased kinase activity of the mutant receptor, but instead showed increased motility and invasion of MDA-MD-134 cells

transfected with G388R compared to the wild type receptor (Bange et al., 2002). A further study investigated this by introducing the equivalent G388R allele into the murine FGFR4 gene, and crossed these knock in mice with TGF α transgenic mice in order to examine the SNP's effect (Seitzer et al., 2010). Validation of the oncogenic potential of the SNP was shown as mammary tumours were larger, in comparison to mice with wild-type SNP, and the development of pulmonary metastases occurred at an earlier stage (Seitzer et al., 2010).

The relationship between the missense mutations in FGFR4 and poorer prognoses in node positive breast cancer has also been demonstrated. In vitro studies in doxorubicin treated apoptotic-resistant cancer cell clones (MDA-MB-134) showed upregulation of FGFR4, as well as increased downstream signalling and upregulation of the pro-survival protein Bcl-xL (Thussbas et al., 2006). Knockdown of FGFR4 increased sensitivity to chemotherapeutic agents and attenuated growth. Therefore, resistance to adjuvant systemic therapy has been attributed to this mutation (Thussbas et al., 2006).

The wild type form of FGFR4 has been proposed to have important tumour suppressive functions via the regulation of genes controlling invasion and motility, e.g. MMP1, suggesting loss of the wild type receptor would adversely influence disease progression (Stadler et al., 2006). Indeed, it has been shown that DNA methylation, exclusive to neoplastic tissue, in breast tumour samples preferentially silenced the wild type allele rather than the polymorphic allele (Zhu et al., 2010). In metastatic lesions, the wild type allele was exclusively methylated, further corroborating the evidence of the mutant allele's tumour enhancing properties (Zhu et al., 2010).

3.2. Endometrial cancer

Endometrial cancer is the most common gynaecological cancer in western countries and the fourth most common cancer in women (Byron et al., 2012; Jemal et al., 2011; Pollock et al., 2007). Most patients are peri- and post-menopausal, however, approximately 25% of endometrial cancer cases occur in pre-menopausal women, particularly in association with hyperestrogenism. Endometrial cancer is split predominately into two types; type I endometrioid endometrial carcinoma (EEC) and type II non-endometrioid endometrial carcinoma (NEEC). Approximately 80% of endometrial carcinomas are EEC, the oestrogen-related, low grade form of the disease, and are usually associated with endometrial hyperplasia, resulting in excessive proliferation of the endometrium due to high oestrogen levels. Both EEC and NEEC present with distinct genetic alterations, however, a minority of cases present with mixed features (Yeramiyan et al., 2013).

Early stage EEC is confined to the endometrium, the lining of the uterus, with little or no invasion into the stroma. Stage I EEC has a survival rate of approximately 80%, decreasing to 15% for stage IV patients. EEC can be treated with surgery, where a full hysterectomy is the most common procedure. Radiotherapy and/or chemotherapy are also used, as well as hormonal therapy, however, alternative treatments to surgery are desirable (Obel et al., 2006; Temkin and Fleming, 2009).

A range of genetic abnormalities are found in endometrial cancer. Microsatellite instability (MSI) is present in 25–30% of endometrial tumours and is most common in EEC (Catasus et al., 1998; Duggan et al., 1994; Risinger et al., 1993). PTEN alterations are also found in 37–61% of EEC and lead to deregulation of the PI3K/AKT pathway (Yeramiyan et al., 2013). Other common mutations include those in PIK3CA and K-RAS (Byron et al., 2008; Yeramiyan et al., 2013). FGFR2 mutations are associated with endometrial cancer and are found in approximately 10–16% of cases (Byron et al., 2008, 2012) (Fig. 3). It is postulated that these FGFR2

mutations could be the driving force in endometrial cancer tumorigenesis.

FGFR2 mutations in endometrial cancer have been identified in a number of independent studies (Byron et al., 2012; Dutt et al., 2008; Pollock et al., 2007). Interestingly, the majority of somatic FGFR2 mutations in endometrial cancer are identical to germline mutations in developmental disorders, for example craniosynostosis syndromes (Pollock et al., 2007). The S252W mutation, the most common FGFR2 mutation in endometrial cancer, occurs in the linker region between the IgII and IgIII loops, the area responsible for providing key contacts with the ligand. This mutation increases the binding affinity of the receptor for a range of FGFs while also leading to violation of ligand specificity of the receptor isoforms (Greulich and Pollock, 2011). It is also possible that this mutation leads to the modified receptor remaining on the cell surface for an extended period of time, rather than undergoing rapid recycling like its wild type counterpart (Ahmed et al., 2008). Mutations in the kinase domain, such as N550K, lead to constitutive activation of the receptor, whilst others, including S373C and Y376C, result in gain of a cysteine residue, allowing formation of intermolecular disulfide bonds (Wilkie et al., 2002). All of these mutations then affect downstream signalling mechanisms, leading to increased cell proliferation and migration, as well as premature differentiation. Initial studies have shown inhibition of FGFR2 using PD173074 or TKI258, as well as receptor knockdown, in endometrial cancer cells leads to a reduction in cell survival (Byron et al., 2008; Dutt et al., 2008; Konecny et al., 2013).

In endometrial cancer, mutations in FGFR2 are mutually exclusive with those in KRAS. However, 77% of endometrial tumours with mutations in FGFR2 also harbour PTEN mutations (Byron et al., 2008). It is therefore possible that the aberrant signalling of the mTOR pathway, in conjunction with the FGFR2 pathway, drives tumorigenesis in this subset of endometrial tumours. This has been demonstrated recently, where treatment of endometrial cancer cells with ponatinib, an FGFR inhibitor, and ridaforolimus, an mTOR inhibitor, resulted in a combined antiproliferative effect (Gozgit et al., 2013). Strong synergy between the two drugs was shown, defined by CI values <0.1, resulting in G₁ arrest of endometrial cancer cells. The ability of FGFR inhibition to synergise with chemotherapeutic drugs has also been shown in endometrial cancer (Byron et al., 2012). Both of these studies support the prospect of dual drug therapy in treatment of this cancer (Gozgit et al., 2013).

3.3. Ovarian cancer

Of all gynaecological cancers, ovarian cancer has the poorest prognosis, despite advances in treatment over the last 40 years (Cole et al., 2010; Colombo and Cavallaro, 2011; McGuire and Markman, 2003). This is attributed to the fact that early symptoms of pain and pressure in the abdomen are vague and thus misdiagnosed as less serious conditions (Colombo and Cavallaro, 2011; Lister-Sharp et al., 2000). It is also an aggressive disease, spreading rapidly from the ovary to other organs of the peritoneal cavity (Colombo and Cavallaro, 2011). Therefore, most cases are diagnosed at a late stage, making treatment difficult.

Ovarian carcinomas are known to have complex cytogenetic abnormalities and are often aneuploid (Brooks et al., 2012). The most common histological type is epithelial ovarian cancer. Other types include endometrioid and clear cell carcinomas (McGuire and Markman, 2003). Interestingly, the prevalence of ovarian cancer in women with endometriosis is higher than that of sporadic ovarian cancer (Taniguchi et al., 2013). It is therefore thought that ovarian cancer can arise from endometriosis precursor lesions, as well as from de novo carcinogenesis (Taniguchi et al., 2013). Current first line of treatment is surgery, ranging from removal of the affected ovary to a full hysterectomy with bilateral salpingo-oophorectomy

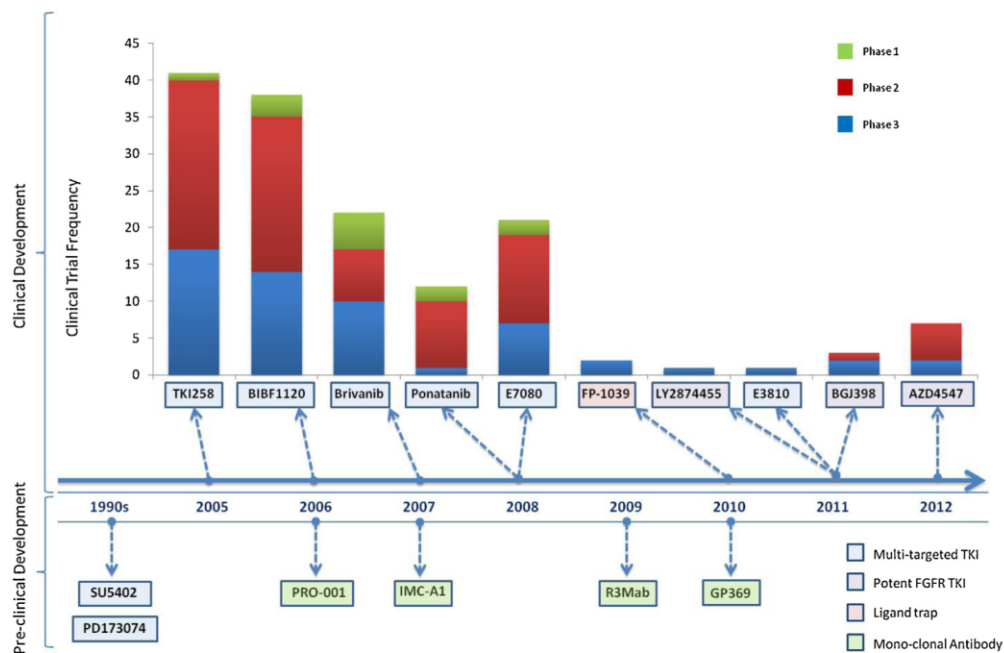


Fig. 3. Timeline of development of FGFR targeted therapies. The timeline illustrates the development of FGFR targeted agents. Agents that have progressed into clinical trials are shown above the arrow. The frequencies of clinical trials that are currently underway for each agent, and what phase these trials are in, are also shown. Agents used only in vitro or in vivo in animal studies are shown below the arrow. Each agent is colour coded according to its mechanism of action/drug class.

Data sourced from www.clinicaltrials.gov and (Bai et al., 2010; Bello et al., 2011; Cai et al., 2008; Gavine et al., 2012; Guagnano et al., 2012; Matsui et al., 2008; Mohammadi et al., 1997, 1998; Noronha et al., 2008; Qing et al., 2009; Sun et al., 2007; Trudel et al., 2005, 2006; Walker and Padhiar, 2010; Zhao et al., 2011).

(McGuire and Markman, 2003). Chemotherapy is also used, however, alternatives to both of these options, for example targeted drug therapy, are a much more attractive option.

Approximately 5–7% of ovarian tumours exhibit FGFR1 amplification (Gorringe et al., 2007; Theillet et al., 1993). FGFR1 copy number gains have been reported in both endometrioid and serous tumours (Gorringe et al., 2007). This study suggested potential for FGFR1 as a novel therapeutic target in ovarian cancer. However, another study demonstrated that reducing FGFR1 levels in epithelial ovarian cancer cells had a cell line specific effect, where in one cell line it increased proliferation 2–3-fold (Cole et al., 2010). This apparent inhibitory effect of FGFR1 on proliferation in epithelial ovarian cancer cells needs more investigation.

The interplay between adhesion molecules and FGFRs is also important in epithelial ovarian cancer, particularly in metastasis (Zecchini et al., 2011). The majority of epithelial ovarian cancer metastases arise from cancer cells that are shed from the ovary and adhere to the surface of abdominal organs and the peritoneal cavity (Bast et al., 2009). Therefore, it is important to understand how adhesion molecules contribute to, and are regulated in, ovarian cancer metastasis. One such mechanism involves the adhesion molecule NCAM, a cell surface glycoprotein (Zecchini et al., 2011). NCAM is not expressed in normal ovarian surface epithelium but is upregulated in tumour tissue (Cho et al., 2006; Zecchini et al., 2011). The contribution of NCAM to epithelial ovarian cancer cell migration relies on its interaction with FGFRs; inhibition of either molecule leads to a decreased ability to migrate (Zecchini et al., 2011). NCAM only interacts with FGFRs, not their ligands, thus FGF2-FGFR1 and NCAM-FGFR1 interactions have different roles; FGF2 induces proliferation, while NCAM provokes migration. Their functions are independent of each other and neither induce both

responses (Zecchini et al., 2011). NCAM is known to interact with FGFR2 and FGFR4 (Cavallaro et al., 2001; Christensen et al., 2006) so blockade of NCAM-FGFR interactions may prove beneficial in prevention of epithelial ovarian cancer metastasis.

Activating mutations in FGFR2 are rare in ovarian cancer (Byron et al., 2010). However, although the incidence is low, those mutations identified in a small subset of ovarian tumours are identical to those found in endometrial cancer, suggesting FGFR2 activating mutations may contribute to ovarian cancer tumorigenesis (Byron et al., 2010).

Clear cell carcinoma (CCC), an epithelial ovarian cancer subtype, is resistant to conventional chemotherapies (Takano et al., 2006; Taniguchi et al., 2013). FGFR2 upregulation has recently been observed in CCC; it is postulated this upregulation occurs during malignant transformation of epithelial cells from endometriomas (Taniguchi et al., 2013). The FGFR signalling cascade may also be implicated in CCC tumorigenesis as a result of enhanced FGF1 levels, independent of FGFR upregulation (Taniguchi et al., 2013). This concurs with earlier data that uncontrolled FGFR signalling can occur in epithelial ovarian cancer via uncontrolled stimulation from its classical ligands (De Cecco et al., 2004; Steele et al., 2001; Valve et al., 2000).

Interestingly, although a class switch from the IIIb to IIIc isoform of FGFR2 and FGFR3 is common in epithelial cells in a variety of carcinomas, the IIIb isoform is thought to predominate in epithelial ovarian cancer cells (Steele et al., 2001, 2006; Taniguchi et al., 2013). In vitro studies have shown FGFR2 and 3 isoform class switch and expression of FGF3 and 19 are associated with cellular transformation (Cole et al., 2010). As well as FGF3, these cells also express high levels of FGF7, the specific ligand of FGFR2-IIIb, and so an autocrine signalling loop is established. Inhibition of FGFR2, FGF3 or FGF7

significantly impacts on cell proliferation, confirming the importance of this signalling circuit in epithelial ovarian cancer cells. This inhibition also significantly reduces the IC50 of cisplatin, showing blockage of FGFR signalling enhances sensitivity of these cells to platinum-based chemotherapeutics. This was also shown *in vivo*, where dual treatment slowed tumour growth as well as augmenting cisplatin cytotoxic effects. Thus, targeting FGFR signalling in ovarian tumours may be an effective therapeutic option.

3.4. Cervical cancer

Cervical cancer is the second most common female cancer and accounts for the most deaths from gynaecological carcinomas worldwide (Brockbank et al., 2013). Chronic infection by oncogenic human papilloma virus (HPV) is the most common risk factor for development of this disease, with chemotherapy and radiation of the primary tumour and pelvic lymph nodes the treatment of choice for cervical cancer (Brockbank et al., 2013). Although inactivation of p53 and RB are the most common mutations in cancer of the cervix (Wingo et al., 2009), recent work has begun to shed light on the possible involvement of aberrant FGFR signalling in this disease.

Approximately 86% of cervical carcinomas express both FGFR2-IIIb and FGFR2-IIIc; this expression is correlated with progression of cervical intraepithelial neoplasia (CIN) (Kawase et al., 2010; Kurban et al., 2004). Expression of both FGFR2 isoforms in cervical tumours opposes that of normal tissue, where FGFR2-IIIb and -IIIc are both expressed weakly on the surface of squamous epithelial cells and the basal layer of the epithelium, respectively (Kawase et al., 2010; Kurban et al., 2004). The FGFR2 ligands, FGF1 and 2, are also expressed in cervical carcinoma (Fujimoto et al., 1997; Hagemann et al., 2007; Kurban et al., 2004). Indeed, it has been suggested that FGF2 levels in patient serum may prove useful in detection of primary tumours and recurrence, as well as monitoring cancer therapy (Chopra et al., 1998; Fujimoto et al., 1997). *In vitro* investigations showed the pattern of FGFR2-IIIc expression in CIN was similar to that of the proliferation marker Ki67, indicative of the relationship between FGFR2-IIIc and cell growth in these cells (Kawase et al., 2010). Furthermore, gene expression analysis of cancer tissues found FGFR2-IIIc to be strongly expressed in areas of cancer cell infiltration. This study showed strong FGFR2 expression in cervical cancer and its correlation with cell growth, but further work is necessary to confirm the importance of FGFR signalling in this cancer.

4. FGFRs as therapeutic targets

Over the past decade, the dysregulation of FGFR signalling has become increasingly implicated in the hallmarks of cancer and pre-clinical evidence has validated the pathway as a critical driver in oncogenesis. Abrogating FGFR signalling can be achieved by targeting different elements of the pathway; FGF ligands, the receptors themselves and downstream signalling outcomes. However, translating this into a therapy for patients has proven difficult; even specific FGFR inhibitors have off-target effects. Further research is required to establish a mechanism of effective targeting of FGFR signalling in cancer without impeding its essential functions in healthy cells. Here, we discuss the current therapeutic options.

4.1. Tyrosine kinase inhibitors (TKIs)

The first FGFR inhibitors to be developed were ATP-competitive small molecules (Fig. 3) (Liang et al., 2012). As other RTKs, for example VEGFR and PDGFR, share similar structural homology to FGFRs, these inhibitors also act on their conserved ATP-binding region, acting as multi-targeted tyrosine kinase inhibitors (TKIs) (Turner and Grose, 2010). Mechanisms of resistance to a single

therapy in cancer cells include the acquisition of mutations or activation of compensatory signalling cascades (Jain and Turner, 2012). Therefore, blocking more than one signalling pathway can be beneficial in treatment. Indeed, these multi-targeted TKIs, including TKI258, are the most clinically advanced in FGFR-targeted treatment to date (Trudel et al., 2005) (Figs. 3 and 4). The lack of specificity, however, can lead to VEGFR/PDGFR-dependent side effects (e.g. hypertension), essentially limiting the doses required to sufficiently abrogate FGFR signalling (Robinson et al., 2010).

The most advanced multi-targeted FGFR inhibitor in clinical development is TKI258 (Fig. 3). A phase II trial investigating the safety and efficacy of dovitinib in the setting of metastatic BC recently ended prematurely due to lack of improved overall response rate. However, it was noted that the subset of patients with FGFR1 amplification had higher response rates to TKI258 than those without amplification (Brooks et al., 2012). FGFR inhibitors with higher potencies are likely to be of greater benefit. Another multi-targeted agent, ponatinib, examined in cell lines and xenograft models, exhibited consistently elevated inhibitory actions over TKI258, cediranib, BIBF1120 and brivanib, in terms of both signalling and impairment of cell growth (Gozgit et al., 2012). Importantly, the doses required to achieve the effective FGFR blockade are achievable in humans (Cortes et al., 2012). These non-specific inhibitors in clinical development do not emulate the definitive tumour impeding results of FGFR blockade that have been achieved *in vitro* and *in vivo* using siRNA knockdown or specific FGFR inhibitors, e.g. PD173074. Unfortunately, early potent pan-FGFR inhibitors like PD173074 have significant toxicity issues rendering them analytical tools only (Knights and Cook, 2010). The complete blockade of FGFR signalling results in hyperphosphataemia and tissue calcification as a result of impaired FGF23 signalling (Brown et al., 2005; Wohrle et al., 2011).

Recently, a number of second generation FGFR specific inhibitors have emerged, for example AZD4547 (Gavine et al., 2012). AZD4547, a pyrazoloamide derivative which also targets the ATP-binding site of the receptor, predominantly inhibits FGFR1-3, exhibiting increased potency and selectivity of FGFRs over other kinases (Gavine et al., 2012). AZD4547 strongly inhibits growth in a number of cell lines that have FGFR deregulated signalling including the breast cancer cell line SUM-52-PE, in which increased apoptosis was additionally observed (Gavine et al., 2012). Importantly, as opposed to multi-targeted inhibitors, VEGFR induced blood pressure elevation does not occur (Gavine et al., 2012). Despite its recent discovery, there are already a number of clinical trials using AZD4547 in cancer, including those investigating use in breast and ovarian cancers (Fig. 4).

4.2. Monoclonal antibodies

Another attractive option for selective FGFR inhibition is the use of monoclonal antibodies (mAb). The success of this type of approach in targeting overexpressed receptor tyrosine kinases is exemplified by the success of trastuzumab targeting HER2/neu, approved for metastatic breast cancer in 1998 (Piccart-Gebhart et al., 2005). There have been fewer attempts at antibody design than TKIs, due to their cost relative to small molecule counterparts. However, mAbs offer some significant advantages over TKIs, including their specificity due to their targeting to a particular receptor splice variant. This circumvents certain toxicity issues that arise upon pan-FGFR inhibition and the ability to recruit cytotoxic immune cells to the tumour site, enhancing the anti-tumour response (Sun et al., 2007). The development of a mAb targeting FGFR1-IIIc had to be halted after trials resulted in rapid weight loss in rodents and monkeys (Sun et al., 2007). The anorexigenic effect was due to the accumulation of mAb in the hypothalamus, blocking an essential regulatory feeding circuit (Sun et al., 2007). More

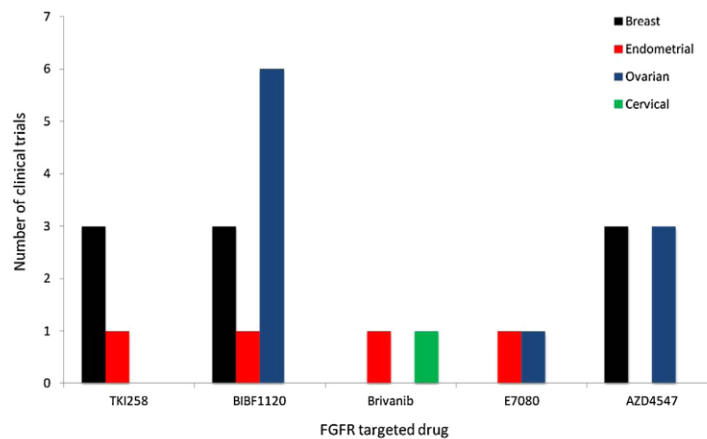


Fig. 4. Number of clinical trials using FGFR targeted drugs in women's cancers. A number of clinical trials are currently underway using FGFR targeted inhibitors in female cancers. The number of phase II and III trials in breast, endometrial, ovarian and cervical cancers are shown.

Data sourced from www.clinicaltrials.gov.

promising antibodies include GP369 directed against FGFR2-IIIb, which exhibited specific and potent inhibition of FGFR2 signalling in amplified cells lines, leading to tumour stasis both in vitro and in vivo in cell line derived xenografts (Bai et al., 2010). Two monoclonal antibodies against FGFR3 have been generated, each with tumour stabilising properties; however both remain in preclinical studies (Qing et al., 2009; Trudel et al., 2006). Although further work on these mAbs is necessary, their development remains an exciting area of FGFR-targeted therapeutics.

4.3. Ligand capture

Attempts to develop an agent capable of exclusively inhibiting mitogenic FGF ligands whilst sparing hormonal FGFs, and therefore preventing impairment of phosphate metabolism, produced FP-10392, a fusion protein comprising the extracellular domain of FGFR1-IIIc and the constant region of IgG1 (Harding et al., 2013). This construct, currently in phase II trials in endometrial cancer, halted tumour growth in xenografts of FGFR1 amplified lung cancer cell lines, but did not result in tumour regression (Harding et al., 2013). This could be due to continual FGFR signalling via mutated receptors exhibiting either constitutive activation or enhanced FGF binding affinity.

4.4. Novel approaches in targeted therapy

A novel and exciting discovery in the field of nanotechnology is the use of drug conjugated gold nanoparticles (AuNP) (Jain et al., 2012). The concept comprises that the drug and delivery vehicle will localise and accumulate at sites of cells overexpressing receptor, i.e. the tumour target tissue. The application of an appropriate wavelength of light will induce AuNP resonance sufficient to cause photothermal tumour specific destruction (Jain et al., 2012; Song et al., 2013). Using the universal FGF1 ligand as a starting point, a highly stable variant conjugated to AuNP was engineered (Szlachcic et al., 2012). In vitro, FGF1-AuNPs were endocytosed exclusively by cells stably transfected with FGFR1 and, when targeted with near infrared radiation (NIR), cytotoxic effects were seen; cells devoid of FGFR expression were not affected (Szlachcic et al., 2012). This study indicates that AuNP can be delivered precisely to FGFR overexpressing cells via FGF mediated delivery, followed by site directed cell destruction induced by NIR. Whether this approach will be

useful in clinical practice remains to be established. Further studies in xenograft models are anticipated.

4.5. Challenges of therapeutic resistance

The efficacy of many molecularly targeted agents is often compromised by de novo or acquired therapeutic resistance. Because of this, we should assume that in trials a proportion of patients we predict to respond will not and a proportion of those who initially respond will develop resistance. Acquired resistance may arise due to development of receptor activating mutations, reliance upon another signalling pathway to maintain cell growth, or upregulation of efflux proteins which effectively pump drugs out of cells before they can perform their cytotoxic roles (Patel et al., 2013). To overcome compensatory signalling mechanisms, for example, dual drug treatment should be considered. Indeed, combination treatment of FGFR inhibitors with mTOR inhibition has proven effective in vitro in BC and EC (Gozgit et al., 2013; Issa et al., 2013).

5. Concluding remarks

FGFR signalling is necessary for a variety of cellular functions in normal physiology. However, due to their promotion of cell growth and survival, FGFRs are commonly mutated or amplified in a range of pathologies, including cancers. Although further investigation into the role of this signalling cascade is necessary in some female cancers, its predominance in, for example, breast cancer is well established. This has led to clinical trials of FGFR inhibitors as a treatment option. Recent data suggest dual therapy, targeting FGFR signalling alongside other cascades or in combination with chemotherapy, may be particularly beneficial in, for example, endometrial cancer. The range of drugs available to target FGFR signalling still require more investigation but the possibilities of potential FGFR inhibition are an exciting field of cancer therapeutics.

References

- Ahmed Z, Schuller AC, Suhling K, Tregidgo C, Ladbury JE. Extracellular point mutations in FGFR2 elicit unexpected changes in intracellular signalling. *Biochem J* 2008;413:37–49.
- Andre F, Job B, Dessen P, Tordai A, Michiels S, Liedtke C, et al. Molecular characterization of breast cancer with high-resolution oligonucleotide comparative genomic hybridization array. *Clin Cancer Res* 2009;15:441–51.

- Bai A, Meetze K, Vo NY, Kollipara S, Mazza EK, Winston WM, et al. GP369, an FGFR2-IIIb-specific antibody, exhibits potent antitumor activity against human cancers driven by activated FGFR2 signaling. *Cancer Res* 2010;70:7630–9.
- Bange J, Prechtl D, Cheburkin Y, Specht K, Harbeck N, Schmitt M, et al. Cancer progression and tumor cell motility are associated with the FGFR4 Arg(388) allele. *Cancer Res* 2002;62:840–7.
- Bast RCJ, Hennessey B, Mills GB. The biology of ovarian cancer: new opportunities for translation; 2009.
- Bello E, Colella G, Scarlato V, Oliva P, Berndt A, Valbusa G, et al. E-3810 is a potent dual inhibitor of VEGFR and FGFR that exerts antitumor activity in multiple preclinical models. *Cancer Res* 2011;71:1396–405.
- Belov AA, Mohammadi M. Molecular mechanisms of fibroblast growth factor signaling in physiology and pathology. *Cold Spring Harb Perspect Biol* 2013, <http://dx.doi.org/10.1101/cshperspect.a015958>, LID – a015958 [pii].
- Bergman A, Sahlin P, Emanuelsson M, Caren H, Tarnow P, Martinsson T, et al. Germine mutation screening of the Saethre-Chotzen-associated genes TWIST1 and FGFR3 in families with BRCA1/2-negative breast cancer. *Scand J Plast Reconstr Surg Hand Surg* 2009;43:251–5.
- Bottcher RT, Niehrs C. Fibroblast growth factor signaling during early vertebrate development. *Endocr Rev* 2005;26:63–77.
- Boyarskikh UA, Zarubina NA, Biltueva JA, Sinkina TV, Voronina EN, Lazarev AF, et al. Association of FGFR2 gene polymorphisms with the risk of breast cancer in population of West Siberia. *Eur J Hum Genet* 2009;17:1688–91.
- Brockbank E, Kokka F, Bryant A, Pomel C, Reynolds K. Pre-treatment surgical para-aortic lymph node assessment in locally advanced cervical cancer. *Cochrane Database Syst Rev* 2013;3:CD008217.
- Brooks AN, Kilgour E, Smith PD. Molecular pathways: fibroblast growth factor signaling: a new therapeutic opportunity in cancer. *Clin Cancer Res* 2012;18:1855–62.
- Brown AP, Courtney CL, King LM, Groom SC, Graziano MJ. Cartilage dysplasia and tissue mineralization in the rat following administration of a FGF receptor tyrosine kinase inhibitor. *Toxicol Pathol* 2005;33:449–55.
- Brunello E, Brunelli M, Bogina G, Calio A, Manfrin E, Nottegar A, et al. FGFR-1 amplification in metastatic lymph-nodal and haematogenous lobular breast carcinoma. *J Exp Clin Cancer Res* 2012;31:103.
- Byron SA, Gartside MG, Wellens CL, Goodfellow PJ, Birrer MJ, Campbell IG, et al. FGFR2 mutations are rare across histologic subtypes of ovarian cancer. *Gynecol Oncol* 2010;117:125–9.
- Byron SA, Gartside MG, Wellens CL, Mallon MA, Keenan JB, Powell MA, et al. Inhibition of activated fibroblast growth factor receptor 2 in endometrial cancer cells induces cell death despite PTEN abrogation. *Cancer Res* 2008;68:6902–7.
- Byron SA, Loch DC, Pollock PM. Fibroblast growth factor receptor inhibition synergizes with Paclitaxel and Doxorubicin in endometrial cancer cells. *Int J Gynaecol Cancer* 2012;22:1517–26.
- Cai ZW, Zhang Y, Borzilleri RM, Qian L, Barbosa S, Wei D, et al. Discovery of brivanib alaninate ((S)-(R)-1-(4-(4-fluoro-2-methyl-1H-indol-5-yloxy)-5-methylpyrrolo[2,1-f][1,2,4] triazin-6-yloxy)propan-2-yl)2-aminopropanoate), a novel prodrug of dual vascular endothelial growth factor receptor-2 and fibroblast growth factor receptor-1 kinase inhibitor (BMS-540215); 2008.
- Catusus L, Matias-Guiu X, Machin P, Munoz J, Prat J. BAX somatic frameshift mutations in endometrioid adenocarcinomas of the endometrium: evidence for a tumor progression role in endometrial carcinomas with microsatellite instability. *Lab Invest* 1998;78:1439–44.
- Cavallaro U, Niedermeyer J, Fuxa M, Christofori G. N-CAM modulates tumour-cell adhesion to matrix by inducing FGF-receptor signalling. *Nat Cell Biol* 2001;3:650–7.
- Cerliani JP, Vanzulli SI, Pinero CP, Bottino MC, Soares A, Nunez M, et al. Associated expressions of FGFR-2 and FGFR-3: from mouse mammary gland physiology to human breast cancer. *Breast Cancer Res Treat* 2012;133:997–1008.
- Chen F, Lv M, Xue Y, Zhou J, Hu F, Chen X, et al. Genetic variants of fibroblast growth factor receptor 2 (FGFR2) are associated with breast cancer risk in Chinese women of the Han nationality. *Immunogenetics* 2012;64:71–6.
- Chioni AM, Grose R. FGFR1 cleavage and nuclear translocation regulates breast cancer cell behavior. *J Cell Biol* 2012;197:801–17.
- Cho EY, Choi Y, Chae SW, Sohn JH, Ahn GH. Immunohistochemical study of the expression of adhesion molecules in ovarian serous neoplasms. *Pathol Int* 2006;56:62–70.
- Chopra V, Dinh TV, Hannigan EV. Circulating serum levels of cytokines and angiogenic factors in patients with cervical cancer. *Cancer Invest* 1998;16:152–9.
- Christensen C, Lauridsen JB, Berezin V, Bock E, Kiselyov VV. The neural cell adhesion molecule binds to fibroblast growth factor receptor 2. *FEBS Lett* 2006;580:3386–90.
- Cole C, Lau S, Backen A, Clamp A, Rushton G, Dive C, et al. Inhibition of FGFR2 and FGFR1 increases cisplatin sensitivity in ovarian cancer. *Cancer Biol Ther* 2010;10:495–504.
- Colombo N, Cavallaro U. The interplay between NCAM and FGFR signalling underlies ovarian cancer progression. *Ebcancermedscience* 2011;5:226.
- Consortium. Autosomal dominant hypophosphataemic rickets is associated with mutations in FGF23. *Nat Genet* 2000;26:345–8.
- Cortes JE, Kantarjian H, Shah NP, Bixby D, Mauro MJ, Flinn I, et al. Ponatinib in refractory Philadelphia chromosome-positive leukemias. *N Engl J Med* 2012;367:2075–88.
- Coughlin SR, Barr PJ, Cousens LS, Fretto LJ, Williams LT. Acidic and basic fibroblast growth factors stimulate tyrosine kinase activity in vivo. *J Biol Chem* 1988;263:988–93.
- Darnell JE Jr. STATs and gene regulation. *Science* 1997;277:1630–5.
- De Cecco L, Marchionni L, Gariboldi M, Reid JF, Lagonigro MS, Caramuta S, et al. Gene expression profiling of advanced ovarian cancer: characterization of a molecular signature involving fibroblast growth factor 2. *Oncogene* 2004;23:8171–83.
- Degnin CR, Laederich MB, Horton WA. Ligand activation leads to regulated intramembrane proteolysis of fibroblast growth factor receptor 3. *Mol Biol Cell* 2011;22:3861–73.
- Dorey K, Amaya E. FGF signalling: diverse roles during early vertebrate embryogenesis. *Development* 2010;137:3731–42.
- Dubrule J, Pourquie O. fgf8 mRNA decay establishes a gradient that couples axial elongation to patterning in the vertebrate embryo. *Nature* 2004;427:419–22.
- Duggan BD, Felix JC, Muderspach LI, Tourgeman D, Zheng J, Shibata D. Microsatellite instability in sporadic endometrial carcinoma. *J Natl Cancer Inst* 1994;86:1216–21.
- Dutt A, Salvesen HB, Chen TH, Ramos AH, Onofrio RC, Hatton C, et al. Drug-sensitive FGFR2 mutations in endometrial carcinoma. *Proc Natl Acad Sci USA* 2008;105:8713–7.
- Easton DF, Pooley KA, Dunning AM, Pharoah PD, Thompson D, Ballinger DG, et al. Genome-wide association study identifies novel breast cancer susceptibility loci. *Nature* 2007;447:1087–93.
- Elbaoumy Elsheikh S, Green AR, Lambros MB, Turner NC, Grainge MJ, Powe D, et al. FGFR1 amplification in breast carcinomas: a chromogenic in situ hybridisation analysis. *Breast Cancer Res* 2007;9:R23.
- Fanale D, Amodeo V, Corsini LR, Rizzo S, Bazan V, Russo A. Breast cancer genome-wide association studies: there is strength in numbers. *Oncogene* 2012;31:2121–8.
- Feldman B, Poueymirou W, Papaioannou VE, DeChiara TM, Goldfarb M. Requirement of FGF-4 for postimplantation mouse development. *Science* 1995;267:246–9.
- Fujimoto J, Ichigo S, Hori M, Hirose R, Sakaguchi H, Tamaya T. Expression of basic fibroblast growth factor and its mRNA in advanced uterine cervical cancers. *Cancer Lett* 1997;111:21–6.
- Furdulj CM, Lew ED, Schlessinger J, Anderson KS. Autophosphorylation of FGFR1 kinase is mediated by a sequential and precisely ordered reaction. *Mol Cell* 2006;21:711–7.
- Gavine PR, Mooney L, Kilgour E, Thomas AP, Al-Kadhimi K, Beck S, et al. AZD4547: an orally bioavailable, potent, and selective inhibitor of the fibroblast growth factor receptor tyrosine kinase family. *Cancer Res* 2012;72:2045–56.
- Gelsi-Boyer V, Orsetti B, Cervera N, Finetti P, Sircoulomb F, Rouge C, et al. Comprehensive profiling of 8p11-12 amplification in breast cancer. *Mol Cancer Res* 2005;3:655–67.
- Ghabrial A, Luschig S, Metzstein MM, Krasnow MA. Branching morphogenesis of the Drosophila tracheal system. *Annu Rev Cell Dev Biol* 2003;19:623–47.
- Glenisson M, Vacher S, Callens C, Susini A, Cizeron-Clairac G, Le Scodan R, et al. Identification of new candidate therapeutic target genes in triple-negative breast cancer. *Genes Cancer* 2012;3:63–70.
- Gorringer KL, Jacobs S, Thompson ER, Sridhar A, Qiu W, Choong DY, et al. High-resolution single nucleotide polymorphism array analysis of epithelial ovarian cancer reveals numerous microdeletions and amplifications. *Clin Cancer Res* 2007;13:4731–9.
- Gotoh N. Regulation of growth factor signaling by FRS2 family docking/scaffold adaptor proteins. *Cancer Sci* 2008;99:1319–25.
- Gozgit JM, Squillace RM, Wongchenko MJ, Miller D, Wardwell S, Moheemad Q, et al. Combined targeting of FGFR2 and mTOR by ponatinib and ridaforolimus results in synergistic antitumor activity in FGFR2 mutant endometrial cancer models. *Cancer Chemother Pharmacol* 2013;71:1315–23.
- Gozgit JM, Wong MJ, Moran L, Wardwell S, Moheemad QK, Narasimhan NI, et al. Ponatinib (AP24534), a multitargeted pan-FGFR inhibitor with activity in multiple FGFR-amplified or mutated cancer models. *Mol Cancer Ther* 2012;11:690–9.
- Greulich H, Pollock PM. Targeting mutant fibroblast growth factor receptors in cancer. *Trends Mol Med* 2011;17:283–92.
- Guagnano V, Kauffmann A, Wohrle S, Stamm C, Ito M, Barys L, et al. FGFR genetic alterations predict for sensitivity to NVP-BGJ398, a selective pan-FGFR inhibitor. *Cancer Discov* 2012;2:1118–33.
- Hacohen N, Kramer S, Sutherland D, Hiroimi Y, Krasnow MA. sprouty encodes a novel antagonist of FGF signaling that patterns apical branching of the Drosophila airways. *Cell* 1998;92:253–63.
- Hagemann T, Bozanovic T, Hooper S, Ljubic A, Slettenaar VI, Wilson JL, et al. Molecular profiling of cervical cancer progression. *Br J Cancer* 2007;96:321–8.
- Harding TC, Long L, Palencia S, Zhang H, Sadra A, Hestir K, et al. Blockade of non-hormonal fibroblast growth factors by FP-1039 inhibits growth of multiple types of cancer. *Sci Transl Med* 2013;5:178ra39.
- Huang P, Stern MJ. FGF signaling in flies and worms: more and more relevant to vertebrate biology. *Cytokine Growth Factor Rev* 2005;16:151–8.
- Huijts PE, van Dongen M, de Goeij MC, van Moolenbroek AJ, Blanken F, Vreeswijk MP, et al. Allele-specific regulation of FGFR2 expression is cell type-dependent and may increase breast cancer risk through a paracrine stimulus involving FGF10. *Breast Cancer Res* 2011;13:R72.
- Hunter DJ, Kraft P, Jacobs KB, Cox DG, Yeager M, Hankinson SE, et al. A genome-wide association study identifies alleles in FGFR2 associated with risk of sporadic postmenopausal breast cancer. *Nat Genet* 2013;39:870–4.
- Issa A, Gill JW, Heideman MR, Sahin O, Wiemann S, Dey JH, et al. Combinatorial targeting of FGF and ErbB receptors blocks growth and metastatic spread of breast cancer models. *Breast Cancer Res* 2013;15:R8.
- Jacquemier J, Adelaide J, Parc P, Penault-Llorca F, Planche J, deLapeyriere O, et al. Expression of the FGFR1 gene in human breast-carcinoma cells. *Int J Cancer* 1994;59:373–8.

- Jain S, Hirst DG, O'Sullivan JM. Gold nanoparticles as novel agents for cancer therapy. *Br J Radiol* 2012;85:101–13.
- Jain VK, Turner NC. Challenges and opportunities in the targeting of fibroblast growth factor receptors in breast cancer. *Breast Cancer Res* 2012;14:208.
- Jang MH, Kim EJ, Choi Y, Lee HE, Kim YJ, Kim JH, et al. FGFR1 is amplified during the progression of in situ to invasive breast carcinoma. *Breast Cancer Res* 2012;14:R115.
- Jemal A, Bray F, Center MM, Ferlay J, Ward E, Forman D. Global cancer statistics. *CA Cancer J Clin* 2011;61:69–90.
- Johnson DE, Williams LT. Structural and functional diversity in the FGF receptor multigene family. *Adv Cancer Res* 1993;60:1–41.
- Kalinina J, Dutta K, Ilghari D, Beenken A, Goetz R, Eliseenkova AV, et al. The alternatively spliced acid box region plays a key role in FGF receptor autoinhibition. *Structure* 2012;20:77–88.
- Kawase R, Ishiwata T, Matsuda Y, Onda M, Kudo M, Takeshita T, et al. Expression of fibroblast growth factor receptor 2 IIIc in human uterine cervical intraepithelial neoplasia and cervical cancer. *Int J Oncol* 2010;36:331–40.
- Kim SW, Dubrowska A, Salamone RJ, Walker JR, Grandinetti KB, Bonamy GM, et al. FGFR2 promotes breast tumorigenicity through maintenance of breast tumor-initiating cells. *PLoS One* 2013;8:e51671.
- Knights V, Cook SJ. De-regulated FGF receptors as therapeutic targets in cancer. *Pharmacol Ther* 2010;125:105–17.
- Konecny GE, Kolarova T, O'Brien NA, Winterhoff B, Yang G, Qi J, et al. Activity of the fibroblast growth factor receptor inhibitors dovitinib (TKI258) and NVP-BGJ398 in human endometrial cancer cells. *Mol Cancer Ther* 2013;12:632–42.
- Kovalenko D, Yang X, Nadeau RJ, Harkins LK, Friesel R. Sef inhibits fibroblast growth factor signaling by inhibiting FGFR1 tyrosine phosphorylation and subsequent ERK activation. *J Biol Chem* 2003;278:14087–91.
- Kurban G, Ishiwata T, Kudo M, Yokoyama M, Sugisaki Y, Naito Z. Expression of keratinocyte growth factor receptor (KGF/FGFR2 IIIb) in human uterine cervical cancer. *Oncol Rep* 2004;11:987–91.
- Kuroso K, Imai Y, Kobayashi M, Yanagimoto K, Suzuki T, Kojima M, et al. Immunohistochemical detection of fibroblast growth factor receptor 3 in human breast cancer: correlation with clinicopathological/molecular parameters and prognosis. *Pathobiology* 2010;77:231–40.
- Liang G, Liu Z, Wu J, Cai Y, Li X. Anticancer molecules targeting fibroblast growth factor receptors. *Trends Pharmacol Sci* 2012;33:531–41.
- Lister-Sharp D, McDonagh MS, Khan KS, Kleijnen J. A rapid and systematic review of the effectiveness and cost-effectiveness of the taxanes used in the treatment of advanced breast and ovarian cancer. *Health Technol Assess* 2000;4:1–113.
- Long J, Shu XO, Cai Q, Gao YT, Zheng Y, Li G, et al. Evaluation of breast cancer susceptibility loci in Chinese women. *Cancer Epidemiol Biomarkers Prev* 2010;19:2357–65.
- Matsui J, Yamamoto Y, Funahashi Y, Tsuruoka A, Watanabe T, Wakabayashi T, et al. E7080, a novel inhibitor that targets multiple kinases, has potent antitumor activities against stem cell factor producing human small cell lung cancer H146, based on angiogenesis inhibition. *Int J Cancer* 2008;122:664–71.
- McGuire WP, Markman M. Primary ovarian cancer chemotherapy: current standards of care. *Br J Cancer* 2003;89(Suppl 3):S3–8.
- Meyer KB, Maia AT, O'Reilly M, Teschendorff AE, Chin SF, Caldas C, et al. Allele-specific up-regulation of FGFR2 increases susceptibility to breast cancer. *PLoS Biol* 2008;6:e108.
- Mohammadi M, Dionne CA, Li W, Li N, Spivak T, Honegger AM, et al. Point mutation in FGF receptor eliminates phosphatidylinositol hydrolysis without affecting mitogenesis. *Nature* 1992;358:681–4.
- Mohammadi M, Froum S, Hamby JM, Schroeder MC, Panek RL, Lu GH, et al. Crystal structure of an angiogenesis inhibitor bound to the FGF receptor tyrosine kinase domain. *Embo J* 1998;17:5896–904.
- Mohammadi M, McMahon G, Sun L, Tang C, Hirth P, Yeh BK, et al. Structures of the tyrosine kinase domain of fibroblast growth factor receptor in complex with inhibitors. *Science* 1997;276:955–60.
- Mohammadi M, Schlessinger J, Hubbard SR. Structure of the FGF receptor tyrosine kinase domain reveals a novel autoinhibitory mechanism; 1996.
- Naski MC, Wang Q, Xu J, Ornitz DM. Graded activation of fibroblast growth factor receptor 3 by mutations causing achondroplasia and thanatophoric dysplasia. *Nature Genet* 1996;13:233–7.
- Noronha G, Cao J, Chow CP, Dneprovskaja E, Fine RM, Hood J, et al. Inhibitors of ABL and the ABL-T315I mutation. *Curr Top Med Chem* 2008;8:905–21.
- Obel JC, Friberg G, Fleming GF. Chemotherapy in endometrial cancer. *Clin Adv Hematol Oncol* 2006;4:459–68.
- Olsen SK, Ibrahim OA, Raucic A, Zhang F, Eliseenkova AV, Yayon A, et al. Insights into the molecular basis for fibroblast growth factor receptor autoinhibition and ligand-binding promiscuity. *Proc Natl Acad Sci USA* 2004;101:935–40.
- Ornitz DM, Itoh N. Fibroblast growth factors. *Genome Biol* 2001;2, REVIEWS3005.
- Ornitz DM, Xu J, Colvin JS, McEwen DG, MacArthur CA, Coulier F, et al. Receptor specificity of the fibroblast growth factor family. *J Biol Chem* 1996;271:15292–7.
- Orr-Urtreger A, Bedford MT, Burakova T, Arman E, Zimmer Y, Yayon A, et al. Developmental localization of the splicing alternatives of fibroblast growth factor receptor-2 (FGFR2); 1993.
- Patel A, Tiwari AK, Chufan EE, Sodani K, Anreddy N, Singh S, et al. PD173074, a selective FGFR inhibitor, reverses ABCB1-mediated drug resistance in cancer cells. *Cancer Chemother Pharmacol* 2013;72:189–99.
- Perou CM, Sorlie T, Eisen MB, van de Rijn M, Jeffrey SS, Rees CA, et al. Molecular portraits of human breast tumours. *Nature* 2000;406:747–52.
- Piccatt-Gebhart MJ, Procter M, Leyland-Jones B, Goldhirsch A, Untch M, Smith I, et al. Trastuzumab after adjuvant chemotherapy in HER2-positive breast cancer. *N Engl J Med* 2005;1659–72.
- Plotnikov AN, Schlessinger J, Hubbard SR, Mohammadi M. Structural basis for FGF receptor dimerization and activation. *Cell* 1999;98:641–50.
- Polanska UM, Fernig DG, Kinnunen T. Extracellular interactome of the FGF receptor–ligand system: complexities and the relative simplicity of the worm. *Dev Dyn* 2009;238:277–93.
- Pollock PM, Gartside MG, Dejeza LC, Powell MA, Mallon MA, Davies H, et al. Frequent activating FGFR2 mutations in endometrial carcinomas parallel germline mutations associated with craniosynostosis and skeletal dysplasia syndromes. *Oncogene* 2007;26:7158–62.
- Qing J, Du X, Chen Y, Chan P, Li H, Wu P, et al. Antibody-based targeting of FGFR3 in bladder carcinoma and t(4;14)-positive multiple myeloma in mice. *J Clin Invest* 2009.
- Raskin L, Pinchev M, Arad C, Lejbkowitz F, Tamir A, Rennert HS, et al. FGFR2 is a breast cancer susceptibility gene in Jewish and Arab Israeli populations. *Cancer Epidemiol Biomarkers Prev* 2008;17:1060–5.
- Reis-Filho JS, Simpson PT, Turner NC, Lambros MB, Jones C, Mackay A, et al. FGFR1 emerges as a potential therapeutic target for lobular breast carcinomas. *Clin Cancer Res* 2006;12:6652–62.
- Rinella ES, Shao Y, Yackowski L, Pramanik S, Oratz R, Schnabel F, et al. Genetic variants associated with breast cancer risk for Ashkenazi Jewish women with strong family histories but no identifiable BRCA1/2 mutation. *Hum Genet* 2013;132:523–36.
- Risinger JI, Berchuck A, Kohler MF, Watson P, Lynch HT, Boyd J. Genetic instability of microsatellites in endometrial carcinoma. *Cancer Res* 1993;53:5100–3.
- Robinson ES, Khankin EV, Karumanchi SA, Humphreys BD. Hypertension induced by vascular endothelial growth factor signaling pathway inhibition: mechanisms and potential use as a biomarker. *Semin Nephrol* 2010;30:591–601.
- Sahlén P, Tarnow P, Martinsson T, Stenman G. Germline mutation in the FGFR3 gene in a TWIST1-negative family with Saethre-Chotzen syndrome and breast cancer. *Genes Chromosomes Cancer* 2009;48:285–8.
- Schlessinger J, Plotnikov AN, Ibrahim OA, Eliseenkova AV, Yeh BK, Yayon A, et al. Crystal structure of a ternary FGF–FGFR–heparin complex reveals a dual role for heparin in FGFR binding and dimerization. *Mol Cell* 2000;6:743–50.
- Schnitt SJ. Classification and prognosis of invasive breast cancer: from morphology to molecular taxonomy. *Mod Pathol* 2010;23(Suppl 2):S60–6.
- Seitzer N, Mayr T, Streit S, Ullrich A. A single nucleotide change in the mouse genome accelerates breast cancer progression. *Cancer Res* 2010;70:802–12.
- Song K, Xu P, Meng Y, Geng F, Li J, Li Z, et al. Smart gold nanoparticles enhance killing effect on cancer cells. *Int J Oncol* 2013;42:597–608.
- Stadler CR, Knyazev P, Bange J, Ullrich A. FGFR4 GLY388 isotype suppresses motility of MDA-MB-231 breast cancer cells by EDG-2 gene repression. *Cellular Signal* 2006;18:783–94.
- Stauber DJ, DiGabriele AD, Hendrickson WA. Structural interactions of fibroblast growth factor receptor with its ligands. *Proc Natl Acad Sci USA* 2000;97:49–54.
- Steele IA, Edmondson RJ, Bulmer JN, Bolger BS, Leung HY, Davies BR. Induction of FGF receptor 2-IIIb expression and response to its ligands in epithelial ovarian cancer. *Oncogene* 2001;20:5878–87.
- Steele IA, Edmondson RJ, Leung HY, Davies BR. Ligands to FGF receptor 2-IIIb induce proliferation, motility, protection from cell death and cytoskeletal rearrangements in epithelial ovarian cancer cell lines. *Growth Factors* 2006;24:45–53.
- Sun HD, Malabunga M, Tonra JR, DiRenzo R, Carrick FE, Zheng H, et al. Monoclonal antibody antagonists of hypothalamic FGFR1 cause potent but reversible hypophagia and weight loss in rodents and monkeys. *Am J Physiol Endocrinol Metab* 2007;292:E964–76.
- Sun S, Jiang Y, Zhang G, Song H, Zhang X, Zhang Y, et al. Increased expression of fibroblast growth factor receptor 2 is correlated with poor prognosis in patients with breast cancer. *J Surg Oncol* 2012;105:773–9.
- Sun X, Meyers EN, Lewandoski M, Martin GR. Targeted disruption of Fgf8 causes failure of cell migration in the gastrulating mouse embryo. *Genes Dev* 1999;13:1834–46.
- Szlachet A, Pala K, Zakrzewska M, Jakimowicz P, Wiedlocha A, Otlewski J. FGF1-gold nanoparticle conjugates targeting FGFR efficiently decrease cell viability upon NIR irradiation. *Int J Nanomedicine* 2012;7:5915–27.
- Takano M, Kikuchi Y, Yaegashi N, Kuzuya K, Ueki M, Tsuda H, et al. Clear cell carcinoma of the ovary: a retrospective multicentre experience of 254 patients with complete surgical staging; 2006.
- Taniguchi F, Itamochi H, Harada T, Terakawa N. Fibroblast growth factor receptor 2 expression may be involved in transformation of ovarian endometrioma to clear cell carcinoma of the ovary. *Int J Gynaecol Cancer* 2013;23:791–6.
- Temkin SM, Fleming G. Current treatment of metastatic endometrial cancer. *Cancer Control* 2009;16:38–45.
- Theillet C, Adelaide J, Louason G, Bonnet-Dorion F, Jacquemier J, Adnane J, et al. FGFR1 and PLAT genes and DNA amplification at 8p12 in breast and ovarian cancers; 1993.
- Thussbas C, Nahrig J, Streit S, Bange J, Kriner M, Kates R, et al. FGFR4 Arg388 allele is associated with resistance to adjuvant therapy in primary breast cancer. *J Clin Oncol* 2006;24:3747–55.
- Tomlinson DC, Knowles MA, Speirs V. Mechanisms of FGFR3 actions in endocrine resistant breast cancer; 2011.
- Torii S, Kusakabe M, Yamamoto T, Maekawa M, Nishida E. Sef is a spatial regulator for Ras/MAP kinase signaling. *Dev Cell* 2004;7:33–44.

- Trudel S, Li ZH, Wei E, Wiesmann M, Chang H, Chen C, et al. CHIR-258, a novel, multitargeted tyrosine kinase inhibitor for the potential treatment of t(4;14) multiple myeloma. *Blood* 2005;105:2941–8.
- Trudel S, Stewart AK, Rom E, Wei E, Li ZH, Kotzer S, et al. The inhibitory anti-FGFR3 antibody, PRO-001, is cytotoxic to t(4;14) multiple myeloma cells. *Blood* 2006;107:4039–46.
- Turner N, Grose R. Fibroblast growth factor signalling: from development to cancer. *Nat Rev Cancer* 2010;10:116–29.
- Turner N, Lambros MB, Horlings HM, Pearson A, Sharpe R, Natrajan R, et al. Integrative molecular profiling of triple negative breast cancers identifies amplicon drivers and potential therapeutic targets. *Oncogene* 2010a;29:2013–23.
- Turner N, Pearson A, Sharpe R, Lambros M, Geyer F, Lopez-Garcia MA, et al. FGFR1 amplification drives endocrine therapy resistance and is a therapeutic target in breast cancer. *Cancer Res* 2010b;70:2085–94.
- Vainikka S, Partanen J, Bellosta P, Coulier F, Birnbaum D, Basilico C, et al. Fibroblast growth factor receptor-4 shows novel features in genomic structure, ligand binding and signal transduction. *Embo J* 1992;11:4273–80.
- Valve E, Martikainen P, Seppanen J, Oksjoki S, Hinkka S, Anttila L, et al. Expression of fibroblast growth factor (FGF)-8 isoforms and FGF receptors in human ovarian tumors. *Int J Cancer* 2000;88:718–25.
- van Rhijn BW, van Tilborg AA, Lurkin L, Bonaventure J, de Vries A, Thiery JP, et al. Novel fibroblast growth factor receptor 3 (FGFR3) mutations in bladder cancer previously identified in non-lethal skeletal disorders; 2002.
- Wakioka T, Sasaki A, Kato R, Shouda T, Matsumoto A, Miyoshi K, et al. Sprouty-related suppressor of Ras signalling. *Nature* 2001;412:647–51.
- Walker K, Padhiar M. AACR-NCI-EORTC—21st International Symposium. *Molecular Targets and Cancer Therapeutics—Part 2. IDrugs* 2010;13:10–2.
- Wang L, Rudert WA, Loutaev I, Roginskaya V, Corey SJ. Repression of c-Cbl leads to enhanced G-CSF Jak-STAT signaling without increased cell proliferation. *Oncogene* 2002;21:5346–55.
- Wesche J, Haglund K, Haugsten EM. Fibroblast growth factors and their receptors in cancer. *Biochem J* 2011;437:199–213.
- Wheldon LM, Khodabukus N, Patey SJ, Smith TG, Heath JK, Hajihosseini MK. Identification and characterization of an inhibitory fibroblast growth factor receptor 2 (FGFR2) molecule, up-regulated in an Apert Syndrome mouse model. *Biochem J* 2011;436:71–81.
- Wilkie AO. Bad bones, absent smell, selfish testes: the pleiotropic consequences of human FGF receptor mutations. *Cytokine Growth Factor Rev* 2005;16:187–203.
- Wilkie AO, Patey SJ, Kan SH, van den Ouweland AM, Hamel BC. FGFs, their receptors, and human limb malformations: clinical and molecular correlations. *Am J Med Genet* 2002;112:266–78.
- Wingo SN, Gallardo TD, Akbay EA, Liang MC, Contreras CM, Boren T, et al. Somatic LKB1 mutations promote cervical cancer progression. *PLoS One* 2009;4:e5137.
- Wohrle S, Bonny O, Beluch N, Gaulis S, Stamm C, Scheibler M, et al. FGF receptors control vitamin D and phosphate homeostasis by mediating renal FGF-23 signaling and regulating FGF-23 expression in bone. *J Bone Miner Res* 2011.
- Xian W, Pappas L, Pandya D, Selfors LM, Derksen PW, de Bruin M, et al. Fibroblast growth factor receptor 1-transformed mammary epithelial cells are dependent on RSK activity for growth and survival. *Cancer Res* 2009;69:2244–51.
- Yan G, Fukabori Y, McBride G, Nikolopoulos S, McKeenan WL. Exon switching and activation of stromal and embryonic fibroblast growth factor (FGF)-FGF receptor genes in prostate epithelial cells accompany stromal independence and malignancy. *Mol Cell Biol* 1993;13:4513–22.
- Yang RB, Ng CK, Wasserman SM, Komuves LG, Gerritsen ME, Topper JN. A novel interleukin-17 receptor-like protein identified in human umbilical vein endothelial cells antagonizes basic fibroblast growth factor-induced signaling. *J Biol Chem* 2003;278:33232–8.
- Yayon A, Klagsbrun M, Esko JD, Leder P, Ornitz DM. Cell surface, heparin-like molecules are required for binding of basic fibroblast growth factor to its high affinity receptor. *Cell* 1991;64:841–8.
- Yeramian A, Moreno-Bueno G, Dolcet X, Catusas L, Abal M, Colas E, et al. Endometrial carcinoma: molecular alterations involved in tumor development and progression. *Oncogene* 2013;32:403–13.
- Zecchini S, Bombardelli L, Decio A, Bianchi M, Mazzarol G, Sanguineti F, et al. The adhesion molecule NCAM promotes ovarian cancer progression via FGFR signalling. *Embo Mol Med* 2011;3:480–94.
- Zhao G, Li WY, Chen D, Henry JR, Li HY, Chen Z, et al. A novel, selective inhibitor of fibroblast growth factor receptors that shows a potent broad spectrum of antitumor activity in several tumor xenograft models. *Mol Cancer Ther* 2011;10:2200–10.
- Zhou BB, Zhang H, Damelin M, Geles KG, Grindley JC, Dirks PB. Tumour-initiating cells: challenges and opportunities for anticancer drug discovery. *Nat Rev Drug Dis* 2009;8:806–23.
- Zhu X, Zheng L, Asa SL, Ezzat S. Loss of heterozygosity and DNA methylation affect germline fibroblast growth factor receptor 4 polymorphism to direct allelic selection in breast cancer. *Am J Pathol* 2010;177:2860–9.

Appendix 4

Nature Structural and Molecular Biology

review:

Grb-ing receptor activation by the tail

Grb-ing receptor activation by the tail

Abbie E Fearon & Richard P Grose

Hyperactivation of receptor tyrosine kinase pathways is a common theme in cancer. The recent demonstration that an imbalance between the fibroblast growth factor receptor 2-binding proteins Grb2 and phospholipase C- γ 1 can lead to invasive behavior in the absence of growth factors highlights an emerging concept in cellular-signaling homeostasis.

Phospholipase C- γ 1 (PLC γ 1) has a central role in mediating signaling downstream of receptor tyrosine kinase (RTK) activation and can drive invasive behavior in cancer cells. In this issue, Timsah *et al.*¹ describe a new homeostatic phenomenon in which phosphorylation-independent competition between the adaptor protein growth factor receptor bound 2 (Grb2) and PLC γ 1 for binding to the C-terminal tail of fibroblast growth factor receptor 2 (FGFR2) influences cell-growth behavior in the absence of stimulatory signal.

FGFR regulation of pro-oncogenic aspects of cell behavior is well documented, with activation of canonical signaling—in pathways including mitogen-activated protein kinase, phosphoinositide 3-kinase and PLC γ —driving proliferation, survival and migration². Specifically, FGFR2 has been implicated as a driver oncogene in breast, gastric and endometrial cancers³. Although researchers have focused mainly on ligand-dependent activation of receptor signaling, previous work from the Ladbury group has uncovered the importance of Grb2 in modulating ligand-independent receptor activity in basal conditions^{3,4}. In elegant biochemical studies, they showed that dimeric Grb2 binds, via each SH3 domain, to the C-terminal tail of unstimulated FGFR2 molecules to form a tetrameric 2:2 complex in which Grb2 functions to prevent the recruitment of downstream signaling proteins (Fig. 1). Ligand binding results in Grb2 phosphorylation and its subsequent dissociation from the

FGFR2 cytoplasmic tail, thus enabling the activation of canonical signaling⁴. In this system, the protein tyrosine phosphatase Shp2 acts as a negative regulator of signaling, partly by dephosphorylating Grb2 and returning it to its FGFR-inhibitory conformation⁵.

PLC γ 1 provides a key signaling axis downstream of RTKs, with its catalytic activity generating second messengers inositol triphosphate (IP3) and diacylglycerol (DAG) from hydrolysis of phosphatidylinositol 4,5-bisphosphate (PIP₂) at the plasma membrane⁵ (Fig. 1b). Although recruitment of PLC γ to the membrane is usually associated with ligand-dependent receptor activation, Timsah *et al.*¹ show that PLC γ 1 can also bind to the C terminus of FGFR2 in an SH3-dependent manner to initiate signaling in the absence of FGF ligand. This occurs when the cellular concentration of PLC γ 1 exceeds that of Grb2 (ref. 1), thus potentially explaining why tumor cells expressing low levels of Grb2 often exhibit enhanced PLC γ 1 activity and metastatic behavior.

Timsah *et al.*¹ used a variety of biochemical and biophysical approaches to dissect the phosphorylation-independent competition between Grb2 and PLC γ 1 for the C terminus of FGFR2. Using RNA interference to titrate Grb2 levels in cells expressing FGFR2, they showed that Grb2 acted as a competitive inhibitor of PLC γ 1 binding. The authors also confirmed this in functional studies on serum-starved cells, using immunoprecipitation and fluorescence lifetime imaging (FLIM) to demonstrate direct interaction of either Grb2 or PLC γ 1 with unstimulated FGFR2. Truncation or mutation of key domains in PLC γ 1, combined with analyses of the formed complexes, confirmed the specific interaction between FGFR2 and the SH3 domain of PLC γ 1 in unstimulated cells.

Using microscale thermophoresis to monitor binding affinity in solution⁶, the authors also determined the relative affinities of the SH3 domains of Grb2 and PLC γ 1 for FGFR2 to be sufficiently similar as to suggest that equimolar concentrations of each would compete equally for FGFR2 in the cell¹.

Stimulation of serum-starved cells with FGF9, a specific ligand for the FGFR2C isoform used in this study⁷, led to Grb2 phosphorylation and subsequent release of receptor inhibition⁴. This allowed recruitment of PLC γ 1—via binding of its N-terminal SH2 domain to phosphotyrosine 769 in FGFR2 (ref. 8)—and subsequent phosphorylation of PLC γ 1 on Y783 in the linker located between the C-SH2 and SH3 domains (Fig. 1a,b). This catalytically active PLC γ 1, recruited to the membrane via pleckstrin homology (PH) domains, hydrolyzes PIP₂ to activate downstream signaling⁵.

A key finding of Timsah *et al.*¹ is that in the absence of receptor stimulation, PLC γ 1 can still be activated, provided that it is able to outcompete Grb2 for a common proline-rich site on the C terminus of FGFR2 (ref. 1) (Fig. 1c). Upon binding via its SH3 domain, PLC γ 1 undergoes a conformational shift that exposes the same Y783 residue that has a critical role in canonical PLC γ 1 signaling. Normally sheltered between the C-terminal SH2 and SH3 domains of PLC γ 1, this residue, when exposed and even when not phosphorylated, is able to interact with the C-terminal SH2 domain to relieve the autoinhibition of PLC γ 1 (ref. 9). Once activated, the catalytic output of PLC γ 1 is identical, whether activation has occurred via phosphorylation-dependent or phosphorylation-independent mechanisms. PLC γ 1 activity can be determined by monitoring either PIP₂ turnover or intracellular Ca²⁺ release, and in unstimulated

Abbie E. Fearon and Richard P. Grose are at the Centre for Tumour Biology, Barts Cancer Institute, Queen Mary University of London, London, UK.
e-mail: r.p.grose@qmul.ac.uk

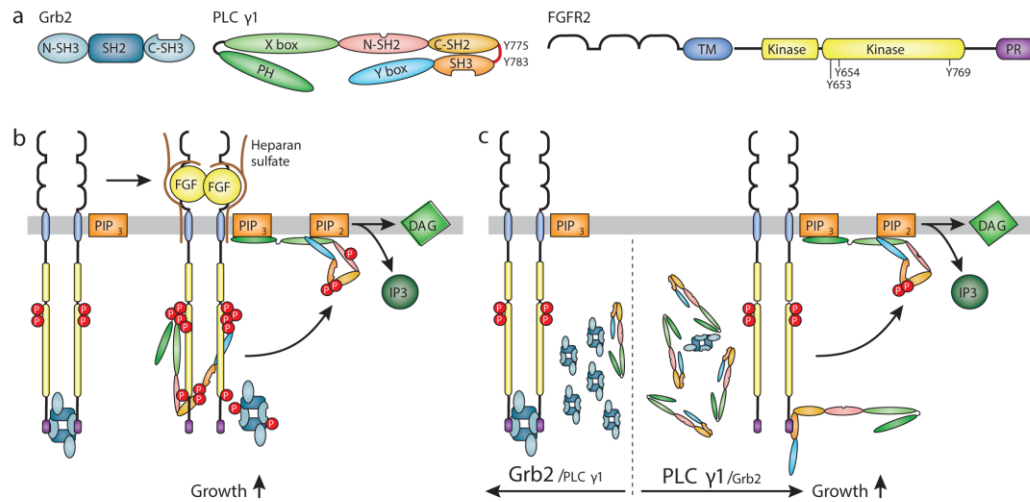


Figure 1 Alternative mechanisms of PLC γ 1 activation downstream of FGFR2. (a) Domain organization of Grb2, PLC γ 1 and FGFR2. N- and C- prefixes denote N- and C-terminal domains, respectively. (b) Mechanism for canonical activation. Left, FGFR2 is kept in an inactive state by formation of a tetrameric complex with Grb2. Upon binding of dimeric Grb2 to the proline-rich C terminus (PR) of FGFR2, low-level phosphorylation of the receptor occurs at Y653 and Y654, thus priming the receptor for downstream signaling. Right, upon ligand binding, trans phosphorylation of the kinase domain initiates several downstream pathways, including PLC γ 1 activation. PLC γ 1 is phosphorylated upon binding of its N-terminal SH2 domain to residue Y775 of FGFR2. This binding induces a conformation shift that results in PLC γ 1 activation and binding to membrane-associated PIP₃ via the PLC γ 1 pleckstrin homology (PH) domain, thus stimulating the hydrolysis of PIP₂ into DAG and IP₃. DAG remains in the membrane, where it activates PKC, whereas IP₃ diffuses into the cytosol and initiates calcium release from the endoplasmic reticulum. Phosphates are shown as red spheres. (c) Mechanism of noncanonical PLC γ 1 activation. Competition between PLC γ 1 and Grb2 for binding to the proline-rich C terminus of the FGFR2 dictates signaling outcome depending on the PLC γ 1/Grb2 ratio. When Grb2 dominates in the cytoplasm, FGFR2 remains in the Grb2-bound inactive state. However, when Grb2 levels are low, PLC γ 1 outcompetes Grb2 for binding to FGFR2. In this scenario, the SH3 domain of PLC γ 1 binds to the proline-rich domain of FGFR2 to result in the activation of PLC γ 1 and growth signaling.

conditions both readouts were significantly higher in cells in which Grb2 levels were depleted by RNA interference. This mechanism, however, appears to be specific to FGFR2, and FGFR1 shows no such interaction¹⁰.

Further functional analysis—with two-dimensional scratch-wound and three-dimensional invasion assays—showed that phosphorylation-independent PLC γ 1 signaling could drive invasive behavior *in vitro* in cells expressing low levels of Grb2 (ref. 1). This was true even when PLC γ 1 was mutated such that it was incapable of binding to phosphotyrosine residues on FGFR2, and the effect was abrogated by treatment with the pharmacological PLC γ 1 inhibitor U73122 (ref. 11). PLC γ 1 is known to promote cancer cell metastasis¹². A comparative analysis of several cell lines and clinical samples representing a broad range of cancers showed a clear relationship between invasiveness and relative expression levels of PLC γ 1 and Grb2, with a low Grb2/PLC γ 1 ratio correlating with aggressiveness¹.

FGFR2 signaling is implicated in a number of cancers, and the uncovered signal-independent mechanism of PLC γ 1 activation therefore provides an interesting new perspective on RTK signaling. However, it appears unlikely that FGFR2 within a typical tumor micro-environment is going to be in an inactivated state, because FGF ligands are likely to be expressed. Nevertheless, it may be that reduced Grb2 levels lead to greater receptor phosphorylation and that the eventual recruitment of PLC γ 1 in the canonical manner leads to increased invasiveness. There are many FGFR inhibitors currently in development or in clinical trials¹³, all of which have been developed to block phosphorylation-dependent signaling, either directly as ATP-competitive small molecules or indirectly as allosteric inhibitors or antibody-based inhibitors of ligand or receptor. One implication of the study by Timsah *et al.*¹ is that even when FGFR2 phosphorylation is blocked, PLC γ 1 recruitment to the ligand-free receptor could still drive malignant behavior.

This observation suggests that researchers may need to think of additional approaches to limit FGFR signaling in cancer.

COMPETING FINANCIAL INTERESTS

The authors declare no competing financial interests.

1. Timsah, Z. *et al.* Nat. Struct. Mol. Biol. 21, 180–188 (2014).
2. Turner, N. & Grose, R. Nat. Rev. Cancer 10, 116–129 (2010).
3. Ahmed, Z. *et al.* J. Cell Biol. 200, 493–504 (2013).
4. Lin, C.C. *et al.* Cell 149, 1514–1524 (2012).
5. Lemmon, M.A. & Schlessinger, J. Cell 141, 1117–1134 (2010).
6. Wienken, C.J., Baaske, P., Rothbauer, U., Braun, D. & Duhr, S. Nat. Commun. 1, 100 (2010).
7. Zhang, X. *et al.* J. Biol. Chem. 281, 15694–15700 (2006).
8. Belleudi, F., Purpura, V. & Torrisi, M.R. PLoS ONE 6, e24194 (2011).
9. Bunney, T.D. *et al.* Structure 20, 2062–2075 (2012).
10. Ahmed, Z. *et al.* Cell. Signal. 22, 23–33 (2010).
11. Bleasdale, J.E. *et al.* Adv. Prostaglandin Thromboxane Leukot. Res. 19, 590–593 (1989).
12. Sala, G. *et al.* Cancer Res. 68, 10187–10196 (2008).
13. Fearon, A.E., Gould, C.R. & Grose, R.P. Int. J. Biochem. Cell Biol. 45, 2832–2842 (2013).

Appendix 5

Trends in Cell Biology review:

**Careless talks costs lives: fibroblast
growth factor receptor signalling and the
consequences of pathway malfunction**

Careless talk costs lives: fibroblast growth factor receptor signalling and the consequences of pathway malfunction

Edward P. Carter, Abbie E. Fearon, and Richard P. Grose

Centre for Tumour Biology, Barts Cancer Institute – a CR-UK Centre of Excellence, Queen Mary University of London, London EC1M 6BQ, England, UK

Since its discovery 40 years ago, fibroblast growth factor (FGF) receptor (FGFR) signalling has been found to regulate fundamental cellular behaviours in a wide range of cell types. FGFRs regulate development, homeostasis, and repair and are implicated in many disorders and diseases; and indeed, there is extensive potential for severe consequences, be they developmental, homeostatic, or oncogenic, should FGF–FGFR signalling go awry, so careful control of the pathway is critically important. In this review, we discuss the recent developments in the FGF field, highlighting how FGFR signalling works in normal cells, how it can go wrong, how frequently it is compromised, and how it is being targeted therapeutically.

Overview of FGF in physiology and pathology

FGFs are a family of 18 either locally or hormonally acting signalling factors that function through four FGF receptor tyrosine kinases (RTKs) to elicit a range of context-dependent cellular outcomes, including proliferation, survival, migration, and differentiation. FGFs are vital to a number of developmental and homeostatic processes and are also primary drivers in the repair response. Given their inherent complexity and critical roles in physiological processes, dysfunction in the FGF family leads to a number of developmental disorders and is consistently found to be a driving force in cancer. Deregulation of the FGF family can take many forms, including receptor amplification, activating mutations, gene fusions, and receptor isoform switching, which presents unique challenges to overcome in order to return FGF function to normal.

In this review, we cover recent studies that highlight new insights into how FGFs signal and their novel roles in development, homeostasis, and repair. We also cover the expanding field of how, and how frequently, FGF signalling goes awry in cancer. Finally, we discuss the many exciting approaches being taken to target aberrant FGF signalling and how they are currently performing in clinical trials.

Corresponding author: Grose, R.P. (r.p.grose@qmul.ac.uk).

Keywords: fibroblast growth factor; fibroblast growth factor receptor; cell signalling; cancer.

0962-8924/

© 2014 Elsevier Ltd. All rights reserved. <http://dx.doi.org/10.1016/j.tcb.2014.11.003>

FGF signalling and regulation

The 18 FGFs cluster into five paracrine subfamilies and one endocrine subfamily [1]. Paracrine FGFs are locally acting and are involved in a plethora of processes, ranging from organogenesis to tissue homeostasis, whereas endocrine FGFs act more globally and are involved in metabolic processes, such as glucose metabolism and phosphate homeostasis [1]. FGFs signal through FGFR tyrosine kinases, of which there are four signalling subtypes. FGFRs are composed of three extracellular immunoglobulin (Ig) like domains linked to an intracellular kinase via a transmembrane α -helix (Figure 1A). Alternate splicing of the extracellular Ig-like domains of FGFRs 1–3 creates 'b' and 'c' isoforms, which differ in their tissue distribution and ligand specificity (reviewed in [2]). A fifth subtype also exists, FGFR1, which lacks an intracellular kinase domain but is still capable of binding to FGFs [3]. Mice deficient in FGFR1 exhibit a number of malformations, including skeletal and heart defects [4]. Interestingly, mice lacking the intracellular portion of FGFR1 do not exhibit any of these abnormalities, suggesting that FGFR1 may function as a decoy receptor [5]. However, others have demonstrated that FGFR1 has a signalling function, enhancing basal ERK signalling through the recruitment of the phosphatase SHP-1 in pancreatic beta cells [6].

Paracrine FGFs utilise heparan sulfate proteoglycans (HS) as binding partners, which stabilise the receptor–ligand structure and enhance resistance to proteolysis, while limiting the action of these FGFs to their site of initial release [7]. Endocrine FGFs exhibit weak interactions with HS, thereby allowing their diffusion away from the site of release and entry into the circulation where they can act hormonally [8]. In place of HS, endocrine FGFs utilise Klotho co-receptors in their receptor binding [8]. Thus, interaction with their respective binding partners provides tight control over the action of different FGF families. Indeed, removing the ability of a paracrine FGF to bind HS, coupled with the substitution of its C-terminal domain with that of an endocrine FGF to facilitate Klotho binding, allows a paracrine FGF to act in an endocrine fashion [9]. Klotho co-receptors have also been demonstrated to inhibit the action of paracrine FGF8, suggesting that

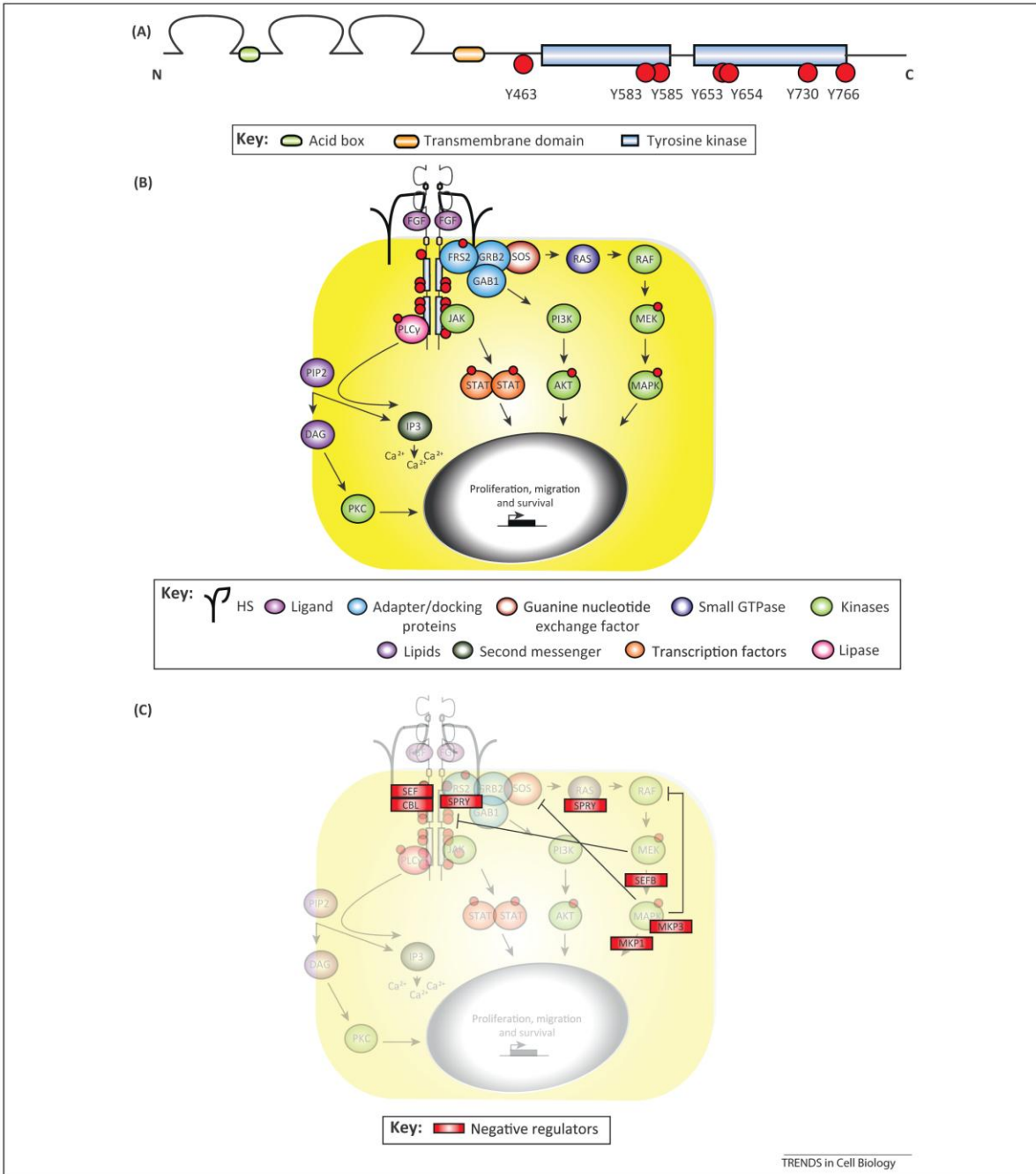


Figure 1. Fibroblast growth factor receptor (FGFR) signalling. (A) Schematic representation of FGFR1. The extracellular domain of FGFR1-4 is comprised of three Ig like loops. The region between the C terminal portion of the second loop and the N terminal portion of the third is responsible for ligand binding. Alternative splicing of these loops leads to varying affinity for different FGF ligands. The acid box (green) between the first and second Ig loops is involved in heparan sulfate proteoglycan (HS) binding. The transmembrane domain is shown in orange. The intracellular portion of the receptor consists of a split kinase domain (blue). Upon ligand binding, dimerisation and subsequent transphosphorylation of the receptor occurs on seven tyrosine residues (red circles). This induces four key downstream pathways: mitogen-activated protein kinase (MAPK), phosphoinositide 3-kinase (PI3K)/AKT, phospholipase Cg (PLCg) and Janus kinase (JAK)/signal transducer and activator of transcription (STAT) (B). These pathways comprise a series of phosphorylation events, culminating in regulation of target genes, which dictate cellular processes, for example proliferation and migration. (C) A number of mechanisms exist to negatively regulate FGFR signalling, including upregulation and recruitment of signalling modulators (red boxes). Further, inhibitory feedback signals, from pathways such as MAPK, act to dampen upstream components of the FGFR signalling axis (black lines).

Klotho-expressing cells have a reduced sensitivity to paracrine FGF stimulation [10].

FGF binding results in receptor dimerisation and increased kinase activity, leading to the ordered phosphorylation of seven tyrosine residues present on the receptor (Y463, Y583, Y585, Y653, Y654, Y730, and Y766 in the case of FGFR1) (Figure 1A) [11]. These, in turn, recruit and activate a number of signalling pathways, including phospholipase C γ (PLC γ) [12], mitogen-activated protein kinase (MAPK) [13], signal transducer and activator of transcription (STAT) [14], and phosphoinositide 3-kinase (PI3K) [15], which control a number of cellular events including; proliferation, migration, and survival (Figure 1B).

FGFR signalling is regulated by a number of factors that exert negative feedback control on several elements of the FGFR cascade (Figure 1C). These include the recruitment of the ubiquitin ligase Cbl, which targets FGFR for internalisation [16]. Further feedback inhibition comes from the induction of the negative regulators MAPK phosphatase 3 [17], sprouty proteins [18], and Sef (similar expression to FGF genes) [19]. As well as recruitment of regulatory proteins, direct phosphorylation of FGFR by ERK has also been reported to reduce FGFR signalling, and therefore, act as a negative feedback loop [20]. Mechanisms are also in place to prevent the aberrant activation of the receptor. In the absence of stimulation, dimerised Grb2 is recruited to the C terminus of FGFR2 via its SH3 domain. Grb2 recruitment promotes receptor dimerisation and phosphorylation, without any subsequent signal transduction [21,22]. This binding site for Grb2 is shared with PLC γ , which competes with Grb2 for receptor binding. However, unlike Grb2, PLC γ recruitment to this site results in increased cellular activity, suggesting that imbalances in Grb2 expression may promote pathological FGF signalling even in the absence of ligand binding [23,24]. Although this has only been demonstrated for FGFR2, similar mechanisms may well exist for other FGFRs.

FGFR signalling outcomes can be dependent on the activating ligand, with different FGF ligands inducing different cellular responses through the same receptor. For instance, FGF10 and FGF7 both signal through FGFR2b, with FGF10 promoting a migratory response with limited proliferation, and FGF7 inducing a more pronounced proliferative, non-migratory, response [25]. This difference in cellular behaviours, mediated through FGFR2, is likely due to the fate of the internalised receptor following ligand binding. Upon activation by FGF10, but not FGF7, FGFR2 is phosphorylated at the Y734 residue; this phosphorylation site recruits the p85 subunit of PI3K and SH3 domain-binding protein 4 (SH3BP4), which in turn recruit and initiate the receptor recycling machinery. Activation without this phosphorylation, that is, following FGF7 stimulation or receptor mutagenesis, instead promotes receptor degradation, thus generating a signalling outcome different from that of FGF10 [25].

Inherent differences in binding affinities for HS, between FGF ligands, can also dictate signalling outcomes in tissues. During branching morphogenesis, in epithelial tissues such as the salivary gland, HS is produced at the sites of branching, forming a gradient that specifies sites of FGF10 binding. Localised FGF10 action induces the

collective migration of epithelial cells, thus promoting branch elongation. Removal of this HS gradient, or reducing the HS binding capabilities of FGF10, results in a uniform action of FGF10 on the tissue. This promotes an epithelial budding response not unlike FGF7, which has a reduced HS binding capability [26].

As well as conventional signal transduction, FGFs and FGFRs can regulate cellular events through their transport to the nucleus [27]. RTKs have been known to localise to the nucleus for many years [28], but the functional implications of this have been examined only recently. In breast cancer cell lines, FGFR1 can translocate to the nucleus following FGF10 stimulation, wherein the receptor can activate the transcription of proteins involved in cell migration [29]. Moreover, FGF2 and FGFR1 have been demonstrated to translocate to the nucleus of pancreatic stellate cells, where they can influence cell migration and proliferation [30]. Nuclear localisation of FGFR1 has also been identified to promote neuronal cell development [31,32], and neurite outgrowth [33], independently of FGF stimulation.

Transport of FGF1 to the nucleus requires receptor binding, but is independent of the kinase activity of the receptor [34]. Once internalised, FGF1 escapes into the cytosol and enters the retrograde pathway through the endoplasmic reticulum, ultimately using the importins karyopherin- α 1 and - β 1 to enter the nucleus [35]. Comparatively little is known about the pathway utilised by FGFR to reach the nucleus. Cleavage of FGFR1 by the protease Granzyme B is required for its nuclear localisation following stimulation by FGF10 [29], although full length FGFR1 has also been identified in the nucleus. However, full length FGFR1 is capable of trafficking to the nucleus independently of FGF stimulation [33].

Beyond the classical FGF ligands, four factors (FGF11-14) share sequence homology with the classic FGF ligands but lack the ability to activate FGFRs, and are not secreted from cells [36]. Rather than acting through FGFRs, these FGF homologous factors (FHF) have been demonstrated to modulate sodium [37] and calcium channels [38,39], where they can affect synaptic transmission and cardiac rhythm.

FGF axis dysfunction in development

FGFs are involved in all stages of mammalian development, from mesoderm formation through organ morphogenesis, myogenesis and limb formation (reviewed in [40]). As a result, mutations in FGFRs have been identified in a number of developmental disorders, which in turn has presented novel insights into the developmental roles of FGF signalling.

Skeletal malformations, notably craniosynostoses and chondrodysplasias, are associated with aberrant FGF signalling [41]. Apert syndrome is one of the most severe forms of craniosynostosis. The majority of patients have one of two mutations in the linker regions between Ig domains II and III of FGFR2, which alter receptor ligand specificity [42,43]. Accordingly, mice expressing one of these FGFR2 mutations, S252W, have a phenotype mimicking Apert syndrome [44]. One such characteristic, impaired bone growth, could be reversed through inhibition of MAPKs, suggesting that these pathways operate downstream of

FGFR2 to regulate bone development [45]. Further studies have suggested that the S252W FGFR2 mutation enhances FGF10 and FGFR2b expression in calvarial tissue, which in turn promotes the premature fusion of cranial coronal sutures [46]. Interestingly, soluble FGFR2 carrying the S252W mutation was able to prevent synostosis in calvarial tissue taken from mice expressing mutant FGFR2, likely due to mutant FGFR2 acting as a ligand trap for FGF10 and/or interfering with FGFR2b signalling [46].

Mutations in FGF signalling are also apparent in developmental disorders that extend beyond skeletal malformations. Kallmann syndrome is a form of hypogonadotropic hypogonadism that presents with anosmia and is associated with a loss of function mutation in FGFR1 [47]. This loss of function is brought about by a mutation in the second Ig loop, which leads to a conformational change in the receptor, diminishing HS and FGF ligand binding [48]. Other loss of function mutations have been identified in FGF8 that result in both reduced release of the growth hormone gonadotropin and pituitary defects, which may contribute to Kallmann syndrome and related conditions [49,50].

Defects in FGF signalling may arise secondarily to another mutation and contribute to developmental disorders. A mutation in the sterile acid motif of P63 affects protein interactions and is found in patients with Hay-Wells syndrome, a type of ectodermal dysplasia [51]. Mice carrying this p63 mutation reflect the human condition and exhibit reduced FGFR2 and FGFR3 transcription [52]. This impaired FGFR signalling was suggested to be responsible for the reduction in self-renewing epidermal cells present in p63 mutant mice [52].

As well as classical FGFs, FHF s have also been implicated in genetic disorders, presenting insights into how they regulate ion channels. A mutation in FGF12 has been reported in patients with Brugada syndrome, a genetic disease characterised by an abnormal electrocardiogram. This mutation in FGF12 reduced its binding to sodium channels present in cardiomyocytes, resulting in reduced action potential amplitude [53].

FGFs in tissue repair and regeneration

The importance of FGFs and their receptors in tissue regeneration and repair is well documented. While the involvement of these proteins has been described in a range of organs, in this review, we focus on their essential role in the skin, liver, and lung.

Skin

Efficient wound healing is crucial for the maintenance of skin integrity. Repair processes are orchestrated by cytokines and growth factors, with the FGF family and their receptors being of particular importance. FGFs 7, 10, and 22, which activate both FGFR1b and 2b, are strongly expressed in both normal and wounded skin and are crucial for maintenance of the epidermal barrier [54]. Activation of these receptors can be autocrine, in the case of FGF22, or paracrine, with FGF7 and FGF10 coming from dermal fibroblasts and gdT-cells [54,55]. Mouse studies have revealed gdT-cells to be critical sources of another ligand, FGF9, which is essential in wound-induced hair follicle neogenesis [56]. These intriguing data showed that

FGF9 coming from gdT-cells at the wound site induced Wnt signalling, and subsequent FGF9 expression in wound fibroblasts, allowing the de novo formation of hair follicles in the regenerating epidermis.

The finding that FGF7 was significantly upregulated in wound healing [57], and that mice expressing dominant negative FGFR2b in keratinocytes display severely delayed wound re-epithelialisation [58], established the importance of FGF signalling in skin repair. The functional significance of FGFR1 and FGFR2 in keratinocytes has been investigated in a number of animal studies. Epidermal-specific deletion of FGFR1 and FGFR2 resulted in impaired wound re-epithelialisation due to reduced proliferation and problems establishing focal contacts [59]. Although FGFR1 knockout alone had no obvious phenotypic consequences, double knockout of FGFR1 and FGFR2 in keratinocytes led to a range of severe phenotypic effects, including hair loss, defective barrier function, hyperproliferation, and inflammation [59]. Changes in the profile of cytokines secreted from keratinocytes led to the attraction of immune cells, leading to further pro-inflammatory cytokine and growth factor production. In addition to the stimulation of keratinocyte proliferation, a pro-fibrotic phenotype in dermal fibroblasts led to progressive dermal fibrosis [59]. These data highlight the importance of stromal-epithelial interactions in the skin and the crucial role of efficient FGF signalling in the prevention of cutaneous inflammation and subsequent fibrosis [54]. Distinct from their role in keratinocytes, FGFR1 and FGFR2 also impact on cutaneous repair by driving injury-induced angiogenesis that nourishes the repair process [60].

Liver

The liver is the only mammalian organ that can regenerate fully following injury. Full restoration of hepatic function can be achieved as a result of well-defined signalling cascades initiated after insults such as toxin-induced necrosis, surgery, or viral infection [61].

The importance of hepatic FGFR2b expression in regeneration is well established [62]. Partial hepatectomy (PH) is the most common method for investigating liver regeneration. In transgenic mice expressing dominant negative FGFR2b, mutant mice subjected to PH demonstrated decreased hepatocyte proliferation [63]. Further investigation, using mice lacking both FGFR1 and FGFR2 in hepatocytes, showed decreased survival after PH, due to an inadequate capacity for detoxification of both anaesthetic compounds and metabolic by-products of liver injury [64].

Interestingly, while FGFR1 and FGFR2 displayed an essential cytoprotective role after partial PH, FGFR4 had the opposite effect. FGFR4 knockout mice exhibited normal regenerative capacity but enhanced fibrosis following toxin-induced liver injury using carbon tetrachloride [65]. Hepatocytes lacking either FGFR1 and 2 or FGFR4 were equally capable of proliferating following PH, whereas mice expressing a dominant negative FGFR2-IIIb construct in the liver showed a severely reduced hepatocyte proliferative capacity [63]. This suggests that signalling from any one of the FGFRs present in hepatocytes is sufficient to support proliferation, but that there are varying, yet essential roles of the different FGFRs in other

aspects of liver regeneration. The differences between FGFR1/2 and FGFR4 may reflect signalling changes as a result of FGFR4 interacting with its co-receptor, b-Klotho [66].

In terms of ligands, FGF7 has been shown to be an essential signal supporting the liver progenitor cell niche, thus helping to promote liver regeneration [67]. In light of the importance of FGFR signalling in the detoxification of anaesthetics, neo-adjuvant FGF7 treatment could be a very useful approach for patients undergoing major liver resections [64]. FGF15 plays a critical role in bile acid homeostasis, and is crucial for liver regeneration, with FGF15 knockout mice showing high mortality rates following PH [68].

Lung

Reactivation of developmental signalling mechanisms is often employed in tissue repair. This is demonstrated in the lung, where the developmentally important FGF, Notch, and Wnt pathways are commonly upregulated following injury [69]. Indeed, the importance of the Wnt–FGF10–Notch signalling axis following injury in intrapulmonary airway re-epithelialisation has been demonstrated *in vivo* [70]. Re-activation of Wnt7b was observed in mice 3 days after naphthalene injury. FGF10 expression was increased in smooth muscle cells in response to Wnt signalling. FGF10 signalling, in turn, upregulated the Notch pathway in variant club cells, leading to re-epithelialisation of the airway. This epithelium–mesenchyme–epithelium signalling relay demonstrates the importance of cellular crosstalk in tissue repair.

The role of FGFR signalling in lung fibrosis is complex. FGF9 has been implicated as a potential driver of lung fibrosis [71], and inhibiting FGFR signalling has been shown to ameliorate bleomycin-induced lung fibrosis in

mouse models, through effects both on the FGFR and also via transforming growth factor β signalling [72]. However, FGF7 expression in bone marrow-derived stem cells attenuates bleomycin-induced lung damage [73]. FGF2 has also been demonstrated to be involved in the repair process following bleomycin- or naphthalene-induced injury. Mice deficient in FGF2 exhibit prolonged inflammation following bleomycin injury and show a marked attenuation in the recovery of epithelial integrity [74].

FGF signalling in cancer

As FGF signalling can promote cell survival, proliferation, and migration, it has a prominent role in cancer (reviewed in [75]). As well as directing the growth of the main body of the tumour, FGF signalling has been implicated in the function of a small population of breast tumour cells, termed tumour initiating cells (TICs), which drive tumour initiation and growth [76]. Breast TICs express high levels of FGFR2 compared to non-TICs, knockdown or inhibition of which results in impaired TIC self-renewal and cancer growth in murine xenograft models of breast cancer [76]. Furthermore, FGFR1 has been implicated in a positive feedback loop between advanced prostate cancer cells and osteoblasts present in the bone. This dynamic interaction leads to metastatic bone lesions that are sensitive to FGFR-based therapies [77]. Many cancers have been suggested to acquire their aberrant growth and invasion through dysregulation of FGF signalling, which can occur through several mechanisms (Figure 2).

Receptor amplification

Recent meta analysis has reported the overall prevalence of FGFR amplification in all cancers to be 11% for FGFR1 and 4% for FGFR2 (Figure 3). Moreover, amplification of either FGFR1 or FGFR2 correlates with poor survival

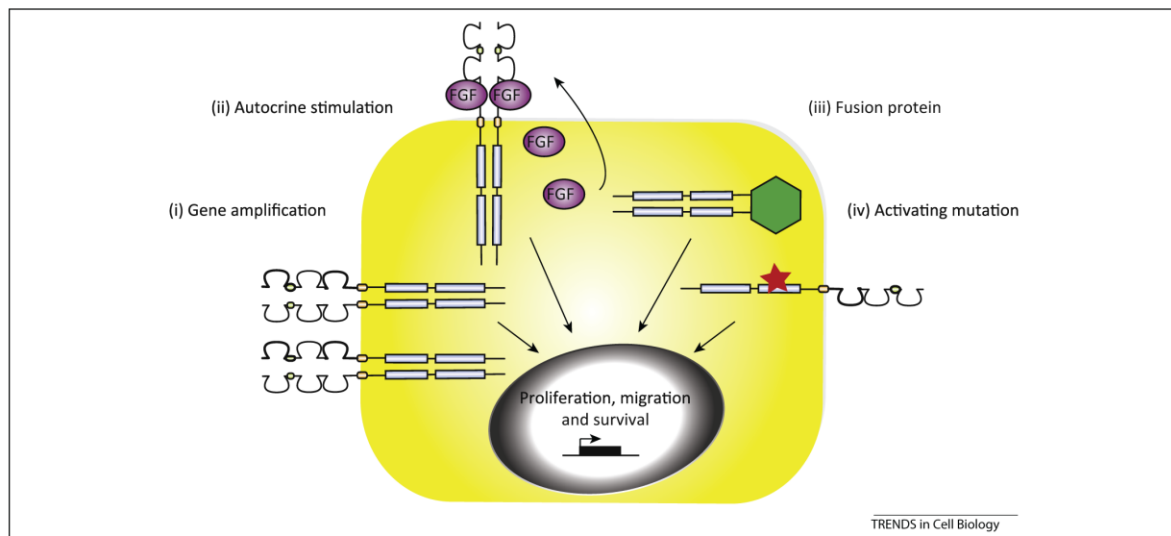


Figure 2. Mechanisms of aberrant fibroblast growth factor receptor (FGFR) signalling in disease. Increased downstream signalling from FGFRs in both developmental disorders and cancer occurs via four main mechanisms: (i) gene amplification, where overexpression of the receptor leads to augmented intracellular signalling; (ii) autocrine stimulation by release of ligands with high affinity for the receptor expressed on the cell; (iii) fusion proteins, whereby the kinase domain is fused to, for example, transforming acidic coiled-coil 1 (TACC1), leading to constitutive activation of the kinase as well as removing the binding site for the regulatory microRNA miR-99a; and (iv) activating mutations, for example, in the kinase domain, which leads to constitutive activation of the receptor.

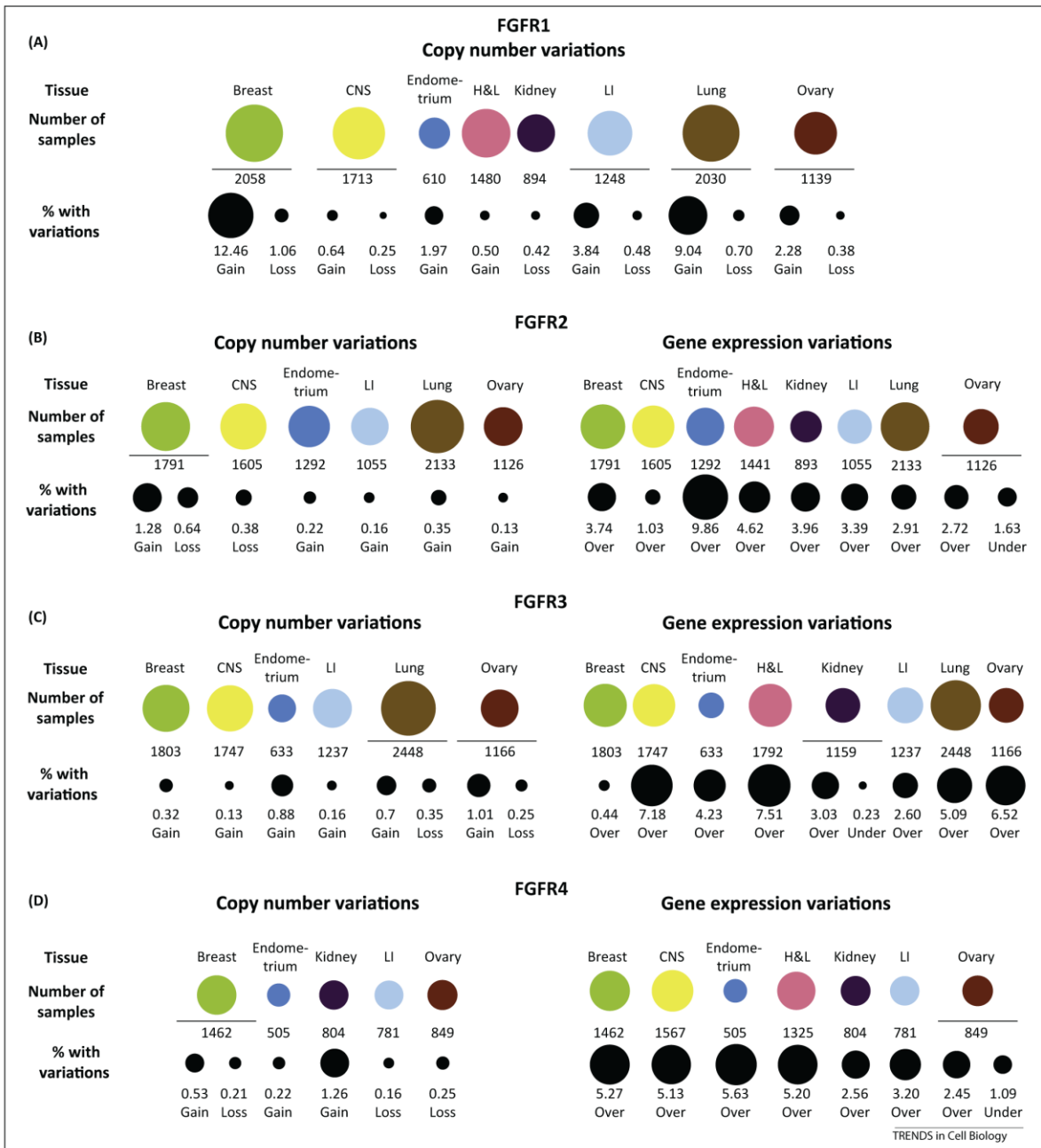


Figure 3. Frequency of fibroblast growth factor receptor (FGFR)1–4 copy number and gene expression variations in cancer. FGFR mutations are found in a range of tumour types and their proportions differ depending on the tissue of origin. In this figure, we show all tissue types and number of tumours screened (A–D, top panels), as well as the proportion of these tumours with copy number or gene expression variations (A–D, bottom panels), as listed in the Catalogue of Somatic Mutations in Cancer (COSMIC). All dots in the plot are in proportion within the same panel. Abbreviations: CNS, central nervous system; LI, large intestine; H&L, haematopoietic and lymphoid. ‘Gain’ and ‘loss’ indicate increased and decreased copy number respectively; ‘over’ and ‘under’ indicate increased and decreased expression of the gene, respectively. Data correct as of September 2014.

[78]. Unsurprisingly, patients who exhibit FGFR amplified tumours respond more favourably to FGFR directed therapies than those harbouring non-amplified tumours [79,80]. As an example, FGFR1 amplifications are found in approximately 22% of lung squamous cell carcinomas

and show an enhanced sensitivity to FGFR-directed therapies. However, contrary to the overall cancer statistics, FGFR amplification in these squamous cell carcinomas does not confer a reduced survival chance, compared with non-amplified cancers [81].

Receptor mutation

FGFR mutations have been identified in many cancers (Figure 4). For example, two point mutations in FGFR2 that lead to enhanced receptor kinase activity have been described in breast cancer [82]. Mice expressing these same FGFR2 mutations in the lung, alongside deletion of p53, develop adenocarcinomas that are sensitive to FGFR-specific inhibitors [83], highlighting a functional consequence for these mutations. Single nucleotide polymorphisms in FGFR2 have also been reported, correlating with poor prognosis in breast cancer [84,85]. Interestingly, these have been postulated to act, not in cancer cells, but in the stromal fibroblasts, where they promote excessive FGFR10 production [86].

FGFR3 mutations are reported to be present in approximately 70% of non-muscle invasive bladder cancers and are associated with enhanced survival [87]. Although FGFR3 mutations are not common in muscle invasive bladder cancers, FGFR3 amplification is found in approximately 45% of these cancers and correlates with reduced survival in patients treated with adjuvant chemotherapy [88]. FGFR3 mutations correlate with enhanced PI3K signalling [89]. Accordingly, mice expressing FGFR3 mutations in the bladder, alongside PTEN deletion, and hence enhanced PI3K signalling, exhibit enhanced urothelial cell proliferation and hypertrophy, providing a functional role for FGFR3 mutations in bladder cancer [90]. FGFR3 mutations are also found in approximately 40% of multiple

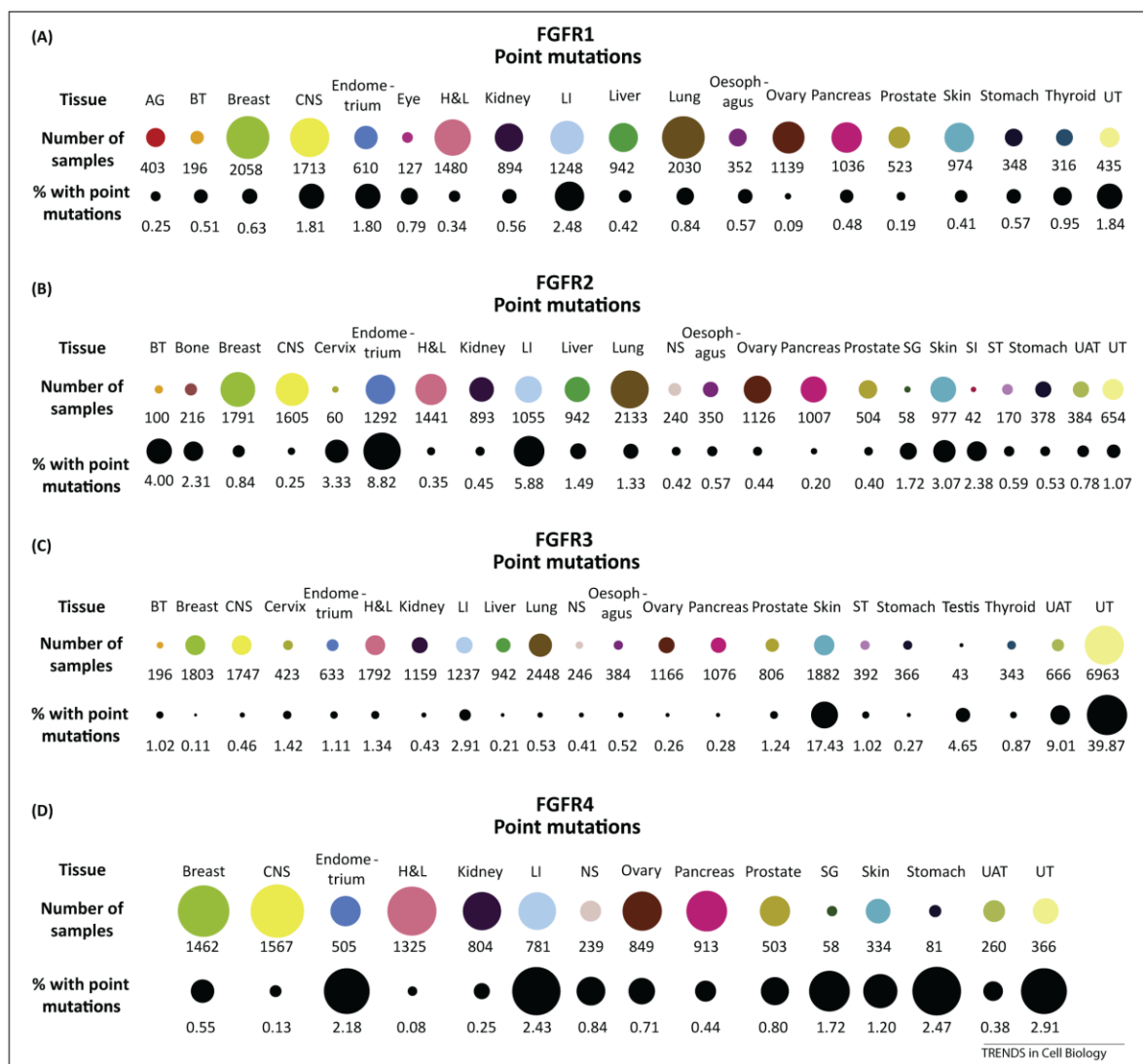


Figure 4. Frequency of fibroblast growth factor receptor (FGFR)1–4 point mutations in cancer. As well as listing copy number and gene expression variations, the Catalogue of Somatic Mutations in Cancer (COSMIC) also details point mutations recorded for FGFR1–4 in all tumours screened. In this review, we show all tissue types and number of tumours screened (A–D, top panels), as well as the proportion of these tumours harbouring an FGFR point mutation (A–D, bottom panels). All dots in the plot are in proportion within the same panel. Abbreviations: AG, autonomic ganglia; BT, biliary tract; CNS, central nervous system; H&L, haematopoietic and lymphoid; LI, large intestine; UT, urinary tract; NS, not specified; SG, salivary gland; SI, small intestine; ST, soft tissue; UAT, upper aerodigestive tract. Data correct as of September 2014.

myeloma patients, leading to enhanced expression of the receptor and poor survival outcomes [91].

Activating mutations in FGFR4 are present in approximately 6% of rhabdomyosarcoma patients and are associated with advanced stage cancer and poor survival [92,93]. Knockdown of FGFR4 in rhabdomyosarcoma cell lines reduces tumour growth and lung metastasis in xenograft models [93].

Gene fusion

Gene fusions involving FGFRs have been documented in many cancers and serve to promote cancer growth (reviewed in [94]). Common fusion partners identified for FGFR1 and FGFR3 are transforming acidic coiled-coil 1 (TACC1) and TACC3, which have been described in a subset of bladder carcinomas [95], non-small cell lung cancer [96], and glioblastoma multiforme [97]. These fusion proteins promote constitutive kinase activity, but lack PLC γ recruitment, which enhances cellular proliferation and oncogenic transformation [95,97]. Expression of FGFR3–TACC3 fusion protein is enhanced by the loss of a binding site for the regulatory microRNA miR-99a [98]. Other fusion partners have been identified for FGFR1, FGFR2, and FGFR3 in a number of cancers with varying prevalence [99,100]. Common to all the identified fusion proteins is an enhanced sensitivity to FGFR inhibitors in the cancers that harbour these fusions.

Isoform switching/autocrine stimulation

Epithelial cells primarily express IIIb receptor isoforms, whereas stromal cells express IIIc. In the tumour micro-environment, cancerous cells have been reported to adopt the expression of atypical receptor isoforms, thus sensitising the cells to stimulation from FGFs that they would not

otherwise detect. The importance of isoform switching was first established in prostate cancer [101]. More recently, isoform switching from FGFR2b to FGFR2c, induced by transforming growth factor β , has been reported in breast cancer cells. The switch to FGFR2c sensitised the cells to FGF2, allowing them to adopt a more invasive phenotype [102]. FGFR2c expression has been documented in many epithelial cancers, where it appears to enhance cell proliferation and migration [103–105]. Indeed, pancreatic cell lines overexpressing FGFR2c exhibit enhanced tumour growth in in vivo models [103].

Cancerous cells can produce FGFs that signal back to the cell in an autocrine loop to promote growth and invasion. For example, the growth of squamous cell carcinoma cell lines can be inhibited with FGF2 ligand traps that effectively shut down an FGF2/FGFR1 autocrine loop [106]. Conditional deletion of the phosphatase PTEN in the epidermis results in the spontaneous formation of skin tumours in mice [107]. Loss of PTEN enhances mTOR signalling and FGF10 production, driving epidermal cell proliferation. This aberrant growth was abrogated through epidermal deletion of FGFR2, demonstrating that PTEN deletion could create an FGF10 autocrine loop [107]. An autocrine loop for FGF19 has also been reported in prostate cancer [108]. As well as promoting cancer cell growth, the adoption of FGF autocrine loops has been identified as a mechanism of developing drug resistance in cancer cell lines [109,110].

FGF directed therapeutics

Given the importance of FGF signalling in a number of pathologies, great efforts have been made to target this pathway, with a number of therapeutics entering the clinic and many more in active development (Table 1). Given the

Table 1. Table of FGFR directed therapies currently in clinical trials^a

Compound	Company	Status	Indication
Multi TKI inhibitors			
AP24534 (Ponatinib)	Ariad Pharma	Approved Phase II	CML, ALL Gastrointestinal stromal tumours, lung/thyroid cancer, AML
BIBF1120 (Nintedanib)	Boehringer Ingelheim	Submitted Phase III	NSCLC Ovarian cancer, IPF
E7080 (Lenvatinib)	Eisai	Submitted Phase II/III	Thyroid cancer Hepatocellular carcinoma, endometrial cancer, melanoma, glioma, NSCLC
TSU-68 (Orantinib)	Taiho Pharma	Phase III	Hepatocellular carcinoma
ENMD-2076	CASI Pharma	Phase I/II	Breast/ovarian cancer
E3810 (Lucitanib)	Clovis Oncology/Servier	Phase I/II	ER ⁺ Breast cancer, Solid tumours
TKI258 (Dovitinib)	Novartis	Phase II	Multiple cancers including advanced endometrial and breast cancers
ARQ 087	ArQule	Phase I	Solid tumours
FGFR selective TKI inhibitors			
AZD4547	Astra Zeneca	Phase II	Solid tumours
BGJ398	Novartis	Phase II	Solid tumours, melanoma
LY2874455	Lilly	Phase I	Advanced cancer
Debio 1347	Debiopharm	Phase I	Solid tumours
TAS-120	Taiho Pharma	Phase I/II	Solid tumours, multiple myeloma
JNJ42756493	Astex pharma/Janssen	Phase I	Neoplasms, lymphoma
FGFR Antibodies			
MGFR18775	Genentech/Roche	Phase I	Solid tumours, multiple myeloma
KRN23	Kyowa HAKKO Kirin	Phase II	X-linked hypophosphatemia
FGF Traps			
FP-1039 (GSK3052230)	Five prime therapeutics/GSK	Phase I	Solid tumours

^aStages of development and indications are based upon information obtained from clinicaltrials.gov. Information correct as of September 2014.

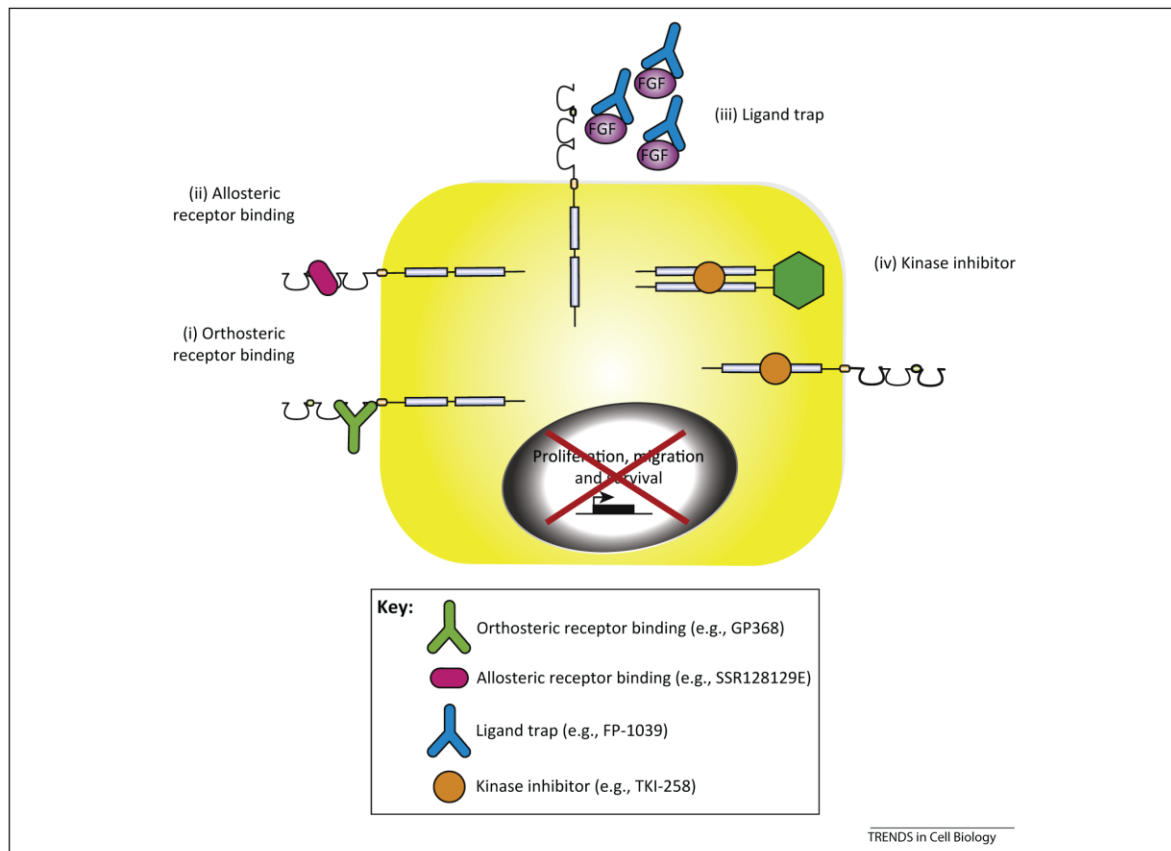


Figure 5. Mechanisms of fibroblast growth factor receptor (FGFR) inhibition. Given the importance of FGFR signalling in a range of pathologies, numerous drugs have been, and currently are, under development to target this pathway. These therapeutics fall into one of four categories: (i) orthosteric inhibitors, where inhibitors target the ligand binding domain of the receptor, therefore preventing FGF attachment and induction of downstream signals; (ii) allosteric inhibitors, which bind to the extracellular portion of the receptor, preventing it being internalised and transducing a signal, even when ligand is bound; (iii) ligand trap, consisting of the ligand binding domain of, for example, FGFR1 bound to the Fc portion of IgG1, resulting in sequestration of ligand, and therefore, prevention of receptor stimulation; and (iv) small molecule kinase inhibitors, the most common therapeutic option, targeting the ATP-binding pocket of the intracellular kinase domain of the receptor.

interest in developing FGF targeted therapies, a number of different approaches have been employed (Figure 5).

Kinase inhibitors

Small molecule inhibitors that target the tyrosine kinase domain of RTKs are the furthest developed of the FGFR directed therapeutics. These compounds are promiscuous, often hitting RTKs beyond FGFR. For instance, AP24534 (Ponatinib) primarily targets BCR-ABL, ($IC_{50} = 0.37$ nM) and is less potent towards FGFR (e.g., FGFR1 $IC_{50} = 2.2$ nM) (Table 2) [111]. Nevertheless, broad-spectrum tyrosine kinase inhibitors (TKIs) effectively inhibit proliferation in a panel of FGFR amplified cancer cell lines, suggesting that they would be beneficial against cancers harbouring FGFR mutations [112]. This has been reflected in recent clinical trials, which report that the broad spectrum TKIs, TKI258 (Dovitinib), and E3810 (Lucitanib), have better responses in patients with cancers harbouring FGFR amplifications [79,80]. Eight such compounds are currently in clinical trials (Table 1), with Ponatinib approved for the treatment of chronic myeloid leukaemia and Nintedanib submitted for

non-small cell lung cancer. Although the broad nature of these inhibitors is therapeutically beneficial, affecting multiple pathways such as those of the FGFR and the vascular endothelial growth factor receptor, it has also led to many of them exhibiting particularly dire toxicity profiles. Of note is the recent temporary withdrawal of Ponatinib due to a high incidence (27%) of sometimes fatal arterial and venous thrombosis [113]. These adverse vascular side effects may be overcome by the emerging class of tyrosine kinase inhibitors (TKIs), which exhibit enhanced selectivity for FGFRs over other RTKs. Currently, six FGFR-selective TKIs are in Phase I/II clinical trials, mainly for solid tumours, having shown promising anti-tumour effects in preclinical models (Table 1) [114–116]. Somewhat unsurprisingly, these FGFR-selective TKIs are more efficacious in cancer cell lines exhibiting FGFR mutations [117–119], suggesting clinical utility in patients with tumours exhibiting FGFR mutations or amplifications. These compounds also appear to avoid the vascular side effects associated with broad spectrum TKIs but do, however, induce hyperphosphatemia, through disruption to hormonal FGF23 signalling [120,121].

Table 2. IC₅₀ values for tyrosine kinase inhibitors of FGFR, VEGFR, and PDGFR

Compound	IC ₅₀ values (nM)										Refs
	FGFR1	FGFR2	FGFR3	FGFR4	VEGFR1	VEGFR2	VEGFR3	PDGFR a	PDGFR b	Other	
AP24534 (Ponatinib)	2.2	1.6	18.2	7.7	3.7	1.5	2.3	1.1	7.7	Abl (0.37) LYN (0.24)	[111]
BIBF1120 (Nintedanib)	69	37	108	610	34	21	13	59	65	FLT-3 (26) LcK (16)	[131]
E7080 (Lenvatinib)	46				22	4	5.2	51	39		[132]
TSU-68 (Orantinib)	1200				2100				8		[133]
ENMD-2076	92.7	70.8				58.2	15.9	56.4		Aurora A (14)	[134]
E3810 (Lucitanib)	17.5	82.5	238.5		7	25	10	175	525	CSF-1R (5)	[135]
TKI258 (Dovitinib)	8		9		10	13	8	27	210	FLT-3 (1) KIT (2)	[136]
ARQ 087	Not available										
AZD4547	0.2	1.8	2.5	165		24					[114]
BGJ398	0.9	1.4	1	60							[115]
LY2874455	2.8	2.6	6.4	6							[116]
Debio 1347	Not available										
TAS-120	Not available										
JNJ42756493	Not available										

Orthosteric receptor binding

Alternatives to small molecule inhibitors may present a preferable option, by allowing for more direct action against specific FGFRs, thus avoiding potential side effects. Antibody based approaches offer an effective means of isoform specific FGFR blockade. Early attempts with an anti-FGFR1 antibody were effective, but failed at the preclinical stage due to an accumulation of the antibody in the hypothalamus of treated monkeys and rats, leading to rapid weight loss [122]. Targeting other FGFRs has proved more successful, with an antibody directed at FGFR3 exerting anti-tumour activity in mouse models of bladder carcinoma and multiple myeloma, without significant side effects [123]. A further anti-FGFR3 antibody, MGFR1877S, is currently in Phase I trials for solid tumours and multiple myeloma (Table 1). Moreover, an FGFR2 directed antibody, GP369, has been demonstrated to reduce growth of xenograft tumours harbouring FGFR2 amplifications [124]. Antibody based therapies also appear to be effective in diseases beyond cancer; an anti-FGF23 antibody, KRN23, is in Phase II trials for x-linked hypophosphatemia [125].

Other approaches include FP-1039, an FGF-ligand trap consisting of the extracellular portion of FGFR1c fused to the Fc domain of IgG1. The use of the FGFR1c receptor allows targeting of mitogenic FGF ligands, without affecting hormonal FGFs, thus reducing toxicity while providing anti-tumour activity in lung and endometrial cancer models [126]. FP-1039 is currently in Phase I trials for solid tumours. Another ligand trap, using the extracellular portion of FGFR3, is effective in a mouse model of achondroplasia, where genetically engineered disease-associated mutations in FGFR3 result in prolonged ligand-mediated activation and skeletal abnormalities. Achondroplastic mice receiving an FGFR3 ligand trap from birth showed increased chondrocyte differentiation and proliferation and enhanced survival, with no overt toxicity [127]. An alternative model, utilising induced pluripotent stem cells to model chondrocyte dysfunction in achondroplasia, showed that statin treatment resulted in the degradation of mutated FGFR3, leading to reduced signalling and a restoration of chondrocyte differentiation [128].

Allosteric receptor binding

A small molecule allosteric modulator of FGFR signalling, SSR128129E, has also been described [129]. SSR128129E is capable of manipulating the signalling of multiple FGFRs, promoting the formation of an FGF: FGFR complex, which is not internalised, thus limiting signalling outputs [129]. Therapeutically, SSR128129E has been shown to reduce cancer progression in a mouse model of pancreatic cancer and also reduces inflammation in a model of arthritis [130]. Moreover, SSR128129E did not appear to induce any vascular side effects in the mice, indicating that this approach may be preferable over classic TKIs.

Concluding remarks

Where to now? Dissecting canonical signalling pathways is still valuable, but interest in novel signalling mechanisms, including crosstalk with other signalling pathways, endocrine roles of FGFs, and nuclear roles for FGFRs are areas of growing interest.

Therapeutic approaches are developing apace but these bring with them new challenges for the field; how to screen and stratify patients for the appropriate treatments, what biomarkers are available to monitor responses to treatment, what mechanisms are used to drive resistance to FGFR inhibition, and what models should we be using to address FGFR signalling in a physiologically relevant context.

The FGF field is developing in a number of exciting directions, highlighting the critical nature of appropriate cellular communication. Our improved understanding of how this can go awry, coupled with the prospect of novel inhibitors coming to clinic points towards a bright future for FGF research.

Acknowledgements

We apologise to colleagues whose work we were unable to cite due to space constraints. We thank Breast Cancer Campaign and Cancer Research UK for funding.

References

- 1 Belov, A.A. and Mohammadi, M. (2013) Molecular mechanisms of fibroblast growth factor signaling in physiology and pathology. *Cold Spring Harb. Perspect. Biol.* 5 Published online June 1, 2013. <http://dx.doi.org/10.1101/cshperspect.a015958>

- 2 Holzmann, K. et al. (2011) Alternative splicing of fibroblast growth factor receptor IgIII loops in cancer. *J. Nucleic Acids* 2012, 950508
- 3 Sleeman, M. et al. (2001) Identification of a new fibroblast growth factor receptor, FGFR5. *Gene* 271, 171–182
- 4 Catela, C. et al. (2009) Multiple congenital malformations of Wolf-Hirschhorn syndrome are recapitulated in Fgfr1 null mice. *Dis. Model Mech.* 2, 283–294
- 5 Bluteau, G. et al. (2014) Targeted disruption of the intracellular domain of receptor FgfrL1 in mice. *PLoS ONE* 9, e105210
- 6 Silva, P.N. et al. (2013) Fibroblast growth factor receptor like-1 (FGFRL1) interacts with SHP-1 phosphatase at insulin secretory granules and induces beta-cell ERK1/2 protein activation. *J. Biol. Chem.* 288, 17859–17870
- 7 Goetz, R. and Mohammadi, M. (2013) Exploring mechanisms of FGF signalling through the lens of structural biology. *Nat. Rev. Mol. Cell Biol.* 14, 166–180
- 8 Goetz, R. et al. (2007) Molecular insights into the klotho-dependent, endocrine mode of action of fibroblast growth factor 19 subfamily members. *Mol. Cell Biol.* 27, 3417–3428
- 9 Goetz, R. et al. (2012) Conversion of a paracrine fibroblast growth factor into an endocrine fibroblast growth factor. *J. Biol. Chem.* 287, 29134–29146
- 10 Goetz, R. et al. (2012) Klotho coreceptors inhibit signaling by paracrine fibroblast growth factor 8 subfamily ligands. *Mol. Cell Biol.* 32, 1944–1954
- 11 Lew, E.D. et al. (2009) The precise sequence of FGF receptor autophosphorylation is kinetically driven and is disrupted by oncogenic mutations. *Sci. Signal.* 2, ra6
- 12 Mohammadi, M. et al. (1991) A tyrosine-phosphorylated carboxy-terminal peptide of the fibroblast growth factor receptor (Fg) is a binding site for the SH2 domain of phospholipase C-gamma 1. *Mol. Cell Biol.* 11, 5068–5078
- 13 Kouhara, H. et al. (1997) A lipid-anchored Grb2-binding protein that links FGF-receptor activation to the Ras/MAPK signaling pathway. *Cell* 89, 693–702
- 14 Hart, K.C. et al. (2000) Transformation and Stat activation by derivatives of FGFR1, FGFR3, and FGFR4. *Oncogene* 19, 3309–3320
- 15 Ong, S.H. et al. (2001) Stimulation of phosphatidylinositol 3-kinase by fibroblast growth factor receptors is mediated by coordinated recruitment of multiple docking proteins. *Proc. Natl. Acad. Sci. U.S.A.* 98, 6074–6079
- 16 Wong, A. et al. (2002) FRS2 alpha attenuates FGF receptor signaling by Grb2-mediated recruitment of the ubiquitin ligase Cbl. *Proc. Natl. Acad. Sci. U.S.A.* 99, 6684–6689
- 17 Smith, T.G. et al. (2006) Negative feedback predominates over cross-regulation to control ERK MAPK activity in response to FGF signalling in embryos. *FEBS Lett.* 580, 4242–4245
- 18 Ding, W. et al. (2003) Functional analysis of the human Sprouty2 gene promoter. *Gene* 322, 175–185
- 19 Kovalenko, D. et al. (2003) Sef inhibits fibroblast growth factor signaling by inhibiting FGFR1 tyrosine phosphorylation and subsequent ERK activation. *J. Biol. Chem.* 278, 14087–14091
- 20 Zakrzewska, M. et al. (2013) ERK-mediated phosphorylation of fibroblast growth factor receptor 1 on Ser777 inhibits signaling. *Sci. Signal.* 6, ra11
- 21 Lin, C.C. et al. (2012) Inhibition of basal FGF receptor signaling by dimeric Grb2. *Cell* 149, 1514–1524
- 22 Ahmed, Z. et al. (2013) Grb2 controls phosphorylation of FGFR2 by inhibiting receptor kinase and Shp2 phosphatase activity. *J. Cell Biol.* 200, 493–504
- 23 Timsah, Z. et al. (2014) Competition between Grb2 and Plcgamma1 for FGFR2 regulates basal phospholipase activity and invasion. *Nat. Struct. Mol. Biol.* 21, 180–188
- 24 Fearon, A.E. and Grose, R.P. (2014) Grb-ing receptor activation by the tail. *Nat. Struct. Mol. Biol.* 21, 113–114
- 25 Francavilla, C. et al. (2013) Functional proteomics defines the molecular switch underlying FGF receptor trafficking and cellular outputs. *Mol. Cell* 51, 707–722
- 26 Makarenkova, H.P. et al. (2009) Differential interactions of FGFs with heparan sulfate control gradient formation and branching morphogenesis. *Sci. Signal.* 2, ra55
- 27 Coleman, S.J. et al. (2014) The ins and outs of fibroblast growth factor receptor signalling. *Clin. Sci. (Lond.)* 127, 217–231
- 28 Mills, I.G. (2011) Nuclear translocation and functions of growth factor receptors. *Semin. Cell Dev. Biol.* 23, 165–171
- 29 Chioni, A.M. and Grose, R. (2012) FGFR1 cleavage and nuclear translocation regulates breast cancer cell behavior. *J. Cell Biol.* 197, 801–817
- 30 Coleman, S.J. et al. (2014) Nuclear translocation of FGFR1 and FGF2 in pancreatic stellate cells facilitates pancreatic cancer cell invasion. *EMBO Mol. Med.* 6, 467–481
- 31 Lee, Y.W. et al. (2012) A novel nuclear FGF Receptor-1 partnership with retinoid and Nur receptors during developmental gene programming of embryonic stem cells. *J. Cell. Biochem.* 113, 2920–2936
- 32 Baron, O. et al. (2012) Cooperation of nuclear fibroblast growth factor receptor 1 and Nurr1 offers new interactive mechanism in postmitotic development of mesencephalic dopaminergic neurons. *J. Biol. Chem.* 287, 19827–19840
- 33 Lee, Y.W. et al. (2013) NGF-induced cell differentiation and gene activation is mediated by integrative nuclear FGFR1 signaling (INFS). *PLoS ONE* 8, e68931
- 34 Zakrzewska, M. et al. (2011) Translocation of exogenous FGF1 into cytosol and nucleus is a periodic event independent of receptor kinase activity. *Exp. Cell Res.* 317, 1005–1015
- 35 Zhen, Y. et al. (2012) Nuclear import of exogenous FGF1 requires the ER-protein LRRC59 and the importins Kpnalpha1 and Kpnbeta1. *Traffic* 13, 650–664
- 36 Smallwood, P.M. et al. (1996) Fibroblast growth factor (FGF) homologous factors: new members of the FGF family implicated in nervous system development. *Proc. Natl. Acad. Sci. U.S.A.* 93, 9850–9857
- 37 Liu, C.J. et al. (2003) Modulation of the cardiac sodium channel Nav1.5 by fibroblast growth factor homologous factor 1B. *J. Biol. Chem.* 278, 1029–1036
- 38 Yan, H. et al. (2013) FGF14 regulates presynaptic Ca²⁺ channels and synaptic transmission. *Cell Rep.* 4, 66–75
- 39 Hennessey, J.A. et al. (2013) Fibroblast growth factor homologous factors modulate cardiac calcium channels. *Circ. Res.* 113, 381–388
- 40 Pownall, M.E. and Isaacs, H.V. (2010) FGF Signalling in Vertebrate Development, Morgan & Claypool Life Science, (San Rafael (CA))
- 41 Hatch, N.E. (2010) FGF signaling in craniofacial biological control and pathological craniofacial development. *Crit. Rev. Eukaryot. Gene Expr.* 20, 295–311
- 42 Yu, K. et al. (2000) Loss of fibroblast growth factor receptor 2 ligand-binding specificity in Apert syndrome. *Proc. Natl. Acad. Sci. U.S.A.* 97, 14536–14541
- 43 Park, W.J. et al. (1995) Analysis of phenotypic features and FGFR2 mutations in Apert syndrome. *Am. J. Hum. Genet.* 57, 321–328
- 44 Wang, Y. et al. (2005) Abnormalities in cartilage and bone development in the Apert syndrome FGFR2(+/S252W) mouse. *Development* 132, 3537–3548
- 45 Chen, P. et al. (2014) A Ser252Trp mutation in fibroblast growth factor receptor 2 (FGFR2) mimicking human Apert syndrome reveals an essential role for FGF signaling in the regulation of endochondral bone formation. *PLoS ONE* 9, e87311
- 46 Yokota, M. et al. (2014) Therapeutic effect of nanogel-based delivery of soluble FGFR2 with S252W mutation on craniosynostosis. *PLoS ONE* 9, e101693
- 47 Dode, C. et al. (2003) Loss-of-function mutations in FGFR1 cause autosomal dominant Kallmann syndrome. *Nat. Genet.* 33, 463–465
- 48 Thurman, R.D. et al. (2012) Molecular basis for the Kallmann syndrome-linked fibroblast growth factor receptor mutation. *Biochem. Biophys. Res. Commun.* 425, 673–678
- 49 McCabe, M.J. et al. (2011) Novel FGF8 mutations associated with recessive holoprosencephaly, craniofacial defects, and hypothalamopituitary dysfunction. *J. Clin. Endocrinol. Metab.* 96, E1709–E1718
- 50 Arauz, R.F. et al. (2010) A hypomorphic allele in the FGF8 gene contributes to holoprosencephaly and is allelic to gonadotropin-releasing hormone deficiency in humans. *Mol. Syndromol.* 1, 59–66
- 51 McGrath, J.A. et al. (2001) Hay-Wells syndrome is caused by heterozygous missense mutations in the SAM domain of p63. *Hum. Mol. Genet.* 10, 221–229
- 52 Ferone, G. et al. (2012) Mutant p63 causes defective expansion of ectodermal progenitor cells and impaired FGF signalling in AEC syndrome. *EMBO Mol. Med.* 4, 192–205

- 53 Hennessey, J.A. et al. (2013) FGF12 is a candidate Brugada syndrome locus. *Heart Rhythm* 10, 1886–1894
- 54 Yang, J. et al. (2010) Fibroblast growth factor receptors 1 and 2 in keratinocytes control the epidermal barrier and cutaneous homeostasis. *J. Cell Biol.* 188, 935–952
- 55 Jameson, J. et al. (2002) A role for skin γ delta T cells in wound repair. *Science* 296, 747–749
- 56 Gay, D. et al. (2013) Fgf9 from dermal γ delta T cells induces hair follicle neogenesis after wounding. *Nat. Med.* 19, 916–923
- 57 Werner, S. et al. (1992) Large induction of keratinocyte growth factor expression in the dermis during wound healing. *Proc. Natl. Acad. Sci. U.S.A.* 89, 6896–6900
- 58 Werner, S. et al. (1994) The function of KGF in morphogenesis of epithelium and reepithelialization of wounds. *Science* 266, 819–822
- 59 Meyer, M. et al. (2012) FGF receptors 1 and 2 are key regulators of keratinocyte migration in vitro and in wounded skin. *J. Cell Sci.* 125, 5690–5701
- 60 Oladipupo, S.S. et al. (2014) Endothelial cell FGF signaling is required for injury response but not for vascular homeostasis. *Proc. Natl. Acad. Sci. U.S.A.* 111, 13379–13384
- 61 Taub, R. (2004) Liver regeneration: from myth to mechanism. *Nat. Rev. Mol. Cell Biol.* 5, 836–847
- 62 Bohm, F. et al. (2010) Regulation of liver regeneration by growth factors and cytokines. *EMBO Mol. Med.* 2, 294–305
- 63 Steiling, H. et al. (2003) Fibroblast growth factor receptor signalling is crucial for liver homeostasis and regeneration. *Oncogene* 22, 4380–4388
- 64 Bohm, F. et al. (2010) FGF receptors 1 and 2 control chemically induced injury and compound detoxification in regenerating livers of mice. *Gastroenterology* 139, 1385–1396
- 65 Yu, C. et al. (2002) Increased carbon tetrachloride-induced liver injury and fibrosis in FGFR4-deficient mice. *Am. J. Pathol.* 161, 2003–2010
- 66 Lin, B.C. et al. (2007) Liver-specific activities of FGF19 require Klotho beta. *J. Biol. Chem.* 282, 27277–27284
- 67 Takase, H.M. et al. (2013) FGF7 is a functional niche signal required for stimulation of adult liver progenitor cells that support liver regeneration. *Genes Dev.* 27, 169–181
- 68 Uriarte, I. et al. (2013) Identification of fibroblast growth factor 15 as a novel mediator of liver regeneration and its application in the prevention of post-resection liver failure in mice. *Gut* 62, 899–910
- 69 Hines, E.A. and Sun, X. (2014) Tissue crosstalk in lung development. *J. Cell. Biochem.* 115, 1469–1477
- 70 Volckaert, T. et al. (2011) Parabranchial smooth muscle constitutes an airway epithelial stem cell niche in the mouse lung after injury. *J. Clin. Invest.* 121, 4409–4419
- 71 Coffey, E. et al. (2013) Expression of fibroblast growth factor 9 in normal human lung and idiopathic pulmonary fibrosis. *J. Histochem. Cytochem.* 61, 671–679
- 72 Yu, Z.H. et al. (2012) Mutant soluble ectodomain of fibroblast growth factor receptor-2 Il1c attenuates bleomycin-induced pulmonary fibrosis in mice. *Biol. Pharm. Bull.* 35, 731–736
- 73 Aguilar, S. et al. (2009) Bone marrow stem cells expressing keratinocyte growth factor via an inducible lentivirus protects against bleomycin-induced pulmonary fibrosis. *PLoS ONE* 4, e8013
- 74 Guzy, R.D. et al. (2014) FGF2 is required for epithelial recovery, but not for pulmonary fibrosis, in response to bleomycin. *Am. J. Respir. Cell Mol. Biol.* Published online July 2, 2014
- 75 Turner, N. and Grose, R. (2010) Fibroblast growth factor signalling: from development to cancer. *Nat. Rev. Cancer* 10, 116–129
- 76 Kim, S. et al. (2013) FGFR2 promotes breast tumorigenicity through maintenance of breast tumor-initiating cells. *PLoS ONE* 8, e51671
- 77 Wan, X. et al. (2014) Prostate cancer cell-stromal cell crosstalk via FGFR1 mediates antitumor activity of dovitinib in bone metastases. *Sci. Transl. Med.* 6, 252ra122
- 78 Chang, J. et al. (2014) Prognostic value of FGFR gene amplification in patients with different types of cancer: a systematic review and meta-analysis. *PLoS ONE* 9, e105524
- 79 Soria, J.C. et al. (2014) Phase I/IIa study evaluating the safety, efficacy, pharmacokinetics, and pharmacodynamics of lucitanib in advanced solid tumors. *Ann. Oncol.* 25, 2244–2251 2014
- 80 Andre, F. et al. (2013) Targeting FGFR with dovitinib (TKI258): preclinical and clinical data in breast cancer. *Clin. Cancer Res.* 19, 3693–3702
- 81 Weiss, J. et al. (2010) Frequent and focal FGFR1 amplification associates with therapeutically tractable FGFR1 dependency in squamous cell lung cancer. *Sci. Transl. Med.* 2, 62ra93
- 82 Reintjes, N. et al. (2013) Activating somatic FGFR2 mutations in breast cancer. *PLoS ONE* 8, e60264
- 83 Tchaicha, J.H. et al. (2014) Kinase domain activation of FGFR2 yields high-grade lung adenocarcinoma sensitive to a Pan-FGFR inhibitor in a mouse model of NSCLC. *Cancer Res.* 74, 4676–4684
- 84 Hunter, D.J. et al. (2007) A genome-wide association study identifies alleles in FGFR2 associated with risk of sporadic postmenopausal breast cancer. *Nat. Genet.* 39, 870–874
- 85 Easton, D.F. et al. (2007) Genome-wide association study identifies novel breast cancer susceptibility loci. *Nature* 447, 1087–1093
- 86 Huijts, P.E. et al. (2011) Allele-specific regulation of FGFR2 expression is cell type-dependent and may increase breast cancer risk through a paracrine stimulus involving FGF10. *Breast Cancer Res.* 13, R72
- 87 Liu, X. et al. (2014) Clinical significance of fibroblast growth factor receptor-3 mutations in bladder cancer: a systematic review and meta-analysis. *Genet. Mol. Res.* 13, 1109–1120
- 88 Sung, J.Y. et al. (2013) FGFR3 overexpression is prognostic of adverse outcome for muscle-invasive bladder carcinoma treated with adjuvant chemotherapy. *Urol. Oncol.* 32, 49 e23–31
- 89 Juanpere, N. et al. (2012) Mutations in FGFR3 and PIK3CA, singly or combined with RAS and AKT1, are associated with AKT but not with MAPK pathway activation in urothelial bladder cancer. *Hum. Pathol.* 43, 1573–1582
- 90 Foth, M. et al. (2014) Fibroblast growth factor receptor 3 activation plays a causative role in urothelial cancer pathogenesis in cooperation with Pten loss in mice. *J. Pathol.* 233, 148–158
- 91 Kalf, A. and Spencer, A. (2012) The t(4;14) translocation and FGFR3 overexpression in multiple myeloma: prognostic implications and current clinical strategies. *Blood Cancer J.* 2, e89
- 92 Shern, J.F. et al. (2014) Comprehensive genomic analysis of rhabdomyosarcoma reveals a landscape of alterations affecting a common genetic axis in fusion-positive and fusion-negative tumors. *Cancer Discov.* 4, 216–231
- 93 Taylor, J.G., VI et al. (2009) Identification of FGFR4-activating mutations in human rhabdomyosarcomas that promote metastasis in xenotransplanted models. *J. Clin. Invest.* 119, 3395–3407
- 94 Parker, B.C. et al. (2014) Emergence of FGFR family gene fusions as therapeutic targets in a wide spectrum of solid tumours. *J. Pathol.* 232, 4–15
- 95 Williams, S.V. et al. (2012) Oncogenic FGFR3 gene fusions in bladder cancer. *Hum. Mol. Genet.* 22, 795–803
- 96 Wang, R. et al. (2014) FGFR1/3 tyrosine kinase fusions define a unique molecular subtype of non-small cell lung cancer. *Clin. Cancer Res.* 20, 4107–4114
- 97 Singh, D. et al. (2012) Transforming fusions of FGFR and TACC genes in human glioblastoma. *Science* 337, 1231–1235
- 98 Parker, B.C. et al. (2013) The tumorigenic FGFR3–TACC3 gene fusion escapes miR-99a regulation in glioblastoma. *J. Clin. Invest.* 123, 855–865
- 99 Arai, Y. et al. (2013) Fibroblast growth factor receptor 2 tyrosine kinase fusions define a unique molecular subtype of cholangiocarcinoma. *Hepatology* 59, 1427–1434
- 100 Wu, Y.M. et al. (2013) Identification of targetable FGFR gene fusions in diverse cancers. *Cancer Discov.* 3, 636–647
- 101 Yan, G. et al. (1993) Exon switching and activation of stromal and embryonic fibroblast growth factor (FGF)-FGF receptor genes in prostate epithelial cells accompany stromal independence and malignancy. *Mol. Cell. Biol.* 13, 4513–4522
- 102 Shirakihara, T. et al. (2011) TGF- β regulates isoform switching of FGF receptors and epithelial-mesenchymal transition. *EMBO J.* 30, 783–795
- 103 Ishiwata, T. et al. (2012) Enhanced expression of fibroblast growth factor receptor 2 Il1c promotes human pancreatic cancer cell proliferation. *Am. J. Pathol.* 180, 1928–1941
- 104 Kawase, R. et al. (2010) Expression of fibroblast growth factor receptor 2 Il1c in human uterine cervical intraepithelial neoplasia and cervical cancer. *Int. J. Oncol.* 36, 331–340

- 105 Peng, W.X. et al. (2014) Altered expression of fibroblast growth factor receptor 2 isoform IIIc: relevance to endometrioid adenocarcinoma carcinogenesis and histological differentiation. *Int. J. Clin. Exp. Pathol.* 7, 1069–1076
- 106 Marshall, M.E. et al. (2011) Fibroblast growth factor receptors are components of autocrine signaling networks in head and neck squamous cell carcinoma cells. *Clin. Cancer Res.* 17, 5016–5025
- 107 Hertzler-Schaefer, K. et al. (2014) Pten loss induces autocrine FGF signaling to promote skin tumorigenesis. *Cell Rep.* 6, 818–826
- 108 Feng, S. et al. (2013) Endocrine fibroblast growth factor FGF19 promotes prostate cancer progression. *Cancer Res.* 73, 2551–2562
- 109 Ware, K.E. et al. (2013) A mechanism of resistance to gefitinib mediated by cellular reprogramming and the acquisition of an FGF2–FGFR1 autocrine growth loop. *Oncogenesis* 2, e39
- 110 Terai, H. et al. (2013) Activation of the FGF2–FGFR1 autocrine pathway: a novel mechanism of acquired resistance to gefitinib in NSCLC. *Mol. Cancer Res.* 11, 759–767
- 111 O'Hare, T. et al. (2009) AP24534, a pan-BCR–ABL inhibitor for chronic myeloid leukemia, potently inhibits the T315I mutant and overcomes mutation-based resistance. *Cancer Cell* 16, 401–412
- 112 Gozgit, J.M. et al. (2012) Ponatinib (AP24534), a multitargeted pan-FGFR inhibitor with activity in multiple FGFR-amplified or mutated cancer models. *Mol. Cancer Ther.* 11, 690–699
- 113 The Medical Letter Online (2014) In brief: ponatinib (Inclusig) returns. *Med. Lett. Drugs Ther.* 56, 8
- 114 Gavine, P.R. et al. (2012) AZD4547: an orally bioavailable, potent, and selective inhibitor of the fibroblast growth factor receptor tyrosine kinase family. *Cancer Res.* 72, 2045–2056
- 115 Guagnano, V. et al. (2011) Discovery of 3-(2,6-dichloro-3,5-dimethoxyphenyl)-1-[6-[4-(4-ethyl-piperazin-1-yl)-phenylamino]-pyrimidin-4-yl]-1-methyl-urea (NVP-BGJ398), a potent and selective inhibitor of the fibroblast growth factor receptor family of receptor tyrosine kinase. *J. Med. Chem.* 54, 7066–7083
- 116 Zhao, G. et al. (2011) A novel, selective inhibitor of fibroblast growth factor receptors that shows a potent broad spectrum of antitumor activity in several tumor xenograft models. *Mol. Cancer Ther.* 10, 2200–2210
- 117 Konecny, G.E. et al. (2013) Activity of the fibroblast growth factor receptor inhibitors dovitinib (TKI258) and NVP-BGJ398 in human endometrial cancer cells. *Mol. Cancer Ther.* 12, 632–642
- 118 Xie, L. et al. (2013) FGFR2 gene amplification in gastric cancer predicts sensitivity to the selective FGFR inhibitor AZD4547. *Clin. Cancer Res.* 19, 2572–2583
- 119 Zhang, J. et al. (2012) Translating the therapeutic potential of AZD4547 in FGFR1-amplified non-small cell lung cancer through the use of patient-derived tumor xenograft models. *Clin. Cancer Res.* 18, 6658–6667
- 120 Sequist, L.V. et al. (2014) Phase I study of BGJ398, a selective pan-FGFR inhibitor in genetically preselected advanced solid tumors. [abstract]. In Proceedings of the 105th Annual Meeting of the American Association for Cancer Research. San Diego, CA. Philadelphia (PA): AACR 2014. Abstract nr CT326
- 121 Dienstmann, R. et al. (2014) First in human study of JNJ-42756493, a potent pan fibroblast growth factor receptor (FGFR) inhibitor in patients with advanced solid tumors [abstract]. In Proceedings of the 105th Annual Meeting of the American Association for Cancer Research. San Diego, CA. Philadelphia (PA): AACR 2014. Abstract nr CT325
- 122 Sun, H.D. et al. (2007) Monoclonal antibody antagonists of hypothalamic FGFR1 cause potent but reversible hypophagia and weight loss in rodents and monkeys. *Am. J. Physiol. Endocrinol. Metab.* 292, E964–E976
- 123 Qing, J. et al. (2009) Antibody-based targeting of FGFR3 in bladder carcinoma and t(4;14)-positive multiple myeloma in mice. *J. Clin. Invest.* 119, 1216–1229
- 124 Bai, A. et al. (2010) GP369, an FGFR2-IIIb-specific antibody, exhibits potent antitumor activity against human cancers driven by activated FGFR2 signaling. *Cancer Res.* 70, 7630–7639
- 125 Carpenter, T.O. et al. (2014) Randomized trial of the anti-FGF23 antibody KRN23 in X-linked hypophosphatemia. *J. Clin. Invest.* 124, 1587–1597
- 126 Harding, T.C. et al. (2013) Blockade of nonhormonal fibroblast growth factors by FP-1039 inhibits growth of multiple types of cancer. *Sci. Transl. Med.* 5, ra39
- 127 Garcia, S. et al. (2013) Postnatal soluble FGFR3 therapy rescues achondroplasia symptoms and restores bone growth in mice. *Sci. Transl. Med.* 5, 203ra124
- 128 Yamashita, A. et al. (2014) Statin treatment rescues FGFR3 skeletal dysplasia phenotypes. *Nature* 513, 507–511
- 129 Herbert, C. et al. (2013) Molecular mechanism of SSR 128129E, an extracellularly acting, small-molecule, allosteric inhibitor of FGF receptor signaling. *Cancer Cell* 23, 489–501
- 130 Bono, F. et al. (2013) Inhibition of tumor angiogenesis and growth by a small-molecule multi-FGF receptor blocker with allosteric properties. *Cancer Cell* 23, 477–488
- 131 Hilberg, F. et al. (2008) BIBF 1120: triple angiokinase inhibitor with sustained receptor blockade and good antitumor efficacy. *Cancer Res.* 68, 4774–4782
- 132 Matsui, J. et al. (2008) E7080, a novel inhibitor that targets multiple kinases, has potent antitumor activities against stem cell factor producing human small cell lung cancer H146, based on angiogenesis inhibition. *Int. J. Cancer* 122, 664–671
- 133 Laird, A.D. et al. (2000) SU6668 is a potent antiangiogenic and antitumor agent that induces regression of established tumors. *Cancer Res.* 60, 4152–4160
- 134 Fletcher, G.C. et al. (2010) ENMD-2076 is an orally active kinase inhibitor with antiangiogenic and antiproliferative mechanisms of action. *Mol. Cancer Ther.* 10, 126–137
- 135 Bello, E. et al. (2011) E-3810 is a potent dual inhibitor of VEGFR and FGFR that exerts antitumor activity in multiple preclinical models. *Cancer Res.* 71, 1396–1405
- 136 Trudel, S. et al. (2005) CHIR-258, a novel, multitargeted tyrosine kinase inhibitor for the potential treatment of t(4;14) multiple myeloma. *Blood* 105, 2941–2948